CONTROL OF SYSTEMS SUBJECT TO UNCERTAINTY AND CONSTRAINTS

A Dissertation

by

ELIZABETH ROXANA VILLOTA CERNA

Submitted to the Office of Graduate Studies of
Texas A&M University
in partial fulfillment of the requirements for the degree of

DOCTOR OF PHILOSOPHY

December 2007

Major Subject: Mechanical Engineering

CONTROL OF SYSTEMS SUBJECT TO UNCERTAINTY AND CONSTRAINTS

A Dissertation

by

ELIZABETH ROXANA VILLOTA CERNA

Submitted to the Office of Graduate Studies of
Texas A&M University
in partial fulfillment of the requirements for the degree of

DOCTOR OF PHILOSOPHY

Approved by:

Chair of Committee,	Suhada Jayasuriya
Committee Members,	Shankar Bhattacharyya
	Alan Palazzolo
	Alexander Parlos
Head of Department,	Dennis L. O'Neal

December 2007

Major Subject: Mechanical Engineering

ABSTRACT

Control of Systems Subject to Uncertainty and Constraints. (December 2007)
Elizabeth Roxana Villota Cerna, B.S., Universidad Nacional de Ingenieria;
M.S., Pontificia Universidade Catolica do Rio de Janeiro
Chair of Advisory Committee: Dr. Suhada Jayasuriya

All practical control systems are subject to constraints, namely constraints arising from the actuator's limited range and rate capacity (*input constraints*) or from imposed operational limits on plant variables (*output constraints*). A linear control system typically yields the desirable small signal performance. However, the presence of input constraints often causes undesirable large signal behavior and potential instability. An anti-windup control consists of a remedial solution that mitigates the effect of input constraints on the closed-loop without affecting the small signal behavior. Conversely, an override control addresses the control problem involving output constraints and also follows the idea that large signal control objectives do not alter small signal performance. Importantly, these two remedial control methodologies must incorporate model uncertainty into their design to be considered reliable in practice. In this dissertation, shared principles of design for the remedial compensation problem are identified which simplify the picture when analyzing, comparing and synthesizing for the variety of existing remedial schemes. Two performance objectives, each one related to a different type of remedial compensation, and a general structural representation associated with both remedial compensation problems will be considered. The effect of remedial control on the closed-loop will be evaluated in terms of two general frameworks which permit the unification and comparison of all known remedial compensation schemes. The difference systems describing the performance objectives will be further employed for comparison of remedial compensation schemes

under uncertainty considerations and also for synthesis of compensators. On the basis of the difference systems and the general structure for remedial compensation, systematic remedial compensation synthesis algorithms for anti-windup and override compensation will be given and compared. Successful application of the proposed robust remedial control synthesis algorithms will be demonstrated via simulation.

To my parents, Jaime Villota and Magnolia Cerna, for their unconditional love and support.

ACKNOWLEDGMENTS

This is the opportunity that I have to thank all the people that have walked by my side during all the years that I spent working on my dissertation and away from home. First and foremost among them is my advisor, Suhada Jayasuriya. His continuous help and guidance were fundamental in the development of my dissertation work. Dr. J. thanks a lot for the tremendous support, encouragement and patience. I will always be greatly indebted to you! My thanks also to the members of my dissertation committee, Shankar Bhattacharyya, Alan Palazzolo and Alexander Parlos, who not only contributed to my academic formation, but also were kind enough to answer all my questions.

My learning experience at Texas A&M was greatly enhanced by many graduate students and post-doctoral fellows. The numerous discussions about almost every topic provided a special balance to my mind and soul. Thanks to my office mates over the years, Avinash Dharne, Chen-yang Lan, Asanka Maithripala, Mayank Lal and Sang-Bum Woo, who have patiently answered my computing and scientific questions as well as sharing endless cups of tea and the different tastes of their countries with me. A special acknowledgment goes to a close collaborator, Murray Kerr; thanks for the endless discussions on control theory topics and for inculcating in me your spirit of research.

Outside the lab, many people have made this journey more enjoyable. I want to thank Freder Medina and his parents for making me feel that I was at home. Special thanks for my roommates, Achala Dassanayake, Yetzirah Urthaler, Mayra Miranda and Muge Kazanci. Girls, thanks for all our talks and also for being part of my family in College Station. A special thanks goes to the Peruvian community, my extended family; having them here really helped me whenever I wanted to have a feel of my

country and its people.

Most importantly, I wish to thank my parents, Jaime and Magnolia, and siblings, Nelly, Marco and Jaime. They have been and will always be the pillars of my life! My apologies to my nieces, Sofia and Mia, and to my little brother Jaime for not having much presence in their lives. Special thanks go to my mom, who always encouraged me to follow my dreams; her understanding of my leaving her at home was crucial to keep me working here. She never failed to make me feel loved or put a smile on my face, even in the worst moments. Thank you, Mom, and thank you, Dad, for everything! To you I dedicate my dissertation.

Last, but not least, I want to thank a special person, Alberto Coronado. Thanks, from the bottom of my heart, for all your time, your precious time!

TABLE OF CONTENTS

CHAPTER Page

CHAPTER Page

CHAPTER Page

CHAPTER Page

CHAPTER Page

LIST OF TABLES

LIST OF FIGURES

FIGURE Page

FIGURE Page

FIGURE Page

FIGURE Page

FIGURE Page

CHAPTER I

INTRODUCTION

This dissertation shows shared principles of design that simplify the picture when analyzing and synthesizing remedial compensation for systems subject to uncertainty and constraints. The identification of these principles permits one to discern the advantages and disadvantages of employing certain remedial compensators.

The aim of the introduction is threefold: to give an engineering motivation for studying remedial compensation by understanding the ramifications of the presence of uncertainty and constraints, to describe the remedial compensation strategies which will counteract the undesirable effects of the presence of uncertainty and constraints, and to provide a summarized review of previous works employing remedial compensation in order to identify the main existing deficiencies, which serve to motivate and justify the contributions of this dissertation.

A. Real-world systems are subject to uncertainty and constraints

The presence of uncertainty and plant constraints is well known to control engineers. Control system design is typically model based, with physical systems always uncertain, and hence the necessity for the provision of robustness to uncertainty. Similarly, all physical systems are subject to constraints, namely actuator saturation (input constraints arising from actuator limited range and rate capacity), which cause undesirable large signal behavior and potential instability, and operational limits in plant variables (output constraints arising from efficiency, safety and other concerns) that must be met. Hence it is know well known that a control systems that is not ca-

---

This dissertation follows the style of *IEEE Transactions on Automatic Control.*

pable to operate under constraints and despite uncertainty, is unlikely to perform acceptably.

1. Physical systems are uncertain

The task of a control engineer is to abstract a complex engineering problem, cast it into an appropriate mathematical setting and derive a solution, the latter of which represents a computable method of evaluation of the problem under study. However, by employing mathematical abstractions to represent the real world system dynamics, one has to deal with fundamental gaps between theory and practice. These gaps are reflected in the *uncertainty*[1] about the behavior of the real system when a mathematical prediction is given. This rationale of dealing with uncertainty is applied in the feedback control theory to obtain reliability in spite of faulty predictions. Importantly, a suitably designed feedback compensator will effectively reduce the sensitivity of the system to certain sources of uncertainty, but this will be possible only at the expense of increased sensitivity to other unmodeled effects. Hence, these existent trade-offs require that feedback theory provides with a means for their quantification and subsequently incorporation in the design process. Notably, this quantification, in addition to the mathematical model, requires some quantitative assessment of the model uncertainty.

2. Physical systems subject to constraints

Any conceivable physical system, in every application of control technology, is ultimately limited. In control system design, these limitations typically manifest them-

[1]Uncertainty in its broader sense describes not only the physical phenomena we are unable to predict, but also, many aspects of the physical plant we have chosen to neglect or simplify.

selves as constraints at the input and at the output of the plant. On the one hand, *input* or *manipulated variable* constraints are typically observed at the output of the system actuators, namely actuator saturation. Note that actuators can be limited in amplitude and rate, with all control actuation devices limited in both energy and power. Examples include: amplifiers, which may be constrained to produce outputs in the range of 0-10 V or 0-20 mA, flow valves, which cannot be opened more than 100%, and motor-driven actuators, which have limited speeds and torques. On the other hand, *output* or *state variable* constraints arise from operational limits imposed on the plant variables. Importantly, operational limits are usually related to efficiency, safety and other concerns. Examples include: environmental regulation agencies imposing strict safety limits in noise pollution or emission of pollutants. Evidently, actuator saturation and operational limits are inherent system features and as such, must be must be taken into account in any control system that aims to be practical and reliable.

3. Importance of uncertainty and constraint consideration

The importance of considering model uncertainty and system constraints in the control problem can be evaluated with regards to its practical and intellectual merit.

a. Practical merit

Moderns systems are designed and required to operate efficiently and cost effectively under safety regulations. This requires increasing demand on the throughput of the system and its subsystems. The extent to which the effect of constraints needs to be considered in the control design process depends on the required control system performance in relation to the capacity of the actuators and operational limits, as well as the level of expected disturbances, noise and uncertainty. Although in some

applications it might be possible to ignore these effects, the reliable operation and acceptable performance of most control systems must be assessed in the light of actuator saturation and operational limits. Notably, saturation can cause performance degradation (excessive overshoot and oscillation) and stability problems (limit cycles and instability), which can lead to catastrophic system failure. It has been reported that Chernobyl disaster was due to such an actuator saturation [1]. Saturation is also present in flight control, especially in high-performance aircraft, where catastrophic outcomes have resulted in the case of statically unstable aircraft (conditionally stable systems) [1, 2, 3]. Rate saturation has also been implicated in the YF-22 crash early in 1992 [4] and possibly in the JAS 39 crash of 1993 [5], both of which also experienced serious pilot-induced oscillations (PIO). Furthermore, on the output constraints side, there also exist dramatic examples. The 1984 Bhopal tragedy in India caused by the release of the highly toxic gas methyl isocyanate (MIC) from the Union Carbide Plant [6].

b. Intellectual merit

The practical importance of managing constraints in control system design has inspired long and increasing research interests in the control community [7]. However, despite the fact that for linear systems the effect of plant model uncertainty on controller performance has been reasonably well understood [8], a similar understanding has not been achieved for the case of systems subject to constraints. The presence of both uncertainty and constraints generally affects the behavior of the system in a dramatic way. Therefore, stability and performance analysis accounting for the effect of both uncertainty and constraints simultaneously is crucial for the control design. Some attempts in this regard have recently been done, but with a conservative description of the model uncertainty.

4. Motivating real problem

An inherent motivation for study of the problem of systems with uncertainty and constraints stems from its practical and theoretical importance, as previously detailed. However, an additional motivation arises from the existence of a suitable experimental testbed at the Dynamic Systems and Control Lab, Texas A&M University. This testbed, a multidimensional positioning system, presents a real-world application scenario that permits the study of the effects of constraints on multivariable systems with uncertainty. This system is useful to study the following issues within the setting of multivariable systems: rate/amplitude saturation, operational limitations, uncertainty, marginally stable systems, convexity, conservatism and decentralized control, among others. In this dissertation, the issues of saturation, operational limits and uncertainty are of principal concern and the MPS is an ideal testbed for the contributions in these areas.

B. Remedial compensation strategies for systems subject to uncertainty and constraints: literature review

The extensive literature on the effects of constraints in application areas such as aerospace, chemical, and mechanical engineering emphasizes the broad technological concern for this problem. As such, many researchers have sought to address problems associated with their presence from a number of perspectives, including:

- Synthesizing controllers which *a priori* directly account for the system constraints [9, 10, 11, 12];

- Model predictive control strategies, where the constraints are incorporated into the resulting optimization procedure [13]; and

• **Remedial compensation strategies**: *Anti-windup* and *override* compensation, techniques that are commonly employed in cases where the desire is to handle the effect of constraints that appear occasionally, and where the basic tenet is a two-step controller design paradigm: first, design the linear (unconstrained) controller ignoring constraints in the system, and second, add anti-windup and/or override compensation to minimize the adverse effect of any constraint on the closed-loop system stability and performance. Interestingly, the behavior of the feedback system with anti-windup and/or override compensation must match the initial unconstrained closed-loop system behavior in the absence of input and/or output constraints.

The anti-windup and override augmentation approaches are the most established, having an intuitive interpretation and requiring the least change in the linear control design, the latter providing them with the distinct advantage of being able to be readily retrofitted to existing systems. Importantly, anti-windup control has been used to deal with input constraints[2] whereas override control has been employed for handling output constraints.

Increasing attention has been given to both robust and constrained control problems, yet independently, within the control community. Herein an overview of the study of systems subject to constraints is presented, where the issue of uncertainty[3] is included as the solutions proposed to the input/output constrained control problems are listed. Compared to anti-windup, override control has not been as extensively studied. Therefore, the main focus of the following literature survey is on anti-windup

[2]Note that in the mode selection scheme (e.g. Min-Max-selectors), a switching nonlinearity is introduced at the plant input to select between a group of controllers designed to achieve specific objectives. Hence, in essence, this type of problem can be addressed as an input constraint problem.

[3]Good references on robust control theory are [8, 14].

control, which can handle the input nonlinearities introduced by both the saturation limits and the mode selection schemes.

For anti-windup compensation, the review is organized in terms of the framework employed (architecture and goal), stability and performance analysis, and synthesis approach.

1. Anti-windup compensation

One can easily visualize the effects of actuator saturation in control systems by the significant deterioration in control system performance and by the stability problems. These effects are known as windup effects. The study of windup effects evolved to a formal interpretation of the windup phenomenon as any inconsistency between the unconstrained controller output and the unconstrained controller states when the control signal saturates. Notably, controllers with slow or unstable dynamics are prone to experience windup problems [15]. As such, the first windup effects were observed in PI/PID controllers [16]. Given the windup effects and its formal interpretation, numerous researchers have proposed **anti**-windup techniques to overcome the problem, each one tackling different issues involved. Anti-windup techniques developed before the early 90's were unified [17, 18] in an attempt to formalize the anti-windup control problem and advance to a more systematic theory. Kothare *et al.* [17] pointed out significant weaknesses in the earlier techniques, such as lack of rigorous stability analysis, no robustness consideration, no general extension to MIMO systems, and no clear exposition of performance objectives. Only in the last decade has the anti-windup problem been addressed in a more formal way, with stability guarantees and clear performance specifications, [19, 20, 21].

a. Anti-windup compensation architecture

Many control configurations have been proposed for anti-windup compensation [17, 19, 21, 22, 23, 24, 25, 26, 27, 28]. This presents a potential problem for the anti-windup control system designer, in that it is often difficult to determine the appropriate configuration and what effect, if any, this choice has on the achievement of the design objectives. This issue was addressed by Kothare *et al.* [17] for *static* anti-windup control, where a general framework that unified all known static anti-windup compensation configurations up to that time was presented. The unification was based on a coprime factorization of the unconstrained controller and showed how a framework that captured the two-step controller design paradigm employed two static gain matrices to enforce a variety of control configurations. While uncertainty was not explicitly considered in the work, the unification also holds for systems with uncertainty. This seminal work was advanced by Miyamoto and Vinnicombe [23], where a *dynamic* version of the Kothare's coprime factorization representation was presented using a Q parameter. However, their work omitted the specific form of the Q parameterization for implementation. Importantly, no direct relation of Kothare and Miyamoto's works to more recent configurations is present in the literature. Hence, dealing with these issues remains as an open problem.

Considering previous works, it could appear that all configurations are essentially equivalent and hence the chosen configuration has no inherent effect on the synthesis problem. However, for synthesis purposes, the configurations employed do seem to be of importance. Before presenting relevant distinctions between configurations employed for synthesis, one issue has yet to be solved: the objective of an anti-windup design. The anti-windup compensation goal was initially subjective but has gradually evolved to be: *to preserve the performance of the anti-windup closed-loop system*

in the unsaturated operating range if the system never saturates, while guaranteeing global stability and minimizing the degradation of anti-windup closed-loop system performance whenever saturation is present. The difference (mismatch) system describing the difference between the anti-windup closed-loop system response and the unconstrained closed-loop system response, and having the anti-windup compensator to modify its properties, arises as the ideal setting for analysis and design. With this in mind, the anti-windup configuration proposed by Weston and Postlethwaite [26] for nominal systems was extended by Turner *et al.* [29] for use in the solution of the dynamic robust anti-windup control problem. Aside from the limitation to unstructured uncertainty, this approach has several problems, such as the complicated mismatch structure employed and the subsequent inability to directly enforce robust performance in the design. Grimm *et al.* [30] employed an anti-windup configuration which proved to be effective in accommodating unstructured (nonlinear) uncertainty for static and dynamic anti-windup compensation when placed in a certain mismatch structure. Teel and Kapoor [19] also implicitly proposed a mismatch structure for dynamic anti-windup compensation by including a model of the nominal plant dynamics in the feedback path of the anti-windup controller. Furthermore, an implicit mismatch structure also appeared in the work of Wu and Jayasuriya [31] where they employed the generic anti-windup configuration defined in Edwards and Postlethwaite [24] for dynamic anti-windup compensation. Other mismatch structures were also effectively described by Horowitz [22] and Miyamoto [23]. Considering these anti-windup compensation configurations for static and dynamic, robust anti-windup compensation, it is not clear what the relative advantages and disadvantages are when employed for synthesis. Comparing Turner [28] and Grimm [30] works it could appear that there are inherent advantages of some configurations over others, while other configurations appear to be equivalent. Therefore, resolving this issue is of importance.

For completeness of the literature review, the choice of performance metric ($\mathcal{L}_p$) can also be considered within the anti-windup configuration setting. Notably, only recently has the importance of the performance metric been emphasized in anti-windup control. The original approach was to consider an $\mathcal{L}_2$ gain (i.e, $\mathcal{H}_\infty$) of certain closed-loop transfer functions [21, 20, 19]. However, lately it has been demonstrated that this can be ineffective as a performance metric [30]. Rather a regional $\mathcal{L}_2$ gain may be more suitable [32]. Note that a regional $\mathcal{L}_2$ gain has to be used for non-exponentially stable plants as a global finite $\mathcal{L}_2$ gain cannot be achieved for such systems by bounded control. The advantages of employing this regional gain, when one is working with exponentially stable systems, is that, by addressing the exogenous input dependence, tighter quantification of performance is provided and hence relative optimization of the anti-windup closed-loop system performance becomes possible.

b. Anti-windup compensation stability and performance analysis

With the incorporation of constraints in the system design, special care must be taken when analyzing stability, as the feedback loop is no longer linear. The elements of the unconstrained closed-loop system remain linear, even the anti-windup controller to be designed is linear, but also a saturation nonlinearity is present. Importantly, a system like this can be considered within the Lure's Problem setting. Hence the first attempts to analyze (anti-)windup control system stability by the direct application of the Popov [33] and Circle [34] criteria. Other methods reported include the scaled small gain theorem [35], the describing function analysis [36], the incremental gain analysis [37], and the invariant subspace technique [38]. Following their unification work for AW configurations, Kothare *et al.* [18] presented a general framework for analyzing stability of anti-windup bumpless transfer schemes where sufficient conditions for stability analysis provided by the passivity theorem were reduced to equivalent

linear matrix inequalities (LMI) by the use of multipliers. These multipliers preserved positivity for the different descriptions of nonlinearities studied, e.g. time varying, static or slope restricted memoryless[4]. However, none of these results can accommodate plant uncertainty. Recently, limited to SISO systems, the Circle and Popov criteria have also been employed to analyze stability with both structured and unstructured uncertainties in the linear plant [40]. In the more general MIMO setting with uncertainty, construction of LMIs guaranteeing the absolute stability for systems with unstructured uncertainty was developed [29, 30]. With this being done, it seems interesting to define a framework for analyzing stability of systems with uncertainty, as done by Kothare *et al.*[18] for the nominal plant case.

Importantly, the advantage of presenting the anti-windup control problem in terms of the mismatch system permits the analysis of stability to only be defined in the nonlinear feedback loop (with the nonlinearity being a deadzone), as pointed out by Weston and Postlethwaite [26] for the nominal plant case. It should be noted that the majority of this work on stability analysis was limited to stable systems. Exceptions include the work of Hess and Wu [41, 42] at the SISO level and Pare and Teel [43, 44] at the MIMO level. This area is beyond the scope of our work and will not be explored further.

The explicit incorporation of the performance measurement in the analysis of the anti-windup problem was given by Mulder *et al.* [20] where a Lyapunov function was found useful in order to state the stability requirements together with the performance properties. Similar ideas were followed by Grimm, Turner [21, 27, 28, 29] and others, for the case of stable plants and uncertain plants. More specifically, in these works, the

[4]Multipliers that preserve positivity for repeated single-input single-output (SISO) nonlinearities are of our interest as they relate to the case of decentralized saturation and parametric (structured) uncertainty [39].

performance measure was represented by the gain relation between two defined signals and the anti-windup design objective was to minimize this measure according to an appropriate ($\mathcal{L}_2$) metric. Notably, a framework for analysis of the of different types of performance with stability guarantees, and accommodating uncertainty, appears as a necessity.

c. Anti-windup compensation synthesis

In addition to the analysis of stability and performance, the anti-windup synthesis problem has been considered from a number of perspectives. The early work [22, 34, 36, 45, 46] utilized SISO classical techniques for the enforcement of absolute stability for the nominal plant case. A recent extension of SISO classical work is done by Wu and Jayasuriya [31] where the SISO QFT design methodology was employed for the synthesis of anti-windup controllers satisfying robust stability, non-overshooting, limit cycles and robust performance specifications. Importantly, the extension of the SISO classical tools for anti-windup control to the multivariable case has not been achieved. Extensions to MIMO systems have employed modern control techniques [20, 21, 24, 23, 28], some of which permit synthesis of control systems with consideration of uncertainty [29, 30], but typically only unstructured. Grimm *et al.* [30], revisiting the paradigm given by Mulder *et al.* [20], introduced robustness into the synthesis scheme by accounting for (nonlinear) unstructured model uncertainty. Interestingly, Turner and Postlethwaite [29] considered additive unstructured uncertainty in the plant for plant order controller synthesis, the latter with no clear definition of robustness performance. The importance of the LMI tools employed in much of this work [21, 28, 29, 30] is evident, where various stability and performance tests for the closed-loop system are formulated in an $\mathcal{L}_2$ setting as convex feasibility

problems, the latter possible to be solved employing computationally efficient solvers[5]. Notably, all of this work on LMIs for the anti-windup problem was limited to exponentially stable plants. The LMI approach has also been used for the case of unstable nominal plants [47]. No further description of the asymptotically unstable plant case will be given, as this will not be a focus of the present work. Recalling the description of the structured LTI uncertainty from robust control theory, it seems natural to define the robust anti-windup control problem with structured uncertainty considerations. Evidently, it could appear that researchers [29, 30] are implicity trying to extend the robust control methods [48, 49, 50] to saturating systems and solve the robust anti-windup compensation problem. Specifically, the ideal problem solution for the robust control problem accounting for nonlinearities described by sectors or more restrictive assumptions, in addition to block structured and unstructured, real and complex, linear uncertainty, is of interest in the present work.

2. Override compensation

The problem of designing compensators for systems with output constraints has always been linked to that of designing compensators for input constrained systems. Little literature can be found that explicitly studies the problem of output constraints. With this being the case, it is even more unlikely to find works on override compensation. Importantly, one of the most comprehensive accounts on override compensation can be found in Glattfelder *et al.* [33, 51], where an analysis of performance and stability of systems subject to output constraints is given, along with some guidelines for designing compensators. However, as in the case of previous anti-windup works,

[5]The main limitation of this LMI-based synthesis technique is that LMI constraints are not always feasible, specially in the case of static anti-windup compensation, thus leaving the linear anti-windup design problem not completely solved.

one can say that the design of compensators is not done in a systematical way and that much of the work is limited to SISO systems [51]. Building on the anti-windup compensation work, Turner and Postlethwaite [52, 53] addresses the synthesis of override compensators using LMIs and providing stability and performance guarantees. Evidently, these papers denote an advance towards systematization, with direct application to MIMO systems. All in all, much work still needs to be done. In terms of the override design objective, the authors in Turner and Postlethwaite [52, 53] propose to measure the performance of the system by considering how much the actual output deviates from the ideal limited output. The ideal limited output they consider corresponds to the saturated version of the override system response. Notably, one can argue that the most desirable response is the saturated version of the linear closed-loop system output response. Furthermore, in an attempt to preserve the linear behavior as much as possible, the authors choose an extra minimization problem, the reduction of the override compensator output such that the effect of override compensation on closed-loop is minimized. Again, this selection may address indirectly the objective of preserving the linear responses but does not employ the actual objectives, namely the output responses of the system. In terms of the controller synthesis, the work in Turner and Postlethwaite [52, 53] only furnishes static override compensation and, from the anti-windup literature, it is known that the main drawback of static compensation is that the LMI constraints may be infeasible.

The anti-windup literature provides valuable results that can easily be extended to the override compensation problem [54]. The engineering community is awaiting systematic and efficient algorithms for override compensator synthesis, with guarantees of existence of solutions. In that regard, providing advances on systematization of the override compensation problem is also an interest in the present work.

C. Contribution of dissertation

Control design for linear plants with constraints is not an easy task. The presence of both constraints and uncertainty produces a challenging control problem. The main goal of this dissertation is to provide a degree of simplicity in several aspects of the remedial compensation problem, which is intriguing given the amount of remedial compensation schemes that continuously appear. In order to reach this goal, the following projects have been completed, each one amounting to a contribution of this dissertation, and described in the following paragraphs.

One level of simplicity occurs in the structure of the remedial compensation schemes. As a first contribution, this dissertation contributes to the remedial compensation problem by providing a clear theoretical system interpretation with a fundamental structure. Based on this fundamental structure, the remedial control problem can be defined to include the variety of interaction patterns between the unconstrained closed-loop system and the remedial compensator. Once the remedial compensation problem is redefined, we contribute with extending an abstract framework that facilitated the unification of all existing static anti-windup compensation schemes [17] to cope also with *dynamic* anti-windup compensation. Moreover, another abstract framework is defined that facilitates unification of all existing and potential *static* and *dynamic* override compensation schemes. The unifying framework is what we call the conditioning of the controller, for anti-windup compensation, and conditioning of the plant, for override compensation. In particular, this conditioning provides with a description of the remedial compensation problem in terms of the parameters (H_1, H_2, Q). Hence, these parameters can now determine the freedom one possesses during the control synthesis process. Building on this unification and on the performance objectives, we contribute with depicting a difference (mismatch)

system describing the effect of the saturation nonlinearity on the system response. The unification of remedial schemes, under the difference system, offers insight into the difficulties faced when employing specific remedial structures and facilitates improved transparency in remedial control system design. In particular, the effect of plant uncertainty on the achievement of the remedial performance objectives can be analyzed in this mismatch setting. From this analysis, we contribute to the robust remedial compensation problem and specially to W&P anti-windup configuration [26] by showing that any compensation scheme based on a model of the plant and hence implicitly relying on a pole-zero cancelation is prone to fail if some hidden cancelation of unstable poles occurs.

Before exploring a source of simplicity in the remedial compensation design, a second contribution of this dissertation is to consider the mismatch system in order to define the robust remedial compensation synthesis problem in this setting. We contribute to the anti-windup synthesis problem by redefining the performance objective and extending the static/dynamic full-authority and external feedback augmentations to incorporate structured (parametric) plant uncertainty. We contribute to the override synthesis problem by providing systematization to the synthesis process. By further exploring similitudes with the anti-windup synthesis method, we show that a static or (plant-order) dynamic override compensator can be constructed by solving only convex LMIs. Notably, for each case, static and dynamic, robust override compensation synthesis schemes are considered.

Another level of simplicity in remedial compensation can be found in the design area. A third contribution to the remedial compensation problem is to provide robust anti-windup compensation synthesis algorithms based on the fundamental structure and show that existing anti-windup compensation schemes arise as special cases. Similar conclusions could also be obtained for the override compensation synthesis

problem.

One important aspect of the contributions consists of the demonstration of the efficacy of the emerging methodologies. Hence, a fourth contribution is that of validating the research developments in practical applications via simulations.

D. Notation

The notation employed in this dissertation is standard throughout.

$\mathbb{R}$ is the set of real numbers. Given a matrix A, A^T denotes its transpose, A^{-1} denotes its inverse (if it exists), $\det(A)$ its determinant, $\mathrm{Im}(A)$ its image space, $\mathrm{Ker}(A)$ its null space, $\mathrm{rank}(A)$ its rank and $\mathrm{He}\, A = A^T + A$. The matrix inequality $A > B$ ($A \geq B$) means that A and B are square Hermitian matrices and $A - B$ is positive (semi-) definite. Furthermore, $\mathrm{diag}[a_1, .., a_n]$ denotes a $n \times n$ diagonal matrix with a_i as its $i-$th diagonal element.

Given a signal $u(t)$, $t \geq 0$, its $\mathcal{L}_2$ norm is defined as $\|u(\cdot)\|_2 = \sqrt{\int_0^\infty |u(t)|^2 dt}$, whenever the integral on the right hand side converges to a finite value. Moreover, defining $\mathcal{L}_2$ as the space of signals with finite $\mathcal{L}_2$ norm, whenever a signal $s(\cdot)$ has finite $\mathcal{L}_2$ norm, we say that $s(\cdot)$ belongs to the space $\mathcal{L}_2$, namely $s(\cdot) \in \mathcal{L}_2$. $\|\mathcal{U}\|_{\mathcal{L}_2 \mapsto \mathcal{L}_2}$ denotes the induced $\mathcal{L}_2$ norm of a possibly nonlinear operator $\mathcal{U} : \mathbb{U}_1 \mapsto \mathbb{U}_2$ from one Lebesgue space to another. The distance between a vector $u \in \mathbb{R}^{n_u}$ and a compact set, $\mathcal{U}$, is denoted $\mathrm{dist}(u, \mathcal{U}) = \inf_{w \in \mathcal{U}} \|u - w\|$. $\mathcal{RH}_\infty$ denotes the set of all real rational transfer function matrices, analytic in the closed right-half complex plane.

A state space representation of a transfer function matrix is denoted by:

$$G(s) = \left[\begin{array}{c|c} A & B \\ \hline C & D \end{array}\right].$$

The term $\tilde{n}_\S$ denotes the order of the system $\S$. Additionally, unless a distinction

needs to be made, the same symbol will be used to denote a time domain signal and its Laplace transform.

CHAPTER II

REMEDIAL COMPENSATION STRATEGIES: GENERAL ARCHITECTURE, GOAL AND MISMATCH SYSTEM

This chapter presents the architecture on which the remedial strategies for constrained control are based. Moreover, the large signal performance goal is described, together with an structure suitable for the achievement of this goal.

A. Definitions

The Introduction, it has been identified some of catastrophic, consequences of having limited actuation and/or not imposing limitations on the performance output. This section of the dissertation is used to make a precise mathematical definition of the actuation and performance output limitation notions.

1. Saturation nonlinearity

In the case of actuator saturation, a control system commands an actuator to produce a determined outcome, but with this outcome limited to lie within a restricted range due to the physical nature of the actuator (e.g. finite capacity of the valve, compressor, pump, etc.). The latter may even further constrain the rate of change of the actuator's outcome. This limited operating range of the actuator's rate and amplitude can be represented by a function that maps the actuator's input (output of the linear controller) into a range of capabilities according to the function illustrated in Fig. 1, which is usually referred to as the *saturation function or nonlinearity*.

On the other hand, the case of a limited performance output may arise because a certain process output may be required to lie between prespecified limits. Different from the case of actuator saturation that is a inherently property of all control

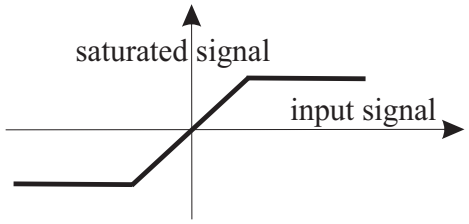

Fig. 1. Input/output representation of saturation phenomenon.

systems, limited performance output is a design requirement that must be taken into account due to stringent product specifications, safety limits or environmental regulations. Having to constrain the outcome of a process corresponds to setting the system performance output to lie within a specified (restricted) range. The *saturation function or nonlinearity* depicted in Fig. 1 can also be used to map the system performance output to the desired limited range of outcomes.

Throughout the whole manuscript, the block diagram in Fig. 2 will be employed to represent the input signal $u(t)$ and its saturated version $\text{sat}(u(t))$. From this representation, it is evident that when the input signal $u(t)$ is less than the saturation limits the outcome of the saturation block is the same output signal $u(t)$. However when $u(t)$ becomes too large, the only possible outcome is the limited saturated version $\text{sat}(u(t))$.

Consider $\check{u}$ and $-\check{u}$ to be the maximal and minimal allowable saturation output, the saturation function[1] can be mathematically represented by:

$$\text{sat}(u) = \begin{cases} \check{u}, & \text{if } u \geq \check{u} \\ u, & \text{if } -\check{u} \leq u \leq \check{u} \\ -\check{u}, & \text{if } u \leq -\check{u}. \end{cases} \tag{2.1}$$

In the case where the input signal u is a vector representing a finite number of

[1]The saturation we have considered here is called symmetric.

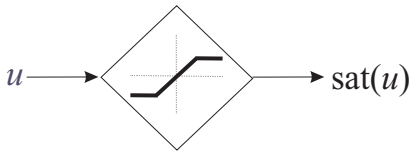

Fig. 2. A signal u and its saturated version $\text{sat}(u)$.

actuation channels or performance output variables, the vector saturation is composed by separated saturation functions at each input channel. Then, u_i denotes the i-th element of the vector u for each $i = 1, \cdot\cdot, n_u$ and the vector saturation function:

$$\phi(u) = \begin{bmatrix} \text{sat}_1(u_1) \\ \text{sat}_2(u_2) \\ \vdots \\ \text{sat}_{n_u}(u_{n_u}) \end{bmatrix}, \tag{2.2}$$

where $\text{sat}_i(\cdot)$ is defined as in Eqn. 2.1 for all i, is called a decentralized saturation.

2. The unconstrained closed-loop system

A feature of a remedial compensation strategy is to act only when the saturation nonlinearity is active, either due to actuator saturation or limited performance output. Hence, remedial control is not responsible for the behavior of the controlled system whenever the plant input or output does not saturate. This implies that an original linear design in charge of regulating the behavior of the system must exist. In fact, the behavior of this original closed-loop, which is not designed to account for saturation nonlinearities, serves as a standard for remedial control, with remedial control attempting to recover this performance output.

In Fig. 3, the closed-loop without constraints is represented in a block diagram form. The uncertain linear plant is represented by $\mathcal{P}^{\Delta}$ and the linear controller is

represented by $\mathcal{G}$. The plant has a control input $u_l \in \mathbb{R}^{n_u}$, an exogenous input $w \in \mathbb{R}^{n_w}$, a measured output $y_l \in \mathbb{R}^{n_y}$, a performance output $z_l \in \mathbb{R}^{n_z}$, an uncertainty perturbation[2] input $\eta_l \in \mathbb{R}^{n_m}$ and an uncertainty perturbation output $\zeta_l \in \mathbb{R}^{n_m}$. The controller $\mathcal{G}$ has as its inputs the measured plant output y_l and the exogenous input w. Note that the exogenous input w may contain the prefiltered reference r_f, among other inputs (e.g. disturbances).

To be consistent with existing literature, some components of the closed-loop system without saturation nonlinearities will have the following names:

Definition 2.1. For a given remedial control problem, and with the closed-loop system without saturation nonlinearities as presented in Fig. 3, we use the following notation:

- $\mathcal{G}$ is the *unconstrained controller*,
- the closed-loop system shown in Fig. 3 is the *unconstrained closed-loop system*,
- the internal state trajectory of the closed-loop shown in Fig. 3 is the *unconstrained state response* and the trajectories u_l, z_l and y_l are the *unconstrained control input response*, *unconstrained performance output response*, and the *unconstrained measured output response*, respectively. $\lhd$

An important assumption for all remedial compensation is the following:

Assumption 2.2. The unconstrained closed-loop system in Fig. 3 possess acceptable and desired robust stability and performance properties.

---

[2]To be consistent with the notation, being the plant and the controller linear, the uncertainty considered in this dissertation will also be linear.

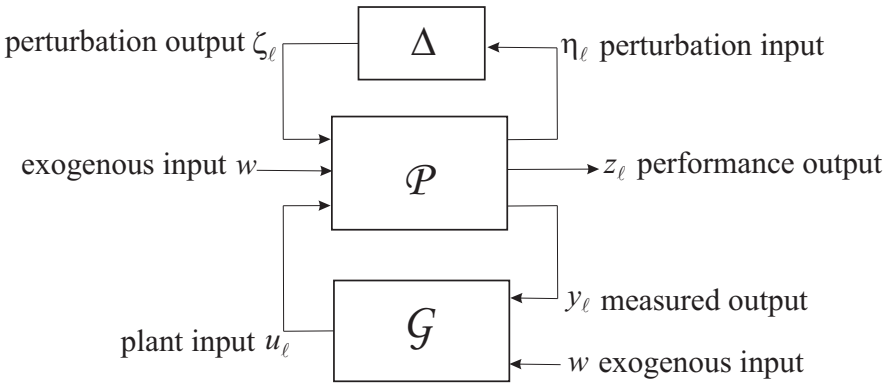

Fig. 3. Linear control design.

3. The constrained closed-loop systems

The remedial control problem arises when saturation has to be incorporated either in the control input path or in the output performance path for the unconstrained closed-loop representation in Fig. 3. Importantly, without any remedial control action, the constrained closed-loop systems are obtained. Figures 4 and 5 represent the input constrained and output constrained closed-loop systems, respectively.

Definition 2.3. For a given remedial control problem, and with the closed-loop systems with saturation nonlinearities as presented in Figs. 4 and 5, we use the following notation:

- the closed-loop system shown in Figs. 4 and 5 is the *constrained closed-loop system*,

- the internal state trajectory of the closed-loop shown in Figs. 4 and 5 is the *constrained state response* and the trajectories u_c, z_c and y_c are the *constrained control input response*, *constrained performance output response*, and the *constrained measured output response*, respectively. $\lhd$

Remark 2.4. For the output constrained control problem, the unconstrained and

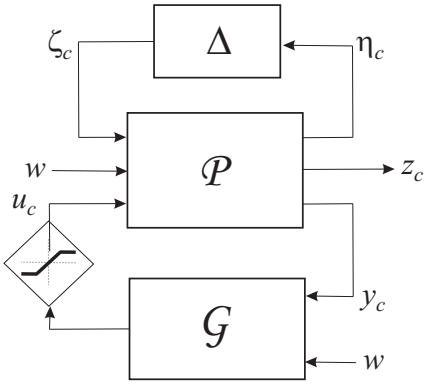

Fig. 4. Input constrained closed-loop system. Real process.

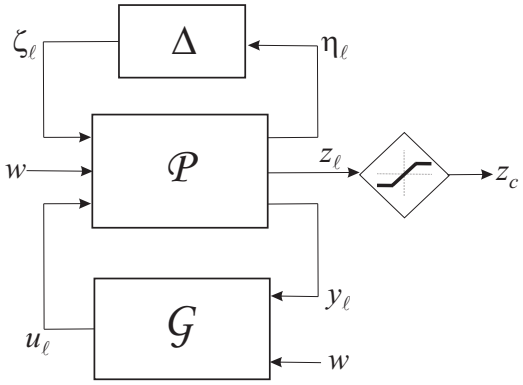

Fig. 5. Output constrained closed-loop system. Ideal process.

constrained responses coincide with the exception of the performance output response. This is the case because, as observed from Fig. 5, the saturation nonlinearity does not affect the feedback loop in the unconstrained closed-loop system. ◁

4. The remedial compensation augmented closed-loop system

The remedial strategies for the constrained control problem can be divided in two. One of them, termed *anti-windup compensation*, which will enter into action when there are input constraints, i.e. actuator rate and amplitude saturation. The other, termed *override compensation*, will play a role only when the output is constrained, i.e. the performance output is required to lie within a limited range.

Figures 6 and 7 present compensation architectures for anti-windup and override control, respectively. The architectures employed in the two remedial strategies are similar in their working principle: the activation of the remedial control action relies on the activation of the saturation nonlinearity. The blocks Λ and Θ represent possibly dynamic and linear systems. For these two compensation architectures for remedial control, additional terminology needs to be defined.

Definition 2.5. With respect to Figs. 6 and 7, we use the following notation:

• the system $\mathcal{R}$ represent either the Λ or Θ systems and is the *remedial compensator*,

• the system $\mathcal{G}_{\mathcal{M}}$ is the *modified unconstrained controller*,

• the closed-loop in Figs. 6 and 7 are the *remedial augmented closed-loop system*, and

• the internal state trajectory of the closed-loop in Figs. 6 and 7 is the *remedial augmented state response*; the trajectories u, z and y are the *remedial augmented control input response*, *remedial augmented performance output response*, and the *remedial augmented measured output response*, respectively. $\lhd$

a. The anti-windup augmented closed-loop system

Definition 2.6. With respect to Fig. 6, we use the following notation:

• the system Λ is the *anti-windup compensator*,

• the system $\mathcal{G}_{\mathcal{M}}$ is the *modified unconstrained controller*,

• the closed-loop in Fig. 6 is the *anti-windup augmented closed-loop system*, and

• the internal state trajectory of the closed-loop is the *anti-windup augmented state response*; the trajectories u, z and y are the *anti-windup augmented control input response*, *anti-windup augmented performance output response*, and the *anti-windup augmented measured output response*, respectively. $\lhd$

b. The override augmented closed-loop system

Definition 2.7. With respect to Fig. 7, we use the following notation:

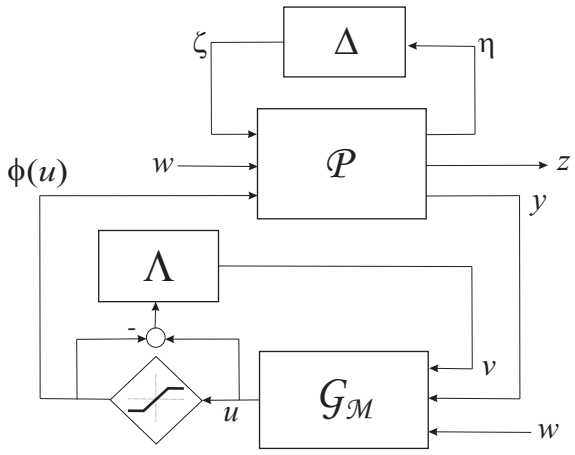

Fig. 6. Anti-windup augmented closed-loop system.

- the system Θ is the *override compensator*,
- the system $\mathcal{G}_{\mathcal{M}}$ is the *modified unconstrained controller*,
- the closed-loop in Fig. 7 is the *override augmented closed-loop system*, and
- the internal state trajectory of the closed-loop is the *override augmented state response*; the trajectories u, z and y are the *override augmented control input response*, *override augmented performance output response*, and the *override augmented measured output response*, respectively. $\lhd$

B. General architecture for remedial compensation

The augmented architectures for remedial control may have to consider certain restrictions in terms of the available connections between the remedial compensator and the unconstrained controller[3]. For example, it may be a possibility that the remedial compensator senses $\text{sat}(u) - u$, or $\text{sat}(z) - z$, but only acts on the output

[3]The introduction of these connections needs an appropriate modification of the unconstrained controller dynamics to allow for the remedial compensator outputs.

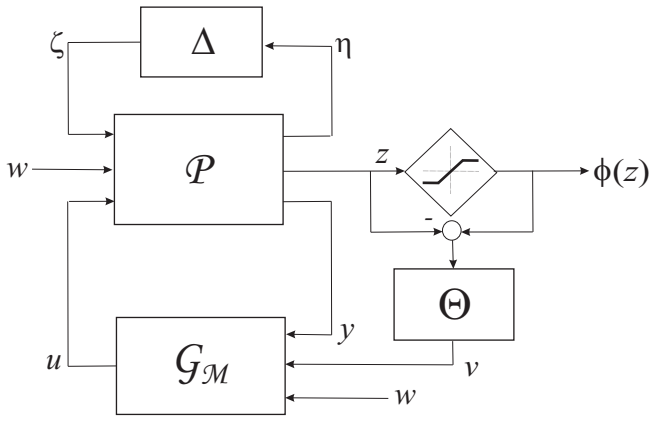

Fig. 7. Override augmented closed-loop system.

of the unconstrained controller. Note, however, that the remedial compensation can not only act on the output of the unconstrained controller but also on the input or internal states of the unconstrained controller. Hence, depending on where the remedial compensator affects the unconstrained controller, it is possible to define a variety of remedial control configurations (external structure) and corresponding functional relations (internal structure). Anti-windup control shows that this variety of configurations sometimes may be a problem, as given the freedom of the anti-windup compensator and unconstrained controller interconnection, many control configurations have been proposed for the anti-windup control (see Introduction). Notably, this presents a potential problem for the anti-windup control system designer as the designer has to choose one configuration for the design[4]. With this in mind, a formal classification of the variety of configurations is performed by defining the *general configuration for remedial control*.

[4]In some cases, the implementation of the remedial compensator, e.g. control systems with analog controllers, does not provide much freedom in selecting configurations

1. External structure of remedial compensation: general configuration

The general configuration for remedial control, as stated by the name, is a generalization of the type of interaction that the block representing the remedial compensator has with the rest of the remedial augmented closed-loop system, see Figs. 6 and 7. In order to define the general configuration, the two structural properties of the remedial compensator are going to be analyzed, being, the selection of the inputs of $\mathcal{R}$ and the selection of the locations where the outputs of $\mathcal{R}$ are injected.

a. Remedial compensator inputs

Figures 6 and 7 show that the input to the remedial compensator is the difference between the saturation nonlinearity input and output, $\text{sat}(u) - u$ or $\text{sat}(z) - z$. Nevertheless, in general, this may not be the case. The remedial compensator could also receive information provided by the unconstrained controller, or even information coming directly from the plant. Keeping in mind that remedial control idea is to act only when the saturation nonlinearities become active, for the remainder of the dissertation, the only input to the remedial compensator $\mathcal{R}$ will be $\text{sat}(u) - u$ or $\text{sat}(z) - z$, as appropriate from the remedial control type considered. This is the ideal selection because, thanks to the linearity of the remedial compensator, for zero initial conditions, the local behavior of the remedial closed-loop system coincides with behavior of the unconstrained closed-loop system.

b. Remedial compensator outputs

From Figs. 6 and 7, the outputs of the remedial compensator act directly on the unconstrained controller. Hence, in order to have a precise characterization of the general configuration for remedial control, the full dynamic equations of the uncon-

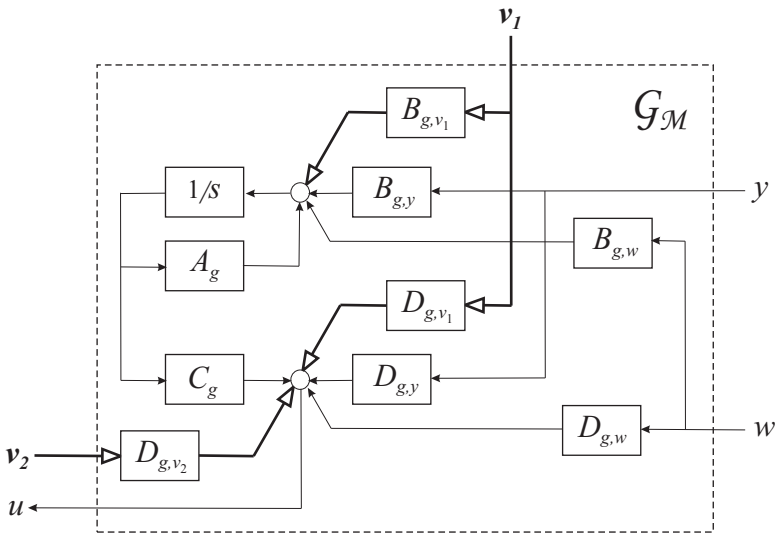

Fig. 8. The remedial compensator output signals in general configuration for remedial control.

strained controller emphasizing the points of injection of the remedial compensator outputs are written below. The unconstrained controller, modified to allow for remedial control outputs, is termed modified unconstrained controller and may be defined as:

$$\mathcal{G}_{\mathcal{M}} = \begin{bmatrix} \mathcal{G}_w & \mathcal{G}_y & \mathcal{G}_v \end{bmatrix} \begin{cases} \dot{x}_g = A_g x_g + B_{g,w} w + B_{g,y} y + B_{g,v_1} v_1 \\ u = C_g x_g + D_{g,w} w + D_{g,y} y + D_{g,v_1} v_1 + D_{g,v_2} v_2 \end{cases}, \quad (2.3)$$

where v_1 and v_2 are the remedial compensator outputs. Importantly, the exact locations where these outputs are injected can be specified by the blocks B_{g,v_1}, D_{g,v_1} and D_{g,v_2} of Fig. 8. There are a variety of possible interactions that can be described with these blocks, each one corresponding to a particular authority allowed to the remedial compensator. Consequently, this representation gives generality to the remedial augmented closed-loop system presented in Figs. 6 and 7. For example, the external anti-windup compensation [27] corresponds to $B_{g,v_1} = B_{g,y}$, $D_{g,v_1} = D_{g,y}$ and $D_{g,v_2} = I_{n_u}$. See Section II.B for the recovery of other existing configurations.

2. Internal structure of remedial compensation

Once the external structure of remedial control has been specified, i.e. the inputs and outputs of the remedial compensator are fixed, the (internal) functional relation between such inputs and outputs has to be determined. The following classification of internal structures, starting form the least complicated, will be useful to provide clarity throughout this dissertation. In the following, consistent with the previous section, we assume for simplicity that the only input to the remedial compensator block is $\text{sat}(u) - u$, for anti-windup control, and $\text{sat}(z) - z$, for override control, and that its two outputs are denoted by v_1 and v_2.

The two internal structures presented below correspond to the anti-windup compensation case when substituting $\mathcal{R}$ and r by Λ and u respectively, and to the override control case when substituting $\mathcal{R}$ and r by Θ and z respectively.

a. Static linear remedial compensation

This compensation class constitutes the simplest remedial scheme. This corresponds to having the following static gain implemented in the remedial block:

$$\mathcal{R} = \begin{bmatrix} \mathcal{R}_1 \\ \mathcal{R}_2 \end{bmatrix} \quad \begin{cases} v_1 = & D_{\mathcal{R}_1}(\text{sat}(r) - r) \\ v_2 = & D_{\mathcal{R}_2}(\text{sat}(r) - r) \end{cases}, \tag{2.4}$$

where $D_{\mathcal{R}_1}$ and $D_{\mathcal{R}_2}$ are linear gains or matrices which need to be chosen according to suitable procedures. This static structure for remedial control looks very appealing because of its simplicity. However, Grimm *et al.* [21] shows that in some cases this selection cannot be carried out in a constructive way. Under this situation a more complex structure is necessary.

b. Dynamic linear anti-windup compensation

Dynamic remedial compensation arises naturally as the extension of the static case allowing for the inclusion of dynamics. Mathematically, this inclusion of dynamics can be represented as:

$$\mathcal{R} = \begin{bmatrix} \mathcal{R}_1 \\ \mathcal{R}_2 \end{bmatrix} \quad \begin{cases} \dot{x}_{\mathcal{R}} = & A_{\mathcal{R}} x_{\mathcal{R}} + B_{\mathcal{R}}(\text{sat}(r) - r) \\ v_1 = & C_{\mathcal{R}_1} x_{\mathcal{R}} + D_{\mathcal{R}_1}(\text{sat}(r) - r) \\ v_2 = & C_{\mathcal{R}_2} x_{\mathcal{R}} + D_{\mathcal{R}_2}(\text{sat}(r) - r) \end{cases}, \tag{2.5}$$

where the state $x_{\mathcal{R}} \in \mathbb{R}^{n_{\mathcal{R}}}$, i.e. $n_{\mathcal{R}} \geq 0$. Evidently, when $n_{\mathcal{R}} = 0$, this zero-order remedial anti-windup compensation corresponds to the static case. In all other cases, when $n_{\mathcal{R}} > 0$, the matrices $A_{\mathcal{R}}$, $B_{\mathcal{R}}$, $C_{\mathcal{R}_1}$ and $C_{\mathcal{R}_2}$ constitute additional variables to be chosen when designing the remedial compensator. Importantly, these additional variables constitute extra degrees of freedom in the remedial compensation selection. Therefore, as compared to static remedial compensation, dynamic remedial compensator suitable solves a wider range of remedial problems. The case when the state $x_{\mathcal{R}}$ has the same size as the state of the plant will be called *plant order remedial compensation*. This case will be specially important in Chapters V and VI where it can be shown that setting the remedial compensator to be plant order allows for convenient remedial compensation constructions that are useful for a wide class of systems.

C. Characterizing remedial compensation goals

In the previous sections we have characterized different families of remedial compensators by presenting the general architecture for remedial compensation. Moreover, we have presented a framework that enables the unification of all known (or possible) remedial compensation schemes. In the following development of this dissertation, given a particular external and internal structure, we will provide constructive algo-

rithms for determining a remedial compensator which optimizes a certain performance measure. Hence, the aim of this section is to characterize the choice of such performance measures.

1. Basic goals of remedial compensation

a. Anti-windup compensation goals

The goal of anti-windup compensation was initially subjective, with a variety of goals proposed, all related to reducing the deleterious effects of actuator saturation on the system performance response. These goals were: to recover the unconstrained controller output response [22], to recover the unconstrained closed-loop system performance output response [29, 17, 23, 28, 30, 55] or to minimize a certain closed-loop response that is deemed appropriate to capture the performance of the unconstrained closed-loop system [20, 21]. If one recognizes that the spirit of anti-windup control is to act in order to preserve the unconstrained closed-loop response, then one can see that the unconstrained closed-loop provides the most desirable response of the system. Hence, the ultimate goal of anti-windup design can be formulated as the recovery of the unconstrained response.

Importantly, by having the real plant subject to input saturation, certain limitations to this recovery task arise. This means that not all the unconstrained trajectories can be recovered. Then, for clarity purposes, the unconstrained trajectories can be classified as *reproducible*, *tractable* and *untractable*[5] [56]. Note that reproducible trajectories correspond to plant inputs such that $\|(u_l - \mathrm{sat}(u_l))(\cdot)\|_2 = 0$ and tractable trajectories can be characterized as those plant inputs such that for any positive δ,

[5]Untractable trajectories arise when the actuators are undersize in relation to the control goal.

$\|(u_l - \mathrm{sat}_\delta(u_l))(\cdot)\|_2$ is finite. The δ-restricted saturation function, $\mathrm{sat}_\delta(\cdot)$, serves to characterize all the tractable trajectories and is defined as:

$$\mathrm{sat}_\delta u = \begin{cases} \breve{u} - \delta, & \text{if } u \geq \breve{u} - \delta \\ u, & \text{if } -\breve{u} + \delta \leq u \leq \breve{u} - \delta \\ -\breve{u} + \delta, & \text{if } u \leq -\breve{u} + \delta. \end{cases} \tag{2.6}$$

Based on this $\mathcal{L}_2$ classification, the following properties of anti-windup compensation can be formalized, as done in Grimm [56] and succinctly presented in Teel and Kapoor [19], as follows:

Property 2.8. (Small signal preservation) *The anti-windup closed-loop system is said to guarantee* small signal preservation *if all the unconstrained trajectories such that $u_l(t) = \mathrm{sat}_\delta(u_l(t))$ for all times $t \geq 0$ (namely, such that the unconstrained plant input never exceeds what would be the saturation limits) are exactly reproduced by the anti-windup closed-loop system.*

Property 2.9. (Tracking) *The anti-windup closed-loop system is said to guarantee* tracking *if for any unconstrained trajectory such that $\|(u_l - \mathrm{sat}_\delta(u_l))(\cdot)\|_2$ is finite, the corresponding anti-windup trajectory is such that $\|(z_l - z)(\cdot)\|_2$ is finite (where $z_l - z$ is the difference between the unconstrained and anti-windup augmented performance output).*

Property 2.10. (Global internal stability) *The anti-windup closed-loop system is said to be* globally BIBS stable *(bounded input implies bounded state) if for any bounded selection of external input (corresponding to an unconstrained trajectory), the resulting anti-windup augmented response is bounded.*

Property 2.11. (Local internal stability) *The anti-windup closed-loop system is said to be* locally BIBS stable *if for any bounded selection of external input w (corresponding to an unconstrained trajectory) such that $\|w\|_2 \leq b$ and $b > 0$, the resulting*

anti-windup augmented response is bounded.

In summary, the three properties of anti-windup compensation can be defined as i) preservation of the anti-windup closed-loop system's response in the unconstrained operating range if the system never saturates (*small signal preservation*), ii) guarantee of steady-state tracking[6] whenever input saturation is present and the unconstrained response is recoverable at steady state (*tracking*), and iii) guarantee of *global BIBS stability* for all the anti-windup trajectories.

b. Override compensation goals

The scope of this section is to characterize the override design objective in order to define the override compensation problem. If one recognizes that the unconstrained closed-loop response with constrained performance output provides the most desirable response of the system, then the ultimate goal of override design can be formulated as the recovery of this unconstrained response and the corresponding constrained performance output. At this point, we are able to expand on the difference between anti-windup compensation and override compensation. Anti-windup is employed to act against the detrimental effects of input saturation (already present in the real plant) whereas override is employed to force the real plant output to behave within certain limits by including a saturation nonlinearity at the performance output. On one side, we have the real plant subject to input saturation and whose effects we want to get rid of and, on the other side, we have the real plant subject to output saturation and whose effects we want to accomplish.

The output constrained problem defined in Fig. 5, whose solution is the override

[6]The tracking property ensures steady-state tracking, this is the response of the anti-windup closed-loop system converges asymptotically to the response of the unconstrained system (in an $\mathcal{L}_2$ sense) whenever the latter is recoverable at the steady state.

compensation in Fig. 7, does not consider any limitations on the actuation of the system, hence we can guarantee that all the unconstrained trajectories, including the constrained performance output, are either *reproducible* or *tractable*[7]. Similar to the anti-windup case, reproducible trajectories correspond to plant performance outputs such that $\|(z_l - \text{sat}(z_l))(\cdot)\|_2 = 0$ and tractable trajectories can be characterized as those plant performance outputs such that $\|(z_l - \text{sat}(z_l))(\cdot)\|_2$ is finite.

On the basis of these $\mathcal{L}_2$ classification of trajectories, the following properties of override compensation can be formalized, as done in Grimm [56] and succinctly presented in Teel *et al.* [19] for anti-windup compensation, as follows:

Property 2.12. (Small signal preservation) *The override closed-loop system is said to guarantee* small signal preservation *if all the unconstrained trajectories such that* $z_l(t) = \text{sat}(z_l(t))$ *for all times* $t \geq 0$ *(namely, such that the unconstrained plant output never exceeds what would be the saturation limits) are exactly reproduced by the override closed-loop system.*

Property 2.13. (Tracking) *The override closed-loop system is said to guarantee* tracking *if for any unconstrained trajectory such that* $\|(z_l - \text{sat}(z_l))(\cdot)\|_2$ *is finite, the corresponding override trajectories are such that* $\|(\text{sat}(z_l) - z)(\cdot)\|_2$ *and* $\|(y_l - y)(\cdot)\|_2$ *are finite (where* $\text{sat}(z_l) - z$ *and* $y_l - y$ *are the differences between the constrained and override augmented plant outputs).*

Property 2.14. (Global internal stability) *The override closed-loop system is said to be* globally BIBS stable *(bounded input implies bounded state) if for any bounded selection of external input (corresponding to an unconstrained trajectory), the resulting override augmented response is bounded.*

Property 2.15. (Local internal stability) *The override closed-loop system is said to*

[7]Both reproducibility and tractability characteristics are defined here with respect to the saturation nonlinearity at the plant performance output.

be locally BIBS stable *if for any bounded selection of external input w (corresponding to an unconstrained trajectory) such that $\|w\|_2 \leq b$ and $b > 0$, the resulting override augmented response is bounded.*

In summary, the three properties of override compensation can be defined as i) preservation of the override closed-loop system's response in the unconstrained operating range if the system never saturates (*small signal preservation*), ii) guarantee of steady-state tracking whenever output saturation is present and the unconstrained response is recoverable at steady state (*tracking*), and iii) guarantee of *global BIBS stability* for all the override trajectories.

c. Basic goals

The combination of the three properties listed above, for both anti-windup compensation and override compensation, will define the main objectives of remedial augmentation. For the rest of the dissertation, these three properties will be called *basic goals*, according to the definition below.

Property 2.16. (The global basic properties) The *remedial closed-loop system is said to guarantee the* global basic properties *if*

1. *it is well-posed (i.e. all the signals are well-defined),*
2. *it guarantees the small signal preservation property,*
3. *it guarantees the tracking property, and*
4. *it is globally BIBS stable.* ◁

Property 2.17. (**The local basic properties**) The *remedial closed-loop system is said to guarantee the* local basic properties *if*

1. *it is well-posed (i.e. all the signals are well-defined),*

2. *it guarantees the small signal preservation property,*

3. *it guarantees the tracking property, and*

4. *it is locally BIBS stable.* ◁

2. Performance measures for remedial compensation

The basic properties of a remedial closed-loop system, presented in the preceding section, provide for global BIBS stability (limited to stable plants) or local BIBS stability (applicable to unstable plants) but considering only qualitative performance. To define the design problem, a suitable performance measure can be chosen *quantifying* the difference in performance response and a remedial compensator designed to optimize/modify this measure.

a. Anti-windup compensation

A variety of performance measures can be selected for anti-windup design, each one of them related to a specific anti-windup objective. Nevertheless, a careful look into the anti-windup problem reveals that the finite $\mathcal{L}_2$ gain[8] from u_l to $z_l(\cdot) - z(\cdot)$ is a natural performance measure. This takes place because, on the basis of the small signal preservation property, all anti-windup compensators that guarantee Property 2.8 will provide the same response and hence we can rule out the unconstrained closed-loop system and consider only the effect of u_l whenever it goes beyond the

[8]Other metrics have been proposed more recently, e.g. Hu *et al.* [32] proposes a nonlinear $\mathcal{L}_2$ gain that deals with the input dependence of the performance levels. This nonlinear gain helps to reduce the conservatism on the treatment of the nonlinearity and hence provide a better quantification of performance, and more importantly relative performance between designs, permitting better optimization of the anti-windup closed-loop system performance. Nevertheless, the $\mathcal{L}_2$ metric is simple to use and is therefore commonly employed.

saturation limits. Moreover, the quantification of performance will be given by the mismatch between the unconstrained output and anti-windup output. In fact, the ideal situation occurs when the anti-windup output response perfectly matches the unconstrained one. However, most of the time this is impossible and the most we can aim for is to minimize their difference. The smaller the difference the better the performance of the anti-windup closed-loop.

Mathematically, the quantification of the performance (level of performance) can be given by the smallest constant γ such that (given zero initial conditions):

$$\|z_l(\cdot) - z(\cdot)\|_2 \leq \gamma \|u_l\|_2. \tag{2.7}$$

b. Override compensation

A previously employed selection of performance measure for the override closed-loop system, in Fig. 7, was the $\mathcal{L}_2$ gain of the nonlinear system from the exogenous input w to the performance output z, when z represents an error signal. This error signal can be composed of the mismatch between the input and the output of the saturation nonlinearity in the override augmentation system, and the mismatch between the unconstrained measured output response and the corresponding override response [52]. Nevertheless, a careful look into the override problem reveals that the output constrained system in Fig. 5 presents the ideal signals for override compensation performance evaluation. Hence, considering the $\mathcal{L}_2$ gain from $\text{sat}(z_l) - z_l$ to $\text{sat}(z_l) - z$ and $y_l - y$ it is a natural performance measure.

Based on the basic properties of override control, all unconstrained responses that do not activate the saturation nonlinearity should be disregarded when evaluating the performance of an override design. This is because all override compensators guaranteeing the Property 2.12 will provide the same responses whenever saturation

is not active. Moreover, the mismatch between the output constrained responses and the override responses should be taken into account to evaluate the performance. Given that the output constrained system responses generate the target responses for the override compensation problem, the performance can be formally measured in terms of how small the deviation of the override performance output $\begin{bmatrix} z \\ y \end{bmatrix}$ from the ideal constrained performance output $\begin{bmatrix} \text{sat}(z_l) \\ y_l \end{bmatrix}$ is. The smaller this deviation is, the better the override compensation responses match the ideal constrained responses.

Mathematically, the quantification of the level of performance can be determined by the smallest constant γ, such that (given zero initial conditions):

$$\left\| \begin{bmatrix} (\text{sat}(z_l) - z)(\cdot) \\ (y_l - y)(\cdot) \end{bmatrix} \right\|_2 < \gamma \, \|(\text{sat}(z_l) - z_l)(\cdot)\|_2. \tag{2.8}$$

c. The finite unconstrained response recovery gain for remedial compensation

The following definition is given by Grimm [56] and here is restated for completeness of the presentation.

Definition 2.18. Given a positive constant γ and a decentralized saturation function $\text{sat}(\cdot)$, the remedial closed-loop system is said to have a *global finite unconstrained response recovery gain* smaller than γ if for all possible selections of the input function $w(\cdot)$, the solutions of the unconstrained (or output constrained) closed-loop system and of the remedial closed-loop system, starting with the same initial conditions in the plant and controller and zero initial conditions in the remedial compensator, satisfy the bound in Eqn. 2.7 (or 2.8). $\lhd$

Definition 2.19. Given a positive constant γ and a decentralized saturation function $\text{sat}(\cdot)$, the remedial closed-loop system is said to have a *local finite unconstrained*

response recovery gain smaller than γ if for all possible selections of the input function $w(\cdot)$ such that $\|w\|_2 \leq b$ for a positive b, the solutions of the unconstrained (or output constrained) closed-loop system and of the remedial closed-loop system, starting with the same initial conditions in the plant and controller and zero initial conditions in the remedial compensator, satisfy the bound in Eqn. 2.7 (or 2.8). $\lhd$

For the case of anti-windup compensation, a finite gain to quantify the unconstrained response recovery was also employed [30, 56]. Indeed, the performance measure employed [30, 56] enforces a finite $\mathcal{L}_2$ gain from the signal $\text{sat}_\delta(u_l) - u_l$ to the output $z - z_l$, i.e. $\|z(\cdot) - z_l(\cdot)\|_2 \leq \gamma \|\text{sat}_\delta(u_l(\cdot)) - u_l(\cdot)\|_2$. Interestingly, this quantification of performance corresponds to a strengthening of the tracking property in Definition 2.9. In following chapters, we will show why we consider our performance measure more suitable in representing the mismatch between the unconstrained output and the anti-windup output responses.

D. Setting for remedial compensation: mismatch system

An effective way to guarantee the properties of Definitions 2.16. and 2.17 is to consider the system describing the difference between the unconstrained (or output constrained) system response and the remedial system response, and modify the properties of this system using the remedial compensator. This difference system is employed herein and termed the mismatch system[9].

[9]This definition is consistent with Grimm *et al.* [30]. It should however be noted that this mismatch system has been considered by previous researchers in anti-windup compensation, both implicitly [19, 22, 23, 24, 25, 31], and explicitly [26, 28].

1. Anti-windup compensation

a. Amplitude saturation

Figure 9 is equivalent to Fig. 6 and shows a cascade connection of the unconstrained closed-loop system and the mismatch system for anti-windup compensation. In particular, the mismatch system $\mathcal{W}^{\Delta}$ in Fig. 9 is presented in an LFT representation. The detailed description of the mismatch system components is shown in Fig. 10. For this mismatch system additional terminology needs to be defined.

Definition 2.20. For a given anti-windup problem, when the closed-loop with plant input saturation has the form in Fig. 10, we use the following notation:

- the system $\mathcal{W}^{\Delta}$ is the *mismatch system for anti-windup compensation*,
- the internal state trajectory of the system $\mathcal{W}^{\Delta}$ is the *mismatch state response*; the trajectories u_d, z_d, and η_d are the *mismatch control input response*, *mismatch performance output response* and the *mismatch uncertainty perturbation response*, respectively and
- the function $\psi : \mathbb{R}^{n_u} \mapsto \mathbb{R}^{n_u}$ is defined[10] as $\psi(u) = u - \phi(u),\ \forall u \in \mathbb{R}^{n_u}$. $\lhd$

Notably, the case of *linear plant uncertainty* permits the decomposition of the mismatch system into a nonlinear feedback loop ($\psi(\cdot)$ in positive feedback with T_n^u) and a disturbance filter ($\mathcal{P}_{zu}S_n^u$) [57], as shown in Fig. 11 and defined in Eqns. 2.10 and 2.12 respectively. A graphical interpretation of this decomposition can also be given, as in Weston and Postlethwaite [26] where the closed-loop transfer functions of the mismatch system, T_n^u and $\mathcal{P}_{zu}S_n^u$, are given in terms of a parameter M for the nominal plant case. Other researchers have also employed the mismatch system for

[10] With the function $\phi(\cdot)$ corresponding to the saturation nonlinearity, the function $\psi(\cdot)$ corresponds to the deadzone nonlinearity.

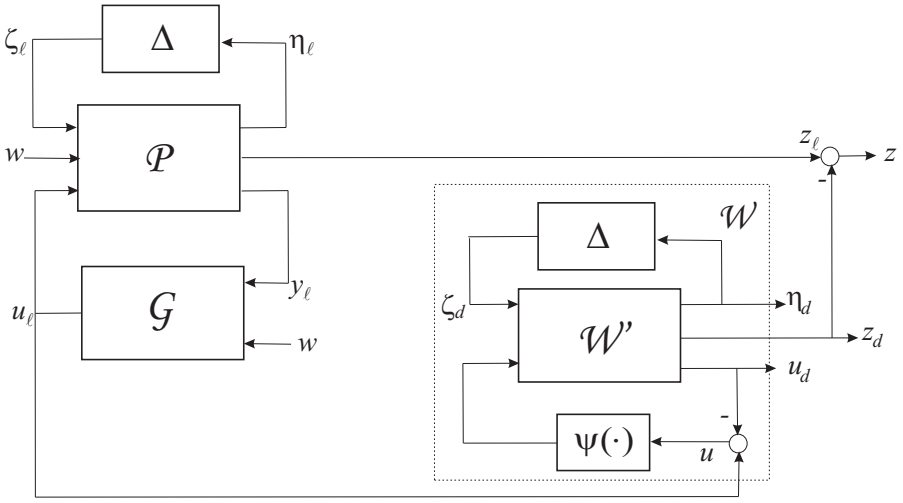

Fig. 9. Cascade interconnection of the unconstrained closed-loop system to the mismatch system for anti-windup compensation.

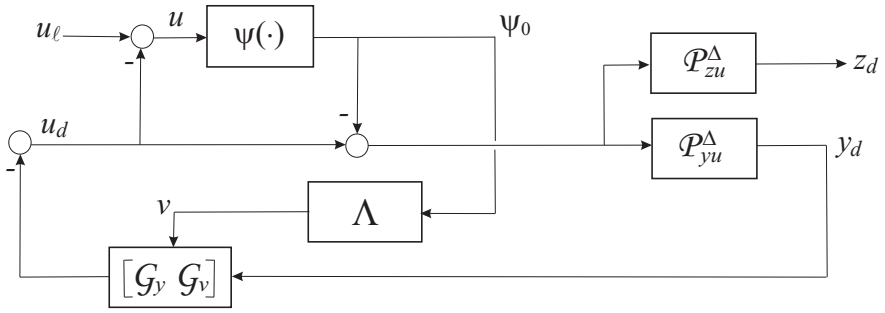

Fig. 10. Detailed representation of the mismatch system for anti-windup compensation.

synthesis [22, 23], but this was limited to an algebraic presentation and hence the geometric interpretation was not clear.

The loop transmission around the nonlinearity L_n^u [22, 25], provides a very convenient representation of the mismatch system and corresponding transfer functions. Additionally, the mismatch transfer functions can also be defined as done in Miyamoto and Vinnicombe [23], where a Q parameter and coprime factorizations, U and V, of the unconstrained controller were employed. Following, L_n^u, Q, U and V are employed to define the closed-loop transfer functions of the mismatch system. Importantly, Q,

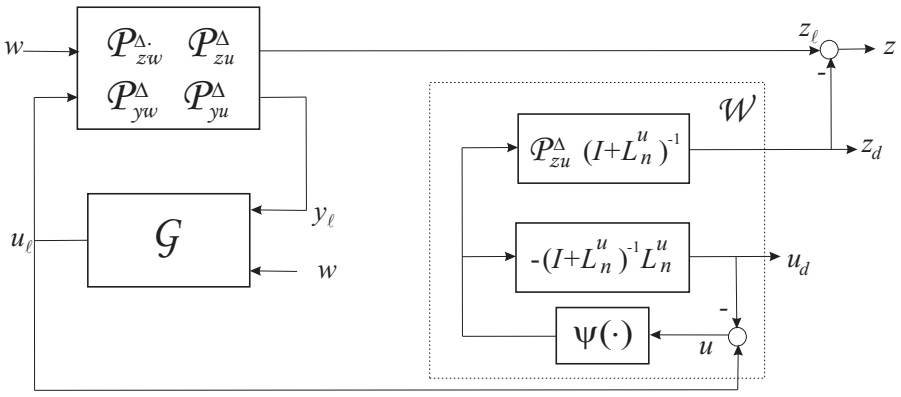

Fig. 11. Cascade interconnection. Mismatch system for anti-windup compensation (linear uncertainty case): nonlinear loop and disturbance filter.

U and V will be explicitly defined in Chapter III.

$$L^u_n = -\frac{u}{\phi(u)} = \tilde{V}(I + \mathcal{G}_y\mathcal{P}_{yu} - \tilde{V}^{-1}) = (\tilde{V} + \tilde{V}\mathcal{G}_y\mathcal{P}_{yu} - I_{n_u}) = (QV + QV\mathcal{G}_y\mathcal{P}_{yu} - I_{n_u}), \tag{2.9}$$

$$T^u_n = (I_{n_u} + L^u_n)^{-1}L^u_n = I_{n_u} - (I_{n_u} + \mathcal{G}_y\mathcal{P}_{yu})^{-1}\tilde{V}^{-1} = I_{n_u} - (I_{n_u} + \mathcal{G}_y\mathcal{P}_{yu})^{-1}V^{-1}Q^{-1}, \tag{2.10}$$

$$S^u_n = (I_{n_u} + L^u_n)^{-1} = (I_{n_u} + \mathcal{G}_y\mathcal{P}_{yu})^{-1}V^{-1}Q^{-1}, \tag{2.11}$$

$$\mathcal{P}_{zu}S^u_n = \mathcal{P}_{zu}(I_{n_u} + L^u_n)^{-1} = \mathcal{P}_{zu}(I_{n_u} + \mathcal{G}_y\mathcal{P}_{yu})^{-1}\tilde{V}^{-1} = \mathcal{P}_{zu}(I_{n_u} + \mathcal{G}_y\mathcal{P}_{yu})^{-1}V^{-1}Q^{-1}, \tag{2.12}$$

where:

$$T^u_n + S^u_n = I_{n_u}. \tag{2.13}$$

Here T^u_n, S^u_n and $\mathcal{P}_{zu}S^u_n$ can be defined as the corresponding closed-loop transfer function matrices for the mismatch system[11]. Note that Eqns. 2.10 and 2.12 are equivalent to Eqns. 3 and 5 in Miyamoto and Vinnicombe [23]. Furthermore, Eqn. 2.10 is equivalent to Eqn. 10.9 in Lurie [25], without the coprime factorizations.

[11]Note that the superscript of the plant has been dropped, and the reference to uncertain or nominal plant will be clarified whenever necessary.

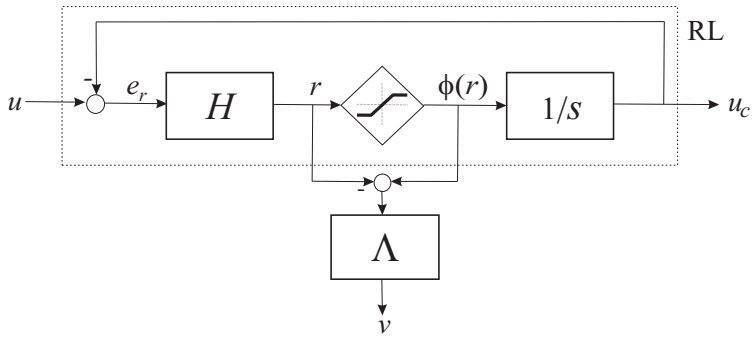

Fig. 12. Model for rate limit (RL). Interconnections for anti-windup compensation.

More recently, with the objective of recovering robustly the unconstrained response, the mismatch structure was also used in an LFT framework [30].

Remark 2.21. When the perturbation uncertainty is nonlinear, the mismatch system is affected by the exogenous input w through η_l. This, however, is not the case for linear uncertainty where the exogenous input plays no role in the definition of the mismatch system. ◁

b. Rate saturation

The rate saturation problem commonly is also important in most systems, most notably in aerospace applications, and hence its practical importance. Different from amplitude saturation, the rate saturation case has a variety of models to represent the phenomenon. Here, for analysis purposes, the rate saturating actuator with finite bandwidth model [58] will be considered. This model of rate saturation is presented in Fig. 12 as RL, where H is a gain matrix.

The anti-windup augmented closed-loop system for rate saturation consists of the construction of Fig. 6, but with the appropriate substitution of the saturation nonlinearity for the rate limit model RL presented in Fig. 12. Note the correspondence among the signals u, u_c and v for the interconnection. The two seemingly different ar-

chitectures for amplitude and rate saturation anti-windup compensation can be made equivalent by conveniently absorbing the rate limit dynamics and the integrator into the plant and unconstrained controller, respectively. Then, by redefining the plant and unconstrained controller as:

$$\begin{bmatrix} \mathcal{P}^r_{yu} \\ \mathcal{P}^r_{yu} \end{bmatrix} = \begin{bmatrix} \mathcal{P}_{yu}\frac{1}{s} \\ \mathcal{P}_{zu}\frac{1}{s} \end{bmatrix}, \tag{2.14}$$

$$\mathcal{G}^r_y = (I_{n_u} + H\frac{1}{s})^{-1}H\mathcal{G}_y, \tag{2.15}$$

we are able to find a mismatch representation, of the anti-windup compensation, for the rate saturation problem, as presented in Figs. 9 and 11, and defined in Eqns. 2.9 to 2.13. Interestingly, provided the plant is exponentially stable, the redefined plant becomes marginally stable due to the presence of the integrator.

2. Override control

Figure 13 is equivalent to Fig. 7 and shows a cascade connection of the unconstrained closed-loop system and the mismatch system for override compensation. In particular, the mismatch system, in Fig. 13, is presented in an LFT representation. The detailed description of the mismatch system components is presented in Fig. 14. For this mismatch system additional terminology needs to be defined.

Definition 2.22. For a given override problem, when the closed-loop with plant output saturation has the form shown in Fig. 14, we use the following notation:

- the system $\mathcal{W}^\Delta$ is the *mismatch system for override compensation*,

- the internal state trajectory of the system $\mathcal{W}^\Delta$ is the *mismatch state response*; the trajectories z_d, y_d, and $\underline{z}_d$ are the *mismatch performance output response*, *mismatch measured output response* and the *mismatch constrained performance*

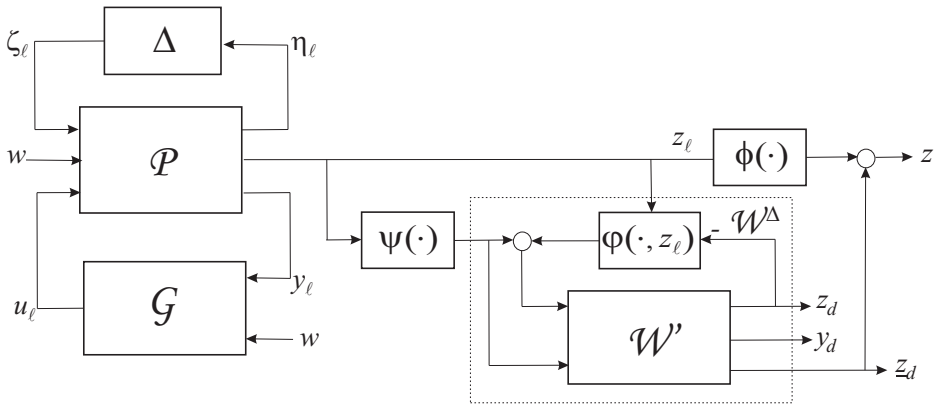

Fig. 13. Cascade interconnection of the output constrained closed-loop system to mismatch system.

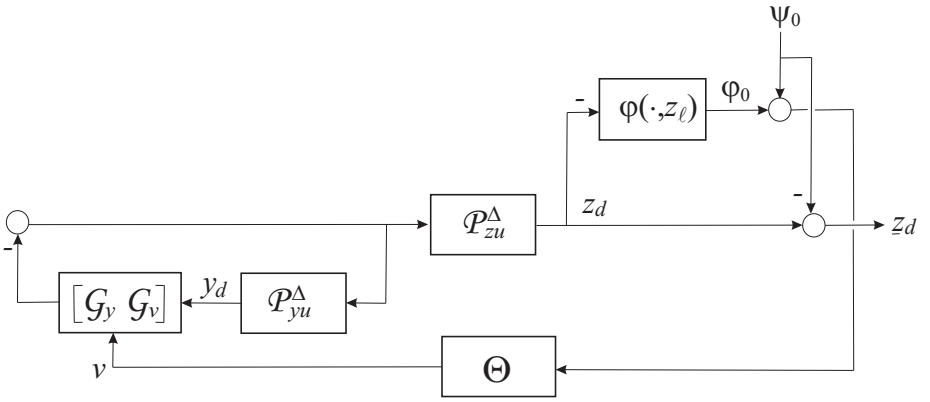

Fig. 14. Detailed representation of the mismatch system for override compensation.

output response,

- the function $\psi : \mathbb{R}^{n_z} \mapsto \mathbb{R}^{n_z}$ is defined as $\psi(r) = r - \phi(r),\ \forall r \in \mathbb{R}^{n_z}$, and
- the function $\varphi : \mathbb{R}^{n_z} \mapsto \mathbb{R}^{n_z}$ is defined as $\varphi(z - z_l, z_l) = \psi(z) - \psi(z_l),\ \forall z, z_l \in \mathbb{R}^{n_z}$. ◁

This mismatch structure is not a new idea, it has been proposed and considered by several researchers within the anti-windup literature [57]. Notably, for the case of *linear plant uncertainty*, the mismatch system presented in Fig. 13 can be decomposed

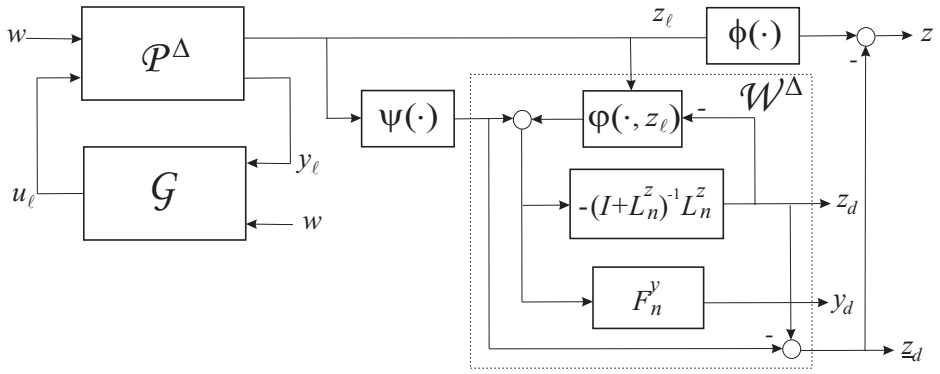

Fig. 15. Cascade interconnection. Mismatch system for override compensation (linear uncertainty case): nonlinear loop and disturbance filter.

into a nonlinear feedback loop ($\varphi(\cdot, z_l)$ in positive feedback with T_n^z) and a disturbance filter (F_n^y), as shown in Fig. 15. For this representation of the mismatch system, the following transfer function matrices are defined:

$$L_n^z = -\frac{z}{\phi(z)} = (I_{n_z} + \mathcal{P}_{zu} S \mathcal{G}_v \Theta)^{-1} - I_{n_z} = (V_{zu}^{-1} Q^{-1} - \mathcal{P}_{zu} S \mathcal{G}_y \mathcal{P}_{yu} \mathcal{G}_v \Theta)^{-1} - I_{n_z}, \quad (2.16)$$

$$S_n^z = (I_{n_z} + L_n^z)^{-1} = I_{n_z} + \mathcal{P}_{zu} S \mathcal{G}_v \Theta = V_{zu}^{-1} Q^{-1} - \mathcal{P}_{zu} S \mathcal{G}_y \mathcal{P}_{yu} \mathcal{G}_v \Theta, \quad (2.17)$$

$$T_n^z = (I_{n_z} + L_n^z)^{-1} L_n^z = -\mathcal{P}_{zu} S \mathcal{G}_v \Theta = I_{n_z} - V_{zu}^{-1} Q^{-1} + \mathcal{P}_{zu} S \mathcal{G}_y \mathcal{P}_{yu} \mathcal{G}_v \Theta, \quad (2.18)$$

$$F_n^y = -\mathcal{P}_{yu} S \mathcal{G}_v \Theta. \quad (2.19)$$

where:

$$T_n^z + S_n^z = I_{n_z}. \quad (2.20)$$

Here L_n^z is the loop transmission around the saturation nonlinearity, similar to the anti-windup compensation case [22, 25]. Moreover, T_n^z, S_n^z and F_n^y are the corresponding closed-loop transfer function matrices for the mismatch system, and $S = (I_{n_y} + \mathcal{G}_y \mathcal{P}_{yu})^{-1}$. Note that T_n^z, S_n^z and F_n^y can also be defined in terms of a parameter Q and coprime factors of the plant, U_{zu} and V_{zu}. In Chapter III, the corresponding Q, U_{zu} and V_{zu} will be explicitly defined.

CHAPTER III

STUDY OF REMEDIAL COMPENSATION ARCHITECTURES

This chapter presents a unified framework for the study of linear systems subject to control input and plant output nonlinearities using remedial compensation schemes.

A. Conditioning of the unconstrained controller and plant: parameterization (H_1, H_2, Q)

The effect of the remedial compensator on the remedial closed-loop dynamics can be interpreted as a conditioning of either the unconstrained controller, in the anti-windup compensation case, or the plant, in the override compensation case. Importantly, when defining the remedial action in this setting, a general framework for studying remedial control design arises. This framework allows for the unification of all known linear remedial control schemes in terms of three parameters (H_1, H_2, Q). Recall that this idea was previously employed by Kothare *et al.* [17] for the study of linear systems subject to control input nonlinearities and working under anti-windup schemes. However, by only considering the parameterization (H_1, H_2, I), the work of Kothare left out *all dynamic* anti-windup compensation schemes. In this sense, the parameterization (H_1, H_2, Q) here described can be considered an extension of Kothare's work as it can include both static and dynamic anti-windup compensation schemes via the Q parameter. Furthermore, an analysis under the general framework given by the (H_1, H_2, Q) parameters can also be insightful in the override compensation case, as shown in the next sections.

1. Anti-windup compensation

This section presents a generalization of the static anti-windup framework for the study of systems subject to control input nonlinearities [17]. This general framework, that permits dynamic anti-windup compensation, is further improved by considering that the anti-windup compensator output v_1 acts on either the unconstrained controller state or unconstrained controller input, and that the anti-windup compensator output v_2 acts on the unconstrained controller output. This is achieved through the freedom of B_{g,v_1}, D_{g,v_1} and D_{g,v_2} in Eqn. 2.3, see also Figs. 6 and 8. Placing this general architecture for anti-windup compensation into an analogous framework to that in Kothare *et al.* [17] gives the following *conditioned controller* $\hat{\mathcal{G}}$:

$$\hat{\mathcal{G}}(s) = \begin{bmatrix} \hat{\mathcal{G}}_y & \mathcal{G}_w \end{bmatrix}, \tag{3.1}$$

where:

$$\hat{\mathcal{G}}_y(s) = \begin{bmatrix} \tilde{U}(s) & I_{n_u} - \tilde{V}(s) \end{bmatrix}, \tag{3.2}$$

as seen in Fig. 16 (see also Miyamoto and Vinnicombe [23]), and:

$$\tilde{V}(s) = Q(s)V(s), \tag{3.3}$$

$$\tilde{U}(s) = Q(s)U(s), \tag{3.4}$$

$$V(s) = \left[\begin{array}{c|c} A_g - \tilde{H}_1 C_g & -\tilde{H}_1 \\ \hline \tilde{H}_2 C_g & \tilde{H}_2 \end{array}\right], \tag{3.5}$$

$$U(s) = \left[\begin{array}{c|c} A_g - \tilde{H}_1 C_g & B_{g,y} - \tilde{H}_1 D_{g,y} \\ \hline \tilde{H}_2 C_g & \tilde{H}_2 D_{g,y} \end{array}\right], \tag{3.6}$$

$$\tilde{H}_1 = \tilde{D}_{\Lambda_1} \tilde{H}_2, \tag{3.7}$$

$$\tilde{H}_2 = (I_{n_u} + \tilde{D}_{\Lambda_2})^{-1}, \tag{3.8}$$

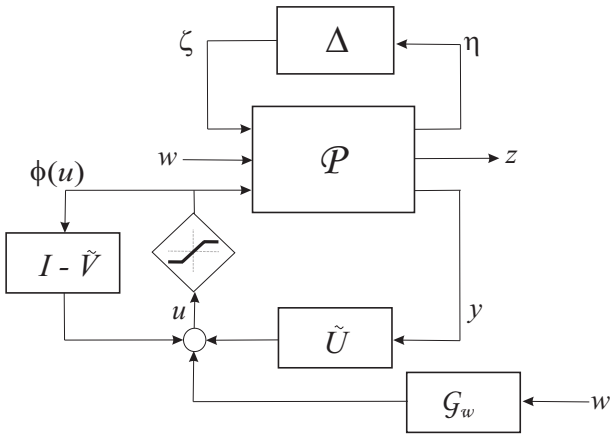

Fig. 16. Conditioned controller $\hat{\mathcal{G}}$.

$$\tilde{D}_{\Lambda_1} = B_{g,v_1} D_{\Lambda_1}, \tag{3.9}$$

$$\tilde{D}_{\Lambda_2} = D_{g,v_1} D_{\Lambda_1} + D_{g,v_2} D_{\Lambda_2}, \tag{3.10}$$

To define $Q(s)$ we require the following additional definitions:

$$\Lambda_1(s) = \Lambda_{1s}(s) + D_{\Lambda_1}, \tag{3.11}$$

$$\Lambda_2(s) = \Lambda_{2s}(s) + D_{\Lambda_2}. \tag{3.12}$$

$$\Lambda_{is}(s) = \left[\begin{array}{c|c} A_\Lambda & B_\Lambda \\ \hline C_{\Lambda_i} & 0 \end{array}\right], \; i = \{1, 2\}, \tag{3.13}$$

$$C(s) = \left[\begin{array}{c|c} A_g - \tilde{H}_1 C_g & B_{g,v_1} \\ \hline \tilde{H}_2 C_g & 0 \end{array}\right]. \tag{3.14}$$

From these definitions one can derive:

$$Q(s) = (I_{n_u} + V D_{g,v_1} \Lambda_{1s} + C\Lambda_{1s} + V D_{g,v_2} \Lambda_{2s})^{-1}. \tag{3.15}$$

The transfer function matrices U and V correspond to minimal realizations of

the left coprime factors of $\mathcal{G}_y$ [17], where:

$$\mathcal{G}_y(s) = V(s)^{-1}U(s), \tag{3.16}$$

for any $\tilde{H}_1$ and $\tilde{H}_2$, provided $\tilde{H}_2$ is invertible.

The above description of the anti-windup closed-loop system has the static configuration described in Kothare *et al.* [17] as a degenerate case, for which $D_{g,v_1} = 0$ and $B_{g,v_1} = I_{n_g}$, such that the feedback location of Λ_1 is the unconstrained controller states, and $\Lambda_{1s} = \Lambda_{2s} = 0$, thus $Q = I_{n_u}$. Therefore the above description can be seen to be a generalization of the configuration in Kothare *et al.* [17] allowing for higher order coprime factorizations of the unconstrained controller $\mathcal{G}_y$ and a higher order for the subsequent conditioned controller $\hat{\mathcal{G}}_y$. Hence this permits dynamic anti-windup compensation via a dynamic Q, combined with either unconstrained controller input or unconstrained controller state feedback of Λ_1. This presentation for the general configuration for anti-windup compensation is equivalent to Miyamoto and Vinnicombe [23], where $Q, Q^{-1} \in \mathcal{RH}_\infty$, but with Q explicitly parameterized in the above description in terms of Λ_1 and Λ_2 and the specific feedback location for Λ_1.

Based on the proposed general configuration for anti-windup compensation, an anti-windup compensator will be termed static if Q is static (i.e. $Q = I_{n_u}$), and conversely dynamic if Q is dynamic. In this way, a static anti-windup compensator adds no additional states to the anti-windup closed-loop system[1], while a dynamic anti-windup compensator does add additional states, being those introduced by Λ. The latter can also be seen from the increase in the order of $\tilde{V}$ and $\tilde{U}$ relative to V and U in Eqns. 3.3 and 3.4 and consequently an increase in order of the conditioned

[1]It is important to distinguish this from the anti-windup static synthesis problem, where only the elements of a gain matrix are modified in the design and the resulting anti-windup compensator may be static or dynamic, depending on the remaining elements in the anti-windup compensator.

controller $\hat{\mathcal{G}}$ (note the cancelation between zeros of Q and poles of V and U).

2. Override compensation

For anti-windup compensation, Kothare *et al.* [17] presented a general framework that unified all the static anti-windup configurations and Villota *et al.* [57] presented its extension via a dynamic Q parameter to account for dynamic anti-windup compensation. Importantly, not a similar study has been performed for override compensation.

The general configuration for override compensation here considered is similar to that in the anti-windup case but accommodated accordingly for the override problem here discussed. This configuration permits static and dynamic override compensation, with v_1 going to either the unconstrained controller state or unconstrained controller input, and v_2 going to the unconstrained controller output. The latter achieved through the freedom of B_{g,v_1}, D_{g,v_1} and D_{g,v_2} in Eqn. 2.3, see also Figs. 7 and 8. Placing this general configuration for override compensation in a framework similar to Villota *et al.* [57], gives the following *conditioned plant* $\hat{\mathcal{P}}$:

$$\hat{\mathcal{P}}(s) = \begin{bmatrix} \hat{\mathcal{P}}_{zu} & \mathcal{P}_{zw} \\ \hat{\mathcal{P}}_{yu} & \mathcal{P}_{yw} \end{bmatrix}, \tag{3.17}$$

where:

$$\hat{\mathcal{P}}_{zu}(s) = [\ \tilde{U}_{zu} \qquad I_{n_z} - \tilde{V}_{zu}\ ], \tag{3.18}$$

$$\hat{\mathcal{P}}_{yu}(s) = [\ \check{U}_{yu} \qquad \mathcal{P}_{yu}\mathcal{G}_v\Theta\tilde{V}_{zu}\ ], \tag{3.19}$$

as seen in Fig. 17, and:

$$\tilde{V}_{zu}(s) = Q(s)V_{zu}(s), \tag{3.20}$$

$$\tilde{U}_{zu}(s) = Q(s)U_{zu}(s), \tag{3.21}$$

$$\check{V}_{*u}(s) = \bar{V}_{*u}(s)\bar{Q}(s), \tag{3.22}$$

$$\check{U}_{*u}(s) = \bar{U}_{*u}(s)\bar{Q}(s), \tag{3.23}$$

$$V_{zu}(s) = \left[\begin{array}{c|c} A_p - \tilde{H}_1 C_{p,z} & -\tilde{H}_1 \\ \hline \tilde{H}_2 C_{p,z} & \tilde{H}_2 \end{array}\right], \tag{3.24}$$

$$U_{zu}(s) = \left[\begin{array}{c|c} A_p - \tilde{H}_1 C_{p,z} & B_{p,u} - \tilde{H}_1 D_{p,zu} \\ \hline \tilde{H}_2 C_{p,z} & \tilde{H}_2 D_{p,zu} \end{array}\right], \tag{3.25}$$

$$\bar{V}_{*u}(s) = \left[\begin{array}{c|c} A_p - B_{p,u}\bar{H}_1 & B_{p,u}\bar{H}_2 \\ \hline -\bar{H}_1 & \bar{H}_2 \end{array}\right], \tag{3.26}$$

$$\bar{U}_{*u}(s) = \left[\begin{array}{c|c} A_p - B_{p,u}\bar{H}_1 & B_{p,u}\bar{H}_2 \\ \hline C_{p,*} - D_{p,*}\bar{H}_1 & D_{p,*u}\bar{H}_2 \end{array}\right], \tag{3.27}$$

$$\tilde{H}_1 = B_{p,u}\tilde{D}_\Theta \tilde{H}_2, \tag{3.28}$$

$$\tilde{H}_2 = (I_{n_z} + D_{p,zu}\tilde{D}_\Theta)^{-1}, \tag{3.29}$$

$$\bar{H}_1 = \bar{H}_2 \tilde{D}_\Theta C_{p,z}, \tag{3.30}$$

$$\bar{H}_2 = (I_{n_u} + \tilde{D}_\Theta D_{p,zu})^{-1}, \tag{3.31}$$

$$\tilde{D}_\Theta = D_{g,v_1} D_{\Theta_1} + D_{g,v_2} D_{\Theta_2}, \tag{3.32}$$

where $*$ substitutes either y or z. To define $Q(s)$ and $\bar{Q}(s)$ we require the following extra definitions:

$$\Theta_1(s) = \Theta_{1s}(s) + D_{\Theta_1}, \tag{3.33}$$

$$\Theta_2(s) = \Theta_{2s}(s) + D_{\Theta_2}, \tag{3.34}$$

$$\mathcal{G}_{v_1}(s) = \mathcal{G}_{v_1 s}(s) + D_{g,v_1}, \tag{3.35}$$

$$\Theta_{is}(s) = \left[\begin{array}{c|c} A_\Theta & B_\Theta \\ \hline C_{\Theta_i} & 0 \end{array}\right], \ i = \{1, 2\}, \tag{3.36}$$

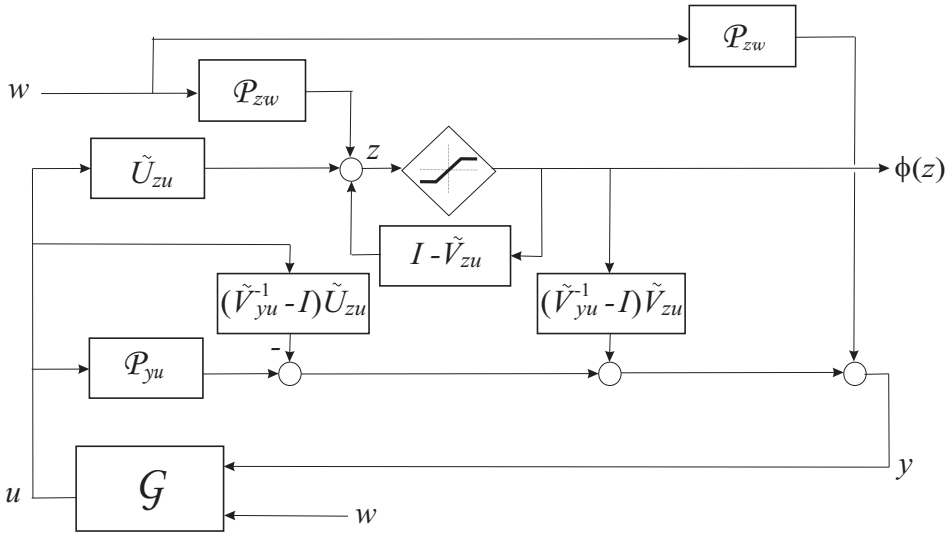

Fig. 17. Conditioned plant $\hat{\mathcal{P}}$.

$$\mathcal{G}_{v_1 s}(s) = \left[\begin{array}{c|c} A_g & B_{g,v_1} \\ \hline C_g & 0 \end{array}\right]. \tag{3.37}$$

From these definitions one can derive:

$$Q(s) = (I_{n_z} + U_{zu} D_{g,v_2} \Theta_{2s} + U_{zu} D_{g,v_1} \Theta_{1s} + U_{zu} \mathcal{G}_{v_1 s} \Theta_1)^{-1}, \tag{3.38}$$

$$\bar{Q}(s) = (I_{n_u} + D_{g,v_2} \Theta_{2s} \bar{U}_{zu} + D_{g,v_1} \Theta_{1s} \bar{U}_{zu} + \mathcal{G}_{v_1 s} \Theta_1 \bar{U}_{zu})^{-1}. \tag{3.39}$$

Similarly to Villota *et al.* [57], the transfer function matrices U_{zu} and V_{zu} ($\bar{U}_{*u}$ and $\bar{V}_{*u}$) correspond to minimal realizations of the left (right) coprime factors of, in this case, $\mathcal{P}_{zu}$ ($\mathcal{P}_{*u}$), where:

$$\mathcal{P}_{zu}(s) = V_{zu}^{-1}(s) U_{zu}(s), \tag{3.40}$$

$$\mathcal{P}_{*u}(s) = \bar{U}_{*u}(s) \bar{V}_{*u}^{-1}(s), \tag{3.41}$$

for any $\tilde{H}_1$ and $\tilde{H}_2$ ($\bar{H}_1$ and $\bar{H}_2$) provided $\tilde{H}_2$ ($\bar{H}_2$) are invertible.

From Fig. 7, it is easy to note that the plant perceives the effect of override com-

pensation as the unconstrained controller does it in the case of dynamic conventional anti-windup configuration for controller input described in Villota *et al.* [57]. This takes place because with the construction of Fig. 7 it is not possible to have internal modification nor affect the output of the plant dynamics (physical system). The limitations of this construction are manifested in the parameters $\tilde{H}_1$ and $\tilde{H}_2$ ($\bar{H}_1$ and $\bar{H}_2$) in Eqns. (3.28) and (3.29) (Eqns. (3.30) and (3.31)) which are not independent, as they are both defined by $\tilde{D}_\Theta$.

On the basis of the presented general configuration for override compensation, for the left (right) plant coprime factorizations, the override compensator is termed static if Q ($\bar{Q}$) is either static (i.e. $Q = I_{n_z}$, $\bar{Q} = I_{n_u}$) or dynamic with $n_Q = n_p + n_g$ ($n_{\bar{Q}} = n_p + n_g$) (i.e. $Q = (I + U_{zu}\mathcal{G}_{v_1 s} D_{\Theta_1})^{-1}$, $\bar{Q} = (I + \mathcal{G}_{v_1 s} D_{\Theta_1} \bar{U}_{zu})^{-1}$), and conversely dynamic if Q ($\bar{Q}$) is dynamic with $n_Q = n_p + n_\Theta$ ($n_{\bar{Q}} = n_p + n_\Theta$) or $n_Q = n_p + n_g + n_\Theta$ ($n_{\bar{Q}} = n_p + n_g + n_\Theta$). To be more precise, for static override compensation the order of $\tilde{V}_{zu}$ and $\tilde{U}_{zu}$ ($\check{V}_{*u}$ and $\check{U}_{*u}$) can be either n_p or $n_p + n_g$ whereas for dynamic override compensation the order can be either $n_p + n_\Theta$ or $n_p + n_g + n_\Theta$ (note the cancelation between zeros of Q ($\bar{Q}$) and poles of V_{zu} and U_{zu} ($\bar{V}_{*u}$ and $\bar{U}_{*u}$)). This is different from the anti-windup compensation case, because, for override compensation, the unconstrained controller dynamics can be embedded in Q ($\bar{Q}$) trough B_{g,v_1} even when the override compensator Θ is static. In other words, what we see in override compensation is that the unconstrained controller dynamics can be employed for "modification" of the plant dynamics whenever the override compensator output v_1 is fed back to the unconstrained controller states or input. Notably, the increase in order of $\tilde{V}_{zu}$ and $\tilde{U}_{zu}$ ($\check{V}_{*u}$ and $\check{U}_{*u}$) produces an increase in order of the conditioned plant $\hat{\mathcal{P}}$. However, this increase in order of the coprime factors is only possible with dynamic override compensation, i.e. Θ adds its states to the override closed-loop system (note the cancelation between zeros of Q ($\bar{Q}$) and poles of $\mathcal{G}$ in

closed-loop).

B. Configurations for remedial compensation: study based on parameterization (H_1, H_2, Q)

We will now discuss several linear remedial compensation schemes and will show them in the framework developed in the preceding section.

1. Anti-windup compensation

a. Full-authority feedback anti-windup augmentation

This configuration corresponds to the case when the anti-windup compensator output v_1 is fed back to the unconstrained controller states and output [27]. Consequently $B_{g,v_1} = I_{n_g}$, $D_{g,v_1} = 0$ and $D_{g,v_2} = I_{n_u}$. Notably, the configuration employed in Grimm *et al.* [30] (also Grimm *et al.* [21] for nominal design) is this configuration. The corresponding Q for dynamic anti-windup compensation is given by:

$$Q(s) = (I_{n_u} + V\Lambda_{2s} + C\Lambda_{1s})^{-1}, \tag{3.42}$$

where:

$$C(s) = \left[\begin{array}{c|c} A_g - \tilde{H}_1 C_g & I_{n_g} \\ \hline \tilde{H}_2 C_g & 0 \end{array}\right], \tag{3.43}$$

$$\tilde{H}_1 = D_{\Lambda_1}\tilde{H}_2, \tag{3.44}$$

$$\tilde{H}_2 = (I_{n_u} + D_{\Lambda_2})^{-1}. \tag{3.45}$$

Note that for this configuration, $\tilde{H}_1$ and $\tilde{H}_2$ are independent, as they are defined by D_{Λ_1} and D_{Λ_2}, which can be assigned independently.

b. External feedback anti-windup augmentation

This configuration corresponds to the case in which the anti-windup compensator output v_1 can modify the input and output of the unconstrained controller [27]. Consequently $B_{g,v_1} = B_{g,y}$, $D_{g,v_1} = D_{g,y}$ and $D_{g,v_2} = I_{n_u}$. The corresponding Q, after simplification using C below, is:

$$Q(s) = (I_{n_u} + V\Lambda_{2s} + U\Lambda_{1s})^{-1}, \tag{3.46}$$

where:

$$C(s) = \left[\begin{array}{c|c} A_g - \tilde{H}_1 C_g & B_{g,y} \\ \hline \tilde{H}_2 C_g & 0 \end{array}\right] = U - V D_{g,y}, \tag{3.47}$$

$$\tilde{H}_1 = B_{g,y} D_{\Lambda_1} \tilde{H}_2, \tag{3.48}$$

$$\tilde{H}_2 = (I_{n_u} + D_{g,y} D_{\Lambda_1} + D_{\Lambda_2})^{-1}. \tag{3.49}$$

For this configuration $\tilde{H}_1$ and $\tilde{H}_2$ are also independent, as they are defined by D_{Λ_1} and D_{Λ_2}, which are independent.

c. Generic anti-windup configuration

The generic anti-windup configuration, as defined in Edwards and Postlethwaite [24] (and see also Wu and Jayasuriya [55] for applications), employs only anti-windup feedback to the unconstrained controller output, hence $B_{g,v_1} = 0$, $D_{g,v_1} = 0$. Consequently, the corresponding Q for dynamic anti-windup compensation is:

$$Q(s) = (I_{n_u} + V\Lambda_{2s})^{-1} = (I + \tilde{H}_2\Lambda_{2s})^{-1}, \tag{3.50}$$

where:

$$V(s) = \left[\begin{array}{c|c} A_g & 0 \\ \hline \tilde{H}_2 C_g & \tilde{H}_2 \end{array}\right] = \tilde{H}_2, \tag{3.51}$$

$$U(s) = \left[\begin{array}{c|c} A_g & B_{g,y} \\ \hline \tilde{H}_2 C_g & \tilde{H}_2 D_{g,y} \end{array}\right] = \tilde{H}_2 \mathcal{G}(s), \tag{3.52}$$

$$\tilde{H}_1 = 0, \tag{3.53}$$

$$\tilde{H}_2 = (I_{n_u} + D_{\Lambda_2})^{-1}. \tag{3.54}$$

Note that for this configuration only $\tilde{H}_2$ is free to be defined via D_{Λ_2}. Subsequently, there is no freedom to change the poles of V or U. Additionally, V is effectively static (assuming zero initial conditions for its states), as its states are uncontrollable.

d. Dynamic conventional anti-windup configuration

Within this type of configuration, we can mention those that adopt a philosophy similar to that of the anti-reset windup. In this case, the anti-windup compensator output $v = v_1$ can only modify either the states or the input of the unconstrained controller and hence $D_{g,v_2} = 0$.

Dynamic conventional anti-windup configuration for unconstrained controller state. Here the configuration scheme considered is similar to the observer technique but with a dynamic feedback compensation instead of the static one [59]. The anti-windup compensator output $v = v_1$ is fed back to the unconstrained controller states, therefore $B_{g,v_1} = I_{n_g}$ and $D_{g,v_1} = 0$. The corresponding dynamic Q is given by:

$$Q(s) = (I_{n_u} + C\Lambda_{1s})^{-1}, \tag{3.55}$$

where:

$$C(s) = \left[\begin{array}{c|c} A_g - \tilde{H}_1 C_g & I_{n_g} \\ \hline \tilde{H}_2 C_g & 0 \end{array}\right], \tag{3.56}$$

$$\tilde{H}_1 = D_{\Lambda_1}, \tag{3.57}$$

$$\tilde{H}_2 = I_{n_u}. \tag{3.58}$$

Note that this configuration only allows modification of $\tilde{H}_1$ through D_{Λ_1}.

Dynamic conventional anti-windup configuration for unconstrained controller input. Here a dynamic representation of the (high gain) conventional anti-windup configuration proposed in Doyle *et al.* [15] as presented in Kothare *et al.* [17] (see also Lurie [25]) is considered. The anti-windup compensator output $v = v_1$ modifies the input of the unconstrained controller, therefore $B_{g,v_1} = B_{g,y}$ and $D_{g,v_1} = D_{g,y}$. This corresponds to Q defined as follows:

$$Q(s) = (I_{n_u} + U\Lambda_{1s})^{-1}, \tag{3.59}$$

where:

$$C(s) = \left[\begin{array}{c|c} A_g - \tilde{H}_1 C_g & B_{g,y} \\ \hline \tilde{H}_2 C_g & 0 \end{array}\right] = U - V D_{g,y}, \tag{3.60}$$

$$\tilde{H}_1 = B_{g,y} D_{\Lambda_1} \tilde{H}_2, \tag{3.61}$$

$$\tilde{H}_2 = (I_{n_u} + D_{g,y} D_{\Lambda_1})^{-1}. \tag{3.62}$$

Note that for this configuration, $\tilde{H}_1$ and $\tilde{H}_2$ are dependent, as they are both defined by D_{Λ_1}.

Remark 3.1. *High gain conventional anti-windup configuration [15].* Complementary to the work presented in Kothare *et al.* [17] for the conventional anti-windup structure, here the version presented in Doyle *et al.* [15] is considered. The design with this configuration starts with some coprime factorization of the unconstrained controller $\mathcal{G}_y = V_o^{-1} U_o$ and proceeds such that the associated loop transfer matrix $L_X = V_o^{-1} X$ has gain and bandwidth much higher than of $L = \mathcal{G}_y \mathcal{P}_{yu}$, where X is the (high) gain to be designed. Let the coprime factors V_o and U_o be defined by $\tilde{H}_{1o}$

and $\tilde{H}_{2o}$. Then designing for X corresponds to the choices:

$$\tilde{H}_1 = \tilde{H}_{1o}\tilde{H}_{2o}^{-1}X(I_{n_u} + \tilde{H}_{2o}^{-1}X)^{-1}, \tag{3.63}$$

$$\tilde{H}_2 = (I_{n_u} + \tilde{H}_{2o}^{-1}X)^{-1}. \tag{3.64}$$

Note that this is a static anti-windup configuration, $Q = I_{n_u}$, as X is not adding dynamics to the anti-windup closed-loop system. Also note that $\tilde{H}_1$ and $\tilde{H}_2$ are dependent, as both parameters are defined by X. ◁

e. Weston and Postlethwaite configuration (W&P)

The previous configurations were all natural variations on the general configuration for anti-windup compensation, in that they are all based on a coprime factorization of the unconstrained controller. However, more recent methods employed for anti-windup compensation have used configurations based on a coprime factorization of the nominal plant [29, 19, 26, 28]. Here the latter are related to the general configuration for anti-windup compensation.

The W&P configuration [26] (and extension [60]) is characterized by the anti-windup compensator being defined in terms of a single transfer function matrix $\hat{M}(s)$ and the nominal plant $\mathcal{P}_{yu}^o$ (see Fig. 6). This anti-windup compensator modifies the input of the unconstrained controller, and therefore $B_{g,v} = B_{g,y}$ and $D_{g,v} = D_{g,y}$. The corresponding elements Λ_1 and Λ_2 of the anti-windup compensator are shown below:

$$\Lambda_1(s) = \mathcal{P}_{yu}^o(I_{n_u} + \Lambda_2) = \mathcal{P}_{yu}^o\hat{M}, \tag{3.65}$$

$$\Lambda_2(s) = \hat{M} - I_{n_u}, \tag{3.66}$$

where $\hat{M} = \hat{M}_s + D_{\hat{M}}$ is a transfer function that is bi-proper for well-posedness of the system. From these definitions one can derive the following Q (after cancelations

based on C below):

$$Q(s) = ((V + U\mathcal{P}^o_{yu})\hat{M})^{-1}, \tag{3.67}$$

where the definition $\mathcal{P}^o_{yu} = \mathcal{P}^o_{yu,s} + D_{p,yu}$ permits the definition of U and V in terms of $\hat{M}$ and $\mathcal{P}^o_{yu}$, and:

$$C(s) = \left[\begin{array}{c|c} A_g - \tilde{H}_1 C_g & B_{g,y} \\ \hline \tilde{H}_2 C_g & 0 \end{array}\right] = U - V D_{g,y}, \tag{3.68}$$

$$\tilde{H}_1 = B_{g,y} D_{p,yu} (I_{n_u} + D_{g,y} D_{p,yu})^{-1}, \tag{3.69}$$

$$\tilde{H}_2 = ((I_{n_u} + D_{g,y} D_{p,yu}) D_{\hat{M}})^{-1}. \tag{3.70}$$

For this configuration, $\tilde{H}_1$ cannot be modified as it is defined by the unconstrained controller and the nominal plant $\mathcal{P}^o_{yu}$ and hence the poles of V and U cannot be modified by $\hat{M}$ (the only way is to change $\mathcal{P}^o_{yu}$). However, $\tilde{H}_2$ is independent as it is defined by $D_{\hat{M}}$, with $\hat{M}$ to be designed.

Importantly, the unknowns in Q are given in terms of $\hat{M}$, the coprime factors of the unconstrained controller and the nominal plant, which are necessarily non-zero and dynamic (assuming the plant and linear controller are dynamic). Hence Q must be dynamic in this configuration (except for pathological cases). However, it should be noted that the anti-windup synthesis problem may be static if $\hat{M}$ is chosen to be a coprime factor of the nominal plant and of plant order. This case is described below.

Equivalence of W&P [26] and Teel and Kapoor (T&K) [19] configurations

Within the framework proposed by W&P [26] one can also choose $\hat{M} = M_o$, where $\mathcal{P}^o_{zu} = \mathcal{P}^o_{yu} = N_o M_o^{-1}$ and M_o being plant order, to give a static synthesis problem,

where:

$$M_o(s) = \left[\begin{array}{c|c} A_p + B_{p,u}F & B_{p,u} \\ \hline F & I_{n_u} \end{array}\right], \tag{3.71}$$

and F is the design parameter. In this case the corresponding Q below can be derived:

$$Q(s) = (VM_o + UN_o)^{-1}, \tag{3.72}$$

where the choice of $M_o = M_{os} + D_{M_o}$ defines the anti-windup compensator elements, Λ_1 and Λ_2, and the unconstrained controller coprime factors, V and U. Therefore:

$$\Lambda_1(s) = N_o, \tag{3.73}$$

$$\Lambda_2(s) = M_{os}, \tag{3.74}$$

$$\tilde{H}_1 = B_{g,y}D_{p,yu}(I_{n_u} + D_{g,y}D_{p,yu})^{-1}, \tag{3.75}$$

$$\tilde{H}_2 = (I_{n_u} + D_{g,y}D_{p,yu})^{-1}. \tag{3.76}$$

Observe that this configuration is simply the one proposed in Teel and Kapoor [19], where $F = k$ and k is the gain matrix in Eqn. 11 of Teel and Kapoor [19], restricted to be linear. Hence T&K [19] and W&P [26] configurations are equivalent under the restriction that $\hat{M} = M_o$ in [26], where M_o is plant order, and the coprime factorization of the plant is linear (i.e. $k(x_{aw})$ is a linear function of x_{aw}) in Weston and Postlethwaite [19]. The additional advantage of employing the T&K configuration is the possibility of synthesizing for a nonlinear, dynamic anti-windup compensator (e.g. $k_{\sigma(\cdot)}(x_{aw})$ where the selection function $\sigma(\cdot)$ can be based on switching among a family of linear gains). A nonlinear compensator is proven to be useful when seeking for highly improved performance [61].

Extension of W&P configuration

To exploit a similar degree of freedom to that of $\tilde{H}_2$ for the coprime factorization of the unconstrained controller, the addition of an extra parameter E to the coprime factorization of the nominal plant was proposed [60]. Then M_o becomes:

$$M_o(s) = \left[\begin{array}{c|c} A_p + B_{p,u}F & B_{p,u}E \\ \hline F & E \end{array}\right]. \tag{3.77}$$

Employing this coprime factorization of the nominal plant results in the following anti-windup compensator:

$$\Lambda_1(s) = N_o = \left[\begin{array}{c|c} A_p + B_{p,u}F & B_{p,u}E \\ \hline C_{p,u} + D_{p,u}F & D_{p,u}E \end{array}\right], \tag{3.78}$$

$$\Lambda_2(s) = M_o - I_{n_u} = \left[\begin{array}{c|c} A_p + B_{p,u}F & B_{p,u}E \\ \hline F & E - I_{n_u} \end{array}\right]. \tag{3.79}$$

This modification permits a bi-proper Λ_2, so that $D_{\Lambda_2} \neq 0$ and $\tilde{H}_2$ can be modified. This allows further modification of the coprime factors of the controller, compared to the previous selection of M_o where $D_{\Lambda_2} = 0$ and $\tilde{H}_2$ is fixed.

f. IMC configuration

The IMC configuration [17] is the simplest. For instance, it can be obtained from the W&P configuration by choosing $\hat{M} = I_{n_u}$. Notably, there is no synthesis problem when IMC is employed. However, this methodology is of interest due to its application in practice. For this configuration the corresponding Q and anti-windup compensator elements are:

$$\Lambda_1(s) = \mathcal{P}^o_{yu}, \tag{3.80}$$

$$\Lambda_2(s) = 0, \tag{3.81}$$

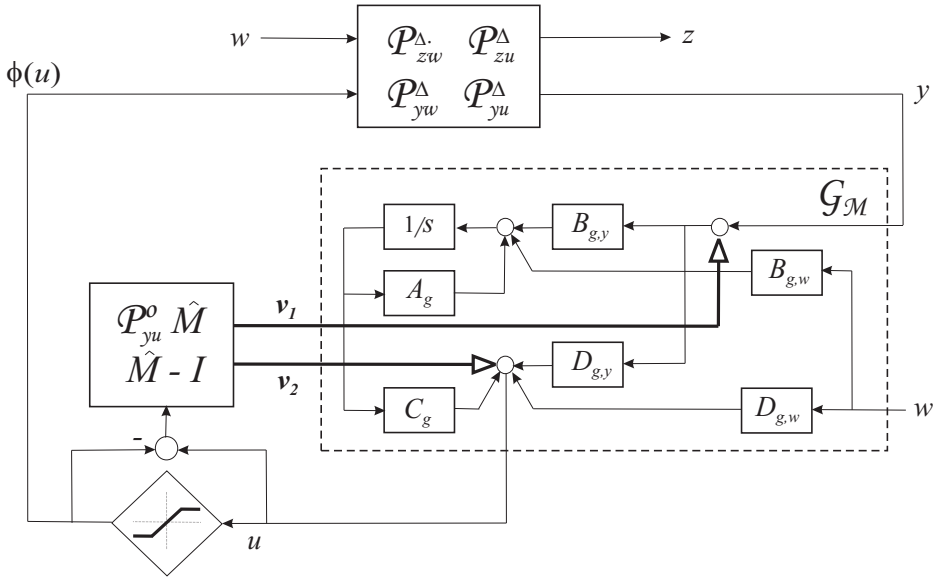

Fig. 18. Weston and Postlethwaite (W&P) configuration.

$$Q(s) = (I_{n_u} + U\mathcal{P}^o_{yu,s})^{-1}, \tag{3.82}$$

$$\tilde{H}_1 = B_{g,y}D_{p,yu}(I_{n_u} + D_{g,y}D_{p,yu})^{-1}, \tag{3.83}$$

$$\tilde{H}_2 = (I_{n_u} + D_{g,y}D_{p,yu})^{-1}, \tag{3.84}$$

where $\mathcal{P}^o_{yu} = \mathcal{P}^o_{yu,s} + D_{p,yu}$.

2. Override compensation

The objective in this section is to understand the relative advantages of employing a variety of override configurations, the latter obtained as special cases of the general configuration for override compensation adopted here. This work is of interest because we want to preclude the appearance of a myriad of configurations for override compensation, as happened in the case of anti-windup compensation. Similar configurations to the anti-windup compensation case have already been proposed [52, 54].

a. GOC for controller state/output

Then $B_{g,v_1} = I_{n_g}$, $D_{g,v_1} = 0$ and $D_{g,v_2} = I_{n_u}$. For a dynamic override compensator Θ with its outputs v_1 and v_2 affecting the unconstrained controller states and output respectively, the corresponding dynamic Q and $\bar{Q}$ are:

$$Q(s) = (I_{n_z} + U_{zu}\Theta_{2s} + U_{zu}\mathcal{G}_{v_1 s}\Theta_1)^{-1}, \tag{3.85}$$

$$\bar{Q}(s) = (I_{n_u} + \Theta_{2s}\bar{U}_{zu} + \mathcal{G}_{v_1 s}\Theta_1\bar{U}_{zu})^{-1} \tag{3.86}$$

where:

$$\tilde{H}_1 = B_{p,u}D_{\Theta_2}\tilde{H}_2, \tag{3.87}$$

$$\tilde{H}_2 = (I_{n_z} + D_{p,zu}D_{\Theta_2})^{-1}, \tag{3.88}$$

$$\bar{H}_1 = \bar{H}_2 D_{\Theta_2} C_{p,z}, \tag{3.89}$$

$$\bar{H}_2 = (I_{n_u} + D_{\Theta_2}D_{p,zu})^{-1}, \tag{3.90}$$

$$\mathcal{G}_{v_1 s}(s) = \left[\begin{array}{c|c} A_g & I_{n_g} \\ \hline C_g & 0 \end{array}\right]. \tag{3.91}$$

Note that for this configuration Q ($\bar{Q}$) is dynamic with $n_Q = n_p + n_g + n_\Theta$ ($n_{\bar{Q}} = n_p + n_g + n_\Theta$).

The case of a static override compensator Θ differs with its dynamic version in that:

$$Q(s) = (I_{n_z} + U_{zu}\mathcal{G}_{v_1 s}D_{\Theta_1})^{-1}, \tag{3.92}$$

$$\bar{Q}(s) = (I_{n_u} + \mathcal{G}_{v_1 s}D_{\Theta_1}\bar{U}_{zu})^{-1}. \tag{3.93}$$

Note that for this case Q ($\bar{Q}$) is dynamic with $n_Q = n_p + n_g$ ($n_{\bar{Q}} = n_p + n_g$) even though the override compensator is static.

b. GOC for controller input/output

Then $B_{g,v_1} = B_{g,y}$, $D_{g,v_1} = D_{g,y}$ and $D_{g,v_2} = I_{n_u}$. For a dynamic compensator Θ with its outputs v_1 and v_2 affecting the unconstrained controller input and output respectively, the corresponding dynamic Q and $\bar{Q}$ are:

$$Q(s) = (I_{n_z} + U_{zu}\Theta_{2s} + U_{zu}D_{g,y}\Theta_{1s} + U_{zu}\mathcal{G}_{v_1 s}\Theta_1)^{-1}, \tag{3.94}$$

$$\bar{Q}(s) = (I + \Theta_{2s}\bar{U}_{zu} + D_{g,y}\Theta_{1s}\bar{U}_{zu} + \mathcal{G}_{v_1 s}\Theta_1\bar{U}_{zu})^{-1} \tag{3.95}$$

where:

$$\tilde{H}_1 = B_{p,u}(D_{g,y}D_{\Theta_1} + D_{\Theta_2})\tilde{H}_2, \tag{3.96}$$

$$\tilde{H}_2 = (I_{n_z} + D_{p,zu}(D_{g,y}D_{\Theta_1} + D_{\Theta_2}))^{-1}, \tag{3.97}$$

$$\tilde{H}_1 = \bar{H}_2(D_{g,y}D_{\Theta_1} + D_{\Theta_2})C_{p,z}, \tag{3.98}$$

$$\tilde{H}_2 = (I_{n_u} + (D_{g,y}D_{\Theta_1} + D_{\Theta_2})D_{p,zu})^{-1}, \tag{3.99}$$

$$\mathcal{G}_{v_1 s}(s) = \left[\begin{array}{c|c} A_g & B_{g,y} \\ \hline C_g & 0 \end{array}\right]. \tag{3.100}$$

Note that for this configuration Q ($\bar{Q}$) is dynamic with $n_Q = n_p + n_g + n_\Theta$ ($n_{\bar{Q}} = n_p + n_g + n_\Theta$).

The case of a static override compensator Θ differs with its dynamic version in that:

$$Q(s) = (I_{n_z} + U_{zu}\mathcal{G}_{v_1 s}D_{\Theta_1})^{-1}, \tag{3.101}$$

$$\bar{Q}(s) = (I_{n_u} + \mathcal{G}_{v_1 s}D_{\Theta_1}\bar{U}_{zu})^{-1}. \tag{3.102}$$

Note that for this case Q ($\bar{Q}$) is dynamic with $n_Q = n_p + n_g$ ($n_{\bar{Q}} = n_p + n_g$) even though the override compensator is static.

c. GOC for controller state

Then $B_{g,v_1} = I_{n_g}$, $D_{g,v_1} = 0$ and $D_{g,v_2} = 0$. For a dynamic override compensator Θ with its output $v = v_1$ affecting only the unconstrained controller states, the corresponding dynamic Q and $\bar{Q}$ are:

$$Q(s) = (I_{n_z} + U_{zu}\mathcal{G}_{v_1 s}\Theta_1)^{-1}, \tag{3.103}$$

$$\bar{Q}(s) = (I_{n_u} + \mathcal{G}_{v_1 s}\Theta_1\bar{U}_{zu})^{-1}, \tag{3.104}$$

where:

$$\tilde{H}_1 = 0, \tag{3.105}$$

$$\tilde{H}_2 = I_{n_z}, \tag{3.106}$$

$$\bar{H}_1 = 0, \tag{3.107}$$

$$\bar{H}_2 = I_{n_u}, \tag{3.108}$$

$$\mathcal{G}_{v_1 s}(s) = \left[\begin{array}{c|c} A_g & I_{n_g} \\ \hline C_g & 0 \end{array}\right]. \tag{3.109}$$

Note that for this configuration Q ($\bar{Q}$) is dynamic with $n_Q = n_p + n_g + n_\Theta$ ($n_{\bar{Q}} = n_p + n_g + n_\Theta$). However, $\tilde{H}_1$ and $\tilde{H}_2$ ($\bar{H}_1$ and $\bar{H}_2$) are fixed, leaving no room for further manipulation.

The case of a static override compensator Θ differs with its dynamic version in that:

$$Q(s) = (I_{n_z} + U_{zu}\mathcal{G}_{v_1 s}D_{\Theta_1})^{-1}, \tag{3.110}$$

$$\bar{Q}(s) = (I_{n_u} + \mathcal{G}_{v_1 s}D_{\Theta_1}\bar{U}_{zu})^{-1}. \tag{3.111}$$

Note that for this case Q ($\bar{Q}$) is dynamic with $n_Q = n_p + n_g$ ($n_{\bar{Q}} = n_p + n_g$) even though the override compensator is static.

d. GOC for controller input

Then $B_{g,v_1} = B_{g,y}$, $D_{g,v_1} = D_{g,y}$ and $D_{g,v_2} = 0$. For a dynamic override compensator Θ with its output $v = v_1$ affecting only the unconstrained controller input, the corresponding dynamic Q and $\bar{Q}$ are:

$$Q(s) = (I_{n_z} + U_{zu} D_{g,y} \Theta_{1s} + U_{zu} \mathcal{G}_{v_1 s} \Theta_1)^{-1}, \tag{3.112}$$

$$\bar{Q}(s) = (I_{n_u} + D_{g,y} \Theta_{1s} \bar{U}_{zu} + \mathcal{G}_{v_1 s} \Theta_1 \bar{U}_{zu})^{-1}, \tag{3.113}$$

where:

$$\tilde{H}_1 = B_{p,u} D_{g,y} D_{\Theta_1} \tilde{H}_2, \tag{3.114}$$

$$\tilde{H}_2 = (I_{n_z} + D_{p,zu} D_{g,y} D_{\Theta_1})^{-1}, \tag{3.115}$$

$$\bar{H}_1 = \bar{H}_2 D_{g,y} D_{\Theta_1} C_{p,z}, \tag{3.116}$$

$$\bar{H}_2 = (I_{n_u} + D_{g,y} D_{\Theta_1} D_{p,zu})^{-1}, \tag{3.117}$$

$$\mathcal{G}_{v_1 s}(s) = \left[\begin{array}{c|c} A_g & B_{g,y} \\ \hline C_g & 0 \end{array}\right]. \tag{3.118}$$

Note that for this configuration Q ($\bar{Q}$) is dynamic with $n_Q = n_p + n_g + n_\Theta$ ($n_{\bar{Q}} = n_p + n_g + n_\Theta$).

The case of a static override compensator Θ differs with its dynamic version in that:

$$Q(s) = (I_{n_z} + U_{zu} \mathcal{G}_{v_1 s} D_{\Theta_1})^{-1}, \tag{3.119}$$

$$\bar{Q}(s) = (I_{n_u} + \mathcal{G}_{v_1 s} D_{\Theta_1} \bar{U}_{zu})^{-1}. \tag{3.120}$$

Note that for this configuration Q ($\bar{Q}$) is dynamic with $n_Q = n_p + n_g$ ($n_{\bar{Q}} = n_p + n_g$) even though the override controller is static.

e. GOC for controller output

Then $B_{g,v_1} = 0$, $D_{g,v_1} = 0$ and $D_{g,v_2} = I_{n_u}$. For a dynamic override compensator Θ with its output affecting only the unconstrained controller output $v = v_2$, the corresponding dynamic Q and $\bar{Q}$ are:

$$Q(s) = (I_{n_z} + U_{zu}\Theta_{2s})^{-1}, \tag{3.121}$$

$$\bar{Q}(s) = (I_{n_u} + \Theta_{2s}\bar{U}_{zu})^{-1}, \tag{3.122}$$

where:

$$\tilde{H}_1 = B_{p,u}D_{\Theta_2}\tilde{H}_2, \tag{3.123}$$

$$\tilde{H}_2 = (I_{n_z} + D_{p,zu}D_{\Theta_2})^{-1}, \tag{3.124}$$

$$\bar{H}_1 = \bar{H}_2 D_{\Theta_2} C_{p,z}, \tag{3.125}$$

$$\bar{H}_2 = (I_{n_u} + D_{\Theta_2}D_{p,zu})^{-1}. \tag{3.126}$$

Note that for this configuration Q ($\bar{Q}$) is dynamic with $n_Q = n_p + n_\Theta$ ($n_{\bar{Q}} = n_p + n_\Theta$).

The case of a static override compensator Θ differs with its dynamic version in that:

$$Q(s) = I_{n_z}, \tag{3.127}$$

$$\bar{Q}(s) = I_{n_u}. \tag{3.128}$$

Note that for this case Q ($\bar{Q}$) is static (i.e. $Q = I_{n_z}$, $\bar{Q} = I_{n_u}$).

C. Comparison of remedial architectures based on the internal structure

In this section the configurations presented in Section III.D are analyzed and compared based on their internal structure and the results of Section III.C.

1. Anti-windup compensation

a. Static anti-windup compensation

In the case of static anti-windup compensation, $Q = I_{n_u}$ and the effect of anti-windup compensation can be seen as the modification of the coprime factors of the unconstrained controller via $\tilde{H}_1$ and $\tilde{H}_2$ (equivalently D_{Λ_1} and D_{Λ_2}) and the corresponding configuration. This restriction to static anti-windup compensation was also considered in Kothare *et al.* [17], where the choice of $\tilde{H}_1$ and $\tilde{H}_2$ was seen to modify the poles and zeros of $\hat{\mathcal{G}}_y$, as defined in Eqn. 3.1 herein.

Considering V and U as defined in Eqns. 3.5 and 3.6, $\tilde{H}_1$ modifies the poles of the coprime factors via $A_g - \tilde{H}_1 C_g$ and $\tilde{H}_2$ acts as an output gain matrix, neither changing the poles nor zeros of the coprime factors. Considering the conditioned controller $\hat{\mathcal{G}}$, it is desirable to change both its poles and zeros (this also permits maximum control of the system via anti-windup compensation). The poles of $\hat{\mathcal{G}}_y$ are modified via $\tilde{H}_1$ and the zeros are modified via both $\tilde{H}_1$ and $\tilde{H}_2$. Hence, independently employing both degrees of freedom (DOF) is desirable, as it permits maximum control over the poles and zeros of $\hat{\mathcal{G}}_y$.

Considering the configurations in Section III.D for anti-windup compensation, it can be seen that not all configurations employ both DOF independently. The full-authority and external feedback anti-windup configurations employ both DOF independently via the modification of D_{Λ_1} and D_{Λ_2}. This however is not the case for the generic anti-windup configuration or dynamic conventional anti-windup. For the generic anti-windup configuration $D_{\Lambda_1} = 0$ and therefore $\tilde{H}_1 = 0$ and the poles of the coprime factors are just the poles of the unconstrained controller, and hence the poles of $\hat{\mathcal{G}}_y$ cannot be modified, with the zeros being modified only by the gain matrix $\tilde{H}_2$ (or D_{Λ_2}). For the dynamic conventional anti-windup, $D_{\Lambda_2} = 0$ and therefore $\tilde{H}_1$ and

$\tilde{H}_2$ are not independent, with $\hat{\mathcal{G}}_y$ having less freedom in the placement of its poles and zeros. Note that the W&P and IMC configurations are not considered here, as they do not correspond to static anti-windup compensation.

From the above observations, it is evident that for static anti-windup compensation, the employment of either the full-authority or external feedback anti-windup configurations is favorable, as it permits the greatest control of $\hat{\mathcal{G}}_y$ and hence the resulting anti-windup compensation system. In terms of their relative applicability, it is evident that the two methods can only give the same anti-windup compensator when:

$$\begin{bmatrix} B_{g,y} & 0 \\ D_{g,y} & I_{n_u} \end{bmatrix} \begin{bmatrix} D_{\Lambda_1} \\ D_{\Lambda_2} \end{bmatrix}^{\mathrm{EF}} = \begin{bmatrix} D_{\Lambda_1} \\ D_{\Lambda_2} \end{bmatrix}^{\mathrm{FA}}, \tag{3.129}$$

where $(\cdot)^{\mathrm{EF}}$ and $(\cdot)^{\mathrm{FA}}$ denote the external feedback and full-authority feedback anti-windup cases, respectively. Representing this as $Ax = b$, this requires that $b \in \mathcal{R}(A)$, which in turn requires $D_{\Lambda_1}^{\mathrm{FA}} \in \mathcal{R}(B_{g,y})$. Therefore, for a general b the matrix A must be invertible, which requires $B_{g,y}$ to be full row rank. Hence, in general, the unconstrained controller part $\mathcal{G}_y$ must have as many inputs as states. Consequently, choosing the full-authority feedback anti-windup configuration is preferable.

This comparison of full-authority and external feedback anti-windup configurations shows that the choice of internal (v_1 to states) or external (v_1 to input) feedback, respectively, does have an effect on the anti-windup compensator design problem and hence the ability to alleviate the effects of saturation. Both configurations are more likely to be equivalent when $\mathcal{G}_y$ is of low order and necessarily when it has as many inputs as states. This is consistent with previous results [27] (Remark 3), arising from a consideration of the LMI feasibility conditions.

b. Dynamic anti-windup compensation

In the case of dynamic anti-windup compensation, $Q \neq I_{n_u}$ and the effect of anti-windup compensation can be seen to be the modification of the coprime factors of the unconstrained controller, when either Λ_1 or Λ_2 are bi-proper, and the addition of desirable dynamics. Hence when D_{Λ_1} or D_{Λ_2} are non-zero, the discussion above for static anti-windup compensation applies in addition to the potential to provide for additional dynamics. Therefore, in this section it is only necessary to consider the additional effect of the strictly proper components of Λ_1 or Λ_2, being Λ_{1s} and Λ_{2s}, and hence the effect of the resulting Q.

It is difficult to generally describe the effect of Q on the anti-windup closed-loop system. Rather, here we compare the different configurations based on the order of Λ_{1s} and Λ_{2s}. We consider the order of Λ_{1s} and Λ_{2s} necessary to give loop transmission order anti-windup compensation, termed full order anti-windup compensation, and the choice of Λ_{1s} and Λ_{2s} for reduced order (fixed) anti-windup compensator design.

The *full order anti-windup compensation* case corresponds to Q being loop transmission ($L = \mathcal{G}_y\mathcal{P}_{yu}$) order. For the full-authority and external feedback anti-windup configurations, the order added by Λ necessary to give full order anti-windup compensation is that of the plant. This can be seen from Eqns. 3.42 and 3.46 for the full-authority and external feedback anti-windup cases, respectively, where the configurations can be seen to employ the dynamics of the unconstrained controller, via its coprime factors, in the dynamics of Q. For the generic anti-windup configuration, only Λ_{2s} is employed and the order of Λ_{2s} required is full order (loop transmission). This is because the dynamics of the unconstrained controller part $\mathcal{G}_y$ are not exploited in Q. For the dynamic conventional anti-windup configuration, only Λ_{1s} is employed but the order required is only that of the plant due to the employment of the dynamics

of $\mathcal{G}_y$ in Q. For the configuration of W&P, both Λ_{1s} and Λ_{2s} are effectively employed, being defined by the choice of $\hat{M}$. The order of Λ_{1s} and Λ_{2s} necessary to give full order anti-windup compensation is again that of the plant, which corresponds to $\hat{M} = I_{n_u}$ or $\hat{M} = M_o$ where $\mathcal{P}_{yu} = N_o M_o^{-1}$. From this, the IMC configuration ($\hat{M} = I_{n_u}$) and the T&K configuration [19] in its linear version ($\hat{M} = M_o$) are restricted to full order anti-windup compensation (note that in the IMC case there is no synthesis problem).

Based on this reasoning, for dynamic anti-windup compensation, the full-authority and external feedback anti-windup configurations are preferable. The relative utility of the configurations is not as clear as in the static anti-windup compensation. However, when the state and input matrices for each configuration are related through a similarity transformation $\{A_\Lambda^{\mathrm{FA}}, B_\Lambda^{\mathrm{FA}}\} \rightarrow \{T^{-1}A_\Lambda^{\mathrm{EF}}T, T^{-1}B_\Lambda^{\mathrm{EF}}\}$, Q clearly will differ due to the presence of C_Λ and either U or C in its dynamics, which seems to be an additional consideration to that in the static case. Interestingly, under the proposed consideration, the two configurations can only render the same anti-windup compensator, or equivalently the same Q, U and V, when:

$$\left[\begin{array}{cc} B_{g,y} & 0 \\ D_{g,y} & I_{n_u} \end{array}\right] \left[\begin{array}{cc} D_{\Lambda_1} & C_{\Lambda_1} \\ D_{\Lambda_2} & C_{\Lambda_2} \end{array}\right]^{\mathrm{EF}} \left[\begin{array}{cc} I_{n_u} & 0 \\ 0 & T \end{array}\right] = \left[\begin{array}{cc} D_{\Lambda_1} & C_{\Lambda_1} \\ D_{\Lambda_2} & C_{\Lambda_2} \end{array}\right]^{\mathrm{FA}}, \tag{3.130}$$

where T accounts for any nonsingular matrix transformation between B_Λ^{FA} and B_Λ^{EF}. Hence, under the assumption that both configurations possess equivalent representations of the anti-windup compensator state and input matrices, the reasoning in the previous section for static anti-windup compensation will apply to dynamic anti-windup compensation, and this will be independent of Λ_1 being bi-proper or not. Therefore, again the full-authority feedback anti-windup configuration will be preferable. The fact that the full-authority external anti-windup configuration is again preferable agrees with intuition and the insight offered by Grimm *et al.* [27] for the

case of plant order anti-windup compensation. Note that the existence of a similarity transformation between both configurations is not too restrictive for comparison purposes as it is intuitive to consider that both configurations add the same poles to Q^{-1} via the eigenvalues of A_Λ and also that it is always possible to find a nonsingular transformation matrix T whenever $\text{rank}(B_\Lambda^{\text{FA}}) = \text{rank}(B_\Lambda^{\text{EF}})$ [62].

In addition to conditions for full order anti-windup compensation, it is also evident that for *reduced order anti-windup compensation*, which corresponds to Q being less than loop transmission order, some configurations may be more favorable. This is simply shown by noting that some configurations can be seen to give a set of possible Q which is a subset of those of other configurations for a fixed order Λ. It is evident that all configurations offer a set of possible Q which are a subset of those given by the full-authority feedback anti-windup configuration, external feedback anti-windup configuration, or both. Evidently the generic anti-windup configuration gives a set of Q that is a subset of both. The dynamic conventional anti-windup gives a set of Q that is a subset of the full-authority feedback anti-windup case. The W&P configuration gives a set of Q which is a subset of the external feedback anti-windup case, more specifically in the W&P configuration part of the anti-windup compensator dynamics is fixed through $\mathcal{P}_{yu}^o$. Note that, due to the employment of $\mathcal{P}_{yu}^o$, this approach gives at least a full order anti-windup compensation. IMC only permits full order anti-windup compensation, with only one possible Q which is also a subset of the external feedback anti-windup case. From this perspective it is evident that for fixed (low) order anti-windup compensation, either the full-authority and external feedback anti-windup configurations should be employed. It should also be noted that other fixed-order synthesis approaches exist [28], where fixed dynamic elements are added to permit dynamic anti-windup compensator design via a static anti-windup synthesis problem. Such approaches are similar to the W&P configuration, where a subset

of the additional dynamics added by Q is fixed, in this case $\mathcal{P}^o_{yu}$. The advantage of such approaches is that the static anti-windup compensation problem is convex, but this is not necessarily feasible, and additionally optimality of the resulting dynamic controller is lost[2].

Remark 3.2. Note that in Grimm *et al.* [27], Remark 3, it is concluded that the full-authority and external feedback anti-windup configurations possess equivalent LMI feasibility conditions when $B_{g,y}$ is full row rank. But this conclusion was limited to the cases of full order and static anti-windup compensation. Importantly, Eqn. 3.130 shows that the choice of full-authority or external feedback anti-windup configuration has no effect provided $B_{g,y}$ is full row rank, and this is independent of the anti-windup compensator order. ◁

2. Override compensation

a. Static override compensation

For static override compensation with $Q = I_{n_z}$ and $\bar{Q} = I_{n_u}$, the poles of $\hat{\mathcal{P}}_{zu}$ ($\hat{\mathcal{P}}_{yu}$) are modified via $\tilde{H}_1$ ($\bar{H}_1$) and the zeros are modified via both $\tilde{H}_1$ and $\tilde{H}_2$ ($\bar{H}_1$ and $\bar{H}_2$). Hence independently employing both DOF is desirable, as it permits maximum control over the poles and zeros of $\hat{\mathcal{P}}_{zu}$ ($\hat{\mathcal{P}}_{yu}$). On the other side, for static override compensation with $Q = (I_{n_z} + U_{zu}\mathcal{G}_{v_1 s} D_{\Theta_1})^{-1}$ and $\bar{Q} = (I_{n_u} + \mathcal{G}_{v_1 s} D_{\Theta_1} \bar{U}_{zu})^{-1}$, both poles and zeros of $\mathcal{P}_{zu}$ ($\mathcal{P}_{yu}$) are modified by $\tilde{H}_1$, $\tilde{H}_2$ ($\bar{H}_1$, $\bar{H}_2$) and the corresponding Q ($\bar{Q}$). From previous analysis, the override compensation problem here considered does not permit independent control of $\tilde{H}_1$ and $\tilde{H}_2$ ($\bar{H}_1$ and $\bar{H}_2$), as they both depend

[2]It should be noted that, for fixed low order anti-windup compensator design, the anti-windup compensation problem will generally not be convex, as it is not full order [21, 63]. Looking at the anti-windup compensation design from the perspective of a matrix inequality approach may then result in a set of BMIs rather than LMIs.

on $\tilde{D}_\Theta$. Still, some configurations present certain advantages over others, specially those that exploit all the available DOF, $\tilde{H}_1$, $\tilde{H}_2$ and Q ($\bar{H}_1$, $\bar{H}_2$ and $\bar{Q}$), being GOC for controller state/output and GOC for controller input/output. Note that these configurations are the ones that take advantage of all the freedom provided by $\mathcal{G}_v$. Hence, by comparing these configurations in terms of their relative applicability, we see that they provide the same override compensator when:

$$\begin{bmatrix} B_{g,y} & 0 \\ D_{g,y} & I_{n_u} \end{bmatrix} \begin{bmatrix} D_{\Theta_1} \\ D_{\Theta_2} \end{bmatrix}^{\mathrm{IO}} = \begin{bmatrix} D_{\Theta_1} \\ D_{\Theta_2} \end{bmatrix}^{\mathrm{SO}}, \tag{3.131}$$

where $(\cdot)^{\mathrm{IO}}$ and $(\cdot)^{\mathrm{SO}}$ denote the override compensators affecting the input/output and state/output of the unconstrained controller, respectively. The satisfaction of the equality in Eqn. 3.131 requires $B_{g,y}$ to be full row rank. This implies that the unconstrained controller $\mathcal{G}_y$ must have as many inputs as states. In practice, this is not always the case, hence we would prefer to choose static override compensation affecting the unconstrained controller states and output.

b. Dynamic override compensation

As done in the previous case, to describe the effect of the strictly proper components of Θ_1 and Θ_2 on Q and $\bar{Q}$, we choose the configurations that provide more control over the parameters $\tilde{H}_1$, $\tilde{H}_2$ ($\bar{H}_1$, $\bar{H}_2$) and the corresponding Q ($\bar{Q}$). It is difficult to generally describe the effect of Q ($\bar{Q}$) on the override control system. Hence, here an extra consideration for comparison is based on the order of Θ_{1s} and Θ_{2s} necessary to give a Q ($\bar{Q}$) being loop transmission ($\mathcal{G}_y\mathcal{P}_{yu}$) plus plant order ($\mathcal{P}_{zu}$ or $\mathcal{P}_{yu}$), termed full order override compensation, and the choice of Θ_{1s} and Θ_{2s} for reduced order override compensation. Compared to the anti-windup compensation case, the order of Q ($\bar{Q}$) for the full order case in override compensation is bigger because,

for override compensation, the unconstrained controller dynamics is embedded in Q ($\bar{Q}$). Then, Q ($\bar{Q}$) is not only a function of the coprime factors of the plant and the override compensator but also a function of the unconstrained controller. Based on this reasoning, for full order override compensation, only one configuration requires Θ to be loop transmission order, and this is the configuration that only affects the unconstrained controller output, GOC for controller output, thus taking no advantage of the unconstrained controller dynamics. For the other configurations that do so, the order of Θ required for full order override compensation is that of the plant. From these configurations, there are only two that provide the most control over $\tilde{H}_1$ and $\tilde{H}_2$ ($\bar{H}_1$ and $\bar{H}_2$), and they are the ones that exploit all the available freedom in $\mathcal{G}_v$. The relative utility of either of the latter configurations can be quantified after certain assumptions. Suppose that the state and input matrices for each configuration are related through a similarity transformation $\{A_\Theta^{\text{SO}}, B_\Theta^{\text{SO}}\} \rightarrow \{T^{-1}A_\Theta^{\text{IO}}T, T^{-1}B_\Theta^{\text{IO}}\}$, then Q ($\bar{Q}$) in Eqns. 3.85 and 3.94 (Eqns. 3.86 and 3.95) will clearly differ due to the presence of C_Θ and U_{zu} (a function of $\tilde{H}_1$ and $\tilde{H}_2$) in its dynamics; this seems to be an additional consideration to that in the static case. Interestingly, under the proposed consideration, the two configurations can only render the same override compensator, or equivalently the same Q ($\bar{Q}$), U_{zu} and V_{zu} ($\bar{U}_{*u}$ and $\bar{V}_{*u}$), when:

$$\begin{bmatrix} B_{g,y} & 0 \\ D_{g,y} & I_{n_u} \end{bmatrix} \begin{bmatrix} D_{\Theta_1} & C_{\Theta_1} \\ D_{\Theta_2} & C_{\Theta_2} \end{bmatrix}^{\text{SO}} \begin{bmatrix} I_{n_z} & 0 \\ 0 & T \end{bmatrix} = \begin{bmatrix} D_{\Theta_1} & C_{\Theta_1} \\ D_{\Theta_2} & C_{\Theta_2} \end{bmatrix}^{\text{IO}}, \tag{3.132}$$

with $(\cdot)^{\text{IO}}$ and $(\cdot)^{\text{SO}}$ defined as in the static case. Therefore, again, dynamic override compensation affecting the unconstrained controller states and output is preferable.

For reduced order override compensation either of the latter override configurations analyzed should be employed, as they best employ the available DOF of override compensation. Other fixed-order synthesis approaches may also be obtained, as in the

case of anti-windup compensation, where some fixed dynamics elements were added to the override compensator dynamics and the synthesis problem was defined only in terms of static elements.

D. Comparison of remedial architectures based on the mismatch system

The mismatch structure has been proposed and considered by several researchers, although the generalization to uncertain systems has differed. To analyze the effect of the choice of configuration on robust remedial compensation, the general architecture for remedial compensation can be considered within the mismatch setting.

For convenience the discussion is separated into three sections, which consider i) analysis of the poles and zeros of the mismatch structure, for both open and closed-loop transfer functions; ii) comparison of configurations based on the previous analysis; and iii) the mismatch system insights.

1. Analysis of the mismatch system poles and zeros

a. Anti-windup compensation

Poles of L_n^u, T_n^u and $\mathcal{P}_{zu}S_n^u$

The equations for the mismatch system show that generally the poles of the open-loop mismatch L_n^u system are a function of those of the loop transmission $L = \mathcal{G}_y\mathcal{P}_{yu}$, V and Q, and the poles of the closed-loop mismatch system T_n^u are a function of those of the unconstrained closed-loop system and those of Q^{-1}, V^{-1} and $\mathcal{P}_{zu}$. To be more precise, in the proceeding discussion, the poles of the open-loop are first considered, followed by those of the closed-loop, for which the case of static anti-windup compensation is first considered followed by the case of dynamic anti-windup compensation.

The poles of the open-loop mismatch system are easily defined through those of $\mathcal{P}_{yu}$ and QU and therefore Λ_1 and Λ_2. Generally they are those of $\mathcal{P}_{yu}$ and Q for dynamic anti-windup and those of $\mathcal{P}_{yu}$ and V for static anti-windup. Hence, it is evident that the choice of the anti-windup compensation can be made such that the open-loop mismatch system is stable provided that the poles of V are stable (requiring stabilizability of $\mathcal{G}_y$), $\mathcal{P}_{yu}$ is stable and the anti-windup compensator is also stable. Conversely, as the poles of the closed-loop mismatch system are generally those of the unconstrained closed-loop system, those of $V^{-1}Q^{-1}$ (except for any cancelation of the poles of $V^{-1}Q^{-1}$ with the zeros of $(I_{n_u} + \mathcal{G}_y\mathcal{P}_{yu})^{-1}$), and those of $\mathcal{P}_{zu}$, there is no freedom in the design to shift undesirable poles arising from the unconstrained closed-loop system. One can only change the residual for the poles via the placement of the transmission zeros of the closed-loop mismatch system. This reinforces the idea that anti-windup is best employed when the unconstrained closed-loop system has favorable properties. It also has important implications on stability and zero placement, as discussed in the proceedings sections.

For a better understanding of the effect of the poles in the closed-loop mismatch structure, below we perform an analysis through coprime factorizations of the plant ($\mathcal{P}_{yu} = NM^{-1}$) and unconstrained controller ($\mathcal{G}_y = V^{-1}U$), and through the Bezout identity ($VM + UN = I_{n_u}$). The analysis focuses on the poles of T_n^u (see Eqn. 2.10), as the poles of T_n^u are also those of S_n^u and $\mathcal{P}_{zu}S_n^u$, with the latter also having the poles of the plant $\mathcal{P}_{zu}$, which cannot be modified.

Considering the static anti-windup case ($Q = I_{n_u}$), T_n^u from Eqn. 2.10, after substitution of the corresponding coprime factors, gives:

$$T_n^u = I_{n_u} - (I_{n_u} + V^{-1}UNM^{-1})^{-1}V^{-1} = I_{n_u} - M(VM + UN)^{-1}. \tag{3.133}$$

For the case when the coprime factorizations are of minimum order and the

Bezout identity holds, the coprime factorizations are *unique* [23, 64]. The coprime factorizations, with unique coprime factors, are defined as $\mathcal{G}_y = V_u^{-1}U_u$ and $\mathcal{P}_{yu} = N_u M_u^{-1}$, where the poles of $V_u(U_u)$ and $N_u(M_u)$ are distinct subsets of the poles of the unconstrained closed-loop system. Consequently, $\Lambda_1 = D_{\Lambda_1}$ and $\Lambda_2 = D_{\Lambda_2}$ are also uniquely defined, being Λ_{u1} and Λ_{u2}, and there is no synthesis problem.

The objective of the anti-windup compensator is to synthesize a Λ_1 and Λ_2, which will generally not be those Λ_{u1} and Λ_{u2} that satisfy the Bezout identity with minimal coprime factor orders. When Λ_1 and Λ_2 are designed to satisfy some synthesis problem, the minimum order coprime factors $U = U_1$ and $V = V_1$ are determined and, $M = M_1$ and $N = N_1$ are then uniquely defined when the Bezout identity is required to hold. Notably, the orders of M_1 and N_1 will be greater than those of M_u and N_u [64]. This can be expressed as follows:

$$\begin{aligned} U_u N_u + V_u M_u &= I_{n_u}, \\ U_1 N_1 + V_1 M_1 &= I_{n_u}, \end{aligned} \tag{3.134}$$

where:

$$\begin{aligned} V_1 &= \mathcal{K} V_u, \\ U_1 &= \mathcal{K} U_u, \end{aligned} \tag{3.135}$$

$$\begin{aligned} N_1 &= N_u \mathcal{K}^{-1}, \\ M_1 &= M_u \mathcal{K}^{-1}, \end{aligned} \tag{3.136}$$

$$\mathcal{K} = V_1 V_u^{-1}, \tag{3.137}$$

with the coprime factors of the plant $\mathcal{P}_{yu}$ (M_1 and N_1) being the order of the unconstrained closed-loop system. Hence, while in the general case we have Eqn. 3.133 for T_n^u, given U and V from the static anti-windup compensation synthesis problem solution, it is always possible to choose M and N, without loss of generality[3], such

[3]This analysis must be performed for each specific plant case in an uncertain plant family. However, this does not limit the results of the analysis to nominal systems and the results of this section hold for the entire plant family.

that the Bezout identity holds, giving:

$$T_n^u = I_{n_u} - M. \tag{3.138}$$

In the case when Λ_1 and Λ_2 give $U = U_u$ and $V = V_u$, then:

$$T_n^u = I_{n_u} - M_u, \tag{3.139}$$

and therefore T_n^u has order equal to the plant and the poles are a proper subset of the unconstrained closed-loop system. In the general case that Λ_1 and Λ_2 give $U \neq U_u$ and $V \neq V_u$, then:

$$T_n^u = I_{n_u} - M_1 = I_{n_u} - M_u V_u V_1^{-1}, \tag{3.140}$$

and T_n^u is of order equal to that of the unconstrained closed-loop system and the poles are those of the unconstrained closed-loop system.

For the case where a dynamic anti-windup compensation is employed (Q being dynamic), T_n^u is defined in terms of the coprime factorizations of the plant and the unconstrained controller:

$$T_n^u = I_{n_u} - M(VM + UN)^{-1}Q^{-1}. \tag{3.141}$$

The reasoning for the poles of T_n whenever $D_{\Lambda_1} \neq 0$ and the Bezout identity holds is similar to that as above, with the remaining poles defined by those of Q^{-1}, except for any cancelation of the poles of Q^{-1} with the zeros of M. This is seen in the following expressions, where we can have either:

$$T_n^u = I_{n_u} - M_u Q^{-1}, \tag{3.142}$$

or

$$T_n^u = I_{n_u} - M_1 Q^{-1} = I_{n_u} - M_u V_u V_1^{-1} Q^{-1}. \tag{3.143}$$

Notably, the poles of T_n^u comprise the poles of the unconstrained closed-loop and the poles of the anti-windup compensator. Hence, the order of T_n^u is that of the unconstrained closed-loop plus that of the anti-windup compensator.

Note that when $D_{\Lambda_1} = 0$ ($D_{\Lambda_2} \neq 0$), it is not possible to modify the coprime factors of the unconstrained controller, and therefore $U = \tilde{H}_2\mathcal{G}_y$ and $V = \tilde{H}_2$. It is important to note that we can still try to satisfy the Bezout identity by following similar reasoning as before for U_1 and V_1. Again, the resulting T_n^u will have as its poles those of the unconstrained closed-loop and those of the anti-windup compensator, whenever the anti-windup compensator is dynamic. Otherwise, for the static anti-windup compensator case, the poles of T_n^u will be those of the unconstrained closed-loop. Consequently, the implications of having $D_{\Lambda_1} = 0$ are not directly seen in the poles.

Remark 3.3. Observing Q from the previous definition of the general architecture for anti-windup compensation, the poles of Q^{-1} are those of the coprime factors of the unconstrained controller and those of anti-windup compensator Λ. Note that for the general case of anti-windup synthesis, the poles of the coprime factors of the unconstrained controller are canceled by the zeros of M in the equation for T_n^u and hence play no role through Q. Rather, the effect of the poles of the coprime factors of the unconstrained controller is seen in the transmission zeros of the closed-loop mismatch system, as observed in the analysis in the next subsection. $\lhd$

Remark 3.4. Note that it is possible to choose Q to cancel poles of the unconstrained closed-loop system in T_n. However, this will only hold for one specific case (i.e. one set of the closed-loop poles) in the uncertain family of unconstrained closed-loop systems, as discussed in the following subsections. $\lhd$

Zeros of L_n^u, T_n^u *and* $\mathcal{P}_{zu}S_n^u$

The zeros of the mismatch system are more interesting. As anti-windup compensation can be seen as a feedforward control problem, it is the zeros of the mismatch system that are of particular interest. Here we restrict our attention to the zeros of the closed-loop mismatch system, as with the poles of the closed-loop mismatch system generally being invariant to anti-windup compensation, it is the zeros that must be carefully chosen. Similar analysis could be done for the zeros of the open-loop mismatch system.

For the closed-loop mismatch system, the zeros of $\mathcal{P}_{zu}S_n^u$ and S_n^u can be easily defined, as described below. However, for the case of T_n^u, the analysis is more difficult and involved[4]. To overcome this, the zeros of T_n^u are considered from two perspectives. First, we consider the zeros of T_n^u for an invertible MIMO system, and hence the zeros are directly defined via the state-state matrices. However, only the static case is considered for simplicity. The second perspective considers a SISO system. In this case the zeros are defined for both static and dynamic anti-windup compensation, in terms of the numerator and denominator polynomials for the system elements.

In a similar manner to the analysis for the poles, employing the coprime factors of the plant and unconstrained controller, together with the Bezout identity, we have the following for $\mathcal{P}_{zu}S_n^u$:

$$\begin{aligned} \mathcal{P}_{zu}S_n^u &= \mathcal{P}_{zu}(I_{n_u} + \mathcal{G}_y\mathcal{P}_{yu})^{-1}V^{-1}Q^{-1}, \\ &= \mathcal{P}_{zu}M(UN+VM)^{-1}Q^{-1} = \mathcal{P}_{zu}MQ^{-1} = \mathcal{P}_{zu}M_uV_uV^{-1}Q^{-1}, \end{aligned} \tag{3.144}$$

where for the static case ($Q = I_{n_u}$), the zeros of $\mathcal{P}_{zu}S_n$ are the zeros of $\mathcal{P}_{zu}$, the zeros of M_u (i.e. poles of the plant $\mathcal{P}_{yu}$) and the poles of V, and for the dynamic case

[4]In general the transmission zeros of a transfer function matrix are difficult to explicitly define in terms of the control parameters, as they arise from the solution of a generalized eigenvalue problem.

($Q \neq I_{n_u}$) the zeros are those of $\mathcal{P}_{zu}$, M_u and Q^{-1}.

The equations for S_n^u are similarly defined. The zeros of S_n^u are those of M_u plus the poles of V for the static case, and those of M_u and Q^{-1} for the dynamic case, as seen from equation below:

$$\begin{aligned} S_n^u &= (I_{n_u} + \mathcal{G}_y\mathcal{P})^{-1}V^{-1}Q^{-1}, \\ &= M(UN + VM)^{-1}Q^{-1} = MQ^{-1} = M_uV_uV^{-1}Q^{-1}. \end{aligned} \tag{3.145}$$

The definition of the zeros of T_n^u is performed as follows:

MIMO case (T_n^u). When T_n^u is bi-proper, with its feedthrough matrix being invertible, for either static or dynamic anti-windup compensation its zeros are given by the solutions λ of the equation:

$$\det(\lambda I - A_n + B_nD_n^{-1}C_n) = 0, \tag{3.146}$$

with (A_n, B_n, C_n, D_n) being the state space matrices for T_n^u.

In this situation, it is possible to describe the zeros of T_n^u as a function of the static anti-windup variables D_{Λ_1} and D_{Λ_2}, and Q, and therefore Λ_{1s} and Λ_{2s}, for the dynamic case. Limiting the consideration to the static case ($Q = I_{n_u}$) for simplicity, the zeros are given by the solutions of the equation below, where, in addition to static anti-windup compensation, it is assumed that (i) $D_{g,y} = 0$ and $D_{p,yu} = 0$ for simplicity, and (ii) $\tilde{n}_{\mathcal{P}_{yu}} = \tilde{n}_{\mathcal{G}_y}$:

$$\begin{aligned} &\det(\underline{\lambda}\Omega\underline{\lambda} - \underline{\lambda}\Omega A_p - (A_g + \tilde{H}_1(\tilde{H}_2 - I_{n_u})^{-1}C_g)\Omega\underline{\lambda} \\ &+A_g\Omega A_p + B_{g,y}C_{p,yu} + \tilde{H}_1(\tilde{H}_2 - I_{n_u})^{-1}C_g\Omega A_p) = 0, \end{aligned} \tag{3.147}$$

where $\underline{\lambda} = \lambda I_{n_u}$, and

$$\Omega = (B_{p,yu}(\tilde{H}_2 - I_{n_u})^{-1}\tilde{H}_2C_g)^{-1}. \tag{3.148}$$

This representation is however not particularly insightful.

SISO case (T_n). For the SISO case it is possible to describe the elements of T_n^u via their numerator and denominator polynomials. This gives:

$$T_n^u = \frac{\sigma d_{\Lambda_{2s}} d_{\Lambda_{1s}} - d_{\mathcal{P}_{yu}}(\tilde{H}_2^{-1}\kappa d_{\Lambda_{2s}} d_{\Lambda_{1s}} + d_{\mathcal{G}_y} n_{\Lambda_{2s}} d_{\Lambda_{1s}} + d_{\mathcal{G}_y} D_{g,v} d_{\Lambda_{2s}} n_{\Lambda_{1s}} + n_C d_{\Lambda_{2s}} n_{\Lambda_{1s}})}{\sigma d_{\Lambda_{2s}} d_{\Lambda_{1s}}}, \tag{3.149}$$

where $\mathcal{P}_{yu} = \frac{n_{\mathcal{P}_{yu}}}{d_{\mathcal{P}_{yu}}}$, $\mathcal{G}_y = \frac{n_{\mathcal{G}_y}}{d_{\mathcal{G}_y}}$, $V = \frac{\tilde{H}_2 d_{\mathcal{G}_y}}{\kappa}$, $\Lambda_{2s} = \frac{n_{\Lambda_{2s}}}{d_{\Lambda_{2s}}}$, $\Lambda_{1s} = \frac{n_{\Lambda_{1s}}}{d_{\Lambda_{1s}}}$, $C = \frac{n_C}{\tilde{H}_2 \kappa}$, $\kappa = \det(sI_{n_g} - A_g + \tilde{H}_1 C_g)$ and $\sigma = (d_{\mathcal{P}_{yu}} d_{\mathcal{G}_y} + n_{\mathcal{G}_y} n_{\mathcal{P}_{yu}})$; with all the denominator polynomials being monic.

From this expression for T_n^u, it is possible to see how the zeros of T_n^u can be modified using the anti-windup compensation elements and selecting an appropriate configuration. Note that this equation also serves to confirm the definition of the poles of T_n^u for the SISO case. Additionally, considering only the properness of T_n^u, for a strictly proper plant (i.e. any physical system), it is clear that T_n^u will be strictly proper if $\tilde{H}_2 = 1$ ($\tilde{D}_{\Lambda_2} = 0$), otherwise T_n^u will be bi-proper.

b. Override compensation

An analysis of poles and zeros of the mismatch system for override compensation is quite similar to the anti-windup case.

Using coprime factorizations of the unconstrained controller ($\mathcal{G}_y = \bar{M}_y^{-1}\bar{N}_y$) and plant ($\mathcal{P}_{zu} = V_{zu}^{-1}U_{zu} = \bar{U}_{zu}\bar{V}_{zu}^{-1}$, $\mathcal{P}_{yu} = \bar{U}_{yu}\bar{V}_{yu}^{-1}$), along with the Bezout identity ($\bar{N}_y\bar{U}_{yu} + \bar{M}_y\bar{V}_{yu} = I_{n_y}$), Eqns. 2.16, 2.18 and 2.19 can be rewritten as:

$$L_n^z = (I_{n_z} + \bar{U}_{zu}\bar{V}_{zu}^{-1}\bar{V}_{yu}\bar{M}_y\mathcal{G}_v\Theta)^{-1} - I_{n_z}, \tag{3.150}$$

$$T_n^z = -\bar{U}_{zu}\bar{V}_{zu}^{-1}\bar{V}_{yu}\bar{M}_y\mathcal{G}_v\Theta, \tag{3.151}$$

$$F_n^y = -\bar{U}_{yu}\bar{M}_y\mathcal{G}_v\Theta. \tag{3.152}$$

Different from the case of anti-windup compensation, the poles and transmission zeros of the open-loop mismatch system L_n^z cannot be directly specified from the corresponding equation above. Note that this implies having no extra assumptions on the location of poles and zeros of the plant and unconstrained controller. Importantly, the only assumption we have is that of well-posedness of the unconstrained closed-loop. Moreover, implicit assumptions are the stabilizability and detectability of the plant, and the stabilizability of the unconstrained controller.

Poles of T_n^z and F_n^y

From the uniqueness of the coprime factorizations [64], the poles of the mismatch system (i.e. T_n^z in Eqn. 3.151) are the poles of the unconstrained closed-loop system plus additional poles introduced by the override compensator Θ. This is concluded after observing that the coprime factors $\bar{V}_{zu}$ and $\bar{V}_{yu}$ are equal, the poles of $\mathcal{G}_v$ get canceled with the zeros of $\bar{M}_y$, and $\bar{U}_{zu}$ and $\bar{U}_{yu}$, coprime factors of different elements of the plant, share the same poles. Notably, the smallest set of poles of the closed-loop mismatch system corresponds to the static override compensation case, i.e. unconstrained closed-loop poles. Similar to the anti-windup case, there is no freedom in the override design to shift undesirable poles arising from the unconstrained closed-loop system. One can only change the residual for the poles via the placement of the transmission zeros of the closed-loop mismatch system. This also reinforces the fact that both anti-windup and override compensation as remedial strategies are best employed when the unconstrained closed-loop system has favorable properties.

The poles of F_n^y are those of the unconstrained closed-loop plus those of Θ (note the cancelation of the zeros of $\bar{M}_y$ with the poles of $\mathcal{G}_v$).

Zeros of T_n^z and F_n^y

Contrary to the anti-windup compensation case, for override compensation the zeros of T_n^z are well defined. The zeros of T_n^z are those of $\bar{U}_{zu}$ and $\mathcal{G}_v$ for static override compensation, and those of $\bar{U}_{zu}$, $\mathcal{G}_v$ and Θ for dynamic override compensation. The zeros of F_n^y are also clearly defined, being those of $\bar{U}_{yu}$, $\mathcal{G}_v$ and Θ.

2. Comparison of remedial architectures based on the mismatch system poles and zeros

In this section the configurations presented in Section III.B. are analyzed and compared based on the results of Section III.D.I.

a. Anti-windup compensation

Poles of L_n^u and T_n^u

The issue of the poles of the mismatch system is generally trivial. As discussed in Section III.D.1.a., assuming no pole-zero cancelations related to the plant dynamics, the poles of the open-loop mismatch system are simply those of $\mathcal{P}_{yu}$ and QU and the poles of the closed-loop mismatch system are the poles of the unconstrained closed-loop system plus any zeros of QV (with the exception of the zeros of $(I_{n_u} + \mathcal{G}_y\mathcal{P}_{yu})^{-1}$) and $\mathcal{P}_{zu}$, accordingly. However, the case of pole-zero cancelations needs to be considered, as it is implicitly built into the configuration of W&P in the case of the closed-loop mismatch system. Here we first consider the issue of pole-zero cancelation by analyzing the W&P configuration for the closed-loop mismatch system. More specifically, T_n^u is considered as the poles of S_n^u and $\mathcal{P}_{zu}S_n^u$ can be obtained with similar considerations. Pole-zero cancelations in the open-loop mismatch system are then briefly discussed.

In the case of W&P, the incorporation of the nominal plant $\mathcal{P}_{yu}^o$ into the dynamics

of Λ modifies Q correspondingly, such that it becomes:

$$Q = \left[(V_W + U_W P_{yu}^o)\hat{M}\right]^{-1}, \tag{3.153}$$

where U_W and V_W are defined accordingly via $\hat{M}$ (i.e. Λ_1 and Λ_2).

Considering the analysis for the plant being nominal $\mathcal{P}_{yu} = \mathcal{P}_{yu}^o$, T_n is defined as in Eqn. 3.143 giving:

$$\begin{aligned} T_n &= I_{n_u} - M_W Q^{-1} = I_{n_u} - M_u \mathcal{R}^{-1} V_W (I_{n_u} + \mathcal{G}_y \mathcal{P}_{yu}^o)\hat{M} \\ &= I_{n_u} - M_u V_u (I_{n_u} + \mathcal{G}_y \mathcal{P}_{yu}^o)\hat{M} = I_{n_u} - \hat{M}, \end{aligned} \tag{3.154}$$

and the poles of T_n^u are defined to be those of $\hat{M}$. In this case Q effectively cancels the poles of the unconstrained closed-loop system and adds new poles to the closed-loop mismatch system, being those of $\hat{M}$. Hence, this method exploits the potential of pole-zero cancelations with plant dynamics involved, in the definition of the closed-loop mismatch system.

Note that employing this cancelation results in the closed-loop transfer functions defining the mismatch system possessing different poles to those defined above. This can be seen from $T_n^u = I_{n_u} - \hat{M}$ and $S_n = \hat{M}$ having the same poles but $\mathcal{P}_{zu} S_n^u = \mathcal{P}_{zu}\hat{M}$ having the additional poles of $\mathcal{P}_{zu}$.[5]

For the specific case that $\hat{M}$ is chosen such that it represents the denominator M_o in a right coprime representation of the plant $N_o M_o^{-1}$, the W&P configuration [26] corresponds to that of T&K [19]. In this case T_n^u is defined as

$$T_n^u = I_{n_u} - M_o. \tag{3.155}$$

The advantage of synthesizing M_o is that it represents a pole allocation problem given

[5]Hence, internal stability will not be guaranteed by simply ensuring that T_n^u and S_n^u are stable, as the pole-zero cancelations may give rise to hidden unstable modes in the mismatch system.

by the calculation of a gain matrix F as defined in Eqns. 3.71 or 3.77.

From the calculations above, it may seem that the W&P and T&K configurations provide favorable features compared to other configurations, in that they permit arbitrarily allocation of the poles of T_n^u. However, the basis for this is the cancelation of the unconstrained closed-loop poles, as observed in Eqn. 3.89, and this does not hold in the presence of uncertainty. When uncertainty is present, Eqn. 3.154 becomes:

$$T_n = I_{n_u} - M_W Q^{-1} = I_{n_u} - (I_{n_u} + \mathcal{G}_y \mathcal{P}_{yu}^{\Delta})^{-1}(I_{n_u} + \mathcal{G}_y \mathcal{P}_{yu}^{o})\hat{M} \tag{3.156}$$

and, as in the other configurations, the poles of T_n^u are the poles of the unconstrained closed-loop system plus the additional dynamic introduced by Q^{-1} (poles of $\mathcal{P}_{yu}^{o}$ and the unconstrained controller $\mathcal{G}_y$ and the poles of $\hat{M}$). In the T&K configuration [19], we have the poles of T_n^u to be the poles of the unconstrained closed-loop together with the poles of M_o and $\mathcal{G}_y$. Hence, it can be concluded that the possibility of exploiting pole-zero cancelation to permit arbitrary allocation of the poles of the closed-loop mismatch system is limited in practice, as it does not hold for uncertain systems. It is important to emphasize that in the case of the other configurations, the results previously stated do not change whenever uncertainty is considered.

For the case of the open-loop mismatch system poles, these are given by those of $\mathcal{P}_{yu}$ and QU, as seen in Eqn. 3.36 and discussed in Section III.D.2.a. In the dynamic case, the choice of the zeros of Q offers the potential to arbitrarily define the poles of the open-loop mismatch system by canceling the poles of $\mathcal{P}_{yu}^{\Delta}$. However, this is again limited in practicality, as it does not hold for uncertain systems. Therefore, it can be stated that, in practice, a subset of the poles of the closed-loop and open-loop mismatch systems are invariant to the design of the ant-windup compensator. These are given by the poles of the unconstrained closed-loop system plus the poles of the plant $\mathcal{P}_{zu}$ and $\mathcal{P}_{yu}$ for the closed-loop and open-loop mismatch systems, respectively.

Zeros of T_n^u and $\mathcal{P}_{zu}S_n^u$

As described in Section III.D.1.a., the true effect of the anti-windup compensation can be seen as the allocation of the zeros of the closed-loop mismatch system. Section III.D.1.a. presented equations for zeros of T_n^u for both the MIMO case (static) and the SISO case, together with the MIMO descriptions of the zeros of S_n^u and $\mathcal{P}_{zu}S_n^u$. The equations for the MIMO case transmission zeros are not insightful for T_n^u and L_n^u in their current form, and are therefore not discussed. However, the equations for S_n^u and $\mathcal{P}_{zu}S_n^u$ are simpler and are discussed below. The equations for the SISO case of T_n^u are more insightful and are considered here to analyze the zeros, for both the dynamic and static anti-windup compensation, and to compare the configurations.

The equations for the zeros of $\mathcal{P}_{zu}S_n^u$ are given in Section III.D.1.a, and the equations for S_n^u are similarly defined. As in the case of the poles of the closed-loop mismatch system, the W&P configuration [26] is of interest, due to the pole-zero cancelations that arise in this configuration. For W&P, the zeros of $\mathcal{P}_{zu}S_n^u$ can be derived from Eqn. 3.145, and given by:

$$\mathcal{P}_{zu}S_n^u = \mathcal{P}_{zu}^o\hat{M}. \tag{3.157}$$

In this case, the zeros of $\mathcal{P}_{zu}S_n^u$ are the zeros of the nominal plant $\mathcal{P}_{zu}^o$ and $\hat{M}$, the latter of which are completely free. In the case that $\hat{M} = M_o$, where M_o is a modified coprime factorization of the nominal plant $\mathcal{P}_{yu}^o$ of plant order, we have the T&K configuration [19] and:

$$\mathcal{P}_{zu}S_n = \mathcal{P}_{zu}^o M_o. \tag{3.158}$$

In this case, the zeros of $\mathcal{P}_{zu}S_n^u$ are simply the zeros of $\mathcal{P}_{zu}^o$ and M_o. However, if $\mathcal{P}_{zu}^o = \mathcal{P}_{yu}^o$, then $\mathcal{P}_{zu}^o M_o = N_o$ and the zeros of $\mathcal{P}_{zu}S_n^u$ are simply those of the plant $\mathcal{P}_{yu}^o$. Furthermore, as in the case of the poles of the closed-loop transfer matrices for

the mismatch system, when uncertainty is considered, the pole-zero cancelations no longer hold and the zeros will be those of the plant $\mathcal{P}_{zu}$, the coprime factorization of the plant $\mathcal{P}_{yu}$ (M) and Q^{-1}, as for the other configurations.

For the SISO case, a comparison of the configurations can be performed in terms of the allocation of the zeros of T_n^u via an algebraic approach using the equations of Section III.D.1.a. It can be observed from Eqn. 3.149 that, in general, the coefficients of the zero polynomial of T_n^u are nonlinearly dependent on the coefficients of the Λ_1 and Λ_2 that define the anti-windup compensator. Hence, it is difficult to make general statements on the ability to arbitrarily define the zeros of T_n^u through the design of the anti-windup compensator. However, when the poles of Λ_1 and Λ_2 are predefined, which they often are in frequency domain loop shaping and in robust low order design procedures, as they are the poles of T_n^u, the dependency becomes linear. For this degenerate case it can be observed that, in general, it is not possible to arbitrarily specify the zeros of T_n^u, irrespective of the order of the anti-windup compensator. This can be seen from Eqn. 3.149 in Section III.D.1.a. for T_n^u, where importantly for a $d_{\Lambda_{1s}}$ and $d_{\Lambda_{2s}}$ fixed and coprime there are $\tilde{n}_{\mathcal{G}_y}+\tilde{n}_{\Lambda_{1s}}+\tilde{n}_{\Lambda_{2s}}+\tilde{n}_{\mathcal{P}_{yu}}+1$ equations and $\tilde{n}_{\mathcal{G}_y}+\tilde{n}_{\Lambda_{1s}}+\tilde{n}_{\Lambda_{2s}}+1$ unknowns. Clearly this system of equations is overdetermined and hence may not offer a unique solution. However, when $d_{\Lambda_{1s}}=d_{\Lambda_{2s}}$, then there are $\tilde{n}_{\mathcal{G}_y}+\tilde{n}_{\Lambda_{1s}}+\tilde{n}_{\mathcal{P}_{yu}}+1$ equations and $\tilde{n}_{\mathcal{G}_y}+2\tilde{n}_{\Lambda_{1s}}+1$ unknowns. In this case, the system of equations can be underdetermined, overdetermined or uniquely defined, depending on $\tilde{n}_{\Lambda_{1s}}$ being greater than, less than, or equal to $\tilde{n}_{\mathcal{P}_{yu}}$, respectively. The uniquely defined case corresponds to the full order anti-windup compensation problem, which is the lowest order that provides convex feasibility conditions [21]. Hence, we see that for orders greater than or equal to that of the plant, the anti-windup compensation is convex and the zeros can be arbitrarily defined provided feasibility is achieved. Note that the analysis performed has been done just by considering the number of

equations and unknowns. More strictly speaking, for the uniquely defined case, we can refer to a linear system of equations whose matrix of coefficients is nonsingular. From Eqn. 3.149, this is not evident, as the matrix of coefficients is a function of $d_{\mathcal{P}_{yu}}$, $d_{\mathcal{G}_y}$, $n_{\mathcal{P}_{yu}}$ and $n_{\mathcal{G}_y}$ coefficients. Interestingly, full order anti-windup compensation is always feasible when the plant is asymptotically stable [21].

In the case of static compensation, where $\tilde{n}_{\Lambda_{1s}} = \tilde{n}_{\Lambda_{2s}} = 0$, the system will be overdetermined and therefore there may be no choice of $\tilde{H}_1$ and $\tilde{H}_2$ that solves for a given zero polynomial (note that $d_{\Lambda_{1s}} = d_{\Lambda_{2s}} = 1$). This can be seen from the following equations derived from Eqn. 3.149 in Section III.D.1.a.:

$$T_n^u = \frac{(d_{\mathcal{G}_y} d_{\mathcal{P}_{yu}} + n_{\mathcal{G}_y} n_{\mathcal{P}_{yu}}) - d_{\mathcal{P}_{yu}} (\tilde{H}_2^{-1} \kappa)}{d_{\mathcal{G}_y} d_{\mathcal{P}_{yu}} + n_{\mathcal{G}_y} n_{\mathcal{P}_{yu}}}. \tag{3.159}$$

In the case of the zero polynomial (numerator of T_n^u), we observe that there exist $\tilde{n}_{\mathcal{G}_y} + 1$ unknowns, being $\tilde{H}_2$ and the coefficients of the monic polynomial κ, for $\tilde{n}_{\mathcal{G}_y} + \tilde{n}_{\mathcal{P}_{yu}} + 1$ number of equations. Hence the problem is overdetermined. Note that this case corresponds to the anti-windup compensation problem being convex but not necessarily feasible, this occurs even though the plant is asymptotically stable [21].

The previous analysis for the zeros was generic, in that it was based on the general equations for the zeros in terms of the anti-windup compensator elements. However, the choice of anti-windup configuration has an additional effect on the ability to assign the zeros of T_n^u. This can be seen for both static and dynamic anti-windup compensation, as considered below.

For static anti-windup compensation there are $\tilde{n}_{\mathcal{G}_y} + \tilde{n}_{\mathcal{P}_{yu}} + 1$ equations to be solved to define the zeros. The full-authority and external feedback anti-windup augmentations possess $\tilde{n}_{\mathcal{G}_y} + 1$ unknowns, with the two configurations being equivalent whenever the invertibility condition defined through Eqn. 3.129 holds. The generic anti-windup configuration possesses only one unknown. The dynamic conventional

anti-windup possess $\tilde{n}_{\mathcal{G}_y} + 1$ pseudo unknowns, in that they are related through the definition of $\tilde{H}_1$ and $\tilde{H}_2$ (note that the W&P and IMC configurations do not give static anti-windup compensators). This difference between configurations comes as no surprise, as in the static case it is known from Section III.B.1. that some configurations are deficient in their ability to determine $\tilde{H}_1$ and $\tilde{H}_2$ independently via Λ_1 and Λ_2, and viceversa.

From dynamic anti-windup compensation, when $d_{\Lambda_{1s}} = d_{\Lambda_{2s}}$, then there are $\tilde{n}_{\mathcal{G}_y} + \tilde{n}_{\Lambda_{1s}} + \tilde{n}_{\mathcal{P}_{yu}} + 1$ equations to be solved to define the zeros. The difference between the configurations is essentially the same as that for the static case. The full-authority and external feedback augmentations possess $\tilde{n}_{\mathcal{G}_y} + 2\tilde{n}_{\Lambda_{1s}} + 1$ unknowns, being equivalent whenever the invertibility condition defined through Eqn. 3.130 holds. The generic anti-windup configuration possesses only $2\tilde{n}_{\Lambda_{1s}} + 1$ unknowns. The dynamic conventional anti-windup configuration possess $\tilde{n}_{\mathcal{G}_y} + 2\tilde{n}_{\Lambda_{1s}} + 1$ pseudo unknowns, in that they are again related through the definition of $\tilde{H}_1$ and $\tilde{H}_2$. The W&P configuration differs depending on the consideration of the nominal or uncertain plant case. For the nominal case, there is a cancelation as discussed in Section III.D.2.a, and there are $\tilde{n}_{\hat{M}} + 1$ equations to be solved and $\tilde{n}_{\hat{M}} + 1$ unknowns (note the equality). For the uncertain plant case there is no cancelation, and with $\mathcal{P}^o_{yu}$ strictly proper, there are $\tilde{n}_{\mathcal{G}_y} + \tilde{n}_{\mathcal{P}^{\Delta}_{yu}} + \tilde{n}_{\mathcal{P}^o_{yu}} + \tilde{n}_{\hat{M}} + 1$ equations to be solved and $\tilde{n}_{\hat{M}} + 1$ unknowns (note that uncertainty has destroyed the desirable equality property). For the IMC configuration, there is no synthesis problem.

From this consideration of the zeros of T^u_n, it would appear that no configuration generally provides a solvable set of equations (with the poles of Λ_1 and Λ_2 predefined), and hence no configuration permits arbitrary zero placement. This situation is typically worse for the static anti-windup case. Comparing the configurations, the full-authority and the external feedback augmentations possess the most favorable

properties. For these configurations, in the dynamic case with fixed and common poles for Λ_1 and Λ_2, it is possible to have a solvable set of equations whenever $\tilde{n}_{\Lambda_{1s}}$ (or $\tilde{n}_{\Lambda_{2s}}$) is equal to $\tilde{n}_{\mathcal{P}_{yu}}$, hence full order anti-windup compensation. The W&P and T&K configuration are again interesting, as they emphasize the importance of uncertainty. For the nominal case the system of equations is uniquely solved but when uncertainty is considered, the number of unknowns is much greater than the unknowns. Hence the practical consideration of uncertainty is important.

b. Override compensation

Similar considerations to the case of anti-windup compensation have to be taken whenever an override configuration arises. With the poles and zeros of T_n^z and F_n^y clearly defined, the analysis is simpler and can be focused only on the conditioning of the plant, and hence the configurations can be compared with respect to their internal structures and the freedom to allocate poles and zeros of the coprime factors of the plant. Care has to be taken when considering uncertainty, one can think about employing the zeros of the override compensator Θ to cancel some undesirable poles of the unconstrained closed-loop system in T_n^z or in F_n^y, however, this will only hold for a specific case of unconstrained closed-loop poles in a plant family.

3. Mismatch system insights

The mismatch system considered in Section II.D offers an ideal setting to consider the effect of the remedial compensators on the constrained systems, and hence compare the configurations. The mismatch system quantifies the response of the remedial closed-loop system relative to the unconstrained closed-loop (or output constrained) system, and hence the ability of the remedial system to recover the unconstrained (or output constrained) closed-loop system's response. Here we present insights that

are obtained by the consideration of remedial compensation through the mismatch system. These insights will be given in terms of design trade-offs and in terms of the clarity offered by both the LFT (Figs. 9 and 13) and feedforward (Fig. 11 and 15) representations of the remedial closed-loop system comprised of the unconstrained (or output constrained) closed-loop system and the mismatch system. This serves to clarify the properties of, and/or reasons for difficulty in, previous (anti-windup case) or potential (override case) designs.

a. Mismatch anti-windup insights

The mismatch system offers direct insight into the mechanisms involved in anti-windup compensation. This is because it isolates the effect of the anti-windup compensator on the ability of the anti-windup system response to recover the unconstrained responses. In the nominal plant case, the W&P configuration [26] is in a mismatch structure and therefore the analysis performed provides insights into the properties of the mismatch system. Namely, the modes of response and the quantification of the effect of saturation on the measured output of the anti-windup system via y_d, as defined therein. To extend this work to uncertain systems, it is necessary to consider the uncertain mismatch system as given by Eqns. 2.9-2.13 in Section II.D.1 and presented in Fig. 9, both for the general anti-windup architecture. From the equations of Section II.D.1, it is evident that the fundamental equation $T_n^u + S_n^u = I_{n_u}$ holds with the corresponding loop transmission being L_n^u. As the fundamental equation holds, the usual situation in feedback control arises, where there is an inherent trade-off between sensitivity and complementary sensitivity functions. As the mismatch system, and anti-windup compensation, only permits 1 DOF control through Λ, this is a very stringent trade-off.

Considering the W&P configuration [26] for the nominal plant case, this gives a

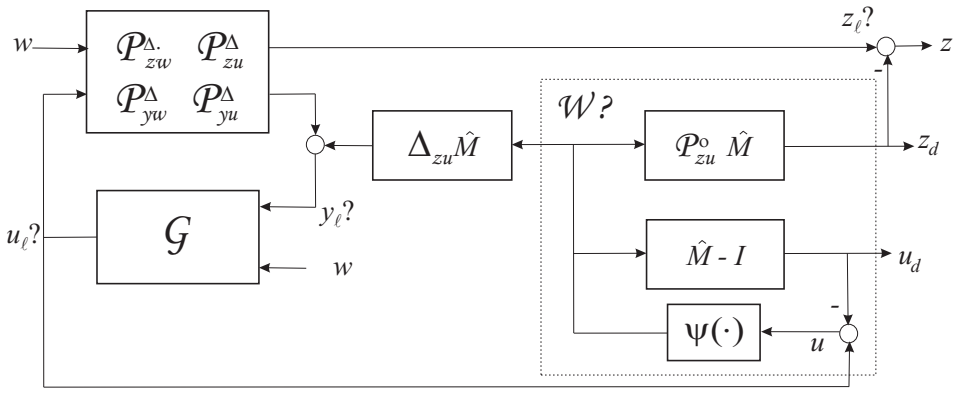

Fig. 19. W&P configuration for additive unstructured uncertainty.

trade-off between the modes of response of the mismatch system, specifically modes 2 and 3, with the system response in mode 2 being governed by T_n^u and in mode 3 being governed by $\mathcal{P}_{zu}S_n^u$, as seen in Fig. 11. In Weston and Potlethwaite [26] it was stated that an ideal design for modes 2 and 3 would be $T_n^u = 0$ and $T_n^u = I_{n_u}$ (i.e. $S_n^u = 0$), respectively. In the present formulation with Q, this corresponds to $QV = S$ and $QV \simeq \infty$, respectively. Clearly this represents a trade-off between modes.

From the graphical interpretation of the mismatch system, in both the LFT representation [30], as shown in Fig. 9, and the standard feedforward representation for nominal [26] and uncertain plant [65], as shown in Fig. 11, the underlying mechanism of anti-windup compensation becomes clear. This is, the design of the anti-windup compensator to minimize the effect of saturation on the output of the system, which can be quantified by the map between u_l and z_d in Figs. 9 and 11. Considering the graphical representation in Fig. 19, it can be seen that the representation of the W&P configuration for uncertain system [29] is not the mismatch system, as noted also therein (see also others [65]). The W&P in the mismatch system, accounting for additive uncertainty, is shown in Fig. 20 and comparing Figs. 19 and 20 it is clear why the design approach with Fig. 19 presented difficulties. Namely, the signals

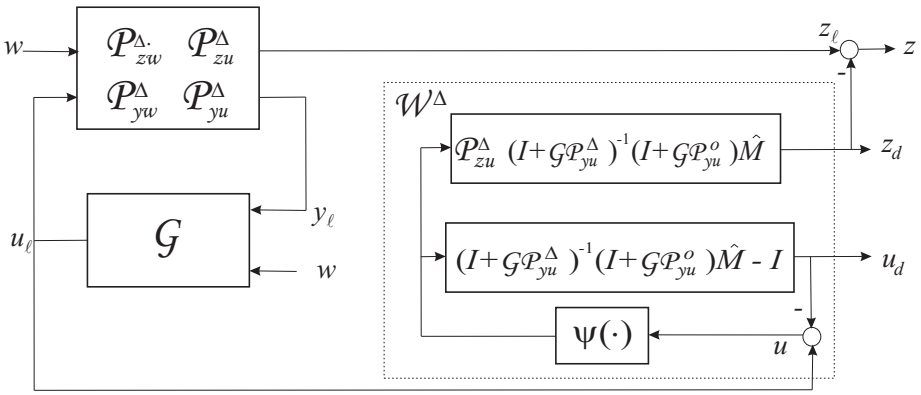

Fig. 20. W&P configuration in the mismatch structure.

considered for the maps do not directly address the basic properties of anti-windup compensation as stated in Section II.C.1.c. Specifically, using the signals in Fig. 19, it is not possible to directly and independently address the robust stability and robust performance goals in the design. As seen in Fig. 20, the relationship between ψu and z_d, which is $\mathcal{P}_{zu}S_n$ and defines the anti-windup system response in mode 3, is defined by $\mathcal{P}^{\Delta}_{zu}(I_{n_u} + \mathcal{G}_y\mathcal{P}^{\Delta}_{yu})^{-1}(I_{n_u} + \mathcal{G}_y\mathcal{P}^{o}_{yu})\hat{M}$, which is not evident in Fig. 19 and not considered in Turner *et al.* [29]. It is therefore evident that the design approach of [29] could be improved through the consideration of Fig. 20 and inclusion of the correct signal maps in the solution of the design problem.[6] [7]

The understanding of anti-windup compensation that results from the standard feedforward representation of Figs. 9 and 11 also provides insights into how the anti-windup compensation should be parameterized in terms of the unconstrained closed-

[6]In terms of the presentation in Galeani *et al.* [66], for the feedback configuration presented in Turner *et al.* [29], the anti-windup compensator is no longer recovering the response of the unconstrained closed-loop system after saturation occurs, but rather a perturbed unconstrained closed-loop system. As defined in Galeani *et al.* [66]: *the response of* $\sum_{UAW}$ *is different from* $\sum_{U}$.

[7]Note also that the T&K configuration [19], to the authors knowledge, has not been employed for anti-windup compensation synthesis with explicit consideration of robustness.

loop system control elements. Considering Fig. 11 and Eqns. 2.9-2.12 it is evident that the choice of a prefilter $\mathcal{F}$, while affecting the response of the unconstrained closed-loop system, does not affect the properties of the mismatch system whenever the plant uncertainty is linear. For the nonlinear uncertainty case, it becomes evident from Fig. 21 that the prefilter dynamics (incorporated in the exogenous input) is not employed to described the mismatch system, but rather its effect can be seen with the input η_l going to a nonlinear uncertainty perturbation. Such insights are useful, as seen when considering some designs [30], which includes the prefilter in the parameterization of the mismatch system and renders a conditioned controller $\hat{\mathcal{G}}$ (or equivalently Q) of increased order. By knowing the properties of the mismatch system in advance, this increase in order of the anti-windup compensator is made evident when placing the design of Grimm *et al.* [30] in the general anti-windup architecture, as shown in Fig. 21:

$$\begin{bmatrix} v_1^1 \\ v_1^2 \\ v_2 \end{bmatrix} = \underbrace{\begin{bmatrix} \tilde{\Lambda}_1^1 \\ \mathcal{F}_i\tilde{\Lambda}_1^2 \\ \tilde{\Lambda}_2 \end{bmatrix}}_{\Lambda} \psi(u), \tag{3.160}$$

where $v_1^1 \in \mathbb{R}^{n_g}$ is fed back to the unconstrained controller states, $v_1^2 \in \mathbb{R}^{n_f}$ is fed back to the unconstrained controller input, $v_2 \in \mathbb{R}^{n_u}$ goes to the unconstrained controller output, $\mathcal{F}_i = C_f(sI_{n_f} - A_f)^{-1}$ and $\tilde{\Lambda}^T = \begin{bmatrix} \tilde{\Lambda}_1^{1T} & \tilde{\Lambda}_1^{2T} & \tilde{\Lambda}_2^T \end{bmatrix}$ is the anti-windup compensator designed in Grimm *et al.* [30]. Interestingly, the prefilter dynamics that appear in part of the anti-windup compensator Λ modifies the corresponding Q parameter to:

$$Q_{\mathcal{F}} = (I_{n_u} + V\tilde{\Lambda}_{2s} + C\tilde{\Lambda}_{1s}^1 + U\mathcal{F}_i\tilde{\Lambda}_1^2)^{-1}, \tag{3.161}$$

where V, U and C are as defined in Eqns. 2.4, Eqn. 2.5 and Eqn. 3.9, respectively, and the subscript $(\cdot)_s$ denotes the strictly proper part of the transfer function matrix.

One can recall that the anti-windup design in Grimm *et al.* [30] is nominal plant order ($\tilde{n}_{\mathcal{P}^o}$) and therefore the minimum order of $Q_{\mathcal{F}}$ in Eqn. 3.134 becomes $\tilde{n}_{\mathcal{P}^o} + \tilde{n}_{\mathcal{G}} + \tilde{n}_{\mathcal{F}}$. Moreover, from Section III.A.1. we know that a nominal plant order anti-windup design for the full-authority configuration with an unconstrained controller not including the prefilter provides a parameter Q of order equal to $\tilde{n}_{\mathcal{P}^o} + \tilde{n}_{\mathcal{G}}$. It is then evident the increase of $\tilde{n}_{\mathcal{F}}$ in the order of $Q_{\mathcal{F}}$ with respect to Q, the latter obtained from a mismatch system not parameterized by the prefilter dynamics. One may think that the increase in order for the conditioned controller given by Eqn. 3.134 provides a better level of global performance, however this is not necessary true as observed from the following argument. The inclusion of the prefilter dynamics does not, theoretically, offer any benefit, as the IMC controller is a feasible solution with or without the prefilter. However, considering Q, we know that for the *same* order of the anti-windup compensator Λ, the use of the prefilter does allow one to exploit existing dynamics and arrive at anti-windup compensators Λ that are not possible without the prefilter. Importantly, these compensators do not offer any benefit from an optimal $\mathcal{L}_2$ setting when the anti-windup compensator Λ is plant order.

b. Mismatch override insights

The insights that the mismatch system provides for anti-windup compensation are very similar to the override compensation case. Figure 13 presents the override system in a cascade connection of the output constrained closed-loop system to the mismatch system. The former is stable by assumption, hence the stability of the conditioned system can be guaranteed by the stability of the mismatch system. The nonlinear loop in the mismatch system consists of a sector bounded nonlinearity $\varphi(\cdot, z_l))$ in a positive feedback loop with the transfer function matrix T_n^z. The stability analysis for this loop can be done by any well known stability criteria (e.g. Small Gain,

MIMO Circle, Popov). Provided the nonlinear loop is stable, the disturbance filter will be guaranteed stable if F_n^y is also stable. Observing the Eqns. 2.18 and 2.19, a requirement for stability is that the override compensator $\Theta \in \mathcal{RH}_\infty$. The analysis of performance can be centered around the disturbance filter F_n^y, and it is quite simple because F_n^y is a linear system. The objective of the disturbance filter is to reject the input $\psi(z)$ as quickly as possible. However, designing for F_n^y is not an easy task because the design parameter Θ, the override compensator, not only is present in the disturbance filter F_n^y, but also in the nonlinear feedback loop. Therefore designing for both T_n^z and F_n^y involves a compromise between the nonlinear loop and the disturbance filter.

Additional observations can also be made in terms of how the override design problem should be parameterized, i.e. which elements of the unconstrained closed-loop system have to be considered in the definition of the design problem. An important consideration is that of including or not the prefilter or disturbance dynamics corresponding to the exogenous input w in the design problem. Figure 15 shows that a possible prefilter dynamics, while affecting the response of the unconstrained closed-loop system and hence the input of the mismatch system $\psi(z_l)$, does not affect the properties of the mismatch system.

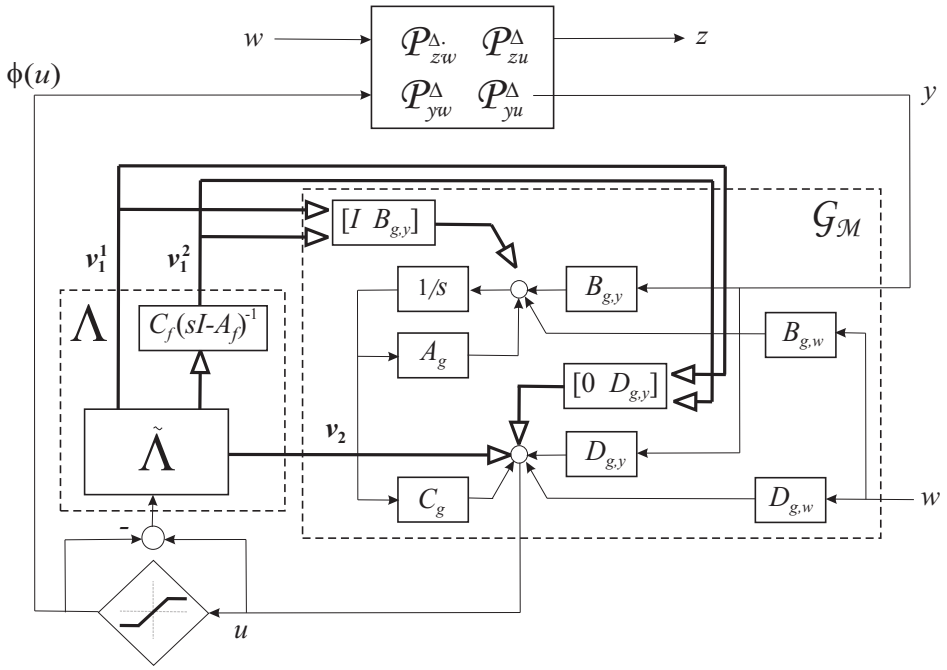

Fig. 21. Parameterization of the anti-windup compensator by the incorporation of the prefilter dynamics.

CHAPTER IV

GLOBAL, FINITE-GAIN ROBUST PERFORMANCE ANALYSIS OF REMEDIAL COMPENSATION

The following systems are introduced and will be used throughout this dissertation. Moreover, the finite performance gain of the remedial closed-loop augmented systems is determined.

A. Realization of the mismatch system

The design of remedial compensators necessitates the model of the plant and the realization of the modified unconstrained controller, the latter allowing for the inclusion of remedial compensation. The state space representations are specified in accordance with the definitions given in Chapter I. Then, the uncertain plant is given as:

$$\mathcal{P}^{\Delta} = \begin{bmatrix} \mathcal{P}^{\Delta}_{zw} & \mathcal{P}^{\Delta}_{zu} \\ \mathcal{P}^{\Delta}_{yw} & \mathcal{P}^{\Delta}_{yu} \end{bmatrix} \begin{cases} \dot{x}_p = A_p x_p + B_{p,\zeta}\zeta_p + B_{p,w} w + B_{p,u} u_p \\ \eta_p = C_{p,\eta} x_p + D_{p,\eta\zeta}\zeta_p + D_{p,\eta w} w + D_{p,\eta u} u_p \\ z_p = C_{p,z} x_p + D_{p,z\zeta}\zeta_p + D_{p,zw} w + D_{p,zu} u_p \\ y_p = C_{p,y} x_p + D_{p,y\zeta}\zeta_p + D_{p,yw} w + D_{p,yu} u_p \\ \zeta_p = \Delta\eta_p \end{cases}, \tag{4.1}$$

and the modified unconstrained controller is given as:

$$\mathcal{G}_{\mathcal{M}} = \begin{bmatrix} \mathcal{G}_w & \mathcal{G}_y & \mathcal{G}_v \end{bmatrix} \begin{cases} \dot{x}_g = A_g x_g + B_{g,w} w + B_{g,y} u_g + B_{g,v_1} u_{v_1} \\ y_g = C_g x_g + D_{g,w} w + D_{g,y} u_g + D_{g,v_1} u_{v_1} + D_{g,v_2} u_{v_2} \end{cases}, \tag{4.2}$$

The corresponding dimensions of the state vectors, inputs and outputs of the plant and modified unconstrained controller have been specified in Section I.B.1. and are: $x_p \in \mathbb{R}^{n_p}$, $\zeta_p \in \mathbb{R}^{n_m}$, $w \in \mathbb{R}^{n_w}$, $u_p \in \mathbb{R}^{n_u}$, $z_p \in \mathbb{R}^{n_z}$, $y_p \in \mathbb{R}^{n_y}$, $\eta_p \in \mathbb{R}^{n_m}$, $x_g \in \mathbb{R}^{n_g}$,

$u_g \in \mathbb{R}^{n_y}$, $u_{v_1} \in \mathbb{R}^{n_{v_1}}$, $u_{v_2} \in \mathbb{R}^{n_{v_2}}$, $y_g \in \mathbb{R}^{n_u}$. We will also specify that the linear nominal plant is order n_p and the modified modified unconstrained controller is order n_g, i.e. $x_p \in \mathbb{R}^{n_p}$ and $n_g \in \mathbb{R}^{n_g}$. Note that the order or the uncertain plant is related to the order of the uncertainty perturbation Δ. The uncertainty perturbation is modeled as a casual, bounded, linear operator in $\mathcal{L}_2$, restricted to have the following spatial structure[1]:

$$\Delta = \text{diag}\left[\delta_1 I_{k_1}, ..., \delta_L I_{k_L}, \Delta_{L+1}, ..., \Delta_{L+F}\right] \text{ with } \delta_q : \mathbb{R} \mapsto \mathbb{R}, \Delta_q : \mathbb{C} \mapsto \mathbb{C}^{k_q \times k_q}, \quad (4.3)$$

with $k_1 + ... + k_L + k_{L+1} + ... + k_{L+F} = n_m$. The perturbations can be normalized to size ϱ in an induced $\mathcal{L}_2$ norm ($\|\Delta\|_{\mathcal{L}_2 \mapsto \mathcal{L}_2} \leq \varrho$). Note that for this $\mathcal{L}_2$ linear uncertainty, with spatial structure as above, the description is consistent with the problem studied in modern robust control (i.e. μ-synthesis). To distinguish the parametric uncertainty from the non-parametric one, the corresponding matrices B_ζ, C_η and $D_{\eta\zeta}$ in Eqn. 4.1 will be partitioned appropriately, with the subscripts $(\cdot)_p$ and $(\cdot)_n$ corresponding to parametric and non-parametric respectively, as follows:

$$B_\zeta = \begin{bmatrix} B_{p,\zeta_p} & B_{p,\zeta_n} \end{bmatrix}, \; C_{p,\eta} = \begin{bmatrix} C_{p,\eta_p} \\ C_{p,\eta_n} \end{bmatrix}, \; D_\eta = \begin{bmatrix} D_{p,\eta_p\zeta_p} & 0 \\ 0 & D_{p,\eta_n\zeta_n} \end{bmatrix}. \quad (4.4)$$

where $B_{p,\zeta_p} \in \mathbb{R}^{n_p \times n_{m_p}}$, $B_{p,\zeta_n} \in \mathbb{R}^{n_p \times n_{m_n}}$, $C_{p,\eta_p} \in \mathbb{R}^{n_{m_p} \times n_p}$, $C_{p,\eta_n} \in \mathbb{R}^{n_{m_n} \times n_p}$, $D_{p,\eta_p} \in \mathbb{R}^{n_{m_p} \times n_{m_p}}$ and $D_{p,\eta_n} \in \mathbb{R}^{n_{m_n} \times n_{m_n}}$, for $n_{m_p} = k_1 + ... + k_L$ and $n_{m_n} = k_{L+1} + ... + k_{L+F}$ with $n_m = n_{m_p} + n_{m_n}$.

For the development of the synthesis procedure, it is useful to consider the mismatch system previously depicted in Figs. 10 and 14 because, conveniently, this system possesses as its inputs and outputs the signals necessary for the definition

[1] A wide variety of uncertainty models can be translated into this standard form by an appropriate selection of the number, size, and dynamic nature of the blocks of Δ (i.e. parameter variations, and unmodeled LTI dynamics).

of remedial performance quantification. This is not a fortuitous fact, recall that the mismatch system was defined to capture the difference between the actual and the unconstrained (or output constrained) responses.

To show the realization of the mismatch system, the realization of the remedial compensator is also necessary. Note that we have given the realization of the static remedial compensator in Eqn. 2.4 and that of the dynamic remedial compensator in Eqn. 2.5.

The dynamics of the mismatch system, as presented in Fig. 22 for anti-windup compensation and Fig. 23 for override compensation, can be captured by the interaction of the uncertain plant $\mathcal{P}^{\Delta}$ in Eqn. 4.1, modified unconstrained controller $\mathcal{G}_{\mathcal{M}}$ in Eqn. 4.2 and remedial compensator $\mathcal{R}$ in Eqn. 2.4 if static and in Eqn. 2.5 if dynamic, via the equations:

$$u_d = u_p = y_g, \;\; z_d = z_p, \;\; y_d = y_p = u_g, \;\; \eta_d = \eta_p, \;\; v_1 = u_{v_1}, \;\; v_2 = u_{v_2}. \tag{4.5}$$

Then, the *compact realization of the mismatch system* can be written with the state $x = \begin{bmatrix} x_{p,d} \\ x_{g,d} \\ x_{\Lambda} \end{bmatrix}$ as detailed below, for *Anti-windup Compensation*:

$$\mathcal{W}^{\Delta} \begin{cases} \dot{x} = Ax + B_{\zeta}\zeta_d + B_{\psi}\psi_0 \\ \eta_d = C_{\eta}x + D_{\eta\zeta}\zeta_d + D_{\eta\psi}\psi_0 \\ z_d = C_z x + D_{z\zeta}\zeta_d + D_{z\psi}\psi_0 \\ u_d = C_u x + D_{u\zeta}\zeta_d + D_{u\psi}\psi_0 \\ \zeta_d = \Delta\eta_d \\ \psi_0 = \psi(u) = \psi(u_l - u_d) \end{cases}, \tag{4.6}$$

and *Override Compensation*:

$$\mathcal{W}^{\Delta}\begin{cases} \dot{x} = Ax + B_{\zeta}\zeta_d + B_{\psi}(\psi_0 + \varphi_0) \\ \eta_d = C_{\eta}x + D_{\eta\zeta}\zeta_d + D_{\eta\psi}(\psi_0 + \varphi_0) \\ z_d = C_z x + D_{z\zeta}\zeta_d + D_{z\psi}(\psi_0 + \varphi_0) \\ y_d = C_y x + D_{y\zeta}\zeta_d + D_{y\psi}(\psi_0 + \varphi_0) \\ \underline{z}_d = z_d - \psi_0 \\ \zeta_d = \Delta\eta_d \\ \psi_0 = \psi(z_l) \\ \varphi_0 = \varphi(-z_d, z_l) = \psi(z) - \psi(z_l) \end{cases}, \tag{4.7}$$

where the matrices A, B_{ζ}, B_{ψ}, C_z, $D_{z\zeta}$, $D_{z\psi}$, C_u, $D_{u\zeta}$, $D_{u\psi}$, C_{η}, $D_{\eta\zeta}$ and $D_{\eta\psi}$ are uniquely determined by the realization of the plant, modified unconstrained controller and the remedial compensation. These matrices can be constructed via the following Notation 4.1.

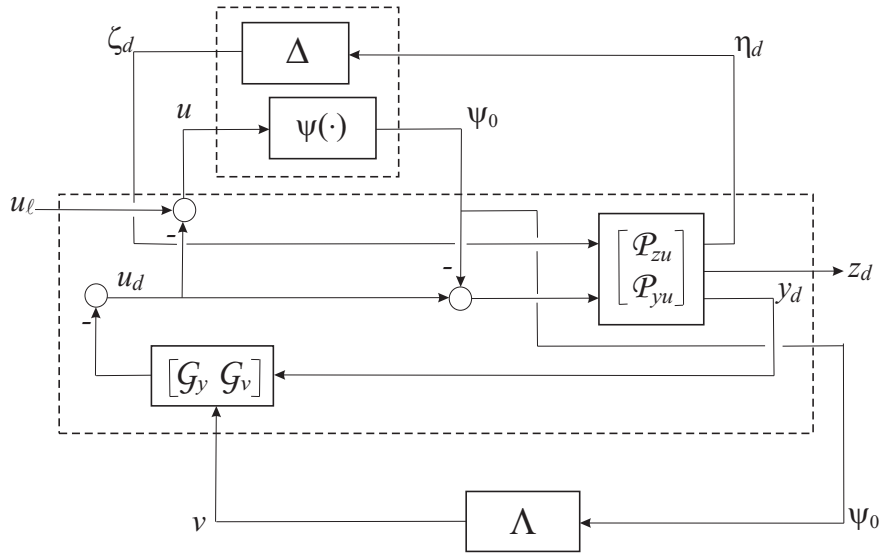

Fig. 22. Detailed LFT representation of the mismatch system for anti-windup compensation.

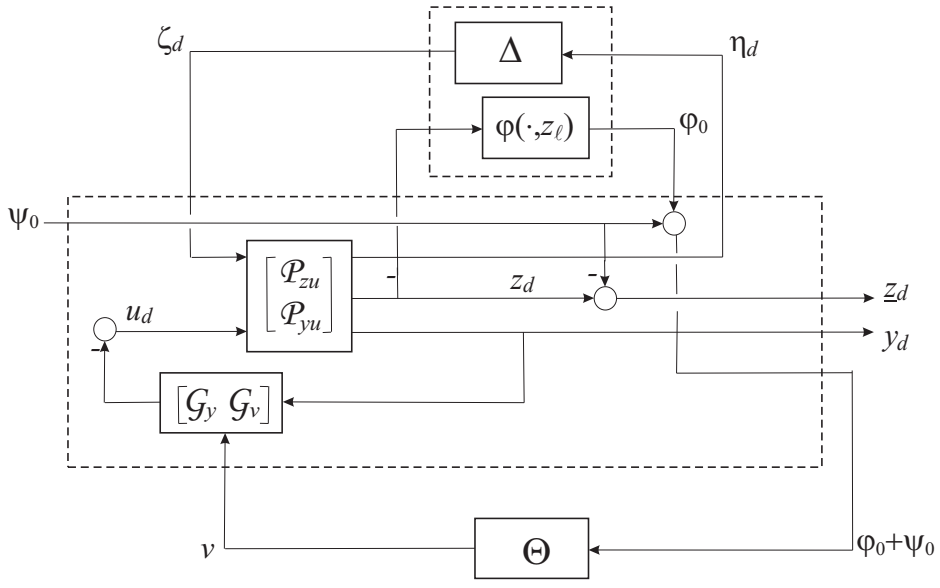

Fig. 23. Detailed LFT representation of the mismatch system for override compensation.

Notation 4.1. Construction of compact representation of mismatch system.

Step 1. Define $n = n_p + n_g + n_\Lambda$ and $n_{\mathrm{CL}} = n_p + n_g$ based on the state vector dimensions of the linear plant $\mathcal{P}^\Delta$, modified unconstrained controller $\mathcal{G}_\mathcal{M}$ and anti-windup compensator in Eqns. 4.1, 4.2 and 2.5 (dynamic version) respectively.

Step 2. On the basis of the realization for the plant $\mathcal{P}^\Delta$ in Eqn. 4.1 and modified unconstrained controller $\mathcal{G}_\mathcal{M}$ in Eqn. 4.2, define $\Upsilon_p \in \mathbb{R}^{n_y \times n_y}$ and $\Upsilon_g \in \mathbb{R}^{n_u \times n_u}$ as:

$$\begin{aligned} \Upsilon_p &= (I_{n_y} + D_{p,yu} D_{g,y}), \\ \Upsilon_g &= (I_{n_y} + D_{g,y} D_{p,yu}). \end{aligned} \tag{4.8}$$

Define $v = \begin{bmatrix} v_1 \\ v_2 \end{bmatrix} \in \mathbb{R}^{n_v}$, where $n_v = n_{v_1} + n_{v_2}$. Also note that n_r substitutes n_u or n_z, depending on the anti-windup or override problem being solved. Then, employing Υ_p and Υ_g and the matrices of the plant $\mathcal{P}^\Delta$ in Eqn. 4.1 and unconstrained controller $\mathcal{G}$ in Eqn. 4.2, define $A_{\mathrm{CL}} \in \mathbb{R}^{n_{\mathrm{CL}} \times n_{\mathrm{CL}}}$, $B_{\mathrm{CL},\zeta} \in \mathbb{R}^{n_{\mathrm{CL}} \times n_m}$, $B_{\mathrm{CL},v} \in \mathbb{R}^{n_{\mathrm{CL}} \times n_v}$, $B_{\mathrm{CL},\psi} \in \mathbb{R}^{n_{\mathrm{CL}} \times n_u}$, $C_{\mathrm{CL},\eta} \in \mathbb{R}^{n_m \times n_{\mathrm{CL}}}$, $D_{\mathrm{CL},\eta\zeta} \in \mathbb{R}^{n_m \times n_m}$, $D_{\mathrm{CL},\eta v} \in \mathbb{R}^{n_m \times n_v}$, $D_{\mathrm{CL},\eta\psi} \in \mathbb{R}^{n_m \times n_r}$, $C_{\mathrm{CL},z} \in \mathbb{R}^{n_z \times n_{\mathrm{CL}}}$, $D_{\mathrm{CL},z\zeta} \in \mathbb{R}^{n_z \times n_m}$, $D_{\mathrm{CL},zv} \in \mathbb{R}^{n_z \times n_v}$, $D_{\mathrm{CL},z\psi} \in \mathbb{R}^{n_z \times n_r}$, $C_{\mathrm{CL},y} \in \mathbb{R}^{n_y \times n_{\mathrm{CL}}}$, $D_{\mathrm{CL},y\zeta} \in \mathbb{R}^{n_y \times n_m}$, $D_{\mathrm{CL},yv} \in \mathbb{R}^{n_y \times n_v}$, $D_{\mathrm{CL},y\psi} \in \mathbb{R}^{n_y \times n_r}$, $C_{\mathrm{CL},u} \in \mathbb{R}^{n_u \times n_{\mathrm{CL}}}$, $D_{\mathrm{CL},u\zeta} \in \mathbb{R}^{n_u \times n_m}$, $D_{\mathrm{CL},uv} \in \mathbb{R}^{n_u \times n_v}$

and $D_{\mathrm{CL},u\psi} \in \mathbb{R}^{n_u \times n_r}$ as:

$$
\begin{aligned}
A_{\mathrm{CL}} &= \begin{bmatrix} A_p - B_{p,u} D_{g,y} \Upsilon_p C_{p,y} & B_{p,u} \Upsilon_g C_g \\ -B_{g,y} \Upsilon_p C_{p,y} & A_g - B_{g,y} \Upsilon_p D_{p,yu} C_g \end{bmatrix}, \\
B_{\mathrm{CL},\zeta} &= \begin{bmatrix} B_{p,\zeta} - B_{p,u} D_{g,y} D_{p,y\zeta} \\ -B_{g,y} \Upsilon_p D_{p,y\zeta} \end{bmatrix}, \\
B_{\mathrm{CL},v} &= \begin{bmatrix} -B_{p,u} \Upsilon_g D_{g,v_1} & -B_{p,u} \Upsilon_g D_{g,v_2} \\ -B_{g,v_1} + B_{g,y} \Upsilon_p D_{p,yu} D_{g,v_1} & B_{g,y} \Upsilon_p D_{p,yu} D_{g,v_2} \end{bmatrix}, \\
B_{\mathrm{CL},\psi^u} &= \begin{bmatrix} B_{p,u} \Upsilon_g \\ -B_{g,y} \Upsilon_p D_{p,yu} \end{bmatrix}, \quad B_{\mathrm{CL},\psi^z} = \begin{bmatrix} 0 \\ 0 \end{bmatrix}, \\
C_{\mathrm{CL},\eta} &= \begin{bmatrix} C_{p,\eta} - D_{p,\eta u} D_{g,y} \Upsilon_p C_{p,y} & D_{p,\eta u} \Upsilon_g C_g \end{bmatrix}, \\
D_{\mathrm{CL},\eta\zeta} &= D_{p,\eta\zeta} - D_{p,\eta u} D_{g,y} D_{p,y\zeta}, \\
D_{\mathrm{CL},\eta v} &= \begin{bmatrix} -D_{p,\eta u} \Upsilon_g D_{g,v_1} & -D_{p,\eta u} \Upsilon_g D_{g,v_2} \end{bmatrix}, \\
D_{\mathrm{CL},\eta\psi^u} &= D_{p,\eta u} \Upsilon_g, \quad D_{\mathrm{CL},\eta\psi^z} = 0, \\
C_{\mathrm{CL},z} &= \begin{bmatrix} C_{p,z} - D_{p,zu} D_{g,y} \Upsilon_p C_{p,y} & D_{p,zu} \Upsilon_g C_g \end{bmatrix}, \\
D_{\mathrm{CL},z\zeta} &= D_{p,z\zeta} - D_{p,zu} D_{g,y} D_{p,y\zeta}, \\
D_{\mathrm{CL},zv} &= \begin{bmatrix} -D_{p,zu} \Upsilon_g D_{g,v_1} & -D_{p,zu} \Upsilon_g D_{g,v_2} \end{bmatrix}, \\
D_{\mathrm{CL},z\psi^u} &= D_{p,zu} \Upsilon_g, \quad D_{\mathrm{CL},z\psi^z} = 0, \\
C_{\mathrm{CL},y} &= \begin{bmatrix} \Upsilon_p C_{p,y} & \Upsilon_p D_{p,yu} C_g \end{bmatrix}, \\
D_{\mathrm{CL},y\zeta} &= \Upsilon_p D_{p,z\zeta}, \\
D_{\mathrm{CL},yv} &= \begin{bmatrix} -\Upsilon_p D_{p,yu} D_{g,v_1} & -\Upsilon_p D_{p,yu} D_{g,v_2} \end{bmatrix}, \\
D_{\mathrm{CL},y\psi^u} &= \Upsilon_p D_{p,yu}, \quad D_{\mathrm{CL},y\psi^z} = 0, \\
C_{\mathrm{CL},u} &= \begin{bmatrix} -D_{g,y} \Upsilon_p C_{p,y} & \Upsilon_g C_g \end{bmatrix}, \\
D_{\mathrm{CL},u\zeta} &= -D_{g,y} D_{p,y\zeta}, \\
D_{\mathrm{CL},uv} &= \begin{bmatrix} -\Upsilon_g D_{g,v_1} & -\Upsilon_g D_{g,v_2} \end{bmatrix}, \\
D_{\mathrm{CL},u\psi^u} &= \Upsilon_g - I_{n_u}, \quad D_{\mathrm{CL},u\psi^z} = 0.
\end{aligned}
\tag{4.9}
$$

Step 3. Using the realization of the linear remedial compensator $\mathcal{R}$ shown in Eqn. 2.4 if static and in Eqn. 2.5 if dynamic, define $D_{\mathcal{R}}$ (where $D_{\mathcal{R}} \in \mathbb{R}^{n_v \times n_r}$) via:

$$D_{\mathcal{R}} = \begin{bmatrix} D_{\mathcal{R}_1} \\ D_{\mathcal{R}_2} \end{bmatrix}. \tag{4.10}$$

If the remedial compensation is linear and *static* then define $A \in \mathbb{R}^{n_{\mathrm{CL}} \times n_{\mathrm{CL}}}$, $B_\zeta \in \mathbb{R}^{n_{\mathrm{CL}} \times n_m}$, $B_\psi \in \mathbb{R}^{n_{\mathrm{CL}} \times n_u}$, $C_\eta \in \mathbb{R}^{n_m \times n_{\mathrm{CL}}}$, $D_{\eta\zeta} \in \mathbb{R}^{n_m \times n_m}$, $D_{\eta\psi} \in \mathbb{R}^{n_m \times n_u}$, $C_z \in \mathbb{R}^{n_z \times n_{\mathrm{CL}}}$, $D_{z\zeta} \in \mathbb{R}^{n_z \times n_m}$, $D_{z\psi} \in \mathbb{R}^{n_z \times n_u}$, $C_y \in \mathbb{R}^{n_y \times n_{\mathrm{CL}}}$, $D_{y\zeta} \in \mathbb{R}^{n_y \times n_m}$, $D_{y\psi} \in \mathbb{R}^{n_y \times n_u}$, $C_u \in \mathbb{R}^{n_u \times n_{\mathrm{CL}}}$, $D_{u\zeta} \in \mathbb{R}^{n_u \times n_m}$, $D_{u\psi} \in \mathbb{R}^{n_u \times n_u}$, via:

$$\begin{aligned}
A &= A_{\mathrm{CL}}, \quad & B_\zeta &= B_{\mathrm{CL},\zeta}, \quad & B_\psi &= B_{\mathrm{CL},\psi}, \\
C_\eta &= C_{\mathrm{CL},\eta}, \quad & D_{\eta\zeta} &= D_{\mathrm{CL},\eta\zeta}, \quad & D_{\eta\psi} &= D_{\mathrm{CL},\eta\psi}, \\
C_y &= C_{\mathrm{CL},y}, \quad & D_{y\zeta} &= D_{\mathrm{CL},y\zeta}, \quad & D_{y\psi} &= D_{\mathrm{CL},y\psi}, \\
C_z &= C_{\mathrm{CL},z}, \quad & D_{z\zeta} &= D_{\mathrm{CL},z\zeta}, \quad & D_{z\psi} &= D_{\mathrm{CL},z\psi}, \\
C_u &= C_{\mathrm{CL},u}, \quad & D_{u\zeta} &= D_{\mathrm{CL},u\zeta} \quad & D_{u\psi} &= D_{\mathrm{CL},u\psi}.
\end{aligned} \tag{4.11}$$

However, if the remedial compensation is linear and *dynamic*, as shown in Eqn. 2.5, then define $A_{\mathcal{R}}$, $B_{\mathcal{R}}$ and $C_{\mathcal{R}}$ where $A_{\mathcal{R}} \in \mathbb{R}^{n_{\mathcal{R}} \times n_{\mathcal{R}}}$, $B_{\mathcal{R}} \in \mathbb{R}^{n_{\mathcal{R}} \times n_r}$, and $C_{\mathcal{R}} \in \mathbb{R}^{n_v \times n_{\mathcal{R}}}$, and the latter is described via:

$$C_{\mathcal{R}} = \begin{bmatrix} C_{\mathcal{R}_1} \\ C_{\mathcal{R}_2} \end{bmatrix}. \tag{4.12}$$

and $A \in \mathbb{R}^{n \times n}$, $B_\zeta \in \mathbb{R}^{n \times n_m}$, $B_\psi \in \mathbb{R}^{n \times n_r}$, $C_\eta \in \mathbb{R}^{n_m \times n}$, $D_{\eta\zeta} \in \mathbb{R}^{n_m \times n_m}$, $D_{\eta\psi} \in \mathbb{R}^{n_m \times n_r}$, $C_z \in \mathbb{R}^{n_z \times n}$, $D_{z\zeta} \in \mathbb{R}^{n_z \times n_m}$, $D_{z\psi} \in \mathbb{R}^{n_z \times n_r}$, $C_y \in \mathbb{R}^{n_y \times n}$,

$D_{y\zeta} \in \mathbb{R}^{n_y \times n_m}$, $D_{y\psi} \in \mathbb{R}^{n_y \times n_r}$, $C_u \in \mathbb{R}^{n_u \times n}$, $D_{u\zeta} \in \mathbb{R}^{n_u \times n_m}$, $D_{u\psi} \in \mathbb{R}^{n_u \times n_r}$ via:

$$
\begin{aligned}
A &= \begin{bmatrix} A_{\mathrm{CL}} & B_{\mathrm{CL},v}C_{\mathcal{R}} \\ 0 & A_{\mathcal{R}} \end{bmatrix}, \qquad B_{\zeta} = \begin{bmatrix} B_{\mathrm{CL},\zeta} \\ 0 \end{bmatrix}, \\
B_{\psi} &= \begin{bmatrix} B_{\mathrm{CL},\psi} + B_{\mathrm{CL},v}D_{\mathcal{R}} \\ B_{\mathcal{R}} \end{bmatrix}, \quad C_{\eta} = \begin{bmatrix} C_{\mathrm{CL},\eta} & D_{\mathrm{CL},\eta v}C_{\mathcal{R}} \end{bmatrix}, \\
D_{\eta\zeta} &= D_{\mathrm{CL},\eta\zeta}, \qquad D_{\eta\psi} = D_{\mathrm{CL},\eta\psi} + D_{\mathrm{CL},\eta v}D_{\mathcal{R}}, \\
C_z &= \begin{bmatrix} C_{\mathrm{CL},z} & D_{\mathrm{CL},zv}C_{\mathcal{R}} \end{bmatrix}, \qquad D_{z\zeta} = D_{\mathrm{CL},z\zeta}, \\
D_{z\psi} &= D_{\mathrm{CL},z\psi} + D_{\mathrm{CL},zv}D_{\mathcal{R}}, \quad C_y = \begin{bmatrix} C_{\mathrm{CL},y} & D_{\mathrm{CL},yv}C_{\mathcal{R}} \end{bmatrix}, \\
D_{y\zeta} &= D_{\mathrm{CL},y\zeta}, \qquad D_{y\psi} = D_{\mathrm{CL},y\psi} + D_{\mathrm{CL},yv}D_{\mathcal{R}}, \\
C_u &= \begin{bmatrix} C_{\mathrm{CL},u} & D_{\mathrm{CL},uv}C_{\mathcal{R}} \end{bmatrix}, \qquad D_{u\zeta} = D_{\mathrm{CL},u\zeta}, \\
D_{u\psi} &= D_{\mathrm{CL},u\psi} + D_{\mathrm{CL},uv}D_{\mathcal{R}}.
\end{aligned}
\tag{4.13}
$$

$\lhd$

If Assumption 2.2 holds, the unconstrained closed-loop system is well-posed and internally stable, then Υ_p and Υ_g are well-defined and all the steps in Notation 3.1. can be completed.

Note that the mismatch system state space representation has been defined for the general architecture for remedial compensation. Defining the remedial compensation synthesis problem in terms of the parameters of the general architecture external structure (B_{g,v_1}, D_{g,v_1} and D_{g,v_2}), besides the remedial compensator $\mathcal{R}$, gives a different insight into the remedial compensation problem. This insight becomes specially important when we attempt to compare existing configurations, for example in the anti-windup compensation case, as seen in the next chapter.

1. Extremal input nonlinearities cases

The states of the mismatch system $x_{p,d} = x_{pl} - x_p$ and $x_{g,d} = x_{gl} - x_g$ correspond to the difference between the unconstrained and remedial internal trajectories for the plant and controller respectively. From Definition 1.16. we know that $x_{pl}(0) = x_p(0)$, $x_{gl}(0) = x_g(0)$ and $x_{\mathcal{R}}(0) = 0$, then, at $t = 0$, we have that $x(0) = 0$. Hence from Figs. 22 and 23, provided $x(0) = 0$, there are two special extreme input nonlinearities we would like to consider.

a. Anti-windup compensation

1. Select $\phi(\cdot) \equiv 0$ in the anti-windup closed-loop system shown in Fig. 6. Then $\psi(u) \equiv u$ in the mismatch system, see Fig. 22, and this is valid for any anti-windup compensator and any unconstrained controller. From Eqn. 4.7 after appropriate substitutions for its matrices according to Eqns. 4.9, 4.11 and 4.13, the mismatch system output response can be written as:

$$\mathcal{W}^{\Delta}_{\psi(\cdot)\equiv I_{n_u}} \begin{cases} \dot{x}_{p,d} = A_p x_{p,d} + B_{p,\zeta}\zeta_d + B_{p,u}u_l \\ z_d = C_{p,z}x_{pd} + D_{p,z\zeta}\zeta_d + D_{p,zu}u_l \\ \eta_d = C_{p,\eta}x_{pd} + D_{p,\eta\zeta}\zeta_d + D_{p,\eta u}u_l \\ \zeta_d = \Delta\eta_d \end{cases} . \tag{4.14}$$

Note that, from Fig. 11, it can be directly concluded that for $\psi(\cdot) \equiv I_{n_u}$, the mismatch control output and mismatch performance output responses are $(I + L^u_n)u_l$ and $\mathcal{P}^{\Delta}_{zu}u_l$, respectively.

2. Select $\phi(\cdot) \equiv I_{n_u}$ in the anti-windup closed-loop system shown in Fig. 6. Then $\psi(u) \equiv 0$ in the mismatch system, see Fig. 22, and this is valid for any anti-windup compensator and any unconstrained controller. From Eqn. 4.7 after

appropriate substitutions for its matrices according to Eqns. 4.9, 4.11 and 4.13, the mismatch system output response can be written with state $x_{\mathrm{CL},d} = \begin{bmatrix} x_{p,d} \\ x_{g,d} \end{bmatrix}$ as:

$$\mathcal{W}^{\Delta}_{\psi(\cdot)\equiv 0} \begin{cases} \dot{x}_{\mathrm{CL},d} = A_{\mathrm{CL}} x_{\mathrm{CL},d} + B_{\mathrm{CL},\zeta}\zeta_d \\ z_d = C_{\mathrm{CL},z} x_{\mathrm{CL},d} + D_{\mathrm{CL},z\zeta}\zeta_d \\ \eta_d = C_{\mathrm{CL},\eta} x_{\mathrm{CL},d} + D_{\mathrm{CL},\eta\zeta}\zeta_d \\ \zeta_d = \Delta\eta_d \end{cases} . \tag{4.15}$$

b. Override compensation

1. Select $\phi(\cdot) \equiv 0$ in the override closed-loop system shown in Fig. 7. Then $\psi(z_l) \equiv z_l$ and $\varphi(-z_d, z_l) = \psi(z) - \psi(z_l) = z - z_l = -z_d$ in the mismatch system, see Fig. 23, and this is valid for any override compensator and any unconstrained controller. From Eqn. 4.8 after appropriate substitutions for its matrices according to Eqns. 4.9, 4.11 and 4.13, the mismatch system output responses can be written as:

$$\mathcal{W}^{\Delta}_{\psi(\cdot)\equiv I_{n_u}} \begin{cases} \dot{x} = Ax + B_\zeta\zeta_d + B_\psi z \\ \eta_d = C_\eta x + D_{\eta\zeta}\zeta_d + D_{\eta\psi} z \\ z_d = C_z x + D_{z\zeta}\zeta_d + D_{z\psi} z \\ y_d = C_y x + D_{y\zeta}\zeta_d + D_{y\psi} z \\ z_d = -z \\ \zeta_d = \Delta\eta_d \end{cases} , \tag{4.16}$$

Note that, from Fig. 15, it can be directly concluded that for $\psi(\cdot) \equiv I_{n_u}$ and $\varphi(\cdot) \equiv I_{n_u}$, the mismatch performance output and mismatch measured output responses are $-L^z_n(I_{n_z} + L^z_n)^{-1} z$ and $-\mathcal{P}^{\Delta}_{yu} S\mathcal{G}_v\Theta$, respectively.

2. Select $\phi(\cdot) \equiv I_{n_u}$ in the override closed-loop system shown in Fig. 7. Then $\psi(\cdot) \equiv 0$ and $\varphi(\cdot) \equiv 0$ in the mismatch system, see Fig. 23, and this is valid for any override compensator and any unconstrained controller. From Eqn. 4.8 after appropriate substitutions for its matrices according to Eqns. 4.9, 4.11 and 4.13, the mismatch system output responses can be written with state $x_{\mathrm{CL},d} = \begin{bmatrix} x_{p,d} \\ x_{g,d} \end{bmatrix}$ as:

$$\mathcal{W}^{\Delta}_{\psi(\cdot)\equiv 0,\varphi(\cdot)\equiv 0} \begin{cases} \dot{x}_{\mathrm{CL},d} = A_{\mathrm{CL}} x_{\mathrm{CL},d} + B_{\mathrm{CL},\zeta}\zeta_d \\ z_d = C_{\mathrm{CL},z} x_{\mathrm{CL},d} + D_{\mathrm{CL},z\zeta}\zeta_d \\ \eta_d = C_{\mathrm{CL},\eta} x_{\mathrm{CL},d} + D_{\mathrm{CL},\eta\zeta}\zeta_d \\ \zeta_d = \Delta\eta_d \end{cases} . \tag{4.17}$$

Remark 4.2. The mismatch system, compared to the constrained closed-loop system, possesses additional inputs and outputs acting at different point locations of the closed-loop. In particular, one of these inputs and outputs corresponds to the remedial compensator. From the mismatch system showed in Figs. 22 and 23, when no remedial compensator exists, we have that $v = 0$ and the connection of the resulting mismatch system to the unconstrained closed-loop system is equivalent to the input constrained system described in Fig. 4 and to the output constrained system in Fig. 5 for anti-windup and override compensation, respectively. ◁

B. Determining the finite unconstrained response gain

1. Anti-windup compensation

Algorithm 4.3 (Linear anti-windup performance analysis of robust unconstrained response recovery gain)

Step 1. Using the compact representation of the mismatch system $\mathcal{W}^{\Delta}$ in Eqn. 4.6, construct A, B_{ζ}, B_{ψ}, C_{η}, $D_{\eta\zeta}$, $D_{\eta\psi}$, C_z, $D_{z\zeta}$, $D_{z\psi}$, C_y, $D_{y\zeta}$, $D_{y\psi}$, C_u, $D_{u\zeta}$, and $D_{u\psi}$, according to Notation 4.1

Step 2. Find a solution $(\bar{Q}, \bar{U}, \bar{V}, \tau, \gamma) \in (\mathbb{R}^{(n_{\mathrm{CL}}+n_{\Lambda})\times(n_{\mathrm{CL}}+n_{\Lambda})}, \mathbb{D}^{n_u\times n_u}, \mathbb{D}^{n_{m_p}\times n_{m_p}}, \mathbb{R}, \mathbb{R})$, with $\gamma > 0$ as small as possible and $\tilde{\varrho} \geq 0$, to the LMI problem:

$$\bar{Q} = \bar{Q}^T > 0, \tag{4.18a}$$

$$\bar{U} = \mathrm{diag}[\mu_1, ..., \mu_{n_u}] > 0, \tag{4.18b}$$

$$\bar{V} = \mathrm{diag}[\nu_1, ..., \nu_{n_{m_p}}] > 0, \tag{4.18c}$$

$$\mathrm{He}\begin{bmatrix} A\bar{Q} & B_{\psi}\bar{U} & \bar{Q}C_z^T & 0 & B_{\zeta_p}\bar{V} & \tau B_{\zeta_n} & \tilde{\varrho}\bar{Q}C_{\eta_n}^T \\ -C_u\bar{Q} & -D_{u\psi}\bar{U}-\bar{U} & 0 & I_{n_u} & -D_{u\zeta_p}\bar{V} & -\tau D_{u\zeta_n} & 0 \\ 0 & D_{z\psi}\bar{U} & -\frac{\gamma}{2}I_{n_z} & 0 & 0 & 0 & 0 \\ 0 & 0 & 0 & -\frac{\gamma}{2}I_{n_u} & 0 & 0 & 0 \\ \tilde{\varrho}C_{\eta_p}\bar{Q} & 0 & \bar{V}D_{z\zeta_p}^T & 0 & \tilde{\varrho}D_{\eta_p\zeta_p}\bar{V}-\bar{V} & 0 & 0 \\ 0 & 0 & \tau D_{z\zeta_n}^T & 0 & 0 & -\frac{\tau}{2}I_{n_{m_n}} & \tau\tilde{\varrho}D_{\eta_n\zeta_n}^T \\ 0 & \tilde{\varrho}D_{\eta_n\psi}\bar{U} & 0 & 0 & 0 & 0 & -\frac{\tau}{2}I_{n_{m_n}} \end{bmatrix} < 0. \tag{4.18d}$$

Theorem 4.4 If $(\bar{Q}, \bar{U}, \bar{V}, \tau, \gamma)$ is a solution to the LMI in Eqn. 4.18, Step 2 of Algorithm 4.3, then the anti-windup augmented closed-loop system guarantees the basic properties of anti-windup and has a robust finite unconstrained response recovery.

Proof. The proof will be provided in Chapter VI.

2. Override compensation

Algorithm 4.5 (Linear override performance analysis of robust unconstrained response recovery gain)

Step 1. Using the compact representation of the mismatch system $\mathcal{W}^{\Delta}$ in Eqn. 4.7, construct A, B_{ζ}, B_{ψ}, C_{η}, $D_{\eta\zeta}$, $D_{\eta\psi}$, C_z, $D_{z\zeta}$, $D_{z\psi}$, C_y, $D_{y\zeta}$, $D_{y\psi}$, C_u, $D_{u\zeta}$, and $D_{u\psi}$, according to Notation 4.1

Step 2. Find a solution $(\bar{Q}, \bar{U}, \bar{V}, \tau, \gamma) \in (\mathbb{R}^{(n_{\mathrm{CL}}+n_{\Theta})\times(n_{\mathrm{CL}}+n_{\Theta})}, \mathbb{D}^{n_u \times n_u}, \mathbb{D}^{n_{m_p}\times n_{m_p}}, \mathbb{R}, \mathbb{R})$, with $\gamma > 0$ as small as possible and $\tilde{\varrho} \geq 0$, to the LMI problem:

$$\bar{Q} = \tilde{Q}^T > 0, \tag{4.19a}$$

$$\bar{U} = \mathrm{diag}[\mu_1, ..., \mu_{n_u}] > 0, \tag{4.19b}$$

$$\bar{V} = \mathrm{diag}[\nu_1, ..., \nu_{n_{m_p}}] > 0, \tag{4.19c}$$

He

$$\begin{bmatrix}
A\bar{Q} & -B_\psi\bar{U} & 0 & 0 & -B_\psi & B_{\zeta_p}\bar{V} & 0 & \tilde{\varrho}\bar{Q}C_{\eta_n}^T \\
-C_z\bar{Q} & -D_{z\psi}\bar{U}-\bar{U} & 0 & 0 & D_{z\psi} & -D_{z\zeta_p}\bar{V} & 0 & -\tilde{\varrho}\bar{U}D_{\eta_n\psi}^T \\
W_yC_y\bar{Q} & -W_yD_{y\psi}\bar{U} & -\frac{\gamma}{2}I_{n_y} & 0 & -W_yD_{y\psi} & W_yD_{y\zeta_p}\bar{V} & \tau W_yD_{y\zeta_n} & 0 \\
W_zC_z\bar{Q} & -W_zD_{z\psi}\bar{U} & 0 & -\frac{\gamma}{2}I_{n_z} & -W_zD_{z\psi} & W_zD_{z\zeta_p}\bar{V} & \tau D_{z\zeta_n} & 0 \\
0 & 0 & 0 & -W_o^TW_z^T & -\frac{\gamma}{2}I_{n_z} & -D_{\eta_p\psi}^T & 0 & \tilde{\varrho}D_{\eta_n\psi}^T \\
\tilde{\varrho}C_{\eta_p}\bar{Q} & -\tilde{\varrho}D_{\eta_p\psi}\bar{U} & 0 & 0 & -D_{\eta_p\psi} & -\bar{V}+\tilde{\varrho}D_{\eta_p\zeta_p}\bar{V} & 0 & 0 \\
\tau B_{\zeta_n}^T & -\tau D_{z\zeta_n}^T & 0 & 0 & 0 & 0 & -\frac{\tau}{2}I_{n_{m_n}} & 0 \\
0 & 0 & 0 & 0 & 0 & 0 & \tau\tilde{\varrho}D_{\eta_n\zeta_n} & -\frac{\tau}{2}I_{n_{m_n}}
\end{bmatrix}$$

$$< 0. \tag{4.19d}$$

Theorem 4.6 If $(\bar{Q}, \bar{U}, \bar{V}, \tau, \gamma)$ is a solution to the LMI in Eqn. 4.19, Step 2 of Algorithm 4.4, then the override augmented closed-loop system guarantees the basic properties of override and has a robust finite unconstrained response recovery.

Proof. The proof will be provided in Chapter VI.

CHAPTER V

GLOBAL, ROBUST REMEDIAL COMPENSATION FOR EXPONENTIALLY STABLE PLANTS

In this chapter we consider the effect of both static and dynamic remedial compensations as detailed in Section II.B. The general architecture for remedial compensation will be the reference for our design algorithms. The specific configurations for anti-windup compensation and their corresponding conditions for design feasibility will appear as special cases of the general architecture for anti-windup compensation. The case of override compensation will be developed only for the corresponding general architecture when the override compensator has access to the unconstrained controller states and output. To guarantee global stability of the remedial compensation closed-loop system we employ absolute stability guaranteed via quadratic stability. All along, the anti-windup community, and lately the override community, has found Lyapunov analysis tools useful in order to state the stability requirements together with the performance properties. This work is no exception, as seen in the development of this and following chapters. Notably, these typical analysis tools have the advantage of being related to LMI conditions. Hence, the satisfaction of these LMI conditions guarantees the global stability, with some performance measure, of the remedial compensation closed-loop system. The LMI conditions given throughout this chapter utilize the notation and definition in Chapter IV.

For the following algorithms, the remedial compensator is allowed to have a static internal structure first, and then a dynamic internal structure. Consideration will be given in both cases to the optimal design based on the finite unconstrained response recovery gain measure presented in Section II.C. The algorithms to be presented here for anti-windup compensation are similar in spirit and structure to the ones presented

in Grimm [56]. However, by presenting the general external structure, our idea is to be able to obtain synthesis algorithms for all remedial compensation schemes and further compare the advantages and disadvantages of employing one structure over the other. The case of override compensation is given here for completeness and comparison purposes with the anti-windup case. Importantly, structured uncertainty is also considered in all synthesis algorithms.

Recall that this chapter will only state results, the proofs of the theorems will be stated in the next chapter.

A. Static remedial compensation

Static anti-windup compensation as described in Section II.B possess a very appealing structure because, with no dynamics involved, it is easy to implement. However, its capabilities are limited [21]. Nevertheless, it is always good to have the algorithms for static compensation at hand such that we can make use of them whenever is possible.

1. Static anti-windup

Static compensation for the input constrained problem will be considered in this part of the dissertation. Recall from Section II.C that the finite unconstrained response recovery gain for anti-windup compensation refers to the $\mathcal{L}_2$ gain from the signal u_l (u_l comes from the unconstrained controller) to the difference of signals $z_l - z$ (z_l comes from the unconstrained closed-loop system and z is from the anti-windup closed-loop system). Therefore, the algorithms presented in this section will guarantee that, regardless of the exogenous disturbance $w \in \mathcal{L}_2$ and when the initial conditions of the plant and controller in the mismatch system are zero, the following is satisfied:

$$\|z_l(\cdot) - z(\cdot)\|_2 \leq \gamma \|u_l(\cdot)\|_2, \tag{5.1}$$

with the finite unconstrained recovery gain γ as small as possible. More specifically, the algorithms in this section are aimed at constructing the gains of a static linear anti-windup compensator that guarantees an optimal finite unconstrained response recovery gain.

a. General external structure static anti-windup

As introduced and described in Section II.B, static anti-windup compensation synthesis amounts to obtaining the gain matrices D_{Λ_1} and D_{Λ_2} of the static anti-windup compensator in Fig. 24. Algorithm 5.1 is now offered in order to provide the most general case of static anti-windup compensation, which corresponds to using the general external structure for anti-windup. In particular, this algorithm will be employed to obtain the corresponding algorithms for the existing static anti-windup external structures (configurations).

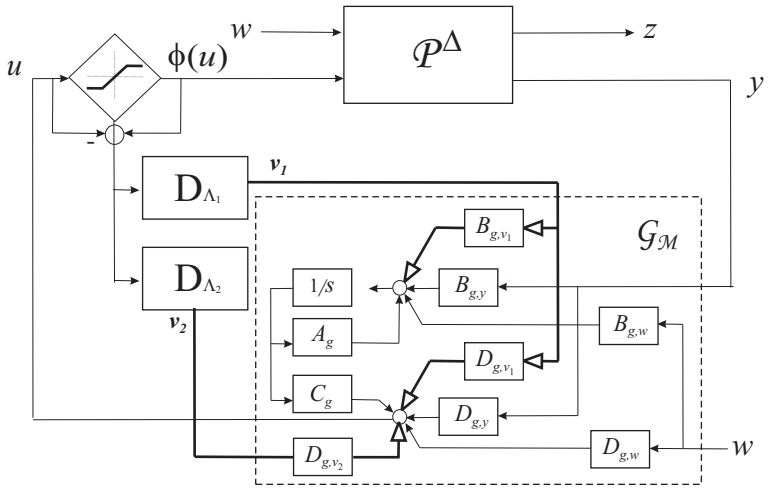

Fig. 24. Static anti-windup compensator is fed back in a general external structure.

Algorithm 5.1 (Static anti-windup compensation design with general external structure)

Step 1. Construct the matrix $\tilde{L}_\perp$ as any full column rank matrix that spans the null space of $\tilde{L}^T$, where:

$$\tilde{L}^T = \begin{bmatrix} D_{g,v_1}^T \Upsilon_g^T B_{p,u}^T & B_{g,v_1}^T - D_{g,v_1}^T \Upsilon_g^T D_{p,yu}^T B_{g,y}^T & -D_{g,v_1}^T \Upsilon_g^T & D_{g,v_1}^T \Upsilon_g^T D_{p,zu}^T \\ D_{g,v_2}^T \Upsilon_g^T B_{p,u}^T & -D_{g,v_2}^T \Upsilon_g^T D_{p,yu}^T B_{g,y}^T & -D_{g,v_2}^T \Upsilon_g^T & D_{g,v_2}^T \Upsilon_g^T D_{p,zu}^T \end{bmatrix}.$$

Let $\bar{L} = \mathrm{diag}[\tilde{L}_\perp, I_{n_u}, I_{n_{m_p}}, I_{n_{m_n}}, I_{n_{m_n}}]$.

Step 2. Find a solution $(X, \bar{U}, \bar{V}, \tau) \in (\mathbb{R}^{n_{\mathrm{CL}} \times n_{\mathrm{CL}}}, \mathbb{D}^{n_u}, \mathbb{D}^{n_{n_m}}, \mathbb{R})$, with $\gamma > 0$ as small as possible and $\tilde{\varrho} \geq 0$, to the LMI problem:

$$X = \begin{bmatrix} X_{11} & X_{12} \\ X_{12}^T & X_{22} \end{bmatrix} = X^T > 0, \tag{5.2a}$$

$$\bar{U} = \mathrm{diag}[\mu_1, ..., \mu_{n_u}] > 0, \tag{5.2b}$$

$$\bar{V} = \mathrm{diag}[\nu_1, ..., \nu_{n_{m_p}}] > 0, \tag{5.2c}$$

$$\mathrm{He}\, \bar{L}^T \begin{bmatrix} A_{\mathrm{CL}} X & B_{\mathrm{CL},\psi}\bar{U} & 0 & 0 & \tilde{\varrho} X C_{\mathrm{CL},\eta_p}^T & \tau B_{\mathrm{CL},\zeta_n} & 0 \\ -C_{\mathrm{CL},u} X & -D_{\mathrm{CL},u\psi}\bar{U} - \bar{U} & 0 & I_{n_u} & -D_{\mathrm{CL},u\zeta_p}\bar{V} & -\tau D_{\mathrm{CL},u\zeta_n} & 0 \\ C_{\mathrm{CL},z} X & D_{\mathrm{CL},z\psi}\bar{U} & -\frac{\gamma}{2} I_{n_z} & 0 & D_{\mathrm{CL},z\zeta_p}\bar{V} & \tau D_{\mathrm{CL},z\zeta_n} & 0 \\ 0 & 0 & 0 & -\frac{\gamma}{2} I_{n_u} & 0 & 0 & 0 \\ \bar{V} B_{\mathrm{CL},\zeta_p}^T & \tilde{\varrho} D_{\mathrm{CL},\eta_p\psi}\bar{U} & 0 & 0 & \tilde{\varrho} D_{\mathrm{CL},\eta_p\zeta_p}\bar{V} - \bar{V} & 0 & 0 \\ 0 & 0 & 0 & 0 & 0 & -\frac{\tau}{2} I_{n_{m_n}} & 0 \\ \tilde{\varrho} C_{\mathrm{CL},\eta_n} X & \tilde{\varrho} D_{\mathrm{CL},\eta_n\psi}\bar{U} & 0 & 0 & 0 & \tau\tilde{\varrho} D_{\mathrm{CL},\eta_n\zeta_n} & -\frac{\tau}{2} I_{n_{m_n}} \end{bmatrix} \bar{L} < 0, \tag{5.2d}$$

$$\mathrm{He} \begin{bmatrix} A_{\mathrm{CL}} X & 0 & X C_{\mathrm{CL},z}^T & \tilde{\varrho} X C_{\mathrm{CL},\eta_p}^T & \tau B_{\mathrm{CL},\zeta_n} & \tilde{\varrho} X C_{\mathrm{CL},\eta_n}^T \\ 0 & -\frac{\gamma}{2} I_{n_u} & 0 & 0 & 0 & 0 \\ 0 & 0 & -\frac{\gamma}{2} I_{n_z} & 0 & 0 & 0 \\ \bar{V} B_{\mathrm{CL},\zeta_p}^T & 0 & D_{\mathrm{CL},z\zeta_p}^T & \tilde{\varrho} D_{\mathrm{CL},\eta_p\zeta_p}^T \bar{V} - \bar{V} & 0 & 0 \\ 0 & 0 & \tau D_{\mathrm{CL},z\zeta_n}^T & 0 & -\frac{\tau}{2} I_{n_m} & \tilde{\varrho} D_{\mathrm{CL},\eta_n\zeta_n}^T \\ 0 & 0 & 0 & 0 & 0 & -\frac{\tau}{2} I_{n_m} \end{bmatrix} < 0, \tag{5.2e}$$

Step 3. Using $m = n_{\mathrm{CL}} + n_{m_p} + n_u + n_{m_n} + n_{m_n} + n_u + n_z$, construct the matrices $\Psi \in \mathbb{R}^{m \times m}$, $\tilde{R} \in \mathbb{R}^{n_u \times m}$, and $\tilde{P} \in \mathbb{R}^{m \times (n_{v_1} + n_{v_2})}$ via:

$$[\Psi, \tilde{R}, \tilde{P}] = V_{\mathrm{static}}(\mathcal{P}^{\Delta}, \mathcal{G}_{\mathcal{M}}, X, \bar{U}, \bar{V}, \tau, \gamma),$$

where the function V_{static} is given in Chapter VI.

Step 4. Find a solution $(D_{\Lambda_1}, D_{\Lambda_2}) \in (\mathbb{R}^{n_{v_1} \times n_u}, \mathbb{R}^{n_{v_2} \times n_u})$ to the LMI problem:

$$\Psi + \tilde{P}^T \begin{bmatrix} D_{\Lambda_1} \\ D_{\Lambda_2} \end{bmatrix} \tilde{R} + \tilde{R}^T \begin{bmatrix} D_{\Lambda_1} \\ D_{\Lambda_2} \end{bmatrix}^T \tilde{P} < 0. \tag{5.3}$$

$\triangleleft$

Note, however, that due to the generality of the presentation in Algorithm 5.1. no concluding remark can be done with respect to under what conditions global stability of the anti-windup closed-loop system is guaranteed. Interestingly, each static anti-windup compensation scheme will require the satisfaction of certain conditions in order to guarantee global stability of the anti-windup closed-loop system. Moreover, we will see that these conditions are necessary and sufficient for the successful construction of anti-windup compensation employing Algorithm 5.1. The list of these conditions is presented in Assumption 5.2.

Assumption 5.2.

1. Full-authority feedback static anti-windup augmentation

   There exists a solution $\bar{X} \in \mathbb{R}^{n_{\mathrm{CL}} \times n_{\mathrm{CL}}}$ to the LMI problem:

$$\bar{X} = \begin{bmatrix} \bar{X}_{11} & \bar{X}_{12} \\ \bar{X}_{12}^T & \bar{X}_{22} \end{bmatrix} = \bar{X}^T > 0, \tag{5.4a}$$

$$A_p \bar{X}_{11} + \bar{X}_{11} A_p^T < 0, \tag{5.4b}$$

$$A_{\mathrm{CL}} \bar{X} + \bar{X} A_{\mathrm{CL}}^T < 0. \tag{5.4c}$$

2. External feedback static anti-windup augmentation

   There exists a solution $\bar{X} \in \mathbb{R}^{n_{\mathrm{CL}} \times n_{\mathrm{CL}}}$ to the LMI problem:

$$\bar{X} = \bar{X}^T > 0, \tag{5.5a}$$

$$M^T \left(\begin{bmatrix} A_p & 0 \\ 0 & A_g \end{bmatrix} \bar{X} + \bar{X} \begin{bmatrix} A_p & 0 \\ 0 & A_g \end{bmatrix}^T \right) M < 0, \tag{5.5b}$$

$$A_{\mathrm{CL}} \bar{X} + \bar{X} A_{\mathrm{CL}}^T < 0, \tag{5.5c}$$

where $M = \text{diag}[I_{n_p}, B_{g\perp}^T]$.

3. Generic static anti-windup configuration

   Global stability conditions for this anti-windup scheme depend on the performance level γ.

4. Conventional static anti-windup configuration for controller state

   There exists a solution $(\bar{X}, \bar{\bar{U}}) \in (\mathbb{R}^{n_{\text{CL}} \times n_{\text{CL}}}, \mathbb{D}^{n_u})$ to the LMI problem:

$$\bar{X} = \bar{X}^T > 0, \tag{5.6a}$$

$$\bar{\bar{U}} = \text{diag}[\bar{\mu}_1, ..., \bar{\mu}_{n_u}] > 0, \tag{5.6b}$$

$$\begin{bmatrix} \tilde{\text{p}}^T(A_{\text{CL}}\bar{X} + \bar{X}A_{\text{CL}}^T)\tilde{\text{p}} & \tilde{\text{p}}^T(B_{\text{CL},\psi}\bar{\bar{U}} - \bar{X}^T C_{\text{CL},u}) \\ (\bar{\bar{U}}B_{\text{CL},\psi}^T - C_{\text{CL},u}\bar{X})\tilde{\text{p}} & -\bar{\bar{U}}D_{\text{CL},u\psi}^T - D_{\text{CL},u\psi}\bar{\bar{U}} - 2\bar{\bar{U}} \end{bmatrix} < 0, \tag{5.6c}$$

$$A_{\text{CL}}\bar{X} + \bar{X}A_{\text{CL}}^T < 0, \tag{5.6d}$$

   with $\tilde{\text{p}}^T = \begin{bmatrix} I_{n_p} & 0 \end{bmatrix}$.

5. Conventional static anti-windup configuration for controller input

   There exists a solution $(\bar{X}, \bar{\bar{U}}) \in (\mathbb{R}^{n_{\text{CL}} \times n_{\text{CL}}}, \mathbb{D}^{n_u})$ to the LMI problem:

$$\bar{X} = \begin{bmatrix} \bar{X}_{11} & \bar{X}_{12} \\ \bar{X}_{12}^T & \bar{X}_{22} \end{bmatrix} = \bar{X}^T > 0, \tag{5.7a}$$

$$\bar{\bar{U}} = \text{diag}[\bar{\mu}_1, ..., \bar{\mu}_{n_u}] > 0, \tag{5.7b}$$

$$M^T \begin{bmatrix} \begin{bmatrix} A_p & 0 \\ 0 & A_g \end{bmatrix} \bar{X} + \bar{X} \begin{bmatrix} A_p & 0 \\ 0 & A_g \end{bmatrix}^T & \bar{X} \begin{bmatrix} 0 \\ C_g^T \end{bmatrix} - \begin{bmatrix} B_{p,u} \\ 0 \end{bmatrix} \bar{\bar{U}} \\ \begin{bmatrix} 0 & C_g \end{bmatrix} \bar{X} - \bar{\bar{U}} \begin{bmatrix} B_{p,u}^T & 0 \end{bmatrix} & -2\bar{\bar{U}} \end{bmatrix} M < 0, \tag{5.7c}$$

$$A_{\mathrm{CL}}\bar{X} + \bar{X}A_{\mathrm{CL}}^T < 0, \tag{5.7d}$$

where $M = \mathrm{diag}[I_{n_p}, \begin{bmatrix} B_{g,y}^T & -D_{g,y}^T \end{bmatrix}_\perp]$.

$\lhd$

Observing the conditions that guarantee global stability of the anti-windup closed-loop system, one can say that Assumption 5.2 corresponding to full-authority anti-windup augmentation is the mildest one when compared to the other anti-windup compensation schemes. In other words, Assumption 5.2 for external anti-windup augmentation and conventional anti-windup configuration for controller input will not hold if Assumption 5.2 for full-authority anti-windup augmentation does not hold. Moreover, note that Assumption 5.2 for the conventional anti-windup configurations emphasizes the well-posedness of the anti-windup closed-loop system.

In the following sections, we will concentrate on showing that, by appropriately choosing the matrix elements B_{g,v_1}, D_{g,v_1} and D_{g,v_2} in the general structure, Algorithm 5.1 permits to recover the algorithms for existing anti-windup compensation schemes synthesis. Observe that $\bar{L}$ is the parameter that carries the information of the compensation schemes, and hence, Steps 1 and 2 of Algorithm 5.1 are the ones that need to be rewritten for each corresponding scheme. The redefinition of Steps 1 and 2 will be considered next.

b. Full-authority feedback static anti-windup augmentation

Step 1. Construct the matrix $\tilde{L}_\perp$ as any full column rank matrix that spans the null space of $\tilde{L}^T$, where $\tilde{L}^T = \begin{bmatrix} 0 & I_{n_g} & 0 & 0 \\ \Upsilon_g^T B_{p,u}^T & -\Upsilon_g^T D_{p,yu}^T B_{g,y}^T & -\Upsilon_g^T & \Upsilon_g^T D_{p,zu}^T \end{bmatrix}$. Let $\bar{L} = \text{diag}[\tilde{L}_\perp, I_{n_u}, I_{n_{m_p}}, I_{n_{m_n}}, I_{n_{m_n}}]$.

Step 2. Find a solution $(X, \bar{V}, \tau) \in (\mathbb{R}^{n_{\text{CL}} \times n_{\text{CL}}}, \mathbb{D}^{n_{n_m}}, \mathbb{R})$, with $\gamma > 0$ as small as possible and $\tilde{\varrho} \geq 0$, to the LMI problem:

$$X = \begin{bmatrix} X_{11} & X_{12} \\ X_{12}^T & X_{22} \end{bmatrix} = X^T > 0, \tag{5.8a}$$

$$\bar{V} = \text{diag}[\nu_1, ..., \nu_{n_{m_p}}] > 0, \tag{5.8b}$$

$$\text{He} \begin{bmatrix} A_p X_{11} & 0 & X_{11} C_{p,z}^T & \tilde{\varrho} X_{11} C_{p,\eta_p}^T & \tau B_{p,\zeta_n} & \tilde{\varrho} X_{11} C_{p,\eta_n}^T \\ B_{p,u}^T & -\frac{\gamma}{2} I_{n_u} & D_{p,zu}^T & 0 & 0 & \tilde{\varrho} D_{p,\eta_n u}^T \\ 0 & 0 & -\frac{\gamma}{2} I_{n_z} & D_{p,z\zeta_p} \bar{V} & \tau D_{p,z\zeta_n} & 0 \\ B_{p,\zeta_p}^T \bar{V} & \tilde{\varrho} D_{p,\eta_p u} & 0 & \tilde{\varrho} D_{p,\eta_p \zeta_p}^T \bar{V} - \bar{V} & \tau \tilde{\varrho} D_{p,\eta_p u} D_{g,y} D_{p,y\zeta_n} & 0 \\ 0 & 0 & 0 & 0 & -\frac{\tau}{2} I_{n_{m_n}} & \tau \tilde{\varrho} D_{p,\eta_n \zeta_n} \\ 0 & 0 & 0 & \tilde{\varrho} D_{p,y\zeta_p}^T D_{g,y}^T D_{p,\eta_n u}^T \bar{V} & 0 & -\frac{\tau}{2} I_{n_{m_n}} \end{bmatrix} < 0, \tag{5.8c}$$

$$\text{He} \begin{bmatrix} A_{\text{CL}} X & 0 & X C_{\text{CL},z}^T & \tilde{\varrho} X C_{\text{CL},\eta_p}^T & \tau B_{\text{CL},\zeta_n} & \tilde{\varrho} X C_{\text{CL},\eta_n}^T \\ 0 & -\frac{\gamma}{2} I_{n_u} & 0 & 0 & 0 & 0 \\ 0 & 0 & -\frac{\gamma}{2} I_{n_z} & 0 & 0 & 0 \\ \bar{V} B_{\text{CL},\zeta_p}^T & 0 & D_{\text{CL},z\zeta_p}^T & \tilde{\varrho} D_{\text{CL},\eta_p \zeta_p}^T \bar{V} - \bar{V} & 0 & 0 \\ 0 & 0 & \tau D_{\text{CL},z\zeta_n}^T & 0 & -\frac{\tau}{2} I_{n_m} & \tilde{\varrho} D_{\text{CL},\eta_n \zeta_n}^T \\ 0 & 0 & 0 & 0 & 0 & -\frac{\tau}{2} I_{n_m} \end{bmatrix} < 0. \tag{5.8d}$$

c. External feedback static anti-windup augmentation

Step 1. Construct the matrix $\tilde{L}_\perp$ as any full column rank matrix that spans the null space of $\tilde{L}^T$, where $\tilde{L}^T = \begin{bmatrix} D_{g,y}^T \Upsilon_g^T B_{p,u}^T & \Upsilon_p^T B_{g,y}^T & -D_{g,y}^T \Upsilon_g^T & D_{g,y}^T \Upsilon_g^T D_{p,zu}^T \\ \Upsilon_g^T B_{p,u}^T & -\Upsilon_g^T D_{p,yu}^T B_{g,y}^T & -\Upsilon_g^T & \Upsilon_g^T D_{p,zu}^T \end{bmatrix}$. Let $\bar{L} = \mathrm{diag}[\tilde{L}_\perp, I_{n_u}, I_{n_{m_p}}, I_{n_{m_n}}, I_{n_{m_n}}]$.

Step 2. Find a solution $(X, \bar{V}, \tau) \in (\mathbb{R}^{n_{\mathrm{CL}} \times n_{\mathrm{CL}}}, \mathbb{D}^{n_{n_m}}, \mathbb{R})$, with $\gamma > 0$ as small as possible and $\tilde{\varrho} \geq 0$, to the LMI problem:

$$X = \begin{bmatrix} X_{11} & X_{12} \\ X_{12}^T & X_{22} \end{bmatrix} = X^T > 0, \tag{5.9a}$$

$$\bar{V} = \mathrm{diag}[\nu_1, ..., \nu_{n_{m_p}}] > 0, \tag{5.9b}$$

$$\mathrm{He}\, \bar{L}^T \begin{bmatrix} A_p X_{11} & X_{12} A_g^T & 0 & X_{11} C_{p,z}^T & \tilde{\varrho} X_{11} C_{p,\eta_p}^T & \tau B_{p,\zeta_n} & \tilde{\varrho} X_{11} C_{p,\eta_n}^T \\ X_{12}^T A_p^T & A_g X_{22} & 0 & 0 & 0 & 0 & 0 \\ B_{p,u}^T & 0 & -\frac{\gamma}{2} I_{n_u} & D_{p,zu}^T & 0 & 0 & \tilde{\varrho} D_{p,\eta_n u}^T \\ 0 & C_{p,z} X_{12} & 0 & -\frac{\gamma}{2} I_{n_z} & D_{p,z\zeta_p} \bar{V} & \tau D_{p,z\zeta_n} & 0 \\ B_{\mathrm{CL},\zeta_p}^T \bar{V} & \tilde{\varrho} C_{p,\eta_p} X_{12} & \tilde{\varrho} D_{p,\eta_p u} & 0 & \tilde{\varrho} D_{p,\eta_p \zeta_p}^T \bar{V} - \bar{V} & 0 & 0 \\ 0 & 0 & 0 & 0 & \tau \tilde{\varrho} D_{p,y\zeta_n}^T D_{g,y}^T D_{p,\eta_p u}^T & -\frac{\tau}{2} I_{n_{m_n}} & \tau \tilde{\varrho} D_{p,\eta_n \zeta_n} \\ 0 & \tilde{\varrho} C_{p,\eta_n} X_{12} & 0 & 0 & \tilde{\varrho} D_{p,y\zeta_p}^T D_{g,y}^T D_{p,\eta_n u}^T \bar{V} & 0 & -\frac{\tau}{2} I_{n_{m_n}} \end{bmatrix} \bar{L} < 0, \tag{5.9c}$$

$$\mathrm{He} \begin{bmatrix} A_{\mathrm{CL}} X & 0 & X C_{\mathrm{CL},z}^T & \tilde{\varrho} X C_{\mathrm{CL},\eta_p}^T & \tau B_{\mathrm{CL},\zeta_n} & \tilde{\varrho} X C_{\mathrm{CL},\eta_n}^T \\ 0 & -\frac{\gamma}{2} I_{n_u} & 0 & 0 & 0 & 0 \\ 0 & 0 & -\frac{\gamma}{2} I_{n_z} & 0 & 0 & 0 \\ \bar{V} B_{\mathrm{CL},\zeta_p}^T & 0 & D_{\mathrm{CL},z\zeta_p}^T & \tilde{\varrho} D_{\mathrm{CL},\eta_p \zeta_p}^T \bar{V} - \bar{V} & 0 & 0 \\ 0 & 0 & \tau D_{\mathrm{CL},z\zeta_n}^T & 0 & -\frac{\tau}{2} I_{n_m} & \tilde{\varrho} D_{\mathrm{CL},\eta_n \zeta_n}^T \\ 0 & 0 & 0 & 0 & 0 & -\frac{\tau}{2} I_{n_m} \end{bmatrix} < 0. \tag{5.9d}$$

d. Generic static anti-windup configuration

Step 1. Construct the matrix $\tilde{L}_\perp$ as any full column rank matrix that spans the null space of $\tilde{L}^T$, where $\tilde{L}^T = \left[\begin{array}{cccc} \Upsilon_g^T B_{p,u}^T & -\Upsilon_g^T D_{p,yu}^T B_{g,y}^T & -\Upsilon_g^T & \Upsilon_g^T D_{p,zu}^T \end{array}\right]$. Let $\bar{L} = \mathrm{diag}[\tilde{L}_\perp, I_{n_u}, I_{n_{mp}}, I_{n_{mn}}, I_{n_{mn}}]$.

Step 2. Find a solution $(X, \bar{U}, \bar{V}, \tau) \in (\mathbb{R}^{n_{\mathrm{CL}} \times n_{\mathrm{CL}}}, \mathbb{D}^{n_u}, \mathbb{D}^{n_{nm}}, \mathbb{R})$, with $\gamma > 0$ as small as possible and $\tilde{\varrho} \geq 0$, to the LMI problem:

$$X = \left[\begin{array}{cc} X_{11} & X_{12} \\ X_{12}^T & X_{22} \end{array}\right] = X^T > 0, \tag{5.10a}$$

$$\bar{U} = \mathrm{diag}[\mu_1, ..., \mu_{n_u}] > 0, \tag{5.10b}$$

$$\bar{V} = \mathrm{diag}[\nu_1, ..., \nu_{n_{mp}}] > 0, \tag{5.10c}$$

$$\mathrm{He}\, \bar{L}^T \left[\begin{array}{ccccccc} A_{\mathrm{CL}} X & B_{\mathrm{CL},\psi}\bar{U} & 0 & 0 & \tilde{\varrho} X C_{\mathrm{CL},\eta_p}^T & \tau B_{\mathrm{CL},\zeta_n} & 0 \\ -C_{\mathrm{CL},u} X & -D_{\mathrm{CL},u\psi}\bar{U} - \bar{U} & 0 & I_{n_u} & -D_{\mathrm{CL},u\zeta_p}\bar{V} & -\tau D_{\mathrm{CL},u\zeta_n} & 0 \\ C_{\mathrm{CL},z} X & D_{\mathrm{CL},z\psi}\bar{U} & -\frac{\gamma}{2} I_{n_z} & 0 & D_{\mathrm{CL},z\zeta_p}\bar{V} & \tau D_{\mathrm{CL},z\zeta_n} & 0 \\ 0 & 0 & 0 & -\frac{\gamma}{2} I_{n_u} & 0 & 0 & 0 \\ \bar{V} B_{\mathrm{CL},\zeta_p}^T & \tilde{\varrho} D_{\mathrm{CL},\eta_p\psi}\bar{U} & 0 & 0 & \tilde{\varrho} D_{\mathrm{CL},\eta_p\zeta_p}\bar{V} - \bar{V} & 0 & 0 \\ 0 & 0 & 0 & 0 & 0 & -\frac{\tau}{2} I_{n_{mn}} & 0 \\ \tilde{\varrho} C_{\mathrm{CL},\eta_n} X & \tilde{\varrho} D_{\mathrm{CL},\eta_n\psi}\bar{U} & 0 & 0 & 0 & \tau\tilde{\varrho} D_{\mathrm{CL},\eta_n\zeta_n} & -\frac{\tau}{2} I_{n_{mn}} \end{array}\right] \bar{L} < 0, \tag{5.10d}$$

$$\mathrm{He} \left[\begin{array}{cccccc} A_{\mathrm{CL}} X & 0 & X C_{\mathrm{CL},z}^T & \tilde{\varrho} X C_{\mathrm{CL},\eta_p}^T & \tau B_{\mathrm{CL},\zeta_n} & \tilde{\varrho} X C_{\mathrm{CL},\eta_n}^T \\ 0 & -\frac{\gamma}{2} I_{n_u} & 0 & 0 & 0 & 0 \\ 0 & 0 & -\frac{\gamma}{2} I_{n_z} & 0 & 0 & 0 \\ \bar{V} B_{\mathrm{CL},\zeta_p}^T & 0 & D_{\mathrm{CL},z\zeta_p}^T & \tilde{\varrho} D_{\mathrm{CL},\eta_p\zeta_p}^T \bar{V} - \bar{V} & 0 & 0 \\ 0 & 0 & \tau D_{\mathrm{CL},z\zeta_n}^T & 0 & -\frac{\tau}{2} I_{n_m} & \tilde{\varrho} D_{\mathrm{CL},\eta_n\zeta_n}^T \\ 0 & 0 & 0 & 0 & 0 & -\frac{\tau}{2} I_{n_m} \end{array}\right] < 0. \tag{5.10e}$$

e. Conventional static anti-windup configuration for controller state

Step 1. Construct the matrix $\tilde{L}_\perp$ as any full column rank matrix that spans the null space of $\tilde{L}^T$, where $\tilde{L}^T = \left[\begin{array}{cccc} 0 & I_{n_g} & 0 & 0 \end{array}\right]$. Let $\bar{L} = \text{diag}[\tilde{L}_\perp, I_{n_u}, I_{n_{m_p}}, I_{n_{m_n}}, I_{n_{m_n}}]$.

Step 2. Find a solution $(X, \bar{U}, \bar{V}, \tau) \in (\mathbb{R}^{n_{\text{CL}} \times n_{\text{CL}}}, \mathbb{D}^{n_u}, \mathbb{D}^{n_{n_m}}, \mathbb{R})$, with $\gamma > 0$ as small as possible and $\tilde{\varrho} \geq 0$, to the LMI problem:

$$X = \left[\begin{array}{cc} X_{11} & X_{12} \\ X_{12}^T & X_{22} \end{array}\right] = X^T > 0, \tag{5.11a}$$

$$\bar{U} = \text{diag}[\mu_1, ..., \mu_{n_u}] > 0, \tag{5.11b}$$

$$\bar{V} = \text{diag}[\nu_1, ..., \nu_{n_{m_p}}] > 0, \tag{5.11c}$$

$$\text{He}\left[\begin{array}{ccccccc} \tilde{\text{p}}^T A_{\text{CL}} X \tilde{\text{p}} & \tilde{\text{p}}^T B_{\text{CL},\psi} \bar{U} & 0 & 0 & \tilde{\text{p}}^T \tilde{\varrho} X C_{\text{CL},\eta_p}^T & \tilde{\text{p}}^T \tau B_{\text{CL},\zeta_n} & 0 \\ -C_{\text{CL},u} X \tilde{\text{p}} & -D_{\text{CL},u\psi} \bar{U} - \bar{U} & 0 & I_{n_u} & -D_{\text{CL},u\zeta_p} \bar{V} & -\tau D_{\text{CL},u\zeta_n} & 0 \\ C_{\text{CL},z} X \tilde{\text{p}} & D_{\text{CL},z\psi} \bar{U} & -\frac{\gamma}{2} I_{n_z} & 0 & D_{\text{CL},z\zeta_p} \bar{V} & \tau D_{\text{CL},z\zeta_n} & 0 \\ 0 & 0 & 0 & -\frac{\gamma}{2} I_{n_u} & 0 & 0 & 0 \\ \bar{V} B_{\text{CL},\zeta_p}^T \tilde{\text{p}} & \tilde{\varrho} D_{\text{CL},\eta_p\psi} \bar{U} & 0 & 0 & \tilde{\varrho} D_{\text{CL},\eta_p\zeta_p} \bar{V} - \bar{V} & 0 & 0 \\ 0 & 0 & 0 & 0 & 0 & -\frac{\tau}{2} I_{n_{m_n}} & 0 \\ \tilde{\varrho} C_{\text{CL},\eta_n} X \tilde{\text{p}} & \tilde{\varrho} D_{\text{CL},\eta_n\psi} \bar{U} & 0 & 0 & 0 & \tau \tilde{\varrho} D_{\text{CL},\eta_n\zeta_n} & -\frac{\tau}{2} I_{n_{m_n}} \end{array}\right] < 0, \tag{5.11d}$$

$$\text{He}\left[\begin{array}{cccccc} A_{\text{CL}} X & 0 & X C_{\text{CL},z}^T & \tilde{\varrho} X C_{\text{CL},\eta_p}^T & \tau B_{\text{CL},\zeta_n} & \tilde{\varrho} X C_{\text{CL},\eta_n}^T \\ 0 & -\frac{\gamma}{2} I_{n_u} & 0 & 0 & 0 & 0 \\ 0 & 0 & -\frac{\gamma}{2} I_{n_z} & 0 & 0 & 0 \\ \bar{V} B_{\text{CL},\zeta_p}^T & 0 & D_{\text{CL},z\zeta_p}^T & \tilde{\varrho} D_{\text{CL},\eta_p\zeta_p}^T \bar{V} - \bar{V} & 0 & 0 \\ 0 & 0 & \tau D_{\text{CL},z\zeta_n}^T & 0 & -\frac{\tau}{2} I_{n_m} & \tilde{\varrho} D_{\text{CL},\eta_n\zeta_n}^T \\ 0 & 0 & 0 & 0 & 0 & -\frac{\tau}{2} I_{n_m} \end{array}\right] < 0, \tag{5.11e}$$

with $\tilde{\text{p}}^T = \left[\begin{array}{cc} I_{n_p} & 0 \end{array}\right]$.

f. Conventional static anti-windup configuration for controller input

Step 1. Construct the matrix $\tilde{L}_\perp$ as any full column rank matrix that spans the null space of $\tilde{L}^T$, where $\tilde{L}^T = \left[\begin{array}{cccc} D_{g,y}^T \Upsilon_g^T B_{p,u}^T & \Upsilon_p^T B_{g,y}^T & -D_{g,y}^T \Upsilon_g^T & D_{g,y}^T \Upsilon_g^T D_{p,zu}^T \end{array}\right]$. Let $\bar{L} = \text{diag}[\tilde{L}_\perp, I_{n_u}, I_{n_{m_p}}, I_{n_{m_n}}, I_{n_{m_n}}]$.

Step 2. Find a solution $(X, \bar{U}, \bar{V}, \tau) \in (\mathbb{R}^{n_{\text{CL}} \times n_{\text{CL}}}, \mathbb{D}^{n_u}, \mathbb{D}^{n_{nm}}, \mathbb{R})$, with $\gamma > 0$ as small as possible and $\tilde{\varrho} \geq 0$, to the LMI problem:

$$X = \left[\begin{array}{cc} X_{11} & X_{12} \\ X_{12}^T & X_{22} \end{array}\right] = X^T > 0, \tag{5.12a}$$

$$\bar{U} = \text{diag}[\mu_1, ..., \mu_{n_u}] > 0, \tag{5.12b}$$

$$\bar{V} = \text{diag}[\nu_1, ..., \nu_{n_{m_p}}] > 0, \tag{5.12c}$$

$$\text{He}\, \bar{L}^T \left[\begin{array}{cccccccc} A_p X_{11} & X_{12} A_g^T & -X_{12} C_g^T & 0 & X_{11} C_{p,z}^T & \tilde{\varrho} X_{11} C_{p,\eta_p}^T & \tau B_{p,\zeta_n} & \tilde{\varrho} X_{11} C_{p,\eta_n}^T \\ X_{12}^T A_p^T & A_g X_{22} & -X_{22} C_g^T & 0 & 0 & 0 & 0 & 0 \\ -\bar{U} B_{p,u}^T & 0 & -\bar{U} & I_{n_u} & 0 & -D_{p,u\zeta_p} \bar{V} & -\tau D_{p,u\zeta_n}^T & 0 \\ B_{p,u}^T & 0 & 0 & -\frac{\gamma}{2} I_{n_u} & D_{p,zu}^T & 0 & 0 & \tilde{\varrho} D_{p,\eta_n u}^T \\ 0 & C_{p,z} X_{12} & -D_{p,zu} \bar{U} & 0 & -\frac{\gamma}{2} I_{n_z} & D_{p,z\zeta_p} \bar{V} & \tau D_{p,z\zeta_n} & 0 \\ B_{\text{CL},\zeta_p}^T \bar{V} & \tilde{\varrho} C_{p,\eta_p} X_{12} & 0 & \tilde{\varrho} D_{p,\eta_p u} & 0 & \tilde{\varrho} D_{p,\eta_p\zeta_p}^T \bar{V} - \bar{V} & 0 & 0 \\ 0 & 0 & 0 & 0 & 0 & \tau \tilde{\varrho} D_{p,y\zeta_n}^T D_{g,y}^T D_{p,\eta_p u}^T & -\frac{\tau}{2} I_{n_{m_n}} & \tau \tilde{\varrho} D_{p,\eta_n\zeta_n} \\ 0 & \tilde{\varrho} C_{p,\eta_n} X_{12} & D_{p,\eta_n u} \bar{U} & 0 & 0 & \tilde{\varrho} D_{p,y\zeta_p}^T D_{g,y}^T D_{p,\eta_n u}^T \bar{V} & 0 & -\frac{\tau}{2} I_{n_{m_n}} \end{array}\right] \bar{L} < 0, \tag{5.12d}$$

$$\text{He} \left[\begin{array}{cccccc} A_{\text{CL}} X & 0 & X C_{\text{CL},z}^T & \tilde{\varrho} X C_{\text{CL},\eta_p}^T & \tau B_{\text{CL},\zeta_n} & \tilde{\varrho} X C_{\text{CL},\eta_n}^T \\ 0 & -\frac{\gamma}{2} I_{n_u} & 0 & 0 & 0 & 0 \\ 0 & 0 & -\frac{\gamma}{2} I_{n_z} & 0 & 0 & 0 \\ \bar{V} B_{\text{CL},\zeta_p}^T & 0 & D_{\text{CL},z\zeta_p}^T & \tilde{\varrho} D_{\text{CL},\eta_p\zeta_p}^T \bar{V} - \bar{V} & 0 & 0 \\ 0 & 0 & \tau D_{\text{CL},z\zeta_n}^T & 0 & -\frac{\tau}{2} I_{n_m} & \tilde{\varrho} D_{\text{CL},\eta_n\zeta_n}^T \\ 0 & 0 & 0 & 0 & 0 & -\frac{\tau}{2} I_{n_m} \end{array}\right] < 0. \tag{5.12e}$$

The next theorem states that Assumption 5.2 provides necessary and sufficient conditions for the static linear anti-windup compensation to be successfully constructed.

Theorem 5.3 *Assumption 5.2 is necessary and sufficient to guarantee that all steps in Algorithm 5.1 can be completed for each anti-windup compensation scheme and the corresponding resulting* $(D_{\Lambda_1}, D_{\Lambda_2})$ *describe a static linear anti-windup compensator that guarantees the anti-windup closed-loop satisfies the basic properties of anti-windup and has finite unconstrained response recovery gain less than* γ. $\lhd$

Since Assumption 5.2 provides necessary and sufficient conditions for the successful construction of a variety of anti-windup compensation schemes, one can say that the success of the static anti-windup schemes synthesis algorithms may or may not depend on the performance measure and on an additional parameter $\bar{U}$. The cases in which the success of static anti-windup compensation synthesis algorithms do not depend on the measure of performance correspond to the full-authority and external feedback anti-windup augmentations, and the conventional anti-windup configurations. However, note that, in the case of the conventional anti-windup configurations, there exists an additional parameter $\bar{U}$ that imposes further restrictions on the achievement of global stability. We will show in the next chapter that the parameter $\bar{U}$ in the conventional anti-windup configuration for controller state case is explicitly enforcing well-posedness of the anti-windup closed-loop system. Notably, this requirement arises as this conventional configuration case only has a limited access to the unconstrained controller. On the other side, the generic anti-windup configuration stands as the only case where global stability of the anti-windup closed-loop system is tied to the performance measure and also the enforcement of well-posedness appears explicitly in the synthesis algorithm.

2. Static override

Static compensation for the output constrained problem will be considered in this part of the dissertation. Recall from Section II.C that the finite unconstrained response recovery gain for override compensation refers to the $\mathcal{L}_2$ gain from the difference signal $\text{sat}(z_l) - z_l$ (z_l comes from the unconstrained closed-loop system and $\text{sat}(z_l)$ corresponds to its saturated version) to the difference of signals $\begin{bmatrix} \text{sat}(z_l) - z \\ y_l - y \end{bmatrix}$ (z_l and y_l come from the unconstrained closed-loop system, $\text{sat}(z_l)$ is the saturated version of z_l and z comes from the anti-windup closed-loop system). Therefore, the algorithms presented in this section will guarantee that, regardless of the exogenous disturbance $w \in \mathcal{L}_2$ and when the initial conditions of the plant and controller in the mismatch system are zero, the following is satisfied:

$$\left\| \begin{bmatrix} \text{sat}(z_l) - z \\ y_l - y \end{bmatrix} (\cdot) \right\|_2 \leq \gamma \|(\text{sat}(z_l) - z_l)(\cdot)\|_2, \tag{5.13}$$

with the finite unconstrained recovery gain γ as small as possible. More specifically, the algorithms in this section are aimed at constructing the gains D_{Θ_1} and D_{Θ_2}, shown in Fig. 25, of a static linear override compensator that guarantees an optimal finite unconstrained response recovery gain. Algorithm 5.4 is now offered in order to provide static override compensation synthesis. Recall that we will perform the calculations for the GOC for controller state/output case.

a. Static GOC for controller state/output

Algorithm 5.4 (Static override compensation)

Step 1. Find a solution $(X, \bar{U}, \bar{V}, \tau, \pi) \in (\mathbb{R}^{n_{\mathrm{CL}} \times n_{\mathrm{CL}}}, \mathbb{D}^{n_u}, \mathbb{D}^{n_{n_m}}, \mathbb{R}, \mathbb{R})$, with $\gamma > 0$ as small as possible and $\tilde{\varrho} \geq 0$, to the LMI problem:

$$X = \begin{bmatrix} X_{11} & Y_{12} \\ Y_{12}^T & Y_{22} \end{bmatrix} = X^T > 0, \tag{5.14a}$$

$$\bar{U} = \mathrm{diag}[\mu_1, ..., \mu_{n_u}] > 0, \tag{5.14b}$$

$$\bar{V} = \mathrm{diag}[\nu_1, ..., \nu_{n_{m_p}}] > 0, \tag{5.14c}$$

$$\mathrm{He}\, \bar{L}^T \begin{bmatrix} \tilde{\mathrm{p}}^T A_{\mathrm{CL}} X \tilde{\mathrm{p}} & -\tilde{\mathrm{p}}^T X C_{\mathrm{CL},z}^T & \tilde{\mathrm{p}}^T C_{\mathrm{CL},y}^T W_y^T & 0 & 0 & \tilde{\mathrm{p}}^T \tilde{\varrho} X C_{\mathrm{CL},\eta_p}^T & \tilde{\mathrm{p}}^T \tau B_{\mathrm{CL},\zeta_n} & 0 \\ 0 & -\bar{U} & 0 & -2\bar{U} W_z^T & 0 & -D_{\mathrm{CL},z\zeta_p} \bar{V} & -\tau D_{\mathrm{CL},z\zeta_n} & 0 \\ 0 & 0 & -\frac{\gamma}{2} I_{n_y} & 0 & 0 & D_{\mathrm{CL},y\zeta_p} \bar{V} & \tau D_{\mathrm{CL},y\zeta_n} & 0 \\ 0 & 0 & 0 & -W_z \bar{U} W_z^T - \frac{\gamma}{2} I_{n_z} & 0 & D_{\mathrm{CL},z\zeta_p} \bar{V} & \tau D_{\mathrm{CL},z\zeta_n} & 0 \\ 0 & 0 & 0 & -I_{n_z} W_o^T W_z^T & -\frac{\gamma}{2} I_{n_z} & 0 & 0 & 0 \\ \bar{V} B_{\mathrm{CL},\zeta_p}^T \tilde{\mathrm{p}} & \tilde{\varrho} D_{\mathrm{CL},\eta_p \psi} \bar{U} & 0 & 0 & 0 & \tilde{\varrho} D_{\mathrm{CL},\eta_p \zeta_p} \bar{V} - \bar{V} & 0 & 0 \\ 0 & 0 & 0 & 0 & 0 & 0 & -\frac{\tau}{2} I_{n_{m_n}} & 0 \\ \tilde{\varrho} C_{\mathrm{CL},\eta_n} X \tilde{\mathrm{p}} & \tilde{\varrho} D_{\mathrm{CL},\eta_n \psi} \bar{U} & 0 & 0 & 0 & 0 & \tau \tilde{\varrho} D_{\mathrm{CL},\eta_n \zeta_n} & -\frac{\tau}{2} I_{n_{m_n}} \end{bmatrix} \bar{L} < 0, \tag{5.14d}$$

$$\mathrm{He} \begin{bmatrix} A_{\mathrm{CL}} X & -X C_{\mathrm{CL},z}^T & X C_{\mathrm{CL},y}^T W_y^T & X C_{\mathrm{CL},z}^T W_z^T & \tilde{\varrho} Y C_{\mathrm{CL},\eta_p}^T & \tau B_{\mathrm{CL},\zeta_n} & \tilde{\varrho} X C_{\mathrm{CL},\eta_n}^T \\ 0 & -\frac{\pi}{2} I_{n_z} & 0 & \bar{U} W_z^T & 0 & 0 & 0 \\ 0 & 0 & -\frac{\gamma}{2} I_{n_y} & 0 & 0 & 0 & 0 \\ 0 & 0 & 0 & -\frac{\gamma}{2} I_{n_z} & 0 & 0 & 0 \\ \bar{V} B_{\mathrm{CL},\zeta_p}^T & 0 & D_{\mathrm{CL},y\zeta_p}^T & D_{\mathrm{CL},z\zeta_p}^T & \tilde{\varrho} D_{\mathrm{CL},\eta_p \zeta_p}^T \bar{V} - \bar{V} & 0 & 0 \\ 0 & 0 & \tau D_{\mathrm{CL},y\zeta_n}^T & \tau D_{\mathrm{CL},z\zeta_n}^T & 0 & -\frac{\tau}{2} I_{n_m} & \tilde{\varrho} D_{\mathrm{CL},\eta_n \zeta_n}^T \\ 0 & 0 & 0 & 0 & 0 & 0 & -\frac{\tau}{2} I_{n_m} \end{bmatrix} < 0, \tag{5.14e}$$

with $\tilde{\mathrm{p}}^T = \begin{bmatrix} I_{n_p} & 0 \end{bmatrix}$ and $\bar{L} = \mathrm{diag}[\begin{bmatrix} -\Upsilon_p^T B_{p,u}^T & \Upsilon_p^T D_{p,zu}^T & -\Upsilon_p^T D_{p,yu}^T W_y^T \end{bmatrix}_\perp, I_{n_z}, I_{n_z}, I_{n_{m_p}}, I_{n_{m_n}}, I_{n_{m_n}}]$.

Step 2. Using $m = n_{\mathrm{CL}} + n_z + n_y + n_z + n_z + n_{m_p} + n_{m_n} + n_{m_n}$, construct the matrices $\Psi \in \mathbb{R}^{m \times m}$, $\tilde{R} \in \mathbb{R}^{n_z \times m}$, and $\tilde{P} \in \mathbb{R}^{m \times (n_{v_1} + n_{v_2})}$ via:

$$[\Psi, \tilde{R}, \tilde{P}] = V_{n_p\text{-dynamic}}(\mathcal{P}^{\Delta}, \mathcal{G}_{\mathcal{M}}, X, Y, \bar{U}, \bar{V}, \tau, \gamma),$$

where the function V_{static} is given in Chapter VI.

Step 3. Find a solution $(D_{\Theta_1}, D_{\Theta_2}) \in (\mathbb{R}^{n_{v_1} \times n_z}, \mathbb{R}^{n_{v_2} \times n_z})$ to the LMI problem:

$$\Psi + \tilde{P}^T \begin{bmatrix} D_{\Theta_1} \\ D_{\Theta_2} \end{bmatrix} \tilde{R} + \tilde{R}^T \begin{bmatrix} D_{\Theta_1} \\ D_{\Theta_2} \end{bmatrix}^T \tilde{P} < 0. \tag{5.15}$$

$\triangleleft$

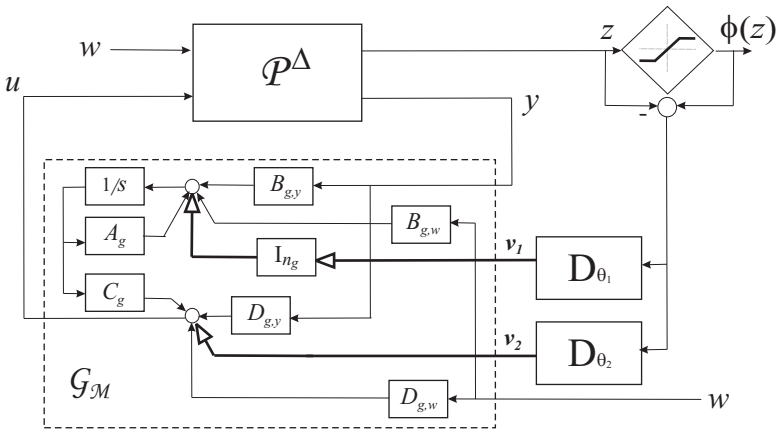

Fig. 25. Static override compensator is fed back to the unconstrained controller states and output.

Note that, a simple inspection of Algorithm 5.4, Step 1, does not offer any information with respect to under what conditions global stability of the override closed-loop system is guaranteed. However, by employing the Finsler Lemma [14], one can prove that the conditions stated below in Assumption 5.5 guarantee global stability for the static override compensation with GOC for controller state/output.

Assumption 5.5. There exists a solution $(\bar{X}, \bar{\bar{U}}) \in (\mathbb{R}^{n_{\mathrm{CL}} \times n_{\mathrm{CL}}}, \mathbb{D}^{n_u})$ to the LMI problem:

$$\bar{X} = \begin{bmatrix} \bar{X}_{11} & \bar{X}_{12} \\ \bar{X}_{12}^T & \bar{X}_{22} \end{bmatrix} = \bar{X}^T > 0, \tag{5.16a}$$

$$A_p \bar{X}_{11} + \bar{X}_{11} A_p^T < 0, \tag{5.16b}$$

$$A_{\mathrm{CL}} \bar{X} + \bar{X} A_{\mathrm{CL}}^T < 0. \tag{5.16c}$$

$\lhd$

Observing the conditions that guarantee global stability of the override closed-loop system, one can say that Assumption 5.5 requires, through Lyapunov inequalities, that both the plant and the unconstrained closed-loop are asymptotically stable,

and also there is a coupling of these Lyapunov inequalities to be satisfied.

Theorem 5.6 *Assumption 5.5 is necessary and sufficient to guarantee that all steps in Algorithm 5.4 can be completed and the corresponding resulting* $(D_{\Theta_1}, D_{\Theta_2})$ *describe a static linear override compensator that guarantees the override closed-loop satisfies the basic properties of override and has finite unconstrained response recovery gain less than* γ. $\lhd$

B. Dynamic remedial compensation

This section considers the effect of incorporating a dynamic, or arbitrary-order, linear remedial compensator in the remedial closed-loop system. Dynamic linear remedial compensation as described in Section II.B possesses a very appealing structure because it can be implemented easily and its capabilities are not limited as the static linear anti-windup compensation case.

1. Dynamic anti-windup

Dynamic compensation for the input constrained problem will be considered in this part of the dissertation. Recall from Section II.C that the finite unconstrained response recovery gain for anti-windup compensation refers to the $\mathcal{L}_2$ gain from the unconstrained controller output u_l to the difference between the unconstrained closed-loop system response and the anti-windup closed-loop system response $z_l - z$. Therefore, the algorithms presented in this section will guarantee that, regardless of the exogenous disturbance $w \in \mathcal{L}_2$ and when the initial conditions of the plant, controller and anti-windup compensator in the mismatch system are zero, the following is satisfied:

$$\|z_l(\cdot) - z(\cdot)\|_2 \leq \gamma \|u_l(\cdot)\|_2, \tag{5.17}$$

with the finite unconstrained recovery gain γ as small as possible. More specifically, the algorithms in this section are aimed at constructing the matrix elements of a dynamic linear anti-windup compensator that guarantees an optimal finite unconstrained response recovery gain. The case when the dynamic anti-windup compensation to be constructed is chosen to be of order equal to the plant, which is called *plant-order* anti-windup compensation, is specially important because it provides very useful synthesis algorithms [21]. Interestingly, plant-order anti-windup compensation algorithms are computationally efficient because the corresponding steps are only given in terms of LMI conditions. On the contrary, arbitrary-order anti-windup compensation presents some steps where a non-convex optimization problem must be solved .

a. General external structure dynamic anti-windup

As introduced and described in Section II.B, dynamic anti-windup compensation synthesis amounts to obtaining the element matrices A_Λ, B_Λ, C_{Λ_1}, C_{Λ_2}, D_{Λ_1} and D_{Λ_2} of the dynamic anti-windup compensator. Figure 26 shows these elements matrices in a compact form. Algorithms 5.7 and 5.8 are now offered in order to provide the most general case of dynamic anti-windup compensation, which corresponds to using the general external structure for anti-windup. Algorithm 5.7 is given for plant-order dynamic anti-windup compensation and Algorithm 5.8 is given for arbitrary-order dynamic anti-windup compensation. Moreover, Algorithms 5.7 and 5.8 will be employed to obtain the corresponding algorithms for the existing dynamic anti-windup configurations.

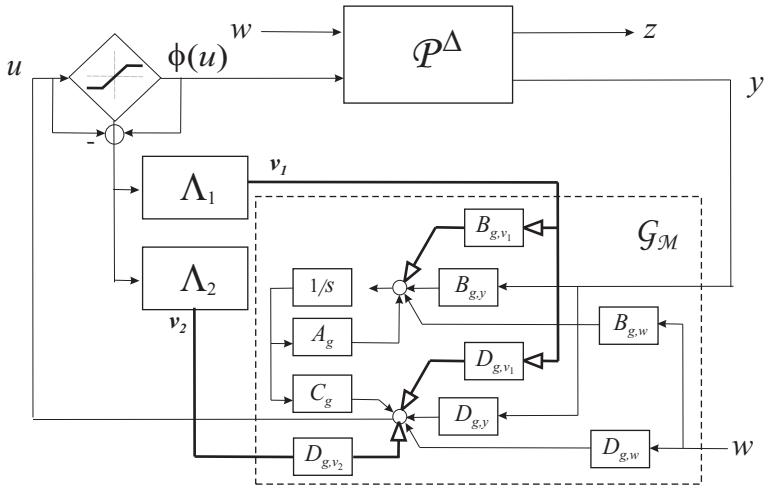

Fig. 26. Dynamic anti-windup compensator is fed back in a general external structure.

Algorithm 5.7 (Plant-order dynamic anti-windup compensation design with general external structure)

Step 1. Construct the matrix $\tilde{L}_\perp$ as any full column rank matrix that spans the null space of $\tilde{L}^T$, where:

$$\tilde{L}^T = \begin{bmatrix} D_{g,v_1}^T \Upsilon_g^T B_{p,u}^T & B_{g,v_1}^T - D_{g,v_1}^T \Upsilon_g^T D_{p,yu}^T B_{g,y}^T & -D_{g,v_1}^T \Upsilon_g^T & D_{g,v_1}^T \Upsilon_g^T D_{p,zu}^T \\ D_{g,v_2}^T \Upsilon_g^T B_{p,u}^T & -D_{g,v_2}^T \Upsilon_g^T D_{p,yu}^T B_{g,y}^T & -D_{g,v_2}^T \Upsilon_g^T & D_{g,v_2}^T \Upsilon_g^T D_{p,zu}^T \end{bmatrix}.$$

Let $\bar{L} = \mathrm{diag}[\tilde{L}_\perp, I_{n_u}, I_{n_{mp}}, I_{n_{mn}}, I_{n_{mn}}]$.

Step 2. Find a solution $(X, Y, \bar{U}, \bar{V}, \tau) \in (\mathbb{R}^{n_{\mathrm{CL}} \times n_{\mathrm{CL}}}, \mathbb{R}^{n_{\mathrm{CL}} \times n_{\mathrm{CL}}}, \mathbb{D}^{n_u}, \mathbb{D}^{n_{nm}}, \mathbb{R})$, with $\gamma > 0$ as small as possible and $\tilde{\varrho} \geq 0$, to the LMI problem:

$$X = \begin{bmatrix} X_{11} & X_{12} \\ X_{12}^T & X_{22} \end{bmatrix} = X^T > 0, \tag{5.18a}$$

$$Y = \begin{bmatrix} Y_{11} & Y_{12} \\ Y_{12}^T & Y_{22} \end{bmatrix} = Y^T > 0, \tag{5.18b}$$

$$X - Y > 0, \tag{5.18c}$$

$$\bar{U} = \mathrm{diag}[\mu_1, ..., \mu_{n_u}] > 0, \tag{5.18d}$$

$$\bar{V} = \mathrm{diag}[\nu_1, ..., \nu_{n_{mp}}] > 0, \tag{5.18e}$$

$$\mathrm{He}\, \bar{L}^T \begin{bmatrix} A_{\mathrm{CL}} X & B_{\mathrm{CL},\psi} \bar{U} & 0 & 0 & \tilde{\varrho} X C_{\mathrm{CL},\eta_p}^T & \tau B_{\mathrm{CL},\zeta_n} & 0 \\ -C_{\mathrm{CL},u} X & -D_{\mathrm{CL},u\psi} \bar{U} - \bar{U} & 0 & I_{n_u} & -D_{\mathrm{CL},u\zeta_p} \bar{V} & -\tau D_{\mathrm{CL},u\zeta_n} & 0 \\ C_{\mathrm{CL},z} X & D_{\mathrm{CL},z\psi} \bar{U} & -\frac{\gamma}{2} I_{n_z} & 0 & D_{\mathrm{CL},z\zeta_p} \bar{V} & \tau D_{\mathrm{CL},z\zeta_n} & 0 \\ 0 & 0 & 0 & -\frac{\gamma}{2} I_{n_u} & 0 & 0 & 0 \\ \bar{V} B_{\mathrm{CL},\zeta_p}^T & \tilde{\varrho} D_{\mathrm{CL},\eta_p\psi} \bar{U} & 0 & 0 & \tilde{\varrho} D_{\mathrm{CL},\eta_p\zeta_p} \bar{V} - \bar{V} & 0 & 0 \\ 0 & 0 & 0 & 0 & 0 & -\frac{\tau}{2} I_{n_{mn}} & 0 \\ \tilde{\varrho} C_{\mathrm{CL},\eta_n} X & \tilde{\varrho} D_{\mathrm{CL},\eta_n\psi} \bar{U} & 0 & 0 & 0 & \tau \tilde{\varrho} D_{\mathrm{CL},\eta_n\zeta_n} & -\frac{\tau}{2} I_{n_{mn}} \end{bmatrix} \bar{L} < 0, \tag{5.18f}$$

$$\text{He}\begin{bmatrix} A_{\text{CL}}Y & 0 & YC_{\text{CL},z}^T & \tilde{\varrho}YC_{\text{CL},\eta_p}^T & \tau B_{\text{CL},\zeta_n} & \tilde{\varrho}YC_{\text{CL},\eta_n}^T \\ 0 & -\frac{\gamma}{2}I_{n_u} & 0 & 0 & 0 & 0 \\ 0 & 0 & -\frac{\gamma}{2}I_{n_z} & 0 & 0 & 0 \\ \bar{V}B_{\text{CL},\zeta_p}^T & 0 & D_{\text{CL},z\zeta_p}^T & \tilde{\varrho}D_{\text{CL},\eta_p\zeta_p}^T\bar{V} - \bar{V} & 0 & 0 \\ 0 & 0 & \tau D_{\text{CL},z\zeta_n}^T & 0 & -\frac{\tau}{2}I_{n_m} & \tilde{\varrho}D_{\text{CL},\eta_n\zeta_n}^T \\ 0 & 0 & 0 & 0 & 0 & -\frac{\tau}{2}I_{n_m} \end{bmatrix} < 0, \tag{5.18g}$$

Step 3. Using $m = n_{\text{CL}} + n_p + n_{m_p} + n_u + n_{m_n} + n_{m_n} + n_u + n_z$, construct the matrices $\Psi \in \mathbb{R}^{m\times m}$, $\tilde{R} \in \mathbb{R}^{n_u\times m}$, and $\tilde{P} \in \mathbb{R}^{m\times(n_{v_1}+n_{v_2})}$ via:

$$[\Psi, \tilde{R}, \tilde{P}] = V_{n_p\text{-dynamic}}(\mathcal{P}^{\Delta}, \mathcal{G}_{\mathcal{M}}, X, Y, \bar{U}, \bar{V}, \tau, \gamma),$$

where the function $V_{n_p\text{-dynamic}}$ is given in Chapter VI.

Step 4. Find a solution $(A_\Lambda, B_\Lambda, C_{\Lambda_1}, C_{\Lambda_2}, D_{\Lambda_1}, D_{\Lambda_2}) \in (\mathbb{R}^{n_p\times n_p}, \mathbb{R}^{n_p\times n_u}, \mathbb{R}^{n_{v_1}\times n_p}, \mathbb{R}^{n_{v_2}\times n_p}, \mathbb{R}^{n_{v_1}\times n_u}, \mathbb{R}^{n_{v_2}\times n_u})$ to the LMI problem:

$$\Psi + \tilde{P}^T\begin{bmatrix} A_\Lambda & B_\Lambda \\ C_{\Lambda_1} & D_{\Lambda_1} \\ C_{\Lambda_2} & D_{\Lambda_2} \end{bmatrix}\tilde{R} + \tilde{R}^T\begin{bmatrix} A_\Lambda & B_\Lambda \\ C_{\Lambda_1} & D_{\Lambda_1} \\ C_{\Lambda_2} & D_{\Lambda_2} \end{bmatrix}^T\tilde{P} < 0. \tag{5.19}$$

$\triangleleft$

Algorithm 5.8 (Arbitrary-order[1] dynamic anti-windup compensation design with general external structure)

Step 1. Step 1 in Algorithm 5.7.

Step 2. Given n_Λ, find a solution $(X, Y, \bar{U}, \bar{V}, \tau) \in (\mathbb{R}^{n_{\mathrm{CL}} \times n_{\mathrm{CL}}}, \mathbb{R}^{n_{\mathrm{CL}} \times n_{\mathrm{CL}}}, \mathbb{D}^{n_u}, \mathbb{D}^{n_{n_m}}, \mathbb{R})$, with $\gamma > 0$ as small as possible and $\tilde{\varrho} \geq 0$, to the LMI problem:

$$\text{Eqns. 5.18a-5.18g,} \tag{5.20a}$$

$$\operatorname{rank}(X - Y) \leq n_\Lambda, \tag{5.20b}$$

Step 3. Using $m = n_{\mathrm{CL}} + n_\Lambda + n_{m_p} + n_u + n_{m_n} + n_{m_n} + n_u + n_z$, construct the matrices $\Psi \in \mathbb{R}^{m \times m}$, $\tilde{R} \in \mathbb{R}^{n_u \times m}$, and $\tilde{P} \in \mathbb{R}^{m \times (n_{v_1} + n_{v_2})}$ via:

$$[\Psi, \tilde{R}, \tilde{P}] = V_{n_\Lambda\text{-dynamic}}(\mathcal{P}^\Delta, \mathcal{G}_\mathcal{M}, X, Y, \bar{U}, \bar{V}, \tau, \gamma, n_\Lambda),$$

where the function $V_{n_\Lambda\text{-dynamic}}$ is given in Chapter VI.

Step 4. Find a solution $(A_\Lambda, B_\Lambda, C_{\Lambda_1}, C_{\Lambda_2}, D_{\Lambda_1}, D_{\Lambda_2}) \in (\mathbb{R}^{n_\Lambda \times n_\Lambda}, \mathbb{R}^{n_\Lambda \times n_u}, \mathbb{R}^{n_{v_1} \times n_\Lambda}, \mathbb{R}^{n_{v_2} \times n_\Lambda}, \mathbb{R}^{n_{v_1} \times n_u}, \mathbb{R}^{n_{v_2} \times n_u})$ to the LMI problem:

$$\Psi + \tilde{P}^T \begin{bmatrix} A_\Lambda & B_\Lambda \\ C_{\Lambda_1} & D_{\Lambda_1} \\ C_{\Lambda_2} & D_{\Lambda_2} \end{bmatrix} \tilde{R} + \tilde{R}^T \begin{bmatrix} A_\Lambda & B_\Lambda \\ C_{\Lambda_1} & D_{\Lambda_1} \\ C_{\Lambda_2} & D_{\Lambda_2} \end{bmatrix}^T \tilde{P} < 0. \tag{5.21}$$

$\lhd$

Note that, the generality of the presentation in Algorithms 5.7 and 5.8 hinders from obtaining any concluding remark with respect to the conditions that guarantee

[1]This algorithm is related to the classic problem of with the It is usually expected that $n_\Lambda < n_p$.

global stability of the anti-windup closed-loop system. Interestingly, for each dynamic anti-windup compensation scheme certain conditions need to be satisfied in order to guarantee global stability of the anti-windup closed-loop system. Moreover, we will see that these conditions are necessary and sufficient for the successful construction of anti-windup compensation employing Algorithms 5.7 and 5.8. The list of these conditions is presented in Assumption 5.9.

Assumption 5.9.

1. Full-authority feedback dynamic anti-windup augmentation

   There exists a solution $(\bar{X}_{11}, \bar{Y}) \in (\mathbb{R}^{n_p \times n_p}, \mathbb{R}^{n_{\mathrm{CL}} \times n_{\mathrm{CL}}})$ to the LMI problem:

$$\bar{X}_{11} = \bar{X}_{11}^T > 0, \tag{5.22a}$$

$$\bar{Y} = \begin{bmatrix} \bar{Y}_{11} & \bar{Y}_{12} \\ \bar{Y}_{12}^T & \bar{Y}_{22} \end{bmatrix} = \bar{Y}^T > 0, \tag{5.22b}$$

$$A_p \bar{X}_{11} + \bar{X}_{11} A_p^T < 0, \tag{5.22c}$$

$$A_{\mathrm{CL}} \bar{Y} + \bar{Y} A_{\mathrm{CL}}^T < 0. \tag{5.22d}$$

2. External feedback dynamic anti-windup augmentation

   There exists a solution $(\bar{X}, \bar{Y}) \in (\mathbb{R}^{n_{\mathrm{CL}} \times n_{\mathrm{CL}}}, \mathbb{R}^{n_{\mathrm{CL}} \times n_{\mathrm{CL}}})$ to the LMI problem:

$$\bar{X} = \begin{bmatrix} \bar{X}_{11} & \bar{Y}_{12} \\ \bar{Y}_{12}^T & \bar{Y}_{22} \end{bmatrix} = \bar{X}^T > 0, \tag{5.23a}$$

$$\bar{Y} = \begin{bmatrix} \bar{Y}_{11} & \bar{Y}_{12} \\ \bar{Y}_{12}^T & \bar{Y}_{22} \end{bmatrix} = \bar{Y}^T > 0, \tag{5.23b}$$

$$M^T \left(\begin{bmatrix} A_p & 0 \\ 0 & A_g \end{bmatrix} \bar{X} + \bar{X} \begin{bmatrix} A_p & 0 \\ 0 & A_g \end{bmatrix}^T \right) M < 0, \tag{5.23c}$$

$$A_{\mathrm{CL}} \bar{Y} + \bar{Y} A_{\mathrm{CL}}^T < 0, \tag{5.23d}$$

where $M = \mathrm{diag}[I_{n_p}, B_{g\perp}^T]$.

3. Generic dynamic anti-windup configuration

   Global stability conditions for this anti-windup scheme depend on the performance level γ.

4. Conventional dynamic anti-windup configuration for controller state

   There exists a solution $(\bar{X}, \bar{Y}, \bar{\bar{U}}) \in (\mathbb{R}^{n_{\mathrm{CL}} \times n_{\mathrm{CL}}}, \mathbb{R}^{n_{\mathrm{CL}} \times n_{\mathrm{CL}}}, \mathbb{D}^{n_u})$ to the LMI problem:

$$\bar{X} = \begin{bmatrix} \bar{X}_{11} & \bar{Y}_{12} \\ \bar{Y}_{12}^T & \bar{Y}_{22} \end{bmatrix} = \bar{X}^T > 0, \tag{5.24a}$$

$$\bar{Y} = \begin{bmatrix} \bar{Y}_{11} & \bar{Y}_{12} \\ \bar{Y}_{12}^T & \bar{Y}_{22} \end{bmatrix} = \bar{Y}^T > 0, \tag{5.24b}$$

$$\bar{\bar{U}} = \mathrm{diag}[\bar{\mu}_1, ..., \bar{\mu}_{n_u}] > 0, \tag{5.24c}$$

$$\begin{bmatrix} \tilde{\mathrm{p}}^T (A_{\mathrm{CL}} \bar{X} + \bar{X} A_{\mathrm{CL}}^T) \tilde{\mathrm{p}} & \tilde{\mathrm{p}}^T (B_{\mathrm{CL},\psi} \bar{\bar{U}} - \bar{X}^T C_{\mathrm{CL},u}) \\ (\bar{\bar{U}} B_{\mathrm{CL},\psi}^T - C_{\mathrm{CL},u} \bar{X}) \tilde{\mathrm{p}} & -\bar{\bar{U}} D_{\mathrm{CL},u\psi}^T - D_{\mathrm{CL},u\psi} \bar{\bar{U}} - 2\bar{\bar{U}} \end{bmatrix} < 0, \tag{5.24d}$$

$$A_{\mathrm{CL}} \bar{Y} + \bar{Y} A_{\mathrm{CL}}^T < 0, \tag{5.24e}$$

with $\tilde{\mathrm{p}}^T = \begin{bmatrix} I_{n_p} & 0 \end{bmatrix}$.

5. Conventional dynamic anti-windup configuration for controller input

   There exists a solution $(\bar{X}, \bar{Y}, \bar{\bar{U}}) \in (\mathbb{R}^{n_{\mathrm{CL}} \times n_{\mathrm{CL}}}, \mathbb{R}^{n_{\mathrm{CL}} \times n_{\mathrm{CL}}}, \mathbb{D}^{n_u})$ to the LMI prob-

lem:

$$\bar{X} = \begin{bmatrix} \bar{X}_{11} & \bar{X}_{12} \\ \bar{X}_{12}^T & \bar{X}_{22} \end{bmatrix} = \bar{X}^T > 0, \tag{5.25a}$$

$$\bar{Y} = \begin{bmatrix} \bar{Y}_{11} & \bar{Y}_{12} \\ \bar{Y}_{12}^T & \bar{Y}_{22} \end{bmatrix} = \bar{Y}^T > 0, \tag{5.25b}$$

$$\bar{\bar{U}} = \mathrm{diag}[\bar{\mu}_1, ..., \bar{\mu}_{n_u}] > 0, \tag{5.25c}$$

$$M^T \begin{bmatrix} \begin{bmatrix} A_p & 0 \\ 0 & A_g \end{bmatrix} \bar{X} + \bar{X} \begin{bmatrix} A_p & 0 \\ 0 & A_g \end{bmatrix}^T & \bar{X} \begin{bmatrix} 0 \\ C_g^T \end{bmatrix} - \begin{bmatrix} B_{p,u} \\ 0 \end{bmatrix} \bar{\bar{U}} \\ \begin{bmatrix} 0 & C_g \end{bmatrix} \bar{X} - \bar{\bar{U}} \begin{bmatrix} B_{p,u}^T & 0 \end{bmatrix} & -2\bar{\bar{U}} \end{bmatrix} M < 0, \tag{5.25d}$$

$$A_{\mathrm{CL}} \bar{Y} + \bar{Y} A_{\mathrm{CL}}^T < 0, \tag{5.25e}$$

where $M = \mathrm{diag}[I_{n_p}, \begin{bmatrix} B_{g,y}^T & -D_{g,y}^T \end{bmatrix}_\perp]$.

◁

Observing the conditions that guarantee global stability of the anti-windup closed-loop system, one can say that Assumption 5.8 corresponding to full-authority and external feedback anti-windup augmentation are the mildest ones when compared to the other anti-windup compensation schemes. This is the case because they only require the plant to be exponentially stable (i.e. A_p is Hurwitz) and the unconstrained closed-loop system to be exponentially stable (i.e. A_{CL} is Hurwitz), as also observed in Grimm [56]. This can be directly concluded from Eqns. 5.24a and 5.24b for the full-authority feedback case, and from Eqns. 5.25a and 5.25b, after applying the Finsler

Lemma [67] to Eqn. 5.25b, for the external feedback augmentation case. The other compensation schemes, although not so evident from the equations, also require both the plant and the unconstrained closed-loop system to be exponentially stable, in addition to other requirements that emphasize the well-posedness of the anti-windup closed-loop system.

In the following sections, we will concentrate on showing that, by appropriately choosing the matrix elements B_{g,v_1}, D_{g,v_1} and D_{g,v_2} in the general structure, Algorithms 5.7 and 5.8 permit to recover the plant-order and arbitrary-order dynamic anti-windup algorithms for the synthesis of existing anti-windup compensation schemes. Observe that $\bar{L}$ is the parameter that carries the information of the compensation schemes, and hence, Steps 1 and 2 of Algorithm 5.7 are the ones that need to be rewritten for each corresponding scheme. Note that when Steps 1 and 2 of Algorithm 5.7 are redefined, automatically Steps 1 and 2 of Algorithm 5.8 get redefined too. The redefinition of Steps 1 and 2 of Algorithm 5.7 will be considered next.

b. Full-authority feedback dynamic anti-windup augmentation

Step 1. Construct the matrix $\tilde{L}_\perp$ as any full column rank matrix that spans the null space of $\tilde{L}^T$, where $\tilde{L}^T = \begin{bmatrix} 0 & I_{n_g} & 0 & 0 \\ \Upsilon_g^T B_{p,u}^T & -\Upsilon_g^T D_{p,yu}^T B_{g,y}^T & -\Upsilon_g^T & \Upsilon_g^T D_{p,zu}^T \end{bmatrix}$. Let $\bar{L} = \text{diag}[\tilde{L}_\perp, I_{n_u}, I_{n_{m_p}}, I_{n_{m_n}}, I_{n_{m_n}}]$.

Step 2. Find a solution $(X_{11}, Y, \bar{V}, \tau) \in (\mathbb{R}^{n_p \times n_p}, \mathbb{R}^{n_{\text{CL}} \times n_{\text{CL}}}, \mathbb{D}^{n_{n_m}}, \mathbb{R})$, with $\gamma > 0$ as small as possible and $\tilde{\varrho} \geq 0$, to the LMI problem:

$$X_{11} = X_{11}^T > 0, \tag{5.26a}$$

$$Y = \begin{bmatrix} Y_{11} & Y_{12} \\ Y_{12}^T & Y_{22} \end{bmatrix} = Y^T > 0, \tag{5.26b}$$

$$X_{11} - Y_{11}^T > 0, \tag{5.26c}$$

$$\bar{V} = \text{diag}[\nu_1, ..., \nu_{n_{m_p}}] > 0, \tag{5.26d}$$

$$\text{He} \begin{bmatrix} A_p X_{11} & 0 & X_{11} C_{p,z}^T & \tilde{\varrho} X_{11} C_{p,\eta_p}^T & \tau B_{p,\zeta_n} & \tilde{\varrho} X_{11} C_{p,\eta_n}^T \\ B_{p,u}^T & -\frac{\gamma}{2} I_{n_u} & D_{p,zu}^T & 0 & 0 & \tilde{\varrho} D_{p,\eta_n u}^T \\ 0 & 0 & -\frac{\gamma}{2} I_{n_z} & D_{p,z\zeta_p} \bar{V} & \tau D_{p,z\zeta_n} & 0 \\ B_{p,\zeta_p}^T \bar{V} & \tilde{\varrho} D_{p,\eta_p u} & 0 & \tilde{\varrho} D_{p,\eta_p \zeta_p}^T \bar{V} - \bar{V} & \tau \tilde{\varrho} D_{p,\eta_p u} D_{g,y} D_{p,y\zeta_n} & 0 \\ 0 & 0 & 0 & 0 & -\frac{\tau}{2} I_{n_{m_n}} & \tau \tilde{\varrho} D_{p,\eta_n \zeta_n} \\ 0 & 0 & 0 & \tilde{\varrho} D_{p,y\zeta_p}^T D_{g,y}^T D_{p,\eta_n u}^T \bar{V} & 0 & -\frac{\tau}{2} I_{n_{m_n}} \end{bmatrix} < 0, \tag{5.26e}$$

$$\text{He} \begin{bmatrix} A_{\text{CL}} Y & 0 & Y C_{\text{CL},z}^T & \tilde{\varrho} Y C_{\text{CL},\eta_p}^T & \tau B_{\text{CL},\zeta_n} & \tilde{\varrho} Y C_{\text{CL},\eta_n}^T \\ 0 & -\frac{\gamma}{2} I_{n_u} & 0 & 0 & 0 & 0 \\ 0 & 0 & -\frac{\gamma}{2} I_{n_z} & 0 & 0 & 0 \\ \bar{V} B_{\text{CL},\zeta_p}^T & 0 & D_{\text{CL},z\zeta_p}^T & \tilde{\varrho} D_{\text{CL},\eta_p \zeta_p}^T \bar{V} - \bar{V} & 0 & 0 \\ 0 & 0 & \tau D_{\text{CL},z\zeta_n}^T & 0 & -\frac{\tau}{2} I_{n_m} & \tilde{\varrho} D_{\text{CL},\eta_n \zeta_n}^T \\ 0 & 0 & 0 & 0 & 0 & -\frac{\tau}{2} I_{n_m} \end{bmatrix} < 0. \tag{5.26f}$$

c. External feedback dynamic anti-windup augmentation

Step 1. Construct the matrix $\tilde{L}_\perp$ as any full column rank matrix that spans the null space of $\tilde{L}^T$, where $\tilde{L}^T = \begin{bmatrix} D_{g,y}^T \Upsilon_g^T B_{p,u}^T & \Upsilon_p^T B_{g,y}^T & -D_{g,y}^T \Upsilon_g^T & D_{g,y}^T \Upsilon_g^T D_{p,zu}^T \\ \Upsilon_g^T B_{p,u}^T & -\Upsilon_g^T D_{p,yu}^T B_{g,y}^T & -\Upsilon_g^T & \Upsilon_g^T D_{p,zu}^T \end{bmatrix}$. Let $\bar{L} = \mathrm{diag}[\tilde{L}_\perp, I_{n_u}, I_{n_{m_p}}, I_{n_{m_n}}, I_{n_{m_n}}]$.

Step 2. Find a solution $(X, Y, \bar{V}, \tau) \in (\mathbb{R}^{n_{\mathrm{CL}} \times n_{\mathrm{CL}}}, \mathbb{R}^{n_{\mathrm{CL}} \times n_{\mathrm{CL}}}, \mathbb{D}^{n_{n_m}}, \mathbb{R})$, with $\gamma > 0$ as small as possible and $\tilde{\varrho} \geq 0$, to the LMI problem:

$$X = \begin{bmatrix} X_{11} & Y_{12} \\ Y_{12}^T & Y_{22} \end{bmatrix} = X^T > 0, \tag{5.27a}$$

$$Y = \begin{bmatrix} Y_{11} & Y_{12} \\ Y_{12}^T & Y_{22} \end{bmatrix} = Y^T > 0, \tag{5.27b}$$

$$X_{11} - Y_{11}^T > 0, \tag{5.27c}$$

$$\bar{V} = \mathrm{diag}[\nu_1, ..., \nu_{n_{m_p}}] > 0, \tag{5.27d}$$

$$\mathrm{He}\, \bar{L}^T \begin{bmatrix} A_p X_{11} & Y_{12} A_g^T & 0 & X_{11} C_{p,z}^T & \tilde{\varrho} X_{11} C_{p,\eta_p}^T & \tau B_{p,\zeta_n} & \tilde{\varrho} X_{11} C_{p,\eta_n}^T \\ Y_{12}^T A_p^T & A_g Y_{22} & 0 & 0 & 0 & 0 & 0 \\ B_{p,u}^T & 0 & -\frac{\gamma}{2} I_{n_u} & D_{p,zu}^T & 0 & 0 & \tilde{\varrho} D_{p,\eta_n u}^T \\ 0 & C_{p,z} Y_{12} & 0 & -\frac{\gamma}{2} I_{n_z} & D_{p,z\zeta_p} \bar{V} & \tau D_{p,z\zeta_n} & 0 \\ B_{\mathrm{CL},\zeta_p}^T \bar{V} & \tilde{\varrho} C_{p,\eta_p} Y_{12} & \tilde{\varrho} D_{p,\eta_p u} & 0 & \tilde{\varrho} D_{p,\eta_p \zeta_p}^T \bar{V} - \bar{V} & 0 & 0 \\ 0 & 0 & 0 & 0 & \tau \tilde{\varrho} D_{p,y\zeta_n}^T D_{g,y}^T D_{p,\eta_p u}^T & -\frac{\tau}{2} I_{n_{m_n}} & \tau \tilde{\varrho} D_{p,\eta_n \zeta_n} \\ 0 & \tilde{\varrho} C_{p,\eta_n} Y_{12} & 0 & 0 & \tilde{\varrho} D_{p,y\zeta_p}^T D_{g,y}^T D_{p,\eta_n u}^T \bar{V} & 0 & -\frac{\tau}{2} I_{n_{m_n}} \end{bmatrix} \bar{L} < 0, \tag{5.27e}$$

$$\mathrm{He} \begin{bmatrix} A_{\mathrm{CL}} Y & 0 & Y C_{\mathrm{CL},z}^T & \tilde{\varrho} Y C_{\mathrm{CL},\eta_p}^T & \tau B_{\mathrm{CL},\zeta_n} & \tilde{\varrho} Y C_{\mathrm{CL},\eta_n}^T \\ 0 & -\frac{\gamma}{2} I_{n_u} & 0 & 0 & 0 & 0 \\ 0 & 0 & -\frac{\gamma}{2} I_{n_z} & 0 & 0 & 0 \\ \bar{V} B_{\mathrm{CL},\zeta_p}^T & 0 & D_{\mathrm{CL},z\zeta_p}^T & \tilde{\varrho} D_{\mathrm{CL},\eta_p \zeta_p}^T \bar{V} - \bar{V} & 0 & 0 \\ 0 & 0 & \tau D_{\mathrm{CL},z\zeta_n}^T & 0 & -\frac{\tau}{2} I_{n_m} & \tilde{\varrho} D_{\mathrm{CL},\eta_n \zeta_n}^T \\ 0 & 0 & 0 & 0 & 0 & -\frac{\tau}{2} I_{n_m} \end{bmatrix} < 0. \tag{5.27f}$$

d. Generic dynamic anti-windup configuration

Step 1. Construct the matrix $\tilde{L}_\perp$ as any full column rank matrix that spans the null space of $\tilde{L}^T$, where $\tilde{L}^T = \left[\begin{array}{cccc} \Upsilon_g^T B_{p,u}^T & -\Upsilon_g^T D_{p,yu}^T B_{g,y}^T & -\Upsilon_g^T & \Upsilon_g^T D_{p,zu}^T \end{array}\right]$. Let $\bar{L} = \mathrm{diag}[\tilde{L}_\perp, I_{n_u}, I_{n_{m_p}}, I_{n_{m_n}}, I_{n_{m_n}}]$.

Step 2. Find a solution $(X, Y, \bar{U}, \bar{V}, \tau) \in (\mathbb{R}^{n_{\mathrm{CL}} \times n_{\mathrm{CL}}}, \mathbb{R}^{n_{\mathrm{CL}} \times n_{\mathrm{CL}}}, \mathbb{D}^{n_u}, \mathbb{D}^{n_{n_m}}, \mathbb{R})$, with $\gamma > 0$ as small as possible and $\tilde{\varrho} \geq 0$, to the LMI problem:

$$X = \left[\begin{array}{cc} X_{11} & X_{12} \\ X_{12}^T & X_{22} \end{array}\right] = X^T > 0, \tag{5.28a}$$

$$Y = \left[\begin{array}{cc} Y_{11} & Y_{12} \\ Y_{12}^T & Y_{22} \end{array}\right] = Y^T > 0, \tag{5.28b}$$

$$X - Y > 0, \tag{5.28c}$$

$$\bar{U} = \mathrm{diag}[\mu_1, ..., \mu_{n_u}] > 0, \tag{5.28d}$$

$$\bar{V} = \mathrm{diag}[\nu_1, ..., \nu_{n_{m_p}}] > 0, \tag{5.28e}$$

$$\mathrm{He}\, \bar{L}^T \left[\begin{array}{ccccccc} A_{\mathrm{CL}} X & B_{\mathrm{CL},\psi}\bar{U} & 0 & 0 & \tilde{\varrho} X C_{\mathrm{CL},\eta_p}^T & \tau B_{\mathrm{CL},\zeta_n} & 0 \\ -C_{\mathrm{CL},u} X & -D_{\mathrm{CL},u\psi}\bar{U} - \bar{U} & 0 & I_{n_u} & -D_{\mathrm{CL},u\zeta_p}\bar{V} & -\tau D_{\mathrm{CL},u\zeta_n} & 0 \\ C_{\mathrm{CL},z} X & D_{\mathrm{CL},z\psi}\bar{U} & -\frac{\gamma}{2} I_{n_z} & 0 & D_{\mathrm{CL},z\zeta_p}\bar{V} & \tau D_{\mathrm{CL},z\zeta_n} & 0 \\ 0 & 0 & 0 & -\frac{\gamma}{2} I_{n_u} & 0 & 0 & 0 \\ \bar{V} B_{\mathrm{CL},\zeta_p}^T & \tilde{\varrho} D_{\mathrm{CL},\eta_p\psi}\bar{U} & 0 & 0 & \tilde{\varrho} D_{\mathrm{CL},\eta_p\zeta_p}\bar{V} - \bar{V} & 0 & 0 \\ 0 & 0 & 0 & 0 & 0 & -\frac{\tau}{2} I_{n_{m_n}} & 0 \\ \tilde{\varrho} C_{\mathrm{CL},\eta_n} X & \tilde{\varrho} D_{\mathrm{CL},\eta_n\psi}\bar{U} & 0 & 0 & 0 & \tau\tilde{\varrho} D_{\mathrm{CL},\eta_n\zeta_n} & -\frac{\tau}{2} I_{n_{m_n}} \end{array}\right] \bar{L} < 0, \tag{5.28f}$$

$$\text{He}\begin{bmatrix} A_{\text{CL}}Y & 0 & YC_{\text{CL},z}^T & \tilde{\varrho}YC_{\text{CL},\eta_p}^T & \tau B_{\text{CL},\zeta_n} & \tilde{\varrho}YC_{\text{CL},\eta_n}^T \\ 0 & -\frac{\gamma}{2}I_{n_u} & 0 & 0 & 0 & 0 \\ 0 & 0 & -\frac{\gamma}{2}I_{n_z} & 0 & 0 & 0 \\ \bar{V}B_{\text{CL},\zeta_p}^T & 0 & D_{\text{CL},z\zeta_p}^T & \tilde{\varrho}D_{\text{CL},\eta_p\zeta_p}^T\bar{V} - \bar{V} & 0 & 0 \\ 0 & 0 & \tau D_{\text{CL},z\zeta_n}^T & 0 & -\frac{\tau}{2}I_{n_m} & \tilde{\varrho}D_{\text{CL},\eta_n\zeta_n}^T \\ 0 & 0 & 0 & 0 & 0 & -\frac{\tau}{2}I_{n_m} \end{bmatrix} < 0. \tag{5.28g}$$

e. Conventional dynamic anti-windup configuration for controller state

Step 1. Construct the matrix $\tilde{L}_\perp$ as any full column rank matrix that spans the null space of $\tilde{L}^T$, where $\tilde{L}^T = \begin{bmatrix} 0 & I_{n_g} & 0 & 0 \end{bmatrix}$. Let $\bar{L} = \text{diag}[\tilde{L}_\perp, I_{n_u}, I_{n_{m_p}}, I_{n_{m_n}}, I_{n_{m_n}}]$.

Step 2. Find a solution $(X, Y, \bar{U}, \bar{V}, \tau) \in (\mathbb{R}^{n_{\text{CL}}\times n_{\text{CL}}}, \mathbb{R}^{n_{\text{CL}}\times n_{\text{CL}}}, \mathbb{D}^{n_u}, \mathbb{D}^{n_{nm}}, \mathbb{R})$, with $\gamma > 0$ as small as possible and $\tilde{\varrho} \geq 0$, to the LMI problem:

$$X = \begin{bmatrix} X_{11} & Y_{12} \\ Y_{12}^T & Y_{22} \end{bmatrix} = X^T > 0, \tag{5.29a}$$

$$Y = \begin{bmatrix} Y_{11} & Y_{12} \\ Y_{12}^T & Y_{22} \end{bmatrix} = Y^T > 0, \tag{5.29b}$$

$$X_{11} - Y_{11} > 0, \tag{5.29c}$$

$$\bar{U} = \text{diag}[\mu_1, ..., \mu_{n_u}] > 0, \tag{5.29d}$$

$$\bar{V} = \text{diag}[\nu_1, ..., \nu_{n_{m_p}}] > 0, \tag{5.29e}$$

$$\text{He}\begin{bmatrix} \tilde{\mathrm{p}}^T A_{\mathrm{CL}} X \tilde{\mathrm{p}} & \tilde{\mathrm{p}}^T B_{\mathrm{CL},\psi} \bar{U} & 0 & 0 & \tilde{\mathrm{p}}^T \tilde{\varrho} X C_{\mathrm{CL},\eta_p}^T & \tilde{\mathrm{p}}^T \tau B_{\mathrm{CL},\zeta_n} & 0 \\ -C_{\mathrm{CL},u} X \tilde{\mathrm{p}} & -D_{\mathrm{CL},u\psi} \bar{U} - \bar{U} & 0 & I_{n_u} & -D_{\mathrm{CL},u\zeta_p} \bar{V} & -\tau D_{\mathrm{CL},u\zeta_n} & 0 \\ C_{\mathrm{CL},z} X \tilde{\mathrm{p}} & D_{\mathrm{CL},z\psi} \bar{U} & -\frac{\gamma}{2} I_{n_z} & 0 & D_{\mathrm{CL},z\zeta_p} \bar{V} & \tau D_{\mathrm{CL},z\zeta_n} & 0 \\ 0 & 0 & 0 & -\frac{\gamma}{2} I_{n_u} & 0 & 0 & 0 \\ \bar{V} B_{\mathrm{CL},\zeta_p}^T \tilde{\mathrm{p}} & \tilde{\varrho} D_{\mathrm{CL},\eta_p\psi} \bar{U} & 0 & 0 & \tilde{\varrho} D_{\mathrm{CL},\eta_p\zeta_p} \bar{V} - \bar{V} & 0 & 0 \\ 0 & 0 & 0 & 0 & 0 & -\frac{\tau}{2} I_{n_{m_n}} & 0 \\ \tilde{\varrho} C_{\mathrm{CL},\eta_n} X \tilde{\mathrm{p}} & \tilde{\varrho} D_{\mathrm{CL},\eta_n\psi} \bar{U} & 0 & 0 & 0 & \tau \tilde{\varrho} D_{\mathrm{CL},\eta_n\zeta_n} & -\frac{\tau}{2} I_{n_{m_n}} \end{bmatrix} < 0, \tag{5.29f}$$

$$\text{He}\begin{bmatrix} A_{\mathrm{CL}} Y & 0 & Y C_{\mathrm{CL},z}^T & \tilde{\varrho} Y C_{\mathrm{CL},\eta_p}^T & \tau B_{\mathrm{CL},\zeta_n} & \tilde{\varrho} Y C_{\mathrm{CL},\eta_n}^T \\ 0 & -\frac{\gamma}{2} I_{n_u} & 0 & 0 & 0 & 0 \\ 0 & 0 & -\frac{\gamma}{2} I_{n_z} & 0 & 0 & 0 \\ \bar{V} B_{\mathrm{CL},\zeta_p}^T & 0 & D_{\mathrm{CL},z\zeta_p}^T & \tilde{\varrho} D_{\mathrm{CL},\eta_p\zeta_p}^T \bar{V} - \bar{V} & 0 & 0 \\ 0 & 0 & \tau D_{\mathrm{CL},z\zeta_n}^T & 0 & -\frac{\tau}{2} I_{n_m} & \tilde{\varrho} D_{\mathrm{CL},\eta_n\zeta_n}^T \\ 0 & 0 & 0 & 0 & 0 & -\frac{\tau}{2} I_{n_m} \end{bmatrix} < 0, \tag{5.29g}$$

$$\tilde{\mathrm{p}}^T = \begin{bmatrix} I_{n_p} & 0 \end{bmatrix}.$$

f. Conventional dynamic anti-windup configuration for controller input

Step 1. Construct the matrix $\tilde{L}_\perp$ as any full column rank matrix that spans the null space of $\tilde{L}^T$, where break $\tilde{L}^T = \begin{bmatrix} D_{g,y}^T \Upsilon_g^T B_{p,u}^T & \Upsilon_p^T B_{g,y}^T & -D_{g,y}^T \Upsilon_g^T & D_{g,y}^T \Upsilon_g^T D_{p,zu}^T \end{bmatrix}$. Let $\bar{L} = \mathrm{diag}[\tilde{L}_\perp, I_{n_u}, I_{n_{m_p}}, I_{n_{m_n}}, I_{n_{m_n}}]$.

Step 2. Find a solution $(X, Y, \bar{U}, \bar{V}, \tau) \in (\mathbb{R}^{n_{\mathrm{CL}} \times n_{\mathrm{CL}}}, \mathbb{R}^{n_{\mathrm{CL}} \times n_{\mathrm{CL}}}, \mathbb{D}^{n_u}, \mathbb{D}^{n_{n_m}}, \mathbb{R})$, with $\gamma > 0$ as small as possible and $\tilde{\varrho} \geq 0$, to the LMI problem:

$$X = \begin{bmatrix} X_{11} & Y_{12} \\ Y_{12}^T & Y_{22} \end{bmatrix} = X^T > 0, \tag{5.30a}$$

$$Y = \begin{bmatrix} Y_{11} & Y_{12} \\ Y_{12}^T & Y_{22} \end{bmatrix} = Y^T > 0, \tag{5.30b}$$

$$X_{11} - Y_{11} > 0, \tag{5.30c}$$

$$\bar{U} = \mathrm{diag}[\mu_1, ..., \mu_{n_u}] > 0, \tag{5.30d}$$

$$\bar{V} = \mathrm{diag}[\nu_1, ..., \nu_{n_{mp}}] > 0, \tag{5.30e}$$

$$\mathrm{He}\,\bar{L}^T \begin{bmatrix} A_p X_{11} & Y_{12} A_g^T & -Y_{12} C_g^T & 0 & X_{11} C_{p,z}^T & \tilde{\varrho} X_{11} C_{p,\eta_p}^T & \tau B_{p,\zeta_n} & \tilde{\varrho} X_{11} C_{p,\eta_n}^T \\ Y_{12}^T A_p^T & A_g Y_{22} & -Y_{22} C_g^T & 0 & 0 & 0 & 0 & 0 \\ -\bar{U} B_{p,u}^T & 0 & -\bar{U} & I_{n_u} & 0 & -D_{p,u\zeta_p} \bar{V} & -\tau D_{p,u\zeta_n}^T & 0 \\ B_{p,u}^T & 0 & 0 & -\frac{\gamma}{2} I_{n_u} & D_{p,zu}^T & 0 & 0 & \tilde{\varrho} D_{p,\eta_n u}^T \\ 0 & C_{p,z} X_{12} & -D_{p,zu} \bar{U} & 0 & -\frac{\gamma}{2} I_{n_z} & D_{p,z\zeta_p} \bar{V} & \tau D_{p,z\zeta_n} & 0 \\ B_{\mathrm{CL},\zeta_p}^T \bar{V} & \tilde{\varrho} C_{p,\eta_p} Y_{12} & 0 & \tilde{\varrho} D_{p,\eta_p u} & 0 & \tilde{\varrho} D_{p,\eta_p\zeta_p}^T \bar{V} - \bar{V} & 0 & 0 \\ 0 & 0 & 0 & 0 & 0 & \tau \tilde{\varrho} D_{p,y\zeta_n}^T D_{g,y}^T D_{p,\eta_p u}^T & -\frac{\tau}{2} I_{n_{m_n}} & \tau \tilde{\varrho} D_{p,\eta_n\zeta_n} \\ 0 & \tilde{\varrho} C_{p,\eta_n} Y_{12} & D_{p,\eta_n u} \bar{U} & 0 & 0 & \tilde{\varrho} D_{p,y\zeta_p}^T D_{g,y}^T D_{p,\eta_n u}^T \bar{V} & 0 & -\frac{\tau}{2} I_{n_{m_n}} \end{bmatrix} \bar{L} < 0, \tag{5.30f}$$

$$\mathrm{He} \begin{bmatrix} A_{\mathrm{CL}} Y & 0 & Y C_{\mathrm{CL},z}^T & \tilde{\varrho} Y C_{\mathrm{CL},\eta_p}^T & \tau B_{\mathrm{CL},\zeta_n} & \tilde{\varrho} Y C_{\mathrm{CL},\eta_n}^T \\ 0 & -\frac{\gamma}{2} I_{n_u} & 0 & 0 & 0 & 0 \\ 0 & 0 & -\frac{\gamma}{2} I_{n_z} & 0 & 0 & 0 \\ \bar{V} B_{\mathrm{CL},\zeta_p}^T & 0 & D_{\mathrm{CL},z\zeta_p}^T & \tilde{\varrho} D_{\mathrm{CL},\eta_p\zeta_p}^T \bar{V} - \bar{V} & 0 & 0 \\ 0 & 0 & \tau D_{\mathrm{CL},z\zeta_n}^T & 0 & -\frac{\tau}{2} I_{n_m} & \tilde{\varrho} D_{\mathrm{CL},\eta_n\zeta_n}^T \\ 0 & 0 & 0 & 0 & 0 & -\frac{\tau}{2} I_{n_m} \end{bmatrix} < 0. \tag{5.30g}$$

g. Weston and Postlethwaite (W&P) anti-windup configuration ($n_\Lambda = n_p$)

Step 1. Construct the matrix $\tilde{L}_\perp$ as any full column rank matrix that spans the null space of $\tilde{L}^T$, where $\tilde{L}^T = \begin{bmatrix} D_{g,y}^T \Upsilon_g^T B_{p,u}^T & \Upsilon_p^T B_{g,y}^T & -D_{g,y}^T \Upsilon_g^T & D_{g,y}^T \Upsilon_g^T D_{p,zu}^T \\ \Upsilon_g^T B_{p,u}^T & -\Upsilon_g^T D_{p,yu}^T B_{g,y}^T & -\Upsilon_g^T & \Upsilon_g^T D_{p,zu}^T \end{bmatrix}$. Let $\bar{L} = \mathrm{diag}[\tilde{L}_\perp, I_{n_u}, I_{n_{m_p}}, I_{n_{m_n}}, I_{n_{m_n}}]$.

Step 2. Find a solution $(X, Y, \bar{V}, \tau) \in (\mathbb{R}^{(n_p+n_{\mathrm{CL}})\times(n_p+n_{\mathrm{CL}})}, \mathbb{R}^{n_{\mathrm{CL}}\times n_{\mathrm{CL}}}, \mathbb{D}^{n_{n_m}}, \mathbb{R})$, with $\gamma > 0$ as small as possible and $\tilde{\varrho} \geq 0$, to the LMI problem:

$$X = \begin{bmatrix} X_p & X_{pY} \\ X_{pY}^T & Y \end{bmatrix} = X^T > 0, \tag{5.31a}$$

$$Y = Y^T > 0, \tag{5.31b}$$

$$\bar{V} = \mathrm{diag}[\nu_1, ..., \nu_{n_{m_p}}] > 0, \tag{5.31c}$$

$$\mathrm{He}\begin{bmatrix} \begin{bmatrix} A_p & 0 \\ B_{\mathrm{CL},v_1} C_{p,y} & A_{\mathrm{CL}} \end{bmatrix} X & 0 & X \begin{bmatrix} C_{p,z}^T \\ 0 \end{bmatrix} & \tilde{\varrho} X \begin{bmatrix} C_{p,\eta_p}^T \\ 0 \end{bmatrix} & \tau \begin{bmatrix} B_{p,\zeta_n}^T \\ 0 \end{bmatrix} & \tilde{\varrho} X \begin{bmatrix} C_{p,\eta_n}^T \\ 0 \end{bmatrix} \\ \begin{matrix} B_{p,u}^T & 0 & B_{p,u}^T \\ 0 & 0 & 0 \\ B_{p,\zeta_p}^T \bar{V} & 0 & B_{p,\zeta_p}^T \bar{V} \\ 0 & 0 & 0 \\ 0 & 0 & 0 \end{matrix} & \begin{matrix} -\frac{\gamma}{2} I_{n_u} \\ 0 \\ \tilde{\varrho} D_{p,\eta_p u} \\ 0 \\ 0 \end{matrix} & \begin{matrix} D_{p,zu}^T \\ -\frac{\gamma}{2} I_{n_z} \\ 0 \\ 0 \\ 0 \end{matrix} & \begin{matrix} 0 \\ D_{p,z\zeta_p} \bar{V} \\ \tilde{\varrho} D_{p,\eta_p\zeta_p}^T \bar{V} - \bar{V} \\ 0 \\ \tilde{\varrho} D_{p,y\zeta_p}^T D_{g,y}^T D_{p,\eta_n u}^T \bar{V} \end{matrix} & \begin{matrix} 0 \\ \tau D_{p,z\zeta_n} \\ \tau \tilde{\varrho} D_{p,\eta_p u} D_{g,y} D_{p,y\zeta_n} \\ -\frac{\tau}{2} I_{n_{m_n}} \\ 0 \end{matrix} & \begin{matrix} \tilde{\varrho} D_{p,\eta_n u}^T \\ 0 \\ 0 \\ \tau \tilde{\varrho} D_{p,\eta_n\zeta_n} \\ -\frac{\tau}{2} I_{n_{m_n}} \end{matrix} \end{bmatrix} < 0, \tag{5.31d}$$

$$\mathrm{He}\begin{bmatrix} A_{\mathrm{CL}} Y & 0 & Y C_{\mathrm{CL},z}^T & \tilde{\varrho} Y C_{\mathrm{CL},\eta_p}^T & \tau B_{\mathrm{CL},\zeta_n} & \tilde{\varrho} Y C_{\mathrm{CL},\eta_n}^T \\ 0 & -\frac{\gamma}{2} I_{n_u} & 0 & 0 & 0 & 0 \\ 0 & 0 & -\frac{\gamma}{2} I_{n_z} & 0 & 0 & 0 \\ \bar{V} B_{\mathrm{CL},\zeta_p}^T & 0 & D_{\mathrm{CL},z\zeta_p}^T & \tilde{\varrho} D_{\mathrm{CL},\eta_p\zeta_p}^T \bar{V} - \bar{V} & 0 & 0 \\ 0 & 0 & \tau D_{\mathrm{CL},z\zeta_n}^T & 0 & -\frac{\tau}{2} I_{n_m} & \tilde{\varrho} D_{\mathrm{CL},\eta_n\zeta_n}^T \\ 0 & 0 & 0 & 0 & 0 & -\frac{\tau}{2} I_{n_m} \end{bmatrix} < 0. \tag{5.31e}$$

Step 3. Complete Step 3 in Algorithm 5.7.

Step 4. Find a solution $(F, E) \in (\mathbb{R}^{n_u \times n_p}, \mathbb{R}^{n_u \times n_u})$ to the LMI problem:

$$\Psi + \tilde{P}^T \left(\begin{bmatrix} A_p & 0 \\ C_{p,y} & 0 \\ 0 & -I_{n_u} \end{bmatrix} + \begin{bmatrix} B_{p,u} \\ D_{p,yu} \\ I_{n_u} \end{bmatrix} \begin{bmatrix} E & F \end{bmatrix} \right) \tilde{R} + \tilde{R}^T \left(\begin{bmatrix} A_p & 0 \\ C_{p,y} & 0 \\ 0 & -I_{n_u} \end{bmatrix} + \begin{bmatrix} B_{p,u} \\ D_{p,yu} \\ I_{n_u} \end{bmatrix} \begin{bmatrix} E & F \end{bmatrix} \right)^T \tilde{P} < 0. \quad (5.32)$$

The next theorems states that Assumption 5.9 provides necessary and sufficient conditions for the plant-order and arbitrary-order dynamic linear anti-windup compensations to be successfully constructed.

Theorem 5.10 *Assumption 5.9 is necessary and sufficient to guarantee that all steps in Algorithm 5.7 can be completed for each anti-windup compensation scheme and the corresponding resulting* $(A_\Lambda, B_\Lambda, C_{\Lambda_1}, C_{\Lambda_2}, D_{\Lambda_1}, D_{\Lambda_2})$ *describe a plant-order dynamic linear anti-windup compensator that guarantees the anti-windup closed-loop satisfies the basic properties of anti-windup and has finite unconstrained response recovery gain less than* γ. $\lhd$

Theorem 5.11 *Assumption 5.9 is necessary and sufficient to guarantee that all steps in Algorithm 5.8 can be completed for each anti-windup compensation scheme and the corresponding resulting* $(A_\Lambda, B_\Lambda, C_{\Lambda_1}, C_{\Lambda_2}, D_{\Lambda_1}, D_{\Lambda_2})$ *describe an arbitrary-order dynamic linear anti-windup compensator that guarantees the anti-windup closed-loop satisfies the basic properties of anti-windup and has finite unconstrained response recovery gain less than* γ. $\lhd$

2. Dynamic override

Dynamic compensation for the output constrained problem will be considered in this part of the dissertation. Recall from Section II.C that the finite unconstrained response recovery gain for override compensation refers to the $\mathcal{L}_2$ gain from the difference signal $\text{sat}(z_l) - z_l$ (z_l comes from the unconstrained closed-loop system and $\text{sat}(z_l)$ corresponds to its saturated version) to the difference of signals $\begin{bmatrix} \text{sat}(z_l) - z \\ y_l - y \end{bmatrix}$ (z_l and y_l come from the unconstrained closed-loop system, $\text{sat}(z_l)$ is the saturated version of z_l and z comes from the anti-windup closed-loop system). Therefore, the algorithms presented in this section will guarantee that, regardless of the exogenous

disturbance $w \in \mathcal{L}_2$ and when the initial conditions of the plant, unconstrained controller and override compensator in the mismatch system are zero, the following is satisfied:

$$\left\| \begin{bmatrix} \text{sat}(z_l) - z \\ y_l - y \end{bmatrix} (\cdot) \right\|_2 \leq \gamma \|(\text{sat}(z_l) - z_l)(\cdot)\|_2, \tag{5.33}$$

with the finite unconstrained recovery gain γ as small as possible. More specifically, the algorithms in this section are aimed at constructing the matrix elements A_Θ, B_Θ, C_{Θ_1}, C_{Θ_2}, D_{Θ_1} and D_{Θ_2}, shown in Fig. 27, of a dynamic linear override compensator that guarantees an optimal finite unconstrained response recovery gain. The case when the dynamic override compensation to be constructed is chosen to be of order equal to the plant, which is called *plant-order* override, is specially important because it provides very useful synthesis algorithms, similar to the case of anti-windup compensation [21]. Interestingly, plant-order override compensation algorithms are computationally efficient because the corresponding steps for compensation synthesis are given only in terms of LMI conditions. On the contrary, arbitrary-order override compensation presents some steps where a non-convex optimization problem must be solved. Algorithms 5.12 and 5.13 are now offered in order to provide plant-order and arbitrary-order dynamic override compensation synthesis, respectively. Recall that we will perform the calculations for the GOC for controller state/output case.

a. Dynamic GOC for controller states/output

Algorithm 5.12 (Plant-order dynamic override compensation)

Step 1. Find a solution $(X, Y, \bar{U}, \bar{V}, \tau, \pi) \in (\mathbb{R}^{n_{\mathrm{CL}} \times n_{\mathrm{CL}}}, \mathbb{R}^{n_{\mathrm{CL}} \times n_{\mathrm{CL}}}, \mathbb{D}^{n_u}, \mathbb{D}^{n_{n_m}}, \mathbb{R}, \mathbb{R})$, with $\gamma > 0$ as small as possible and $\tilde{\varrho} \geq 0$, to the LMI problem:

$$X = \begin{bmatrix} X_{11} & Y_{12} \\ Y_{12}^T & Y_{22} \end{bmatrix} = X^T > 0, \tag{5.34a}$$

$$Y = \begin{bmatrix} Y_{11} & Y_{12} \\ Y_{12}^T & Y_{22} \end{bmatrix} = Y^T > 0, \tag{5.34b}$$

$$X_{11} - Y_{11} > 0, \tag{5.34c}$$

$$\bar{U} = \mathrm{diag}[\mu_1, ..., \mu_{n_u}] > 0, \tag{5.34d}$$

$$\bar{V} = \mathrm{diag}[\nu_1, ..., \nu_{n_{m_p}}] > 0, \tag{5.34e}$$

$$\mathrm{He}\, \bar{L}^T \begin{bmatrix} \tilde{\mathrm{p}}^T A_{\mathrm{CL}} X \tilde{\mathrm{p}} & -\tilde{\mathrm{p}}^T X C_{\mathrm{CL},z}^T & \tilde{\mathrm{p}}^T C_{\mathrm{CL},y}^T W_y^T & 0 & 0 & \tilde{\mathrm{p}}^T \tilde{\varrho} X C_{\mathrm{CL},\eta_p}^T & \tilde{\mathrm{p}}^T \tau B_{\mathrm{CL},\zeta_n} & 0 \\ 0 & -\bar{U} & 0 & -2\bar{U} W_z^T & 0 & -D_{\mathrm{CL},z\zeta_p} \bar{V} & -\tau D_{\mathrm{CL},z\zeta_n} & 0 \\ 0 & 0 & -\frac{\gamma}{2} I_{n_y} & 0 & 0 & D_{\mathrm{CL},y\zeta_p} \bar{V} & \tau D_{\mathrm{CL},y\zeta_n} & 0 \\ 0 & 0 & 0 & -W_z \bar{U} W_z^T - \frac{\gamma}{2} I_{n_z} & 0 & D_{\mathrm{CL},z\zeta_p} \bar{V} & \tau D_{\mathrm{CL},z\zeta_n} & 0 \\ 0 & 0 & 0 & -I_{n_z} W_o^T W_z^T & -\frac{\gamma}{2} I_{n_z} & 0 & 0 & 0 \\ \bar{V} B_{\mathrm{CL},\zeta_p}^T \tilde{\mathrm{p}} & \tilde{\varrho} D_{\mathrm{CL},\eta_p \psi} \bar{U} & 0 & 0 & 0 & \tilde{\varrho} D_{\mathrm{CL},\eta_p \zeta_p} \bar{V} - \bar{V} & 0 & 0 \\ 0 & 0 & 0 & 0 & 0 & 0 & -\frac{\tau}{2} I_{n_{m_n}} & 0 \\ \tilde{\varrho} C_{\mathrm{CL},\eta_n} X \tilde{\mathrm{p}} & \tilde{\varrho} D_{\mathrm{CL},\eta_n \psi} \bar{U} & 0 & 0 & 0 & 0 & \tau \tilde{\varrho} D_{\mathrm{CL},\eta_n \zeta_n} & -\frac{\tau}{2} I_{n_{m_n}} \end{bmatrix} \bar{L} < 0, \tag{5.34f}$$

$$\text{He}\begin{bmatrix} A_{\text{CL}}Y & -YC_{\text{CL},z}^T & YC_{\text{CL},y}^TW_y^T & YC_{\text{CL},z}^TW_z^T & \tilde{\varrho}YC_{\text{CL},\eta_p}^T & \tau B_{\text{CL},\zeta_n} & \tilde{\varrho}YC_{\text{CL},\eta_n}^T \\ 0 & -\frac{\pi}{2}I_{n_z} & 0 & \bar{U}W_z^T & 0 & 0 & 0 \\ 0 & 0 & -\frac{\gamma}{2}I_{n_y} & 0 & 0 & 0 & 0 \\ 0 & 0 & 0 & -\frac{\gamma}{2}I_{n_z} & 0 & 0 & 0 \\ \bar{V}B_{\text{CL},\zeta_p}^T & 0 & D_{\text{CL},y\zeta_p}^T & D_{\text{CL},z\zeta_p}^T & \tilde{\varrho}D_{\text{CL},\eta_p\zeta_p}^T\bar{V}-\bar{V} & 0 & 0 \\ 0 & 0 & \tau D_{\text{CL},y\zeta_n}^T & \tau D_{\text{CL},z\zeta_n}^T & 0 & -\frac{\tau}{2}I_{n_m} & \tilde{\varrho}D_{\text{CL},\eta_n\zeta_n}^T \\ 0 & 0 & 0 & 0 & 0 & 0 & -\frac{\tau}{2}I_{n_m} \end{bmatrix} < 0, \tag{5.34g}$$

with $\tilde{\mathrm{p}}^T = \begin{bmatrix} I_{n_p} & 0 \end{bmatrix}$ and $\bar{L} = \text{diag}[\begin{bmatrix} -\Upsilon_p^TB_{p,u}^T & \Upsilon_p^TD_{p,zu}^T & -\Upsilon_p^TD_{p,yu}^TW_y^T \end{bmatrix}_\perp, I_{n_z}, I_{n_z}, I_{n_{m_p}}, I_{n_{m_n}}, I_{n_{m_n}}]$.

Step 2. Using $m = n_{\text{CL}} + n_p + n_z + n_y + n_z + n_z + n_{m_p} + n_{m_n} + n_{m_n}$, construct the matrices $\Psi \in \mathbb{R}^{m\times m}$, $\tilde{R} \in \mathbb{R}^{n_z\times m}$, and $\tilde{P} \in \mathbb{R}^{m\times(n_{v_1}+n_{v_2})}$ via:

$$[\Psi, \tilde{R}, \tilde{P}] = V_{n_p\text{-dynamic}}(\mathcal{P}^\Delta, \mathcal{G}_\mathcal{M}, X, Y, \bar{U}, \bar{V}, \tau, \gamma),$$

where the function $V_{n_p\text{-dynamic}}$ is given in Chapter VI.

Step 3. Find a solution $(A_\Theta, B_\Theta, C_{\Theta_1}, C_{\Theta_2}, D_{\Theta_1}, D_{\Theta_2}) \in (\mathbb{R}^{n_p\times n_p}, \mathbb{R}^{n_p\times n_z}, \mathbb{R}^{n_{v_1}\times n_p}, \mathbb{R}^{n_{v_2}\times n_p}, \mathbb{R}^{n_{v_1}\times n_z}, \mathbb{R}^{n_{v_2}\times n_z})$ to the LMI problem:

$$\Psi + \tilde{P}^T\begin{bmatrix} A_\Theta & B_\Theta \\ C_{\Theta_1} & D_{\Theta_1} \\ C_{\Theta_2} & D_{\Theta_2} \end{bmatrix}\tilde{R} + \tilde{R}^T\begin{bmatrix} A_\Theta & B_\Theta \\ C_{\Theta_1} & D_{\Theta_1} \\ C_{\Theta_2} & D_{\Theta_2} \end{bmatrix}^T\tilde{P} < 0. \tag{5.35}$$

$\triangleleft$

Algorithm 5.13 (Arbitrary-order dynamic override compensation)

Step 1. Given n_Θ. Find a solution $(X, Y, \bar{U}, \bar{V}, \tau) \in (\mathbb{R}^{n_{\mathrm{CL}} \times n_{\mathrm{CL}}}, \mathbb{R}^{n_{\mathrm{CL}} \times n_{\mathrm{CL}}}, \mathbb{D}^{n_u}, \mathbb{D}^{n_{n_m}}, \mathbb{R})$, with $\gamma > 0$ as small as possible and $\tilde{\varrho} \geq 0$, to the LMI problem:

$$\text{Eqns. 5.34a-5.34g,} \tag{5.36a}$$

$$\mathrm{rank}(X - Y) \leq n_\Theta, \tag{5.36b}$$

Step 2. Using $m = n_{\mathrm{CL}} + n_\Theta + n_z + n_y + n_z + n_z + n_{m_p} + n_{m_n} + n_{m_n}$, construct the matrices $\Psi \in \mathbb{R}^{m \times m}$, $\tilde{R} \in \mathbb{R}^{n_z \times m}$, and $\tilde{P} \in \mathbb{R}^{m \times (n_{v_1} + n_{v_2})}$ via:

$$[\Psi, \tilde{R}, \tilde{P}] = V_{n_\Theta\text{-dynamic}}(\mathcal{P}^\Delta, \mathcal{G}_\mathcal{M}, X, Y, \bar{U}, \bar{V}, \tau, \gamma),$$

where the function $V_{n_\Theta\text{-dynamic}}$ is given in Chapter VI.

Step 3. Find a solution $(A_\Theta, B_\Theta, C_{\Theta_1}, C_{\Theta_2}, D_{\Theta_1}, D_{\Theta_2}) \in (\mathbb{R}^{n_\Theta \times n_\Theta}, \mathbb{R}^{n_\Theta \times n_z}, \mathbb{R}^{n_{v_1} \times n_\Theta}, \mathbb{R}^{n_{v_2} \times n_\Theta}, \mathbb{R}^{n_{v_1} \times n_z}, \mathbb{R}^{n_{v_2} \times n_z})$ to the LMI problem:

$$\Psi + \tilde{P}^T \begin{bmatrix} A_\Theta & B_\Theta \\ C_{\Theta_1} & D_{\Theta_1} \\ C_{\Theta_2} & D_{\Theta_2} \end{bmatrix} \tilde{R} + \tilde{R}^T \begin{bmatrix} A_\Theta & B_\Theta \\ C_{\Theta_1} & D_{\Theta_1} \\ C_{\Theta_2} & D_{\Theta_2} \end{bmatrix}^T \tilde{P} < 0. \tag{5.37}$$

$\lhd$

Note that, from a simple inspection of Algorithm 5.12, Step 1, no concluding remark can be done with respect to under what conditions global stability of the override closed-loop system is guaranteed. However, by employing the Finsler Lemma [14], one can prove that the conditions stated below in Assumption 5.5 guarantee global stability for the static override compensation with GOC for controller state/output.

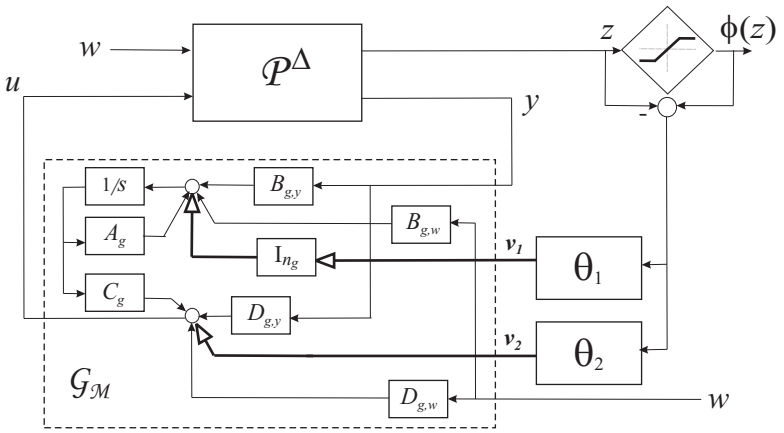

Fig. 27. Dynamic override compensation is fed back to the unconstrained controller states and output.

Assumption 5.14

There exists a solution $(\bar{X}_{11}, \bar{Y}, \bar{\bar{U}}) \in (\mathbb{R}^{n_p \times n_p}, \mathbb{R}^{n_{\mathrm{CL}} \times n_{\mathrm{CL}}}, \mathbb{D}^{n_u})$ to the LMI problem:

$$\bar{X}_{11} = \bar{X}_{11}^T > 0, \tag{5.38a}$$

$$\bar{Y} = \bar{Y}^T > 0, \tag{5.38b}$$

$$A_p \bar{X}_{11} + \bar{X}_{11} A_p^T < 0, \tag{5.38c}$$

$$A_{\mathrm{CL}} \bar{Y} + \bar{Y} A_{\mathrm{CL}}^T < 0. \tag{5.38d}$$

◁

Observing the conditions that guarantee global stability of the override closed-loop system, one can say that Assumption 5.14 requires, through Lyapunov inequalities, that both the plant and the unconstrained closed-loop are asymptotically stable.

The next theorems state that Assumption 5.9 provides necessary and sufficient conditions for the plant-order and arbitrary-order dynamic linear anti-windup compensations to be successfully constructed.

Theorem 5.15 *Assumption 5.14 is necessary and sufficient to guarantee that all steps*

in Algorithm 5.12 can be completed and the corresponding resulting $(A_\Theta, B_\Theta, C_{\Theta_1}, C_{\Theta_2}, D_{\Theta_1}, D_{\Theta_2})$ *describe a plant-order dynamic linear override compensator that guarantees the override closed-loop satisfies the basic properties of override and has finite unconstrained response recovery gain less than* γ. $\lhd$

Theorem 5.16 *Assumption 5.14 is necessary and sufficient to guarantee that all steps in Algorithm 5.13 can be completed and the corresponding resulting* $(A_\Theta, B_\Theta, C_{\Theta_1}, C_{\Theta_2}, D_{\Theta_1}, D_{\Theta_2})$ *describe an arbitrary-order dynamic linear override compensator that guarantees the override closed-loop satisfies the basic properties of override and has finite unconstrained response recovery gain less than* γ. $\lhd$

CHAPTER VI

QUADRATIC STABILITY AND PERFORMANCE OF CONSTRAINED SYSTEMS

This chapter presents the analysis and typical design tools which will be employed to guarantee stability and performance of the linear uncertain plant in feedback with a nonlinear function. More specifically, a quadratic Lyapunov function will be useful in order to guarantee absolute stability with the performance properties.

A. Preliminaries

The following definitions are given to assist in the system theoretic interpretation of the matrix inequalities presented in this dissertation.

1. Absolute stability

Absolute stability is a classical method employed to guarantee the stability of a linear system of the form:

$$\mathcal{L} \left\{ \begin{array}{l} \dot{x} = Ax + Bu \\ y = Cx + Du \end{array} \right. , \tag{6.1}$$

where $u, y \in \mathbb{R}^p$ interconnected with a (memoryless and, perhaps, time-varying) nonlinear function $f : \mathbb{R}^p \times \mathbb{R} \mapsto \mathbb{R}^p$ via:

$$u = f(y, t), \tag{6.2}$$

as observed in Fig. 28. The basic idea of absolute stability is to avoid studying a particular nonlinearity by embedding it inside a set of functions that is easily described and studied. This set of functions are defined in terms of a sector, as defined as follows.

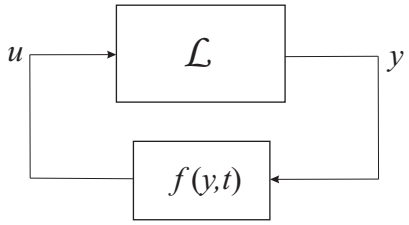

Fig. 28. Absolute stability. Linear system connected to a nonlinearity that belongs to a bounded sector.

Definition 6.1. Let $u \in \mathbb{R}^{n_p}, \mathcal{U} \subset \mathbb{R}^{n_u}, M_1, M_2 \in \mathbb{R}^{n_p \times r}$, and a $W \in \mathbb{R}^{n_p \times n_p}$. Define the $W - product$ of M_1 and M_2 as:

$$\langle M_1, M_2 \rangle_W = M_1^T W M_2.$$

Define the $W - norm$ as $|u|_W = \langle u, u \rangle_W^{\frac{1}{2}}$. We will use $|u| = |u|_I$. Define:

$$\text{dist}(u, \mathcal{U}) = \inf_{w \in \mathcal{U}} |u - w|_I.$$

Definition 6.2. Let $\underline{K}, \bar{K}, W$ be symmetric matrices in $\mathbb{R}^{p \times p}$ where $\bar{K} - \underline{K} > 0$ and $W > 0$. The (nonlinear, time-varying) function $f : \mathbb{R}^p \times \mathbb{R} \mapsto \mathbb{R}^p$ is said to *belong to the sector* $[\underline{K}, \bar{K}]_W$ if for all $y \in \mathbb{R}^p, t \in \mathbb{R}$:

$$\langle f(y,t) - \underline{K}y, f(y,t) - \bar{K}y \rangle \leq 0.$$

Moreover, f is said to belong to the incremental sector $[\underline{K}, \bar{K}]_W$ if f is locally Lipschitz in the first argument, measurable in the second, belongs to the sector $[\underline{K}, \bar{K}]_W$ and for almost all $y \in \mathbb{R}^p, t \in \mathbb{R}$:

$$\langle J_y f(y,t) - \underline{K}, J_y f(y,t) - \bar{K} \rangle_W \geq 0,$$

where $J_y f(y,t)$ is the Jacobian of $f(\cdot, t)$ evaluated at y.

The saturation nonlinearity is of our interest in the constrained problem. The

saturation nonlinearity has been denoted by $\phi : \mathbb{R}^{n_u} \mapsto \mathbb{R}^{n_u}$ (standard decentralized saturation function in Eqn. 2.2) and belongs to the incremental sector $[0, I]_W$ whenever $\phi(0) = 0$ and W is diagonal.

Definition 6.3. A function $\phi : \mathbb{R}^{n_u} \mapsto \mathbb{R}^{n_u}$ is said to belong to $\Phi_W (\phi \in \Phi_W)$ if the function f is locally Lipschitz, belongs to the incremental sector $[0, I]_W$, and $\phi(0) = 0$. Furthermore, $\phi \in \Phi_W$ is said to be *bounded* if there exists a $b \in \mathbb{R}$ such that $|\phi(s)|_W \leq b$ for all $s \in \mathbb{R}^{n_u}$.

Note that any standard decentralized saturation function belongs to $\Phi_W (\phi \in \Phi_W)$ if W is diagonal positive definite. Furthermore, if $\phi(\cdot)$ is a standard decentralized function then $|u - \phi(u)|_I = \text{dist}(u, \mathcal{U})$.

Definition 6.4. The feedback interconnection of $\mathcal{L}$ in Eqn. 6.1 and $u = \phi(y, t)$, as shown in Fig. 28, is said to be *well-posed* if there exists a unique function $\varsigma : \mathbb{R}^n \times \mathbb{R} \mapsto \mathbb{R}^u$, locally Lipschitz in the first argument, measurable in the second, such that $\varsigma(x, t) = \phi(Cx + D\varsigma(x, t), t)$ for all (x, t). Moreover, the interconnection is said to be absolutely stable in the sector $[\underline{K}, \bar{K}]_W$ if for every ϕ that belongs to the sector $[\underline{K}, \bar{K}]_W$ the system is well-posed and such that $x = 0$ is an uniformly globally asymptotically stable equilibrium.

Lemma 6.5 [56] The feedback interconnection of $\mathcal{L}$ in Eqn. 6.1 and $u = \phi(y, t)$, shown in Fig. 28, is well-posed for every ϕ that belongs to the incremental sector $[\underline{K}, \bar{K}]_W$ if and only if:

$$\text{He}\, \langle I - \underline{K}D, I - \bar{K}D \rangle_W > 0. \tag{6.3}$$

2. Quadratic stability

Absolute stability is established by way of quadratic stability.

Definition 6.6. Consider a feedback interconnection of $\mathcal{L}$ in Eqn. 6.1 and $u = \phi(y, t)$, shown in Fig. 28. The feedback interconnection is said to be *quadratically stable* if:

1. the interconnection is well-posed and

2. there exists a matrix $P = P^T > 0$ and a scalar $\epsilon > 0$ such that:

$$2x^T P(Ax + Bu) < -\epsilon x^T x$$

for all $(x, u, t) \neq 0$ such that:

$$u = \phi(Cx + Du, t).$$

Moreover the feedback interconnection is said to be *quadratically stable in the incremental sector* $[\underline{K}, \bar{K}]_W$ if:

1. the interconnection is well-posed for all ϕ belonging to the incremental sector $[\underline{K}, \bar{K}]_W$ and

2. there exists a matrix $P = P^T > 0$ and a scalar $\epsilon > 0$ such that:

$$2x^T P(Ax + Bu) < -\epsilon x^T x$$

for all $(x, u, t) \neq 0$ and all ϕ in the incremental sector $[\underline{K}, \bar{K}]_W$ such that:

$$u = \phi(Cx + Du, t).$$

Lemma 6.7 [56] Consider a feedback interconnection of $\mathcal{L}$ in Eqn. 6.1 and $u = \phi(y, t)$, shown in Fig. 28. If the feedback interconnection is quadratically stable in the incremental sector $[\underline{K}, \bar{K}]_W$, then it is absolute stable in the incremental sector $[\underline{K}, \bar{K}]_W$.

Lemma 6.8 [56] Consider a feedback interconnection of $\mathcal{L}$ in Eqn. 6.1 and $u = \phi(y, t)$, shown in Fig. 28. The following are equivalent:

1. The interconnection is quadratically stable in the incremental sector $[\underline{K}, \bar{K}]_W$.

2. The interconnection is well-posed for all ϕ belonging to the incremental sector $[\underline{K}, \bar{K}]_W$ and there exists a matrix $P = P^T > 0$ and a scalar $\epsilon > 0$ such that:

$$2x^T P(Ax + Bu) < -\epsilon x^T x$$

for all $(x, u, t) \neq 0$ such that:

$$\langle u - \underline{K}(Cx + Du), u - \bar{K}(Cx + Du)\rangle_W \leq 0.$$

3. There exists a matrix $P = P^T > 0$ and a scalar $\tau > 0$ such that:

$$\text{He}\begin{bmatrix} PA - \tau C^T \underline{K} W \bar{K} C & PB + \tau C^T \underline{K} W (I - \bar{K} D) \\ \tau (I - \bar{K} D)^T W \bar{K} C & -\tau (I - \underline{K} D)^T W (I - \bar{K} D) \end{bmatrix} < 0.$$

Corollary 6.9 [56] Consider a feedback interconnection of $\mathcal{L}$ in Eqn. 6.1 and $u = \phi(y, t)$, shown in Fig. 28. The feedback interconnection is quadratically stable in the incremental sector $[0, I]_W$ if and only if there exists a matrix $P = P^T > 0$ and a scalar $\tau > 0$ such that:

$$\begin{bmatrix} PA + A^T P & PB + \tau C^T W \\ \tau W C + B^T P & -\tau (WD + D^T W - 2W) \end{bmatrix} < 0. \tag{6.4}$$

3. Quadratic performance of constrained systems

In this section the tools employed to guarantee quadratic stability are expanded to be used for performance. In particular, consider the system:

$$\tilde{\mathcal{L}} \begin{cases} \dot{x} = Ax + B_1 u_1 + B_2 u_2 \\ y_1 = C_1 x + D_{11} u_1 + D_{12} u_2 \\ y_2 = C_2 x + D_{21} u_1 + D_{22} u_2 \end{cases}, \tag{6.5}$$

where $u_2, y_2 \in \mathbb{R}^p$ interconnected to a (memoryless and, perhaps, time-varying) sector-bounded nonlinear function via:

$$u_2 = \phi(y_2, t), \tag{6.6}$$

as shown in Fig. 29.

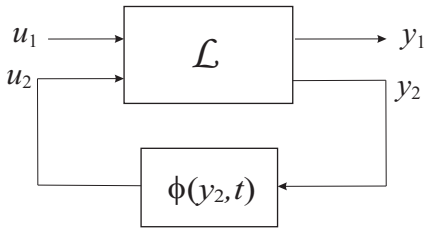

Fig. 29. Accounting for performance in the absolute stability setting.

The following definition merely extends the definition of well-posedness and quadratic stability in Definition 6.4 to allow an additional input and output such that performance can be quantified.

Definition 6.10. The interconnection of $\tilde{\mathcal{L}}$ in Eqn. 6.5 and $u_2 = \phi(y_2, t)$, shown in Fig. 29, is said to be *well-posed* if there exists an unique function $\varsigma : \mathbb{R}^n \times \mathbb{R}^u \times \mathbb{R} \mapsto \mathbb{R}^u$, globally Lipschitz in the first argument, measurable in the others, such that $\varsigma(x, u_1, t) = \phi(C_2 x + D_{21} u_1 + D_{22}\varsigma(x, u_1, t), t)$ for all (x, u_1, t). The feedback interconnection is said to *guarantee quadratic performance level* γ *from* u_1 *to* y_1 if:

1. the interconnection is well-posed and

2. there exists a matrix $P = P^T > 0$ and a scalar $\epsilon > 0$ such that:

$$2x^T P(Ax + B_1 u_1 + B_1 u_2) < -\epsilon|x|^2 - \frac{1}{\gamma}|C_1 x + D_{11} u_1 + D_{12} u_2|^2 + \gamma|u_1|^2$$

for all $(x, u_1, u_2, t) \neq 0$ such that:

$$u_2 = \phi(C_2 x + D_{21} u_1 + D_{22} u_2, t).$$

Moreover the feedback interconnection is said to *guarantee quadratic performance level* γ *from* u_1 *to* y_1 *in the incremental sector* $[\underline{K}, \bar{K}]_W$ if:

1. the interconnection is well-posed for all ϕ belonging to the incremental sector $[\underline{K}, \bar{K}]_W$ and

2. there exists a matrix $P = P^T > 0$ and a scalar $\epsilon > 0$ such that:

$$2x^T P(Ax + B_1 u_1 + B_1 u_2) < -\epsilon|x|^2 - \frac{1}{\gamma}|C_1 x + D_{11}u_1 + D_{12}u_2|^2 + \gamma|u_1|^2, \quad (6.7)$$

for all $(x, u_1, u_2, t) \neq 0$ and all ϕ belonging to the incremental sector $[\underline{K}, \bar{K}]_W$ such that:

$$u_2 = \phi(C_2 x + D_{21}u_1 + D_{22}u_2, t).$$

Well-posedness is now established for the interconnection with performance consideration, this is done following the ideas for the system without input.

Lemma 6.11 [56] Suppose ϕ belongs to the incremental sector $[\underline{K}, \bar{K}]_W$. The feedback interconnection of $\tilde{\mathcal{L}}$ in Eqn. 6.5 and $u_2 = \phi(y_2, t)$, shown in Fig. 29, is well-posed if and only if:

$$\text{He}\,\langle I - \underline{K}D_{22}, I - \bar{K}D_{22}\rangle_W > 0. \quad (6.8)$$

Lemma 6.12 [56] If a feedback interconnection of $\tilde{\mathcal{L}}$ in Eqn. 6.5 and $u_2 = \phi(y_2, t)$, shown in Fig. 29, guarantees quadratic performance level γ from u_1 to y_1, then the interconnection is quadratically stable (when $u_1 = 0$) and the $\mathcal{L}_2$ gain from u_1 to y_1 is less than γ (when $x(0) = 0$).

Lemma 6.13 [56] Consider a feedback interconnection of $\tilde{\mathcal{L}}$ in Eqn. 6.5 and $u_2 = \phi(y_2, t)$, shown in Fig. 29. The following are equivalent:

1. The feedback interconnection guarantees quadratic performance level γ from u_1 to y_1 in the incremental sector $[0, I]_W$.

2. The interconnection is well-posed for all ϕ belonging to the incremental sector $[\underline{K}, \bar{K}]_W$ and there exists a matrix $P = P^T > 0$ and a scalar $\epsilon > 0$ such that:

$$2x^T P(Ax + B_1 u_1 + B_1 u_2) < -\epsilon|x|^2 - \frac{1}{\gamma}|C_1 x + D_{11}u_1 + D_{12}u_2|^2 + \gamma|u_1|^2,$$

for all $(x, u_1, u_2, t) \neq 0$ and all ϕ belonging to the incremental sector $[\underline{K}, \bar{K}]_W$ such that:

$$u_2 = \phi(C_2 x + D_{21}u_1 + D_{22}u_2, t).$$

3. There exists a matrix $P = P^T$ and a scalar $\tau > 0$ such that:

$$\begin{bmatrix} PA + A^T P & PB_2 + \tau C_2 W & PB_1 & C_1^T \\ B_1^T P + \tau W C_2^T & \tau(WD_{22} + D_{22}^T W - 2W) & \tau W D_{21} & D_{12}^T \\ B_1^T P & \tau D_{21}^T W & -\gamma I & D_{11}^T \\ C_1 & D_{12} & D_{11} & -\gamma I \end{bmatrix}.$$

4. Quadratic robust stability

This section requires the definition of the perturbation uncertainty characteristics.

Definition 6.14. Let C_1, D_{11}, D_{12}, C_2, D_{21} and D_{22} be given. Then the uncertainty perturbation $\Delta = \begin{bmatrix} \Delta_p \\ \Delta_n \end{bmatrix}$, where $\Delta_p = \text{diag}\,[\delta_1 I_{k_1}, ..., \delta_L I_{k_L}]$ and $\Delta_n = \text{diag}\,[\Delta_{L+1}, ..., \Delta_{L+F}]$ have the following properties:

1. The perturbation Δ_p is a nonlinear diagonal perturbation (from $y_1 = C_1 x + D_{11}u_1 + D_{13}u_3$ to Δ_p) in the incremental sector $[0, \varrho I]_{W_p}$, and

2. The dynamic nonlinear perturbation Δ_n is said to have *finite incremental gain*

ϱ (from $y_2 = C_2x + D_{22}u_2 + D_{23}u_3$ to Δ_n) if:

$$\|\Delta_n(\sigma_o, y_2) - \Delta_n(\sigma_o, y_2')\|_2 \leq \varrho \left\| \begin{bmatrix} C_2(x - x') \\ D_{22}(u_2 - u_2') \\ D_{23}(u_3 - u_3') \end{bmatrix} \right\|_2, \tag{6.9}$$

for all $x, x', y_2, y_2', u_2, u_2' \in \mathcal{L}_2$.

With the uncertainty perturbation properly defined, we use absolute stability theory to guarantee stability of a linear system of the form:

$$\mathcal{L}^{\Delta} \begin{cases} \dot{x} = Ax + B_1u_1 + B_2u_2 \\ y_1 = C_1x + D_{11}u_1 + D_{13}u_3 \\ y_2 = C_2x + D_{22}u_2 + D_{23}u_3 \\ y_3 = C_3x + D_{31}u_1 + D_{32}u_2 + D_{33}u_3 \end{cases}, \tag{6.10}$$

where $u_1, y_1 \in \mathbb{R}^p$ are interconnected to a (memoryless and perhaps, time varying) sector-bounded nonlinear function via:

$$u_1 = \Delta_p(y_1, t), \tag{6.11}$$

$u_2, y_2 \in \mathbb{R}^p$ are interconnected to a dynamic, possibly nonlinear, system with finite incremental gain ϱ via:

$$u_2 = \Delta_n(\sigma_o, y_2, t), \tag{6.12}$$

and $u_3, y_3 \in \mathbb{R}^p$ are interconnected to a (memoryless and, perhaps, time-varying) sector-bounded nonlinear function via:

$$u_3 = \phi(y_3, t), \tag{6.13}$$

as shown in Fig. 30.

For (global) remedial compensation, we are interested in the sector that the

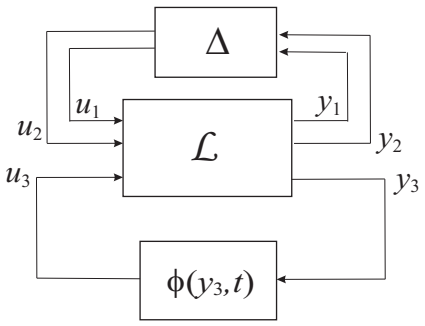

Fig. 30. Absolute stability accounting for model uncertainty.

saturation nonlinearity belongs to, namely the incremental sector $[0, I]_W$, hence from now on we will we will assume that $\phi \in \Phi_W$.

Definition 6.15. Consider a feedback interconnection of $\mathcal{L}^{\Delta}$ in Eqn. 6.9 and, $u_1 = \Delta_p(y_1, t)$, $u_2 = \Delta_n(\sigma_o, y_2, t)$ and $u_3 = \phi(y_3, t)$, shown in Fig. 30. The feedback interconnection is said to be *quadratically robustly stable* if:

1. the interconnection is well-posed and
2. there exists a matrix $P = P^T > 0$ and real scalars $\epsilon > 0$, $\rho \geq 0$ and $\beta \geq 0$ such that:

$$2x^T P(Ax + B_1 u_1 + B_2 u_2) < -\epsilon x^T x + \beta(\langle u_1, \varrho y_1 - u_1 \rangle_{W_p}) + \rho(u_2^T u_2 - \varrho^2 y_2^T y_2)$$

for all $(x, u_1, u_2, u_3, t) \neq 0$ such that:

$$u_3 = \phi(C_3 x + D_{31} u_1 + D_{32} u_2 + D_{33} u_3, t).$$

Moreover the feedback interconnection is said to be *quadratically robustly stable in the incremental sector* $[0, I]_W$ if:

1. the interconnection is well-posed for all ϕ belonging to Φ_W and
2. there exists a matrix $P = P^T > 0$ and real scalars $\epsilon > 0$, $\rho \geq 0$ and $\beta \geq 0$ such

that:

$$2x^T P(Ax + B_1 u_1 + B_2 u_2) < -\epsilon x^T x + \beta(\langle u_1, \varrho y_1 - u_1 \rangle_{W_p}) + \rho(u_2^T u_2 - \varrho^2 y_2^T y_2)$$

for all $(x, u_1, u_2, u_3, t) \neq 0$ and all $\phi \in \Phi_W$ such that:

$$u_3 = \phi(C_3 x + D_{31} u_1 + D_{32} u_2 + D_{33} u_3, t).$$

Lemma 6.16. Consider a feedback interconnection of $\mathcal{L}^\Delta$ in Eqn. 6.9 and, $u_1 = \Delta_p(y_1, t)$, $u_2 = \Delta_p(y_2, t)$ and $u_3 = \phi(y_3, t)$, shown in Fig. 30. The following are equivalent:

1. The interconnection is quadratically robustly stable in the incremental sector $[0, I]_W$.

2. The interconnection is well-posed for all $\phi \in \Phi_W$ and there exists a matrix $P = P^T > 0$ and real scalars $\epsilon > 0$, $\rho \geq 0$ and $\beta \geq 0$ such that:

   $$2x^T P(Ax + B_1 u_1 + B_2 u_2) < -\epsilon x^T x + \beta(\langle u_1, \varrho y_1 - u_1 \rangle_{W_p}) + \rho(u_2^T u_2 - \varrho^2 y_2^T y_2)$$

   for all $(x, u_1, u_2, u_3, t) \neq 0$ such that:

   $$\langle u, u_3 - (C_3 x + D_{31} u_1 + D_{32} u_2 + D_{33} u_3) \rangle_W \leq 0.$$

3. There exists a matrix $P = P^T > 0$ and a scalar $\tau > 0$ such that:

$$\mathrm{He} \begin{bmatrix} PA + \frac{\rho}{2}\varrho^2 C_2^T C_2 & PB_1 & PB_2 & PB_3 \\ \beta\varrho W_p C_1 & \beta(\varrho W_p D_{11} - W_p) & 0 & \beta\varrho W_p D_{13} \\ \rho\varrho^2 D_{22}^T C_2 & 0 & \frac{\rho}{2}(\varrho^2 D_{22}^T D_{22} - I) & \rho\varrho^2 D_{22}^T D_{23} \\ \tau W C_3 & \tau W D_{31}^T & \tau W D_{32}^T & \tau(W D_{33} - W) + \frac{\rho}{2}\varrho^2 D_{23}^T D_{23} \end{bmatrix} < 0. \tag{6.14}$$

5. Quadratic robust performance of constrained systems

In this section the tools employed to guarantee quadratic robust stability are expanded to be used for performance. In particular, consider the system:

$$\tilde{\mathcal{L}}^{\Delta} \begin{cases} \dot{x} = Ax + B_1u_1 + B_2u_2 + B_3u_3 + B_4u_4 \\ y_1 = C_1x + D_{11}u_1 + D_{13}u_3 + D_{14}u_4 \\ y_2 = C_2x + D_{22}u_2 + D_{23}u_3 + D_{24}u_4 \\ y_3 = C_3x + D_{31}u_1 + D_{32}u_2 + D_{33}u_3 + D_{34}u_4 \\ y_4 = C_4x + D_{41}u_1 + D_{42}u_2 + D_{43}u_3 + D_{44}u_4 \end{cases}, \tag{6.15}$$

where $u_1, y_1 \in \mathbb{R}^p$ are interconnected to a (memoryless and perhaps, time varying) sector-bounded nonlinear function via:

$$u_1 = \Delta_p(y_1, t), \tag{6.16}$$

$u_2, y_2 \in \mathbb{R}^p$ are interconnected to a dynamic, possibly nonlinear, system with finite incremental gain ϱ via:

$$u_2 = \Delta_n(\sigma_o, y_2, t), \tag{6.17}$$

and $u_4, y_4 \in \mathbb{R}^u$ are interconnected to a (memoryless and, perhaps, time-varying) sector-bounded nonlinear function via:

$$u_4 = \phi(y_4, t), \tag{6.18}$$

as shown in Fig. 31.

The following definition merely extends the definition of well-posedness and quadratic robust stability in Definition 6.16 to allow an additional input and output such that performance can be quantified.

Definition 6.17. The interconnection of $\tilde{\mathcal{L}}^{\Delta}$ in Eqn. 6.15 and, $u_1 = \Delta_p(y_1, t)$,

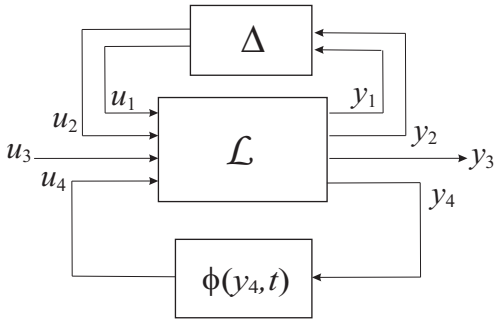

Fig. 31. Absolute stability accounting for model uncertainty and performance.

$u_2 = \Delta_n(\sigma_o, y_2, t)$ and $u_3 = \phi(y_3, t)$, shown in Fig. 31, is said to be *well-posed* if there exist unique functions $\varsigma_1 : \mathbb{R}^n \times \mathbb{R}^p \times \mathbb{R}^u \times \mathbb{R} \mapsto \mathbb{R}^p$, $\varsigma_2 : \mathbb{R}^n \times \mathbb{R}^p \times \mathbb{R}^u \times \mathbb{R} \mapsto \mathbb{R}^p$ and $\varsigma_4 : \mathbb{R}^n \times \mathbb{R}^p \times \mathbb{R}^p \times \mathbb{R}^u \times \mathbb{R} \mapsto \mathbb{R}^u$, globally Lipschitz in the first arguments and measurable in the last arguments, such that $\varsigma_1(x, u_3, u_4, t) = \phi(C_1 x + D_{11}\varsigma_1(x, u_3, u_4, t) + D_{13}u_3 + D_{14}u_4, t)$ for all (x, u_3, u_4, t), $\varsigma_2(x, u_3, u_4, t) = \Delta_p(C_2 x + D_{22}\varsigma_2(x, u_3, u_4, t) + D_{23}u_3 + D_{24}u_4, t)$ for all (x, u_3, u_4, t) and $\varsigma_4(x, u_1, u_2, u_3, t) = \Delta_n(C_4 x + D_{41}u_1 + D_{42}u_2 + D_{43}u_3 + D_{44}\varsigma_4(x, u_1, u_2, u_3, t), t)$ for all (x, u_1, u_2, u_3, t). The feedback interconnection is said to *guarantee quadratic robust performance level* γ *from* u_3 *to* y_3 if:

1. the interconnection is well-posed and

2. there exists a matrix $P = P^T > 0$ and real scalars $\epsilon > 0$, $\rho \geq 0$ and $\beta \geq 0$ such that:

$$2x^T P(Ax + B_1u_1 + B_2u_2 + B_3u_3 + B_4u_4) < -\epsilon|x|^2 - \tfrac{1}{\gamma}|C_3x + D_{31}u_1 + D_{32}u_2 + D_{33}u_3 + D_{34}u_4|^2 + \gamma|u_3|^2 + \beta(\langle u_1, \varrho y_1 - u_1\rangle_{W_p}) + \rho(u_2^T u_2 - \varrho^2 y_2^T y_2)$$

for all $(x, u_1, u_2, u_3, u_4, t) \neq 0$ such that:

$$u_4 = \phi(C_4x + D_{41}u_1 + D_{42}u_2 + D_{43}u_3 + D_{43}u_4, t).$$

Moreover the feedback interconnection is said to *guarantee quadratic robust performance level* γ *from* u_3 *to* y_3 *in the incremental sector* $[0, I]_W$ if:

1. the interconnection is well-posed for all $\phi \in \Phi$ and

2. there exists a matrix $P = P^T > 0$ and real scalars $\epsilon > 0$, $\rho \geq 0$ and $\beta \geq 0$ such that:

$$\begin{aligned} 2x^T P(Ax + B_1u_1 + B_2u_2 + B_3u_3 + B_4u_4) < -\epsilon|x|^2 - \tfrac{1}{\gamma}|C_3x + D_{31}u_1 + D_{32}u_2 \\ +D_{33}u_3 + D_{34}u_4|^2 + \gamma|u_3|^2 + \beta(\langle u_1, \varrho y_1 - u_1\rangle_{W_p}) + \rho(u_2^T u_2 - \varrho^2 y_2^T y_2), \end{aligned} \tag{6.19}$$

for all $(x, u_1, u_2, u_3, u_4, t) \neq 0$ and all ϕ belonging to the incremental sector $[\underline{K}, \bar{K}]_W$ such that:

$$u_4 = \phi(C_4x + D_{41}u_1 + D_{42}u_2 + D_{43}u_3 + D_{43}u_4, t).$$

Well-posedness is now established for the interconnection with performance considerations, this is done following the ideas for the system without exogenous input.

Lemma 6.18. Suppose $\phi \in \Phi_W$. The feedback interconnection of $\tilde{\mathcal{L}}^\Delta$ in Eqn. 6.15 and, $u_1 = \Delta_p(y_1, t)$, $u_2 = \Delta_n(\sigma_o, y_2, t)$ and $u_4 = \phi(y_4, t)$, shown in Fig. 31, is well-posed if and only if:

$$\text{He}\begin{bmatrix} \beta(\varrho W_p D_{11} - W_p) & 0 & \beta\varrho W_p D_{14} \\ 0 & \frac{\rho}{2}(\varrho^2 D_{22}^T D_{22} - I) & \rho\varrho^2 D_{22}^T D_{24} \\ \tau W D_{41}^T & \tau W D_{42} & \tau(W D_{44} - W) + \frac{\rho}{2}\varrho^2 D_{24}^T D_{24} \end{bmatrix} < 0. \tag{6.20}$$

Lemma 6.19. If a feedback interconnection of $\tilde{\mathcal{L}}^\Delta$ in Eqn. 6.15 and, $u_1 = \Delta_p(y_1, t)$, $u_2 = \Delta_n(\sigma_o, y_2, t)$ and $u_3 = \phi(y_3, t)$, shown in Fig. 31, guarantees quadratic robust performance level γ from u_3 to y_3, then the interconnection is quadratically robustly stable (when $u_3 = 0$) and the $\mathcal{L}_2$ gain from u_3 to y_3 is less than γ (when $x(0) = 0$).

Lemma 6.20. Consider a feedback interconnection of $\tilde{\mathcal{L}}^\Delta$ in Eqn. 6.15 and, $u_1 = \Delta_p(y_1, t)$, $u_2 = \Delta_n(\sigma_o, y_2, t)$ and $u_3 = \phi(y_3, t)$, shown in Fig. 31. The following are equivalent:

1. The feedback interconnection guarantees quadratic robust performance level γ from u_3 to y_3 in the incremental sector $[0, I]_W$.

2. The interconnection is well-posed for all $\phi \in \Psi$ and there exists a matrix $P = P^T > 0$ and real scalars $\epsilon > 0$, $\rho \geq 0$ and $\beta \geq 0$ such that:

$$2x^T P(Ax + B_1u_1 + B_2u_2 + B_3u_3 + B_4u_4) < -\epsilon|x|^2 - \tfrac{1}{\gamma}|C_3x + D_{31}u_1 + D_{32}u_2 + D_{33}u_3 + D_{34}u_4|^2 + \gamma|u_3|^2 + \beta(\langle u_1, \varrho y_1 - u_1\rangle_{W_p}) + \rho(u_2^T u_2 - \varrho^2 y_2^T y_2),$$

for all $(x, u_1, u_2, u_3, u_4, t) \neq 0$ and all $\phi \in \Phi_W$ such that:

$$u_4 = \phi(C_4x + D_{41}u_1 + D_{42}u_2 + D_{43}u_3 + D_{43}u_4, t).$$

3. There exists a matrix $P = P^T > 0$ and real scalars $\epsilon > 0$, $\rho \geq 0$ and $\beta \geq 0$ such that:

$$\text{He}\begin{bmatrix} PA & PB_4 & C_3^T & PB_3 & PB_1 & PB_2 & \rho\varrho C_2^T \\ \beta W C_4 & \tau(WD_{44} - W) & 0 & \tau W D_{43} & \tau W D_{41} & \tau W D_{42} & 0 \\ 0 & D_{34} & -\frac{\gamma}{2}I & 0 & D_{31} & 0 & 0 \\ 0 & 0 & D_{33}^T & -\frac{\gamma}{2}I & 0 & 0 & 0 \\ \beta\varrho W_p C_1 & \beta\varrho W_p D_{14} & 0 & 0 & \beta(\varrho W_p D_{11} - W_p) & 0 & 0 \\ 0 & 0 & D_{32}^T & 0 & 0 & -\frac{\rho}{2}I & 0 \\ 0 & \rho\varrho D_{24} & 0 & 0 & 0 & \rho\varrho D_{22} & -\frac{\rho}{2}I \end{bmatrix} < 0.$$

B. Robust remedial compensation analysis

In this section, we plan to use Lemma 6.20 to guarantee quadratic robust performance of the remedial closed-loop systems. In particular, we intend to apply Lemma 6.20 to the mismatch systems presented in Chapter IV. Note that Figs. 22 and 23 show the mismatch closed-loop systems with the corresponding input and outputs as defined in Eqns. 4.6 and 4.7. The realization of the mismatch systems are rewritten at this part for clarity of presentation.

1. Anti-windup compensation

The mismatch system for anti-windup compensation can be written with the state $x = \begin{bmatrix} x_{p,d} \\ x_{g,d} \\ x_\Lambda \end{bmatrix}$, inputs ζ_d and ψ_0, and outputs η_d, z_d and u_d as:

$$\mathcal{W} \begin{cases} \dot{x} = Ax + B_\zeta \zeta_d + B_\psi \psi_0 \\ \eta_d = C_\eta x + D_{\eta\zeta}\zeta_d + D_{\eta\psi}\psi_0 \\ z_d = C_z x + D_{z\zeta}\zeta_d + D_{z\psi}\psi_0 \\ u_d = C_u x + D_{u\zeta}\zeta_d + D_{u\psi}\psi_0 \end{cases}, \tag{6.21}$$

interconnected with the feedback connections:

$$\begin{aligned} \zeta_d &= \Delta(\eta_d), \\ \psi_0 &= \psi(u) = u - \phi(u). \end{aligned}$$

The following lemma shows that the function $u \mapsto u - \phi(u) \in \Phi_W$.

Lemma 6.21. Let W be symmetric positive definite. If $\phi : \mathbb{R}^{n_u} \times \mathbb{R} \mapsto \mathbb{R}^{n_u}$ belongs to the sector $[0, I]_W$ then the function $\psi(u) = u - \phi(u, t)$ belongs to the sector $[0, I]_W$. Moreover, if $\phi \in \Phi_W$ then the function $\psi(u) = u - \phi(u, t) \in \Phi_W$.

Proof. The proof follows by applying the definitions.

2. Override compensation

The mismatch system for override compensation can be written with the state $x = \begin{bmatrix} x_{p,d} \\ x_{g,d} \\ x_{\Theta} \end{bmatrix}$, inputs ζ_d, ψ_0 and φ_0, and outputs η_d, z_d, y_d and $\underline{z}_d$ as:

$$\mathcal{W} \begin{cases} \dot{x} = Ax + B_\zeta \zeta_d + B_\psi(\psi_0 + \varphi_0) \\ \eta_d = C_\eta x + D_{\eta\zeta}\zeta_d + D_{\eta\psi}(\psi_0 + \varphi_0) \\ z_d = C_z x + D_{z\zeta}\zeta_d + D_{z\psi}(\psi_0 + \varphi_0) \\ y_d = C_y x + D_{y\zeta}\zeta_d + D_{y\psi}(\psi_0 + \varphi_0) \\ \underline{z}_d = z_d - \psi_0 \end{cases}, \tag{6.22}$$

interconnected with the feedback connections:

$$\zeta_d = \Delta(\eta_d),$$
$$\varphi_0 = \varphi(-z_d, z_l) = \psi(z) - \psi(z_l).$$

Lemma 6.22. Let W be symmetric positive definite. If $\phi : \mathbb{R}^{n_z} \times \mathbb{R} \mapsto \mathbb{R}^{n_z}$ belongs to the sector $[0, I]_W$ then the functions $\psi(z) = z - \phi(z, t)$ and $\varphi(\cdot, z_l) = \psi(z) - \psi(z_l)$ belong to the sector $[0, I]_W$. Moreover, if $\phi \in \Phi_W$ then the functions $\psi, \varphi \in \Phi_W$.

Proof. The proof follows by applying the definitions.

3. Quadratic robust unconstrained response recovery performance

As noted in Chapter IV, the mismatch systems furnish an effective way of ensuring the satisfaction of the basic properties of remedial compensation together with explicit quantification of performance. Having determined, from Lemmas 6.21 and 6.22, that the nonlinear functions $\psi, \varphi \in \Phi_W$ if and only if $\phi \in \Phi_W$. We are now in position to use Lema 6.20 to guarantee quadratic robust performance level, which due to Lemma 6.19 implies robust stability and unconstrained performance recovery.

Property 6.23. Let $W = W^T > 0$. The remedial augmented closed-loop system is said to guarantee quadratic robust unconstrained response recovery performance level γ if the feedback interconnection of Eqn. 6.21 and $\psi_0 = \psi(u)$, and of Eqn. 6.22 and $\varphi_0 = \varphi(-u_d, u_l)$, respectively for anti-windup and override compensation, guarantees quadratic robust performance level γ from u_l to z_d, and from ψ_0 to $\begin{bmatrix} y_d \\ z_d \end{bmatrix}$, respectively.

Lemma 6.24. Let $W = W^T > 0$. The remedial augmented closed-loop system guarantees quadratic robust unconstrained response recovery performance level γ and $\tilde{\varrho} \geq 0$ if and only if there exists a solution $(\bar{Q}, \bar{U}, \bar{V}, \tau, \gamma)$ to the LMI problem in Eqns. 4.18 and 4.19 with $\bar{U} = \tau W^{-1}$ for some $\tau > 0$, $\bar{V} = \alpha W_p^{-1}$ for some $\alpha > 0$ and $\tau = 1/\rho$ for some $\rho > 0$, when the matrices are defined accordingly to Notation 4.1.

Proof. Based on the matrices according to Notation 4.1, given the solution $(\bar{Q}, \bar{U}, \bar{V}, \tau, \gamma)$ to the LMI problem in Eqns. 4.18 and 4.19 with $\bar{U} = \tau W^{-1}$ and $\tau > 0$, $\bar{V} = \alpha W_p^{-1}$ and $\alpha > 0$, and $\tau = 1/\rho$ and $\rho > 0$, after premultiplying and postmultiplying each side of Eqns. 4.18d and 4.19d by the nonsingular matrix diag $= [P, \tau W, I_{n_z}, I_{n_u}, \beta W_p, \tau]$, where $P = P^T = \bar{Q}^{-1} > 0$, Lemma 6.20 guarantees quadratic robust unconstrained response performance level γ. Reversing the arguments the converse can be proved.

Proof of Theorem 4.4. With the unconstrained closed-loop assumed to be exponentially stable, the signal u_l is well-defined, and bounded exogenous input w implies bounded closed-loop trajectories and hence bounded u_l. Lemma 6.24 further guarantees the interconnection of Eqn. 6.21 and $\psi_0 = \psi(u)$ is quadratically robustly stable with $\|z(\cdot) - z_l(\cdot)\|_2 \leq \gamma \|u_l(\cdot)\|_2$, then the anti-windup closed-loop system guarantees the basic-properties of anti-windup.

Proof of Theorem 4.6. With the unconstrained closed-loop assumed to be exponentially stable, the signal z_l is well-defined, and bounded exogenous input w implies

bounded closed-loop trajectories and hence bounded z_l. Lemma 6.24 further guarantees the interconnection of Eqn. 6.21 and $\varphi_0 = \varphi(-u_d, u_l)$ is quadratically robustly stable with $\| \begin{bmatrix} y_d \\ z_d \end{bmatrix} \|_2 \leq \gamma \|z_l(\cdot) - \text{sat}(z_l(\cdot))\|_2$, then the override closed-loop system guarantees the basic-properties of override.

C. Remedial compensation synthesis

For synthesis purposes, further manipulation can be performed in Eqns. 4.18d and 4.19d in Chapter IV, such that the parametrization of the mismatch system state space matrices is affine in the remedial compensator Λ or Θ elements, respectively. However, even employing this parametrization, Theorems 4.4 and 4.6 do not seem appropriate for synthesis as the (unknown) remedial compensator Λ and Θ elements multiply the unknowns $\bar{Q}$, $\bar{U}$, $\bar{V}$ and τ, and hence Eqns. 4.18d and 4.19d become a nonlinear matrix inequality. Converting 4.18d and 4.19d into LMI conditions amenable for synthesis is the motivation for this section.

In order to isolate the dependence on the remedial compensators in the matrix inequalities for analysis, we will use the following construction, detailed in Notation 6.25.

Notation 6.25. Construction of compact representation of mismatch system with explicit presence of remedial compensator.

Step 1. Based on the matrices of the plant $\mathcal{P}^{\Delta}$ in Eqn. 4.1 and unconstrained controller $\mathcal{G}$ in Eqn. 4.2, construct A_{CL}, $B_{\text{CL},\zeta}$, $B_{\text{CL},v}$, $B_{\text{CL},\psi}$, $C_{\text{CL},\eta}$, $D_{\text{CL},\eta\zeta}$, $D_{\text{CL},\eta v}$, $D_{\text{CL},\eta\psi}$, $C_{\text{CL},z}$, $D_{\text{CL},z\zeta}$, $D_{\text{CL},zv}$, $D_{\text{CL},z\psi}$, $C_{\text{CL},y}$, $D_{\text{CL},y\zeta}$, $D_{\text{CL},yv}$, $D_{\text{CL},y\psi}$, $C_{\text{CL},u}$, $D_{\text{CL},u\zeta}$, $D_{\text{CL},uv}$ and $D_{\text{CL},u\psi}$.

Step 2. Define $\bar{A} \in \mathbb{R}^{(n_{\text{CL}}+n_{\mathcal{R}})\times(n_{\text{CL}}+n_{\mathcal{R}})}$, $\bar{B}_{\zeta} \in \mathbb{R}^{(n_{\text{CL}}+n_{\mathcal{R}})\times n_m}$, $\bar{B}_{\psi} \in \mathbb{R}^{(n_{\text{CL}}+n_{\mathcal{R}})\times n_r}$,

$\bar{C}_\eta \in \mathbb{R}^{n_m \times (n_{\mathrm{CL}}+n_{\mathcal{R}})}$, $\bar{D}_{\eta\zeta} \in \mathbb{R}^{n_m \times n_m}$, $\bar{D}_{\eta\psi} \in \mathbb{R}^{n_m \times n_r}$, $\bar{C}_z \in \mathbb{R}^{n_z \times (n_{\mathrm{CL}}+n_{\mathcal{R}})}$, $\bar{D}_{z\zeta} \in \mathbb{R}^{n_z \times n_m}$, $\bar{D}_{z\psi} \in \mathbb{R}^{n_z \times n_r}$, $\bar{C}_y \in \mathbb{R}^{n_y \times (n_{\mathrm{CL}}+n_{\mathcal{R}})}$, $\bar{D}_{y\zeta} \in \mathbb{R}^{n_y \times n_m}$, $\bar{D}_{y\psi} \in \mathbb{R}^{n_y \times n_r}$, $\bar{C}_u \in \mathbb{R}^{n_u \times (n_{\mathrm{CL}}+n_{\mathcal{R}})}$, $\bar{D}_{u\zeta} \in \mathbb{R}^{n_u \times n_m}$, $\bar{D}_{u\psi} \in \mathbb{R}^{n_u \times n_r}$ via:

$$
\begin{aligned}
&\bar{A} = \begin{bmatrix} A_{\mathrm{CL}} & 0 \\ 0 & 0 \end{bmatrix}, \quad \bar{B}_\zeta = \begin{bmatrix} B_{\mathrm{CL},\zeta} \\ 0 \end{bmatrix}, \quad \bar{B}_\psi = \begin{bmatrix} B_{\mathrm{CL},\psi} \\ 0 \end{bmatrix}, \\
&\bar{C}_\eta = \begin{bmatrix} C_{\mathrm{CL},\eta} & 0 \end{bmatrix}, \qquad \bar{D}_{\eta\zeta} = D_{\mathrm{CL},\eta\zeta}, \qquad \bar{D}_{\eta\psi} = D_{\mathrm{CL},\eta\psi}, \\
&\bar{C}_z = \begin{bmatrix} C_{\mathrm{CL},z} & 0 \end{bmatrix}, \qquad \bar{D}_{z\zeta} = D_{\mathrm{CL},z\zeta}, \qquad \bar{D}_{z\psi} = D_{\mathrm{CL},z\psi}, \\
&\bar{C}_y = \begin{bmatrix} C_{\mathrm{CL},y} & 0 \end{bmatrix}, \qquad \bar{D}_{y\zeta} = D_{\mathrm{CL},y\zeta}, \qquad \bar{D}_{y\psi} = D_{\mathrm{CL},y\psi}, \\
&\bar{C}_u = \begin{bmatrix} C_{\mathrm{CL},u} & 0 \end{bmatrix}, \qquad \bar{D}_{u\zeta} = D_{\mathrm{CL},u\zeta}, \qquad \bar{D}_{u\psi} = D_{\mathrm{CL},u\psi}.
\end{aligned}
\tag{6.23}
$$

and $\underline{B} \in \mathbb{R}^{(n_{\mathrm{CL}}+n_{\mathcal{R}}) \times (n_{\mathcal{R}}+n_v)}$, $\underline{C} \in \mathbb{R}^{(n_{\mathcal{R}}+n_r) \times (n_{\mathrm{CL}}+n_{\mathcal{R}})}$, $\underline{D}_\psi \in \mathbb{R}^{(n_{\mathcal{R}}+n_r) \times n_r}$, $\underline{D}_\eta \in \mathbb{R}^{n_m \times (n_{\mathrm{CL}}+n_v)}$, $\underline{D}_z \in \mathbb{R}^{n_z \times (n_{\mathrm{CL}}+n_v)}$, $\underline{D}_y \in \mathbb{R}^{n_y \times (n_{\mathrm{CL}}+n_v)}$, $\underline{D}_u \in \mathbb{R}^{n_u \times (n_{\mathrm{CL}}+n_v)}$ via:

$$
\begin{aligned}
&\underline{B} = \begin{bmatrix} 0 & B_{\mathrm{CL},v} \\ I_{n_{\mathcal{R}}} & 0 \end{bmatrix}, \quad \underline{C} = \begin{bmatrix} 0 & I_{n_{\mathcal{R}}} \\ 0 & 0 \end{bmatrix}, \quad \underline{D}_\psi = \begin{bmatrix} 0 \\ I_{n_r} \end{bmatrix}, \\
&\underline{D}_\eta = \begin{bmatrix} 0 & D_{\mathrm{CL},\eta v} \end{bmatrix} \quad \underline{D}_z = \begin{bmatrix} 0 & D_{\mathrm{CL},zv} \end{bmatrix} \\
&\underline{D}_y = \begin{bmatrix} 0 & D_{\mathrm{CL},yv} \end{bmatrix} \quad \underline{D}_u = \begin{bmatrix} 0 & D_{\mathrm{CL},uv} \end{bmatrix}
\end{aligned}
\tag{6.24}
$$

Step 3. Define $\Xi \in \mathbb{R}^{(n_{\mathcal{R}}+n_v) \times (n_{\mathcal{R}}+n_r)}$ via:

$$
\Xi = \begin{bmatrix} A_{\mathcal{R}} & B_{\mathcal{R}} \\ C_{\mathcal{R}_1} & D_{\mathcal{R}_1} \\ C_{\mathcal{R}_2} & D_{\mathcal{R}_2} \end{bmatrix}. \tag{6.25}
$$

Step 4. Define the matrices $A \in \mathbb{R}^{(n_{\mathrm{CL}}+n_{\mathcal{R}}) \times (n_{\mathrm{CL}}+n_{\mathcal{R}})}$, $B_\zeta \in \mathbb{R}^{(n_{\mathrm{CL}}+n_{\mathcal{R}}) \times n_m}$, $B_\psi \in \mathbb{R}^{(n_{\mathrm{CL}}+n_{\mathcal{R}}) \times n_r}$, $C_\eta \in \mathbb{R}^{n_m \times (n_{\mathrm{CL}}+n_{\mathcal{R}})}$, $D_{\eta\zeta} \in \mathbb{R}^{n_m \times n_m}$, $D_{\eta\psi} \in \mathbb{R}^{n_m \times n_r}$, $C_z \in$

$\mathbb{R}^{n_z\times(n_{\mathrm{CL}}+n_{\mathcal{R}})}$, $D_{z\zeta}\in\mathbb{R}^{n_z\times n_m}$, $D_{z\psi}\in\mathbb{R}^{n_z\times n_r}$, $C_y\in\mathbb{R}^{n_y\times(n_{\mathrm{CL}}+n_{\mathcal{R}})}$, $D_{y\zeta}\in\mathbb{R}^{n_y\times n_m}$, $D_{y\psi}\in\mathbb{R}^{n_y\times n_r}$, $C_u\in\mathbb{R}^{n_u\times(n_{\mathrm{CL}}+n_{\mathcal{R}})}$, $D_{u\zeta}\in\mathbb{R}^{n_u\times n_m}$, $D_{u\psi}\in\mathbb{R}^{n_u\times n_r}$ via:

$$
\begin{aligned}
A &= \bar{A}+\underline{B}\Xi\underline{C}, \qquad B_\zeta=\bar{B}_\zeta \qquad B_\psi=\bar{B}_\psi+\underline{B}\Xi\underline{D}_\psi,\\
C_\eta &= \bar{C}_\eta+\underline{D}_\eta\Xi\underline{C}, \quad D_{\eta\zeta}=\bar{D}_{\eta\zeta}, \quad D_{\eta\psi}=\bar{D}_{\eta\psi}+\underline{D}_\eta\Xi\underline{D}_\psi\\
C_z &= \bar{C}_z+\underline{D}_z\Xi\underline{C}, \quad D_{z\zeta}=\bar{D}_{z\zeta}, \quad D_{z\psi}=\bar{D}_{z\psi}+\underline{D}_z\Xi\underline{D}_\psi \ .\\
C_y &= \bar{C}_y+\underline{D}_y\Xi\underline{C}, \quad D_{y\zeta}=\bar{D}_{y\zeta}, \quad D_{y\psi}=\bar{D}_{y\psi}+\underline{D}_y\Xi\underline{D}_\psi\\
C_u &= \bar{C}_u+\underline{D}_u\Xi\underline{C}, \quad D_{u\zeta}=\bar{D}_{u\zeta}, \quad D_{u\psi}=\bar{D}_{u\psi}+\underline{D}_u\Xi\underline{D}_\psi
\end{aligned}
\tag{6.26}
$$

$\triangleleft$

Note that the matrices constructed in Notation 6.25 , Step 4, are identical to the like named in Notation 4.1, Step 3.

1. Design of the remedial compensator

Using definitions in Notation 6.25 and 4.1, the following algorithm can be employed to obtain the remedial compensator such that the remedial closed-loop system guarantees quadratic robust unconstrained response recovery.

a. Anti-windup compensation

Algorithm 6.26 (Design of arbitrary-order dynamic anti-windup compensation with general external structure)

Step 1. Step 1 in Algorithm 5.7.

Step 2. Given n_Λ, find a solution $(X,Y,\bar{U},\bar{V},\tau)\in(\mathbb{R}^{n_{\mathrm{CL}}\times n_{\mathrm{CL}}},\mathbb{R}^{n_{\mathrm{CL}}\times n_{\mathrm{CL}}},\mathbb{D}^{n_u},\mathbb{D}^{n_{m_p}},\mathbb{R})$, with $\gamma>0$ as small as possible and $\tilde{\varrho}\geq 0$, to the LMI problem:

$$\text{Eqn. 5.18,} \tag{6.27a}$$

$$\text{rank}(X - Y) \leq n_\Lambda, \tag{6.27b}$$

Step 3. Select any scalar $\rho > 0$ and define the matrix:

$$\bar{U} = \rho W^{-1},$$

if $\bar{U}$ was not obtained from Step 2.

Step 4. Using the solution $(X, Y, \bar{U}, \bar{V}, \tau)$ from Step 2, define the $\bar{Q}_{12} \in \mathbb{R}^{n_{\text{CL}} \times n_\Lambda}$ as a solution of the following equation:

$$XY^{-1}X - X = \bar{Q}_{12}\bar{Q}_{12}^T.$$

define the matrix $\bar{Q}_{12} \in \mathbb{R}^{n_\Lambda \times n_\Lambda}$ as:

$$\bar{Q}_{22} = I_{n_\Lambda} + \bar{Q}_{12}^T X^{-1} \bar{Q}_{12}.$$

Define the matrix $\bar{Q} \in \mathbb{R}^{(n_{\text{CL}}+n_\mathcal{R}) \times (n_{\text{CL}}+n_\mathcal{R})}$ as:

$$\bar{Q} = \begin{bmatrix} X & \bar{Q}_{12} \\ \bar{Q}_{12}^T & \bar{Q}_{22} \end{bmatrix}.$$

Step 5. Using the matrices defined Notation 6.25 and Notation 4.1, define $m = n_{\text{CL}} + n_u + n_z + n_u + n_{m_p} + n_{m_n} + n_{m_n}$ and $\Psi \in \mathbb{R}^{m \times m}$,$\tilde{R} \in \mathbb{R}^{n_u \times m}$, and

$\tilde{P} \in \mathbb{R}^{m\times(n_{v_1}+n_{v_2})}$ via:

$$\Psi = \mathrm{He}\left[\begin{array}{ccccccc} \bar{A}\bar{Q} & \bar{B}_\psi\bar{U} & \bar{Q}\bar{C}_z^T & 0 & \bar{B}_{\zeta_p}\bar{V} & \tau\bar{B}_{\zeta_n} & \tilde{\varrho}\bar{Q}\bar{C}_{\eta_n}^T \\ -\bar{C}_u\bar{Q} & -\bar{D}_{u\psi}\bar{U}-\bar{U} & 0 & I_{n_u} & -\bar{D}_{u\zeta_p}\bar{V} & -\tau\bar{D}_{u\zeta_n} & 0 \\ 0 & \bar{D}_{z\psi}\bar{U} & -\frac{\gamma}{2}I_{n_z} & 0 & 0 & 0 & 0 \\ 0 & 0 & 0 & -\frac{\gamma}{2}I_{n_u} & 0 & 0 & 0 \\ \tilde{\varrho}\bar{C}_{\eta_p}\bar{Q} & 0 & \bar{V}\bar{D}_{z\zeta_p}^T & 0 & \tilde{\varrho}\bar{D}_{\eta_p\zeta_p}\bar{V}-\bar{V} & 0 & 0 \\ 0 & 0 & \tau\bar{D}_{z\zeta_n}^T & 0 & 0 & -\frac{\tau}{2}I_{n_{m_n}} & \tau\tilde{\varrho}\bar{D}_{\eta_n\zeta_n}^T \\ 0 & \tilde{\varrho}\bar{D}_{\eta_n\psi}\bar{U} & 0 & 0 & 0 & 0 & -\frac{\tau}{2}I_{n_{m_n}} \end{array}\right],$$

$$\tilde{P} = \left[\begin{array}{cccccc} \underline{B}^T & -\underline{D}_u^T & 0 & \underline{D}_z^T & \tilde{\varrho}\underline{D}_{\zeta_p}^T & 0 & \tilde{\varrho}\underline{D}_{\zeta_n}^T \end{array}\right]$$

$$\tilde{R} = \left[\begin{array}{ccccccc} \underline{C}\bar{Q} & \bar{U}\underline{D}_\psi & 0 & 0 & 0 & 0 & 0 \end{array}\right]$$

Step 6. Find a solution $(A_\Lambda, B_\Lambda, C_{\Lambda_1}, C_{\Lambda_2}, D_{\Lambda_1}, D_{\Lambda_2}) \in (\mathbb{R}^{n_\Lambda\times n_\Lambda}, \mathbb{R}^{n_\Lambda\times n_u}, \mathbb{R}^{n_{v_1}\times n_\Lambda}, \mathbb{R}^{n_{v_2}\times n_\Lambda}, \mathbb{R}^{n_{v_1}\times n_u}, \mathbb{R}^{n_{v_2}\times n_u})$ to the LMI problem:

$$\Psi + \tilde{P}^T\left[\begin{array}{cc} A_\Lambda & B_\Lambda \\ C_{\Lambda_1} & D_{\Lambda_1} \\ C_{\Lambda_2} & D_{\Lambda_2} \end{array}\right]\tilde{R} + \tilde{R}^T\left[\begin{array}{cc} A_\Lambda & B_\Lambda \\ C_{\Lambda_1} & D_{\Lambda_1} \\ C_{\Lambda_2} & D_{\Lambda_2} \end{array}\right]^T\tilde{P} < 0. \tag{6.28}$$

◁

Theorem 6.27 Let $W = W^T > 0$. There exists an arbitrary-order anti-windup compensator such that the anti-windup augmented closed-loop system guarantees quadratic robust unconstrained response recovery with performance level γ and $\tilde{\varrho} \geq 0$ if and only if there exists a feasible solution $(X, Y, \bar{U}, \bar{V}, \tau)$ to Eqn. 6.27. Moreover, given a feasible $(X, Y, \bar{U}, \bar{V}, \tau)$ to Eqn. 6.27, the steps in Algorithm 6.27 can be completed and the resulting n_Λ-order anti-windup compensator is such that the anti-windup augmented closed-loop system guarantees quadratic robust unconstrained response recovery with performance level γ.

Proof. Proof can be carried out as in Theorem 13.23 [56], but employing the mismatch system $\mathcal{W}^\Delta$ in Eqn. 4.6 which comprises an uncertain plant. First, *the existence part of the anti-windup compensator* is proved. For any $W = W^T > 0$ and

Lemma 6.24, anti-windup augmented closed-loop system guarantees quadratic robust unconstrained response recovery with performance level γ and $\tilde{\varrho} \geq 0$ if and only if there exists a solution $(\bar{Q}, \bar{U}, \bar{V}, \tau, A_\Lambda, B_\Lambda, C_{\Lambda_1}, C_{\Lambda_2}, D_{\Lambda_1}, D_{\Lambda_2})$ to the LMI problem in Eqn. 4.18 with $\bar{U} = \rho W^{-1}, \rho > 0$. Note that Eqn. 4.18d is equal to $\Psi + \tilde{P}^T \Xi \tilde{R} + \tilde{R}^T \Xi^T \tilde{P} < 0$, the latter defined according to Notation 6.25. Hence, there exists a suitable anti-windup compensator if and only if there exists a solution $(\bar{Q}, \bar{U}, \bar{V}, \tau, A_\Lambda, B_\Lambda, C_{\Lambda_1}, C_{\Lambda_2}, D_{\Lambda_1}, D_{\Lambda_2})$ that satisfies $\Psi + \tilde{P}^T \Xi \tilde{R} + \tilde{R}^T \Xi^T \tilde{P} < 0$, $\bar{Q} = \bar{Q}^T > 0$, $\bar{U} = \rho W^{-1}$ and $\rho > 0$. Note that Ψ depends on $\bar{Q}, \bar{U}, \bar{V}, \tau$. Using the elimination lemma [68], we are able to remove Ξ from the problem and reduce the problem to that of there exists a suitable anti-windup compensator if and only if there exists a solution $(\bar{Q}, \bar{U}, \bar{V}, \tau)$ that satisfies $N_{\tilde{P}}^T \Psi N_{\tilde{P}} < 0, N_{\tilde{R}}^T \Psi N_{\tilde{R}} < 0, \bar{U} = \rho W^{-1}$ and $\rho > 0$, where $N_{\tilde{P}}$ and $N_{\tilde{R}}$ are full column rank matrices that span the null space of $\tilde{P}$ and $\tilde{R}$ respectively. To complete this part of the proof , we work with $N_{\tilde{P}}^T \Psi N_{\tilde{P}} < 0$ and $N_{\tilde{R}}^T \Psi N_{\tilde{R}} < 0$ inequalities to show that these conditions are equivalent to the existence of a solution to Step 2 of Algorithm 6.26
($N_{\tilde{P}}^T \Psi N_{\tilde{P}} < 0$). Using Notations 4.1 and 6.25, $\tilde{P}$ can be constructed:

$$\tilde{P}^T = \begin{bmatrix} 0 & -B_{p,u}\Upsilon_g D_{g,v_1} & -B_{p,u}\Upsilon_g D_{g,v_2} \\ 0 & -B_{g,v_1} + B_{g,y} D_{p,yu} \Upsilon_g D_{g,v_1} & B_{g,y}\Upsilon_p D_{p,yu} D_{g,v_2} \\ I_{n_\Lambda} & 0 & 0 \\ 0 & -\Upsilon_g D_{g,v_1} & -\Upsilon_g D_{g,v_2} \\ 0 & 0 & 0 \\ 0 & -D_{p,zu}\Upsilon_g D_{g,v_1} & -D_{p,zu}\Upsilon_g D_{g,v_2} \\ 0 & -\tilde{\varrho} D_{p,\eta_p u}\Upsilon_g D_{g,v_1} & -\tilde{\varrho} D_{p,\eta_p u}\Upsilon_g D_{g,v_2} \\ 0 & 0 & 0 \\ 0 & -\tilde{\varrho} D_{p,\eta_n u}\Upsilon_g D_{g,v_1} & -\tilde{\varrho} D_{p,\eta_n u}\Upsilon_g D_{g,v_2} \end{bmatrix}.$$

Define $m = n_p + n_g + n_u + n_z + n_u + n_m$ and note that the n =rank($\tilde{P}$)=$n_\Lambda + n_{v_1} + n_{v_2}$, then the matrix that spans the null space of $\tilde{P}$, $N_{\tilde{P}} \in \mathbb{R}^{m \times (m-n)}$. With $\tilde{P}$ explicitly defined as above, one can attempt to obtain directly a matrix whose columns form the bases of the null space of $\tilde{P}$. This was successfully done previously due to the

special configurations employed [21, 27], however, for the general architecture for anti-windup compensation, this is not possible. To define a matrix that spans the null space of $\tilde{P}$, the most we can do is try to take advantage of what is known and group the unknowns in one single matrix. This is detailed in the following. Rearranging the columns of the matrix $\tilde{P}$ through the following transformation matrix T:

$$\tilde{P} = \tilde{P}_o \underbrace{\begin{bmatrix} I_{n_p+n_g} & 0 & 0 & 0 & 0 & 0 \\ 0 & 0 & I_{n_u} & 0 & 0 & 0 \\ 0 & 0 & 0 & 0 & I_{n_z} & 0 \\ 0 & I_{n_\Lambda} & 0 & 0 & 0 & 0 \\ 0 & 0 & 0 & I_{n_u} & 0 & 0 \\ 0 & 0 & 0 & 0 & 0 & I_{n_m} \end{bmatrix}}_{T},$$

permits to rewrite $N_{\tilde{P}}^T \Psi N_{\tilde{P}} < 0$ as indicated below:

$$N_{\tilde{P}}^T \Psi N_{\tilde{P}} = N_{\tilde{P}}^T T^T \underbrace{T^{-T} \Psi T^{-1}}_{\bar{\Psi}} \underbrace{T N_{\tilde{P}}}_{N_{\tilde{P}_o}} = N_{\tilde{P}_o}^T \bar{\Psi} N_{\tilde{P}_o} < 0,$$

where the null space of $\tilde{P}_o$ can be the image of:

$$N_{\tilde{P}_o} = \begin{bmatrix} \tilde{L} & 0 & 0 \\ 0 & 0 & 0 \\ 0 & I_{n_u} & 0 \\ 0 & 0 & I_{n_m} \end{bmatrix},$$

with $\tilde{L}_\perp \in \mathbb{R}^{(m-n_\Lambda-n_u-n_m)\times(m-n-n_u-n_m)}$ being any matrix that spans the null space of $\tilde{L}^T$:

$$\tilde{L}^T = \begin{bmatrix} D_{g,v_1}^T \Upsilon_g^T B_{p,u}^T & B_{g,v_1}^T - D_{g,v_1}^T \Upsilon_g^T D_{p,yu}^T B_{g,y}^T & -D_{g,v_1}^T \Upsilon_g^T & D_{g,v_1}^T \Upsilon_g^T D_{p,zu}^T \\ D_{g,v_2}^T \Upsilon_g^T B_{p,u}^T & -D_{g,v_2}^T \Upsilon_g^T D_{p,yu}^T B_{g,y}^T & -D_{g,v_2}^T \Upsilon_g^T & D_{g,v_2}^T \Upsilon_g^T D_{p,zu}^T \end{bmatrix}.$$

Additionally, assuming $\bar{Q} = \begin{bmatrix} X & \bar{Q}_{12} \\ \bar{Q}_{12}^T & \bar{Q}_{22} \end{bmatrix}$ where $X \in \mathbb{R}^{n_{\mathrm{CL}} \times n_{\mathrm{CL}}}$, $\bar{Q}_{12} \in \mathbb{R}^{n_{\mathrm{CL}} \times n_\Lambda}$ and $\bar{Q}_{22} \in \mathbb{R}^{n_\Lambda \times n_{\mathrm{CL}}}$, then $N_{\tilde{P}}^T \Psi N_{\tilde{P}}$ if and only if:

$$N_{\tilde{P}}^T \Psi N_{\tilde{P}} = \mathrm{He}$$
$$\bar{L}^T \begin{bmatrix} A_{\mathrm{CL}} X & B_{\mathrm{CL},\psi}\bar{U} & 0 & 0 & \tilde{\varrho} X C_{\mathrm{CL},\eta_p}^T & \tau B_{\mathrm{CL},\zeta_n} & 0 \\ -C_{\mathrm{CL},u} X & -\bar{U} - D_{\mathrm{CL},u\psi}\bar{U} & 0 & I_{n_u} & -D_{\mathrm{CL},u\zeta_p}\bar{V} & -\tau D_{\mathrm{CL},u\zeta_n} & 0 \\ C_{\mathrm{CL},z} X & D_{\mathrm{CL},z\psi}\bar{U} & -\frac{\gamma}{2} I_{n_z} & 0 & D_{\mathrm{CL},z\zeta_p}\bar{V} & \tau D_{\mathrm{CL},z\zeta_n} & 0 \\ 0 & 0 & 0 & -\frac{\gamma}{2} I_{n_u} & 0 & 0 & 0 \\ \bar{V} B_{\mathrm{CL},\zeta_p}^T & \tilde{\varrho} D_{\mathrm{CL},\eta_p\psi}\bar{U} & 0 & 0 & -\bar{V} + \tilde{\varrho} D_{\mathrm{CL},\eta_p\zeta_p}\bar{V} & 0 & 0 \\ 0 & 0 & 0 & 0 & 0 & -\frac{\tau}{2} I_{n_{m_n}} & 0 \\ \tilde{\varrho} C_{\mathrm{CL},\eta_n} X & \tilde{\varrho} D_{\mathrm{CL},\eta_n\psi}\bar{U} & 0 & 0 & 0 & \tau\tilde{\varrho} D_{\mathrm{CL},\eta_n\zeta_n} & -\frac{\tau}{2} I_{n_{m_n}} \end{bmatrix} \bar{L} < 0,$$

where $\bar{L} = \mathrm{diag}[\tilde{L}_\perp, I_{n_u}, I_{n_m}]$.

($N_{\tilde{R}}^T \Psi N_{\tilde{R}} < 0$) Note that $\tilde{R} = \tilde{R}_o \bar{T}$, where $\tilde{R}_o = \begin{bmatrix} \underline{C} & \underline{D}_\psi & 0 & 0 \\ 0 & 0 & 0 & \end{bmatrix}$ and $\bar{T} = \mathrm{diag}[\bar{Q}, \bar{U}, I_{n_u}, I_{n_z}, I_{n_m}]$, where $\bar{T}$ is invertible, then one can write $N_{\tilde{R}}^T \Psi N_{\tilde{R}} < 0$ as:

$$N_{\tilde{R}}^T \Psi N_{\tilde{R}} = N_{\tilde{R}}^T \bar{T} \underbrace{\bar{T}^{-1} \Psi \bar{T}^{-1}}_{\bar{\Psi}} \underbrace{\bar{T} N_{\tilde{R}}}_{N_{\tilde{R}_o}} = N_{\tilde{R}_o}^T \bar{\Psi} N_{\tilde{R}_o} < 0,$$

where a matrix that spans the null space of $\tilde{R}_o$ is given by $N_{\tilde{R}_o}$. If $P = \bar{Q}^{-1}$ and $W = \rho \bar{U}^{-1}$, then:

$$\bar{\Psi} = \mathrm{He} \begin{bmatrix} P\bar{A} & P\bar{B}_\psi & \bar{C}_z^T & 0 & P\bar{B}_{\zeta_p}\bar{V} & \tau P\bar{B}_{\zeta_n} & \tilde{\varrho}\bar{C}_{\eta_n}^T \\ -\bar{C}_u & -W\bar{D}_{u\psi} - W & 0 & W I_{n_u} & -\bar{D}_{u\zeta_p}\bar{V} & -\tau\bar{D}_{u\zeta_n} & 0 \\ 0 & \bar{D}_{z\psi} & -\frac{\gamma}{2} I_{n_z} & 0 & 0 & 0 & 0 \\ 0 & 0 & 0 & -\frac{\gamma}{2} I_{n_u} & 0 & 0 & 0 \\ \tilde{\varrho}\bar{C}_{\eta_p} & 0 & \bar{V}\bar{D}_{z\zeta_p}^T & 0 & \tilde{\varrho} D_{\eta_p\zeta_p}\bar{V} - \bar{V} & 0 & 0 \\ 0 & 0 & \tau\bar{D}_{z\zeta_n}^T & 0 & 0 & -\frac{\tau}{2} I_{n_{m_n}} & \tau\tilde{\varrho}\bar{D}_{\eta_n\zeta_n}^T \\ 0 & \tilde{\varrho}\bar{D}_{\eta_n\psi} & 0 & 0 & 0 & 0 & -\frac{\tau}{2} I_{n_{m_n}} \end{bmatrix}$$

and:

$$\tilde{R}_o = \begin{bmatrix} 0 & 0 & I_{n_\Lambda} & 0 & 0 & 0 & 0 & 0 & 0 \\ 0 & 0 & 0 & I_{n_u} & 0 & 0 & 0 & 0 & 0 \end{bmatrix},$$

thus a matrix that spans the null space of $\tilde{R}_o$ is $N_{\tilde{R}_o} \in \mathbb{R}^{m\times(m-n_u-n_\Lambda)}$ is:

$$N_{\tilde{R}_o} = \begin{bmatrix} I_{n_p} & 0 & 0 & 0 & 0 & 0 & 0 \\ 0 & I_{n_g} & 0 & 0 & 0 & 0 & 0 \\ 0 & 0 & 0 & 0 & I_{n_u} & 0 & 0 \\ 0 & 0 & 0 & 0 & 0 & I_{n_z} & 0 \\ 0 & 0 & 0 & 0 & 0 & 0 & I_{n_m} \end{bmatrix}^T .$$

If $P = \begin{bmatrix} \tilde{Y} & \tilde{Y}_2 \\ \tilde{Y}_2^T & \tilde{Y}_3 \end{bmatrix}$, where $\tilde{Y} \in \mathbb{R}^{n_{\mathrm{CL}}\times n_{\mathrm{CL}}}$, $\tilde{Y}_2 \in \mathbb{R}^{n_{\mathrm{CL}}\times n_\Lambda}$, $\tilde{Y}_3 \in \mathbb{R}^{n_\Lambda\times n_\Lambda}$ and $M = \mathrm{diag}[Y, I_{n_u}, I_{n_z}, I_{n_m}]$, where $Y = \tilde{Y}^{-1}$ then

$$M^T N_{\tilde{R}}^T \Psi N_{\tilde{R}} M = M^T N_{\tilde{R}_o}^T \bar{\Psi} N_{\tilde{R}_o} M =$$

$$\mathrm{He}\begin{bmatrix} A_{\mathrm{CL}}Y & 0 & YC_{\mathrm{CL},z}^T & \tilde{\varrho}YC_{\mathrm{CL},\eta_p}^T & \tau B_{\mathrm{CL},\zeta_n} & \tilde{\varrho}YC_{\mathrm{CL},\eta_n}^T \\ 0 & -\frac{\gamma}{2}I_{n_u} & 0 & 0 & 0 & 0 \\ 0 & 0 & -\frac{\gamma}{2}I_{n_z} & 0 & 0 & 0 \\ \bar{V}B_{\mathrm{CL},\zeta_p}^T & 0 & D_{\mathrm{CL},z\zeta_p}^T & \tilde{\varrho}D_{\mathrm{CL},\eta_p\zeta_p}^T\bar{V} - \bar{V} & 0 & 0 \\ 0 & 0 & \tau D_{\mathrm{CL},z\zeta_n}^T & 0 & -\frac{\tau}{2}I_{n_m} & \tilde{\varrho}D_{\mathrm{CL},\eta_n\zeta_n}^T \\ 0 & 0 & 0 & 0 & 0 & -\frac{\tau}{2}I_{n_m} \end{bmatrix} < 0$$

(Step 2). Given X and $\tilde{Y}^{-1} = Y$, we wish to find conditions such that a $\bar{Q} = \bar{Q}^T > 0$, $\bar{Q} = \begin{bmatrix} X & \bar{Q}_{12} \\ \bar{Q}_{12}^T & \bar{Q}_{22} \end{bmatrix}$ and $\bar{Q}^{-1} = \begin{bmatrix} \tilde{Y} & \tilde{Y}_2 \\ \tilde{Y}_2^T & \tilde{Y}_3 \end{bmatrix}$. Lemma 6 [68] shows that a $\bar{Q}$ exists if and only if there exist $X = X^T > 0$, $Y = Y^T > 0$, $X - Y \geq 0$ and $\mathrm{rank}(X-Y) \leq n_\Lambda$. Thus, there exists an anti-windup compensator such that the anti-windup augmented closed-loop system guarantees quadratic robust unconstrained response recovery performance level γ and $\tilde{\varrho} \geq 0$ if and only if there exists a solution $(X, Y, \bar{U}, \bar{V}, \tau)$ to Eqn. 6.27.

To complete the other part of the proof, *the algorithm is successful*. Given the solution $(X, Y, \bar{U}, \bar{V}, \tau)$ to Eqn. 6.27. Steps 3 and 4 are constructive, then the resulting X, Y are such that $X = X^T$, $Y = Y^T$, $X - Y \geq 0$ and $\mathrm{rank}(X - Y) \leq n_\Lambda$. Thus,, there

exists a $\bar{Q}_{12}$ such that $\bar{Q}_{12}\bar{Q}_{12}^T = XY^{-1}X - X$ and $\bar{Q}_{22} = I_{n_\Lambda} + \bar{Q}_{12}^T X^{-1}\bar{Q}_{12}$ can be constructed. Then, Lemma 6 [68] can be employed for:

$$\bar{Q}^{-1} = \begin{bmatrix} X & \bar{Q}_{12} \\ \bar{Q}_{12}^T & \bar{Q}_{22} \end{bmatrix} = \begin{bmatrix} Y & ? \\ ? & ? \end{bmatrix}$$

With $\bar{Q}$ and $\bar{U}$ selected, then Ψ, $\tilde{P}$ and $\tilde{R}$ can be constructed as detailed in Step 5, and there exists a solution to the LMI at Step 6. This conclude our proof. $\lhd$

From Theorem 6.27 and its proof, the functions used in the algorithm for anti-windup compensation can be given.

$[\Psi, \tilde{R}, \tilde{P}] = V_{n_\Lambda\text{-dynamic}}(\mathcal{P}^\Delta, \mathcal{G}_\mathcal{M}, X, Y, \bar{U}, \bar{V}, \tau, \gamma)$.

Construct the matrices $\Psi, \tilde{R}, \tilde{P}$ from Step 3 in Algorithm 6.26.

$[\Psi, \tilde{R}, \tilde{P}] = V_{n_p\text{-dynamic}}(\mathcal{P}^\Delta, \mathcal{G}_\mathcal{M}, X, Y, \bar{U}, \bar{V}, \tau, \gamma)$.

Construct the matrices $\Psi, \tilde{R}, \tilde{P}$ from Step 3 in Algorithm 6.26, with $n_\Lambda = n_p$.

$[\Psi, \tilde{R}, \tilde{P}] = V_{\text{static}}(\mathcal{P}^\Delta, \mathcal{G}_\mathcal{M}, X, \bar{U}, \bar{V}, \tau, \gamma)$.

Construct the matrices $\Psi, \tilde{R}, \tilde{P}$ from Step 3 in Algorithm 6.26 with $n_\Lambda = 0$.

b. Override compensation

Algorithm 6.28 (Design of arbitrary-order dynamic override compensation with GOC for controller states/input)

Step 1. Given n_Θ, find a solution $(X, Y, \bar{U}, \bar{V}, \tau, \pi) \in (\mathbb{R}^{n_{\text{CL}} \times n_{\text{CL}}}, \mathbb{R}^{n_{\text{CL}} \times n_{\text{CL}}}, \mathbb{D}^{n_z}, \mathbb{D}^{n_{m_p}}, \mathbb{R}, \mathbb{R})$, with $\gamma > 0$ as small as possible and $\tilde{\varrho} \geq 0$, to the LMI problem:

$$\text{Eqn. 5.34}, \tag{6.29a}$$

$$\text{rank}(X - Y) \leq n_\Theta, \tag{6.29b}$$

Step 2. Using the solution $(X, Y, \bar{U}, \bar{V}, \tau)$ from Step 2, define the $\bar{Q}_{12} \in \mathbb{R}^{n_{\mathrm{CL}} \times n_\Theta}$ as a solution of the following equation:

$$XY^{-1}X - X = \bar{Q}_{12}\bar{Q}_{12}^T.$$

define the matrix $\bar{Q}_{12} \in \mathbb{R}^{n_\Theta \times n_\Theta}$ as:

$$\bar{Q}_{22} = I_{n_\Theta} + \bar{Q}_{12}^T X^{-1} \bar{Q}_{12}.$$

Define the matrix $\bar{Q} \in \mathbb{R}^{(n_{\mathrm{CL}}+n_{\mathcal{R}}) \times (n_{\mathrm{CL}}+n_{\mathcal{R}})}$ as:

$$\bar{Q} = \begin{bmatrix} X & \bar{Q}_{12} \\ \bar{Q}_{12}^T & \bar{Q}_{22} \end{bmatrix}.$$

Step 3. Using the matrices defined Notation 6.25 and Notation 4.1, define $m = n_{\mathrm{CL}} + n_z + n_z + n_u + n_{m_p} + n_{m_n} + n_{m_n}$ and $\Psi \in \mathbb{R}^{m \times m}$, $\tilde{R} \in \mathbb{R}^{n_z \times m}$, and $\tilde{P} \in \mathbb{R}^{m \times (n_v)}$ via:

$$\Psi = \mathrm{He}\begin{bmatrix}
\bar{A}\bar{Q} & -\bar{B}_\psi\bar{U} & 0 & 0 & -\bar{B}_\psi & \bar{B}_{\zeta_p}\bar{V} & 0 & \tilde{\varrho}\bar{Q}\bar{C}_{\eta_n}^T \\
-\bar{C}_z\bar{Q} & -\bar{U}-\bar{D}_{z\psi}\bar{U} & 0 & 0 & \bar{D}_{z\psi} & -\bar{D}_{z\zeta_p}\bar{V} & 0 & -\tilde{\varrho}\bar{U}\bar{D}_{\eta_n\psi}^T \\
W_y\bar{C}_y\bar{Q} & -W_y\bar{D}_{y\psi}\bar{U} & -\frac{\gamma}{2}I_{n_y} & 0 & -W_y\bar{D}_{y\psi} & W_y\bar{D}_{y\zeta_p}\bar{V} & \tau W_y\bar{D}_{y\zeta_n} & 0 \\
W_z\bar{C}_z\bar{Q} & -W_z\bar{D}_{z\psi}\bar{U} & 0 & -\frac{\gamma}{2}I_{n_z} & -W_z\bar{D}_{z\psi} & W_z\bar{D}_{z\zeta_p}\bar{V} & \tau\bar{D}_{z\zeta_n} & 0 \\
0 & 0 & 0 & -W_o^T W_z^T & -\frac{\gamma}{2}I_{n_z} & -\bar{D}_{\eta_p\psi}^T & 0 & \tilde{\varrho}\bar{D}_{\eta_n\psi}^T \\
\tilde{\varrho}\bar{C}_{\eta_p}\bar{Q} & -\tilde{\varrho}\bar{D}_{\eta_p\psi}\bar{U} & 0 & 0 & -\bar{D}_{\eta_p\psi} & -\bar{V}+\tilde{\varrho}\bar{D}_{\eta_p\zeta_p}\bar{V} & 0 & 0 \\
\tau\bar{B}_{\zeta_n}^T & -\tau\bar{D}_{z\zeta_n}^T & 0 & 0 & 0 & 0 & -\frac{\tau}{2}I_{n_{m_n}} & 0 \\
0 & 0 & 0 & 0 & 0 & 0 & \tau\tilde{\varrho}\bar{D}_{\eta_n\zeta_n} & -\frac{\tau}{2}I_{n_{m_n}}
\end{bmatrix},$$

$$\tilde{P} = \begin{bmatrix} \underline{B}^T & -\underline{D}_z^T & 0 & \underline{D}_y^T W_y^T & \underline{D}_z^T W_z^T & \tilde{\varrho}\underline{D}_{\zeta_p}^T & 0 & \tilde{\varrho}\underline{D}_{\zeta_n}^T \end{bmatrix}$$

$$\tilde{R} = \begin{bmatrix} \underline{C}\bar{Q} & -\bar{U}\underline{D}_\psi & \underline{D}_\psi & 0 & 0 & 0 & 0 & 0 \end{bmatrix}$$

Step 4. Find a solution $(A_\Theta, B_\Theta, C_{\Theta_1}, C_{\Theta_2}, D_{\Theta_1}, D_{\Theta_2}) \in (\mathbb{R}^{n_\Theta \times n_\Theta}, \mathbb{R}^{n_\Theta \times n_u},$

$\mathbb{R}^{n_{v_1}\times n_\Theta}, \mathbb{R}^{n_{v_2}\times n_\Theta}, \mathbb{R}^{n_{v_1}\times n_u}, \mathbb{R}^{n_{v_2}\times n_u}$) to the LMI problem:

$$\Psi + \tilde{P}^T \begin{bmatrix} A_\Theta & B_\Theta \\ C_{\Theta_1} & D_{\Theta_1} \\ C_{\Theta_2} & D_{\Theta_2} \end{bmatrix} \tilde{R} + \tilde{R}^T \begin{bmatrix} A_\Theta & B_\Theta \\ C_{\Theta_1} & D_{\Theta_1} \\ C_{\Theta_2} & D_{\Theta_2} \end{bmatrix}^T \tilde{P} < 0. \tag{6.30}$$

◁

Theorem 6.29 Let $W = W^T > 0$. There exists an override compensator (GOC for controller state/input) such that the override augmented closed-loop system guarantees quadratic robust unconstrained response recovery with performance level γ and $\tilde{\varrho} \geq 0$ if and only if there exists a feasible solution $(X, Y, \bar{U}, \bar{V}, \tau)$ to Eqn. 6.29. Moreover, given a feasible $(X, Y, \bar{U}, \bar{V}, \tau)$ to Eqn. 6.29, the steps in Algorithm 6.28 can be completed and the resulting override compensator is such that the override augmented closed-loop system guarantees quadratic robust unconstrained response recovery with performance level γ.

Proof. This theorem can be proved following the ideas in Theorem 6.27.

D. Example: mass-spring-damper system

In this part, remedial compensation techniques are applied to the uncertain mass-spring damper system. The results show that the remedial compensation schemes, considered in this dissertation, are capable of improving the performance over the constrained closed-loop responses, for the anti-windup case, and over the unconstrained closed-loop responses, for the override case.

1. The uncertain plant and the unconstrained controller

The mass-spring-damper system has its dynamics governed by the following equations of motion:

$$\begin{aligned} \cdot x_p &= \begin{bmatrix} 0 & 1 \\ -k/m & -f/m \end{bmatrix} x_p + \begin{bmatrix} 0 \\ 1/m \end{bmatrix} u \\ z &= \begin{bmatrix} 1 & 0 \end{bmatrix} x_p \text{ performance output for anti-windup compensation} \\ z &= \begin{bmatrix} 0 & 1 \end{bmatrix} x_p \text{ performance output for override compensation} \\ y &= \begin{bmatrix} 1 & 0 \end{bmatrix} x_p \end{aligned}, \quad (6.31)$$

where $x_p = [q, \dot{q}]^T$ represent the position and velocity of the body attached to the spring. Moreover, m represents the mass of the body, k is the elastic constant of the spring and f is the damping factor. The system is considered to be subjected to external forces such as u and w, u usually corresponds to the actuation of the controller on the mass and w is an exogenous input. To make the system more realistic, we will consider that the values of the parameter are not precisely known, but are believed to lie in known intervals. In particular, the actual mass m, elastic constant k and damping factor f are within 10% of their corresponding nominal values, m_o, k_o and f_o. We choose the following nominal parameter values:

$$m_o = 0.1\text{kg}, \;\; k_o = 1\frac{kg}{s}, \;\; f_o = 0.005\frac{kg}{s}. \quad (6.32)$$

Assuming the w is an exogenous reference input corresponding to the desired mass position, the following linear unconstrained controller has been designed:

$$u = C_{fb}(s)(C_{ff}(s)w - y), \quad (6.33)$$

with:

$$C_{fb}(s) = 200\frac{(s+5)^2}{s(s+80)}, \;\; C_{ff}(s) = \frac{5}{s+5}. \tag{6.34}$$

Note that this controller was designed to provide a fast response with zero steady-state error to step references change, robust to parametric uncertainties.

2. Robust anti-windup design

a. Unconstrained closed-loop responses

The response of the unconstrained closed-loop system, with zero initial conditions, resulting from an input reference that switches between ± 0.9 meters every five seconds and going back to zero permanently after 10 seconds, is shown in Fig. 32. Observe that what seems to be a thick line is in fact the response of a family of plants generated by randomly selecting parameter values within the intervals previously described. The plant input has peaks of 8N for the first and third step changes, and of 16N for the biggest step change that occurs after 5 seconds. Note that the peaks are almost similar for all the plant cases.

b. Input constrained responses

When the actuator output, in this case the exerted force u, is limited to lie within the interval $[-1, +1]$N, the closed-loop response of the plant family corresponds to the dotted lines in Fig. 33. To show the degradation with respect to the unconstrained responses, the latter are also shown with solid lines, Notably, the plant family responses converge to a limit cycle and present persistent oscillating responses, each one with a different peak.

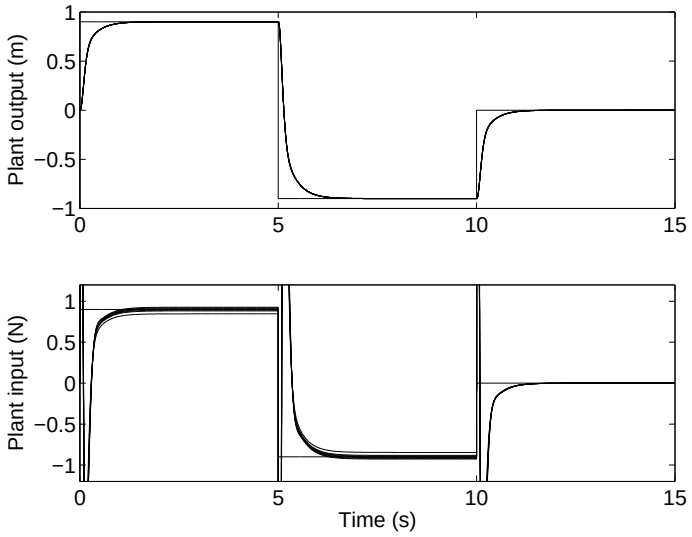

Fig. 32. The response of the unconstrained uncertain mass-spring-damper system.

c. Anti-windup design

For the anti-windup design, the full-authority anti-windup augmentation is chosen as the configuration scheme. Furthermore, the corresponding synthesis algorithms for static and dynamic anti-windup compensation, presented in Chapter V, are applied.

Static anti-windup design was not possible due to the infeasibility of the LMI conditions in Assumption 5.2. However a plant-order anti-windup design was successful. An observation of our design is that the prefilter dynamics was embedded in the unconstrained controller dynamics before employing Algorithm 5.7 for the synthesis of the full-authority anti-windup compensator[1]. The unconstrained response recovery gain obtained for this compensator is 63.3, exactly the same value as the $\mathcal{H}_\infty$ norm of the open-loop system from the plant input u to the performance output z. Note that the performance output considered for the anti-windup compensation is the position

[1]As an aside comment, the inclusion of the prefilter dynamics resulted in an anti-windup compensator with better closed-loop responses than one not including the prefilter dynamics, recall the discussion in the mismatch insights section, Chapter III.

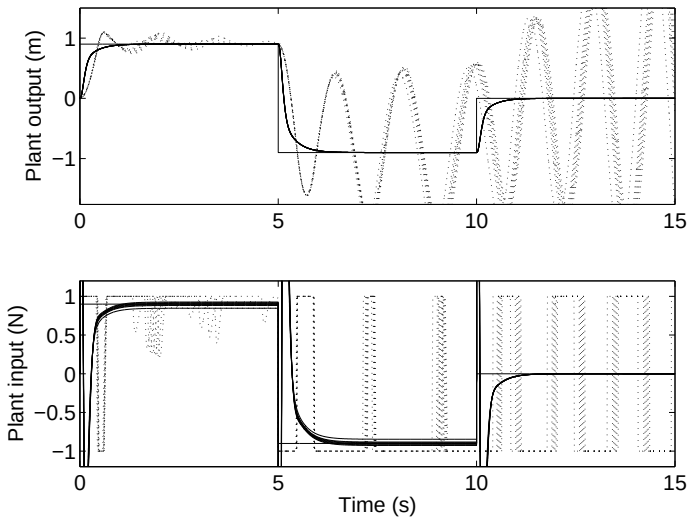

Fig. 33. The response of the input constrained uncertain mass-spring-damper system (dotted lines).

of the mass q.

The resulting anti-windup augmented closed-loop trajectories are shown in Fig. 34. The trajectories present relative improvement with respect to the input constrained closed-loop trajectories presented in Fig. 33, and this occurs for all plant cases randomly considered.

3. Nominal override design

a. Unconstrained closed-loop responses

The system is the mass-spring-damper, however, only the nominal plant case will be considered. We select the velocity of the mass $\dot{q}$ as the performance output, constrained to lie within the interval $[-2, +2]\frac{m}{s}$. Moreover, another design objective will be that of keeping the plant output q as close as possible to the corresponding unconstrained closed-loop plant response. The unconstrained controller is the one previously described.

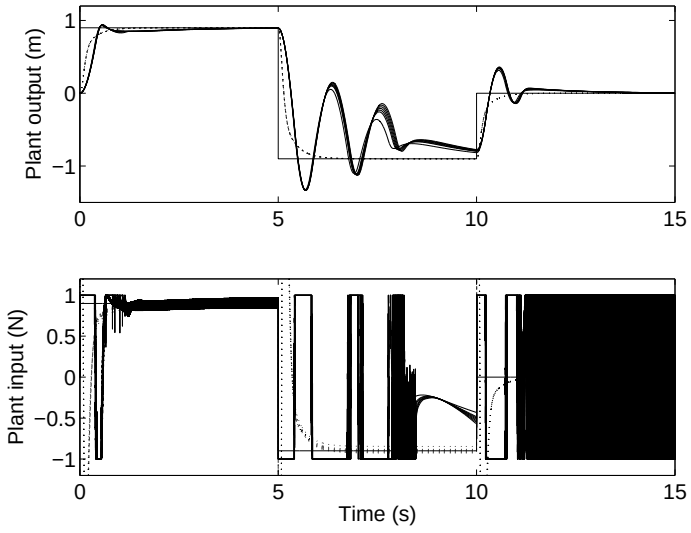

Fig. 34. Plant-order full-authority anti-windup augmented closed-loop system response of the uncertain mass-spring-damper system (solid lines).

Figure 35 shows the unconstrained closed-loop responses of the system with a thick solid line. These responses are caused by the same exogenous reference considered in the anti-windup design part. We observe that the performance output overpasses the limits $[-2, +2]\frac{m}{s}$ during the step changes, hence override compensation will be designed to act at these time intervals. Note that a consideration during the design is that system actuation will be able to provide the required control effort such that the override goal is achieved.

b. Output constrained responses and override design

An static override compensator is first designed according to Algorithm 5.4 and its equivalent representation for performance analysis described in Algorithm 4.5. The proof of Theorem 6.29 further relates these two algorithms. The override closed-loop trajectories obtained with this compensator are shown in Fig, 36. The solid thin lines in the plant responses correspond to the ideal output constrained responses, namely

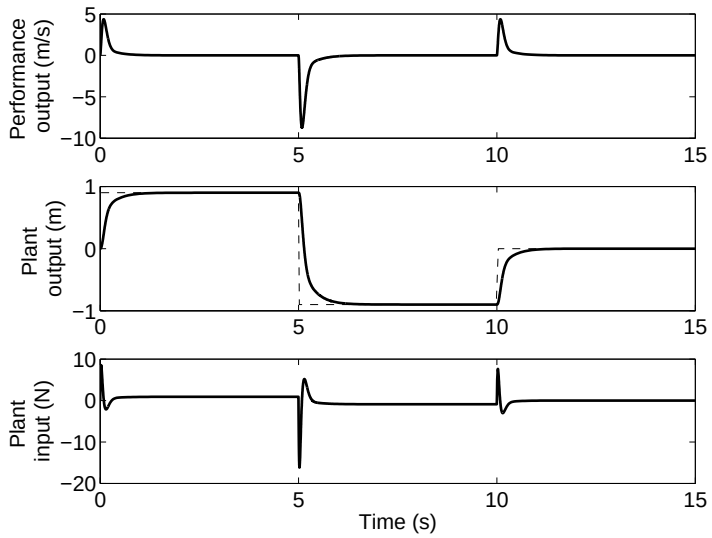

Fig. 35. The response of the unconstrained nominal mass-spring-damper system. Performance output is velocity, $\cdot x$, and plant output is amplitude x.

the saturated version of the unconstrained performance output and the unconstrained plant output. The thick solid lines depict the closed-loop responses when override control is employed. Notably, during steps changes, the performance output stays within the bounds with an error of $\pm 2\%$. Additionally, note the dependency between plant output and performance output. With the performance output $\dot{q}$ limited in amplitude, the plant output q is also limited, but in slope. Then, by removing this constrain on the plant output, we are left with a good match of the unconstrained responses. The plant input responses for the override closed-loop system show the high demand on the actuation of the system.

A plant-order override design was also attempted by following the steps in Algorithm 5.12, however, the resulting compensator had very high poles, making the implementation difficult.

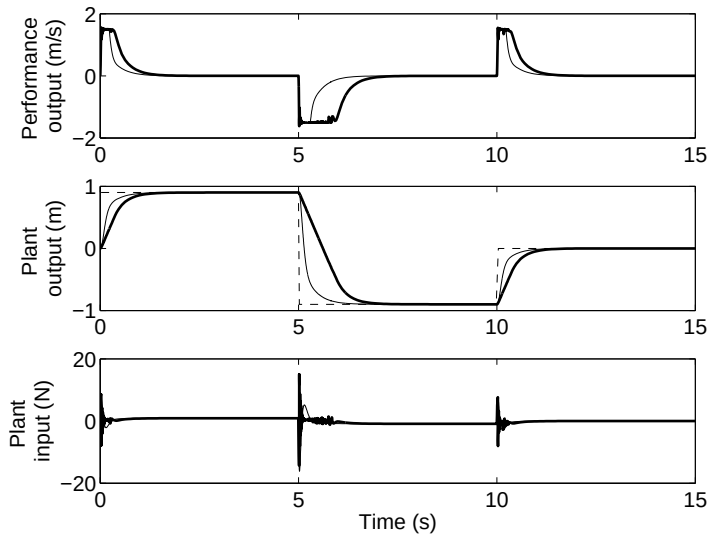

Fig. 36. The response of the output constrained nominal mass-spring-damper system and the response of the override closed-loop system.

CHAPTER VII

MULTIDIMENSIONAL POSITIONING SYSTEM (MPS)

The Multidimensional Positioning System (MPS) has been designed and assembled in the Mechatronics Laboratory at Texas A&M University for inhouse research in multi-degree-of-freedom positioning of a single magnetically levitated moving part (platen) at micro and nano scales. The working principle of the MPS is a linear motor capable of providing forces for both suspension and translation without contact. Reference [69] and references therein give a detail description of the facility.

Positional control for the MPS consists of six degree-of-freedom (DOF) control of the platen in the presence of external disturbances, model uncertainties and constraints. The platen has attached three windings (coils) on its bottom surface and is levitated above a two-dimensional superimposed concentrated-field magnet matrix (stator). The platen is modeled as a rigid body. The motion of a rigid body undergoing six DOF is nonlinear, hence a linear, time invariant motion about an equilibrium point is considered. Linear control design methods are then used based on the linearized model without considering the presence of constraints. This linear control design is the first step towards a second design that will take into account the constraints and which will attempt to employ the anti-windup/override techniques described in previous chapters.

This chapter is organized as follows: A description of the analytical model, and the sensing and actuation systems is first presented. Model based controllers with and without uncertainty considerations are then designed. For the controllers that incorporate an uncertainty description in the design, approximate uncertainty bounds are obtained. After a failed attempt in the implementation of the robust controllers, improved uncertainty characterizations are urged. Not only identification of the MPS

is considered, but also description of the uncertainty using model validation ideas is presented. Finally, it would be ideal to employ the synthesis algorithms presented in Chapter V to construct remedial compensation for this system, however, further theory is required as the MPS is not an asymptotically stable system.

A. MPS model

Figure 37 depicts the MPS formed by the stator and the platen. On the stator, there is attached a two-dimensional superimposed concentrated-field magnet matrix. On the bottom surface of the platen are attached the windings (coils) that energize the actuation of the system. The currents pass through the coils and generate forces and torques in the center of mass of the platen due to the interaction between the current distribution and the magnet array [70]. Subsequently, the platen has six DOF, namely three displacements and three rotations. More specifically, the currents in the coils flow in the orthogonally interwoven multi-phase η_1 and η_2 windings generating air gap magnetic field traveling in the η_1 and η_2 directions, respectively. These η_1 and η_2 coil currents interact only with the corresponding η_1 and η_2 magnet array components, thus generating horizontal translation. The current distribution and equal magnetic poles of the magnet array create a repulsive force that lifts the platen against gravity, thus generating vertical translation. The motors (I and II) drive the platen in the η_2 direction, and the third motor (III), in the η_1 direction. Rotational motion is generated as the repulsion forces in the η_3 direction and horizontal forces do not pass through the center of mass of the platen. To avoid thermal problems the platen is suspended by air bearings. The air bearings are modeled as three linear springs and the platen is modeled as a rigid body. A set of orthogonal (b_1, b_2, b_3) body fixed axes defines the motion of the platen with respect to the inertial frame (stator) whereas a

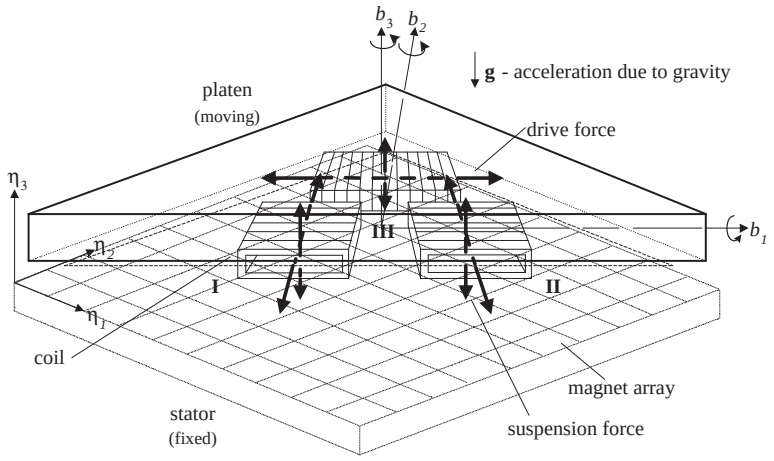

Fig. 37. 6 DOF positioner.

(η_1, η_2, η_3) coordinate system is fixed to the stator.

1. Nonlinear model

Let the unitary vectors $\hat{b}_i$ and $\hat{\eta}_i$ denote the body and inertial coordinates which are initially assumed to be collinear. Defining the following variables: angular velocity vector of the platen with respect to body frame $\vec{\omega} = \sum_{i=1}^{3} \omega_i \hat{b}_i$, linear centroid velocity vector $\vec{v} = \sum_{i=1}^{3} v_i \hat{\eta}_i$, linear position vector of centroid relative to inertial frame $\vec{x} = \sum_{i=1}^{3} x_i \hat{\eta}_i$, angular position vector of centroid with respect to inertial frame $\vec{\beta} = \sum_{i=1}^{3} \beta_i \hat{\eta}_i$, magnetic force vector acting on the centroid of each coil attached to the platen $\vec{F}_j = \sum_{i=1}^{3} F_{ji} \hat{b}_i \; j = [\mathrm{I}, \mathrm{II}, \mathrm{III}]$, disturbance force vector acting on the platen centroid excluding any magnetic force $\vec{F}_d = \sum_{i=1}^{3} F_{di} \hat{\eta}_i$, magnetic torque vector about the platen centroid $\vec{\tau} = \sum_{i=1}^{3} \tau_i \hat{b}_i = \sum_{j=1}^{\mathrm{III}} \vec{r}_j \times \vec{F}_j$, and disturbance torque vector acting on

the platen centroid excluding any magnetic torque $\vec{\tau}_d = \sum_{i=1}^{3} \tau_{di}\hat{\eta}_i$. Let $\vec{r}_j$ $j = [\mathrm{I}, \mathrm{II}, \mathrm{III}]$ denote the position of each coil centroid with respect to the platen centroid.

The relation between the inertial and body coordinates is given by the Euler angles, where $\hat{b} = E\hat{\eta}$ and E is a matrix transformation for a 3, 2, 1 (that is, η_3, η_2, η_1) rotation sequence.

The inertia tensor of the platen is defined as $\underline{I}$, where $\underline{I}_{ij}$ $(i, j = [1, 2, 3])$, is an entry of the inertia tensor. The physical parameters, m, k_{x_3}, k_{β_1}, k_{β_2} and g, denote the mass of the platen, linear spring constant, rotational spring constants and acceleration of the gravity, respectively. The spring constants are generated by the air bearings action. The nonlinear equations of motion for the platen suspended by the magnetic forces and the air bearings are given as follows:

$$\begin{bmatrix} \dot{\omega}_1 \\ \dot{\omega}_2 \\ \dot{\omega}_3 \end{bmatrix} = -\begin{bmatrix} \underline{I}^i_{11} & \underline{I}^i_{12} & \underline{I}^i_{13} \\ \underline{I}^i_{21} & \underline{I}^i_{22} & \underline{I}^i_{23} \\ \underline{I}^i_{31} & \underline{I}^i_{32} & \underline{I}^i_{33} \end{bmatrix} \left\{ \begin{bmatrix} k_{\beta_1} & 0 & 0 \\ 0 & k_{\beta_2} & 0 \\ 0 & 0 & 0 \end{bmatrix} \begin{bmatrix} \beta_1 \\ \beta_2 \\ \beta_3 \end{bmatrix} + \begin{bmatrix} 0 & -\omega_3 & \omega_2 \\ \omega_3 & 0 & -\omega_1 \\ -\omega_2 & \omega_1 & 0 \end{bmatrix} \begin{bmatrix} \underline{I}_{11} & \underline{I}_{12} & \underline{I}_{13} \\ \underline{I}_{21} & \underline{I}_{22} & \underline{I}_{23} \\ \underline{I}_{31} & \underline{I}_{32} & \underline{I}_{33} \end{bmatrix} \begin{bmatrix} \omega_1 \\ \omega_2 \\ \omega_3 \end{bmatrix} - \begin{bmatrix} \tau_1 \\ \tau_2 \\ \tau_3 \end{bmatrix} - E^T \begin{bmatrix} \tau_{d1} \\ \tau_{d2} \\ \tau_{d3} \end{bmatrix} \right\}, \tag{7.1}$$

$$\begin{bmatrix} \dot{\beta}_1 \\ \dot{\beta}_2 \\ \dot{\beta}_3 \end{bmatrix} = E^T \begin{bmatrix} \omega_1 \\ \omega_2 \\ \omega_3 \end{bmatrix}, \tag{7.2}$$

$$\begin{bmatrix} \dot{v}_1 \\ \dot{v}_2 \\ \dot{v}_3 \end{bmatrix} = -\frac{1}{m} \left\{ \begin{bmatrix} 0 & 0 & 0 \\ 0 & 0 & 0 \\ 0 & 0 & k_{x_3} \end{bmatrix} \begin{bmatrix} x_1 \\ x_2 \\ x_3 \end{bmatrix} + \begin{bmatrix} 0 \\ 0 \\ g \end{bmatrix} - E^T \begin{bmatrix} F_1 \\ F_2 \\ F_3 \end{bmatrix} - \begin{bmatrix} F_{d1} \\ F_{d2} \\ F_{d3} \end{bmatrix} \right\}, \tag{7.3}$$

$$\begin{bmatrix} \dot{x}_1 \\ \dot{x}_2 \\ \dot{x}_3 \end{bmatrix} = \begin{bmatrix} v_1 \\ v_2 \\ v_3 \end{bmatrix}, \tag{7.4}$$

where $\underline{I}^i_{ij}$ denotes the ij-th element of the inverse of the inertia tensor.

The magnetic forces $\vec{F}_j$ $j = [\mathrm{I}, \mathrm{II}, \mathrm{III}]$ (related to each coil) depend on the instantaneous centroid location of the platen, $\vec{x} = [x_1, x_2, x_3]^T$, and the current applied to the coils:

$$\begin{bmatrix} i_{Aj} \\ i_{Bj} \\ i_{Cj} \end{bmatrix} = \frac{2\mathbf{e}^{\gamma_1 x_3}}{\mu_o M_o \eta_o N_m G} \begin{bmatrix} 1 & 0 \\ \frac{1}{2} & \frac{\sqrt{3}}{2} \\ -\frac{1}{2} & \frac{\sqrt{3}}{2} \end{bmatrix} \mathbf{e}^{-\gamma_1 x_i \mathrm{J}} \begin{bmatrix} F_{j3} \\ F_{ji} \end{bmatrix}, \tag{7.5}$$

where i_A, i_B and i_C are the three phase currents and $\mathbf{e}^{\gamma_1 x_i \mathrm{J}}$ is a transformation matrix given by:

$$\mathbf{e}^{\gamma_1 x_i \mathrm{J}} = \begin{bmatrix} \cos\gamma_1 x_i & \sin\gamma_1 x_i \\ -\sin\gamma_1 x_i & \cos\gamma_1 x_i \end{bmatrix}, \tag{7.6}$$

with $i = [1, 2]$. The magnet remanence is $\mu_o M_o$, the winding turn density is η_o, the number of active pitches is N_m, the pitch is l, the fundamental wave number is $\gamma_1 = \frac{2\pi}{l}$ and the nominal air gap is x_{3o}. See Table I in Appendix for the mechanical and electromagnetic parameter values of the MPS.

For simplicity, the quadrature and direct currents i_q and i_d can also be considered for analysis and synthesis of the controllers. The relation between the quadrature/direct current and the phase currents is given by:

$$\begin{bmatrix} i_{Aj} \\ i_{Bj} \\ i_{Cj} \end{bmatrix} = \begin{bmatrix} 1 & 0 \\ \frac{1}{2} & \frac{\sqrt{3}}{2} \\ -\frac{1}{2} & \frac{\sqrt{3}}{2} \end{bmatrix} \mathbf{e}^{-\gamma_1 x_i \mathrm{J}} \begin{bmatrix} i_{dj} \\ i_{qj} \end{bmatrix}, \tag{7.7}$$

where $j = [\mathrm{I}, \mathrm{II}, \mathrm{III}]$.

The $\mathbb{R}^{12\times1}$ state vector is formed by the linear and rotational positions and the corresponding velocities:

$$\vec{\zeta} = \begin{bmatrix} \omega_1 & \omega_2 & \omega_3 & \beta_1 & \beta_2 & \beta_3 & v_1 & v_2 & v_3 & x_1 & x_2 & x_3 \end{bmatrix}^T. \tag{7.8}$$

The external disturbance vector incorporates the disturbance forces and torques:

$$\vec{q} = \begin{bmatrix} \begin{bmatrix} \tau_{d1} & \tau_{d2} & \tau_{d3} \end{bmatrix} E\frac{1}{\underline{I}^T} & O_{1\times3} & \frac{F_{d1}}{m} & \frac{F_{d2}}{m} & \frac{F_{d3}}{m} & O_{1\times3} \end{bmatrix}^T. \tag{7.9}$$

The control input vector may include the magnetic torques and forces acting on the platen centroid or the direct and quadrature currents in each coil:

$$\vec{u} = \begin{bmatrix} \tau_1 & \tau_2 & \tau_3 & F_1 & F_2 & F_3 \end{bmatrix}^T. \tag{7.10}$$

$$\vec{i} = \begin{bmatrix} i_{q\mathrm{I}} & i_{q\mathrm{II}} & i_{q\mathrm{III}} & i_{d\mathrm{I}} & i_{d\mathrm{II}} & i_{d\mathrm{III}} \end{bmatrix}^T. \tag{7.11}$$

Finally, the equation of motion is nonlinear and can be written as:

$$\dot{\vec{\zeta}} = g(\vec{\zeta}, \vec{u}) + \vec{q} = f(\vec{\zeta}, \vec{i}) + \vec{q}, \tag{7.12}$$

where $f(\vec{\zeta}, \vec{u})$ and $g(\vec{\zeta}, \vec{i})$ capture Eqns. 7.1 to 7.7 and 7.1 to 7.4, respectively.

2. Perturbed motion about equilibrium

Consider the following equilibrium state vector:

$$\vec{\zeta_o} = \begin{bmatrix} 0 & 0 & 0 & 0 & 0 & 0 & 0 & 0 & 0 & 0 & 0 & 2.324\text{mm} \end{bmatrix}^T. \tag{7.13}$$

This equilibrium state corresponds to the body frame being collinear with the inertial frame with zero angular and translational velocities (the air bearings are off).

Considering the perturbed motion:

$$\vec{\zeta} = \vec{\zeta_o} + \delta\vec{\zeta}, \quad \vec{u} = \vec{u}_o + \delta\vec{u}, \quad \vec{i} = \vec{i}_o + \delta\vec{i}, \tag{7.14}$$

the linearized equation about $\vec{\zeta}_o$ is given by:

$$\delta\dot{\vec{\zeta}} = A\,\delta\vec{\zeta} + B_u\delta\vec{u} = A\,\delta\vec{\zeta} + B_i\delta\vec{i}, \tag{7.15}$$

where:

$$A = \begin{bmatrix} & \begin{bmatrix} -\underline{I}^i_{11}k_{\beta_1} & -\underline{I}^i_{12}k_{\beta_2} & 0 \\ -\underline{I}^i_{21}k_{\beta_1} & -\underline{I}^i_{22}k_{\beta_2} & 0 \\ -\underline{I}^i_{31}k_{\beta_1} & -\underline{I}^i_{32}k_{\beta_2} & 0 \end{bmatrix} & & \\ O_{3\times3} & & O_{3\times3} & O_{3\times3} \\ I_{3\times3} & O_{3\times3} & O_{3\times3} & O_{3\times3} \\ & & & \begin{bmatrix} 0 & 0 & 0 \\ 0 & 0 & 0 \\ 0 & 0 & -\dfrac{k_{x_3}}{m} \end{bmatrix} \\ O_{3\times3} & O_{3\times3} & O_{3\times3} & \\ O_{3\times3} & O_{3\times3} & I_{3\times3} & O_{3\times3} \end{bmatrix}, \tag{7.16}$$

$$B_u = \begin{bmatrix} \begin{bmatrix} \underline{I}^i_{11} & \underline{I}^i_{12} & \underline{I}^i_{13} \\ \underline{I}^i_{21} & \underline{I}^i_{22} & \underline{I}^i_{23} \\ \underline{I}^i_{31} & \underline{I}^i_{32} & \underline{I}^i_{33} \end{bmatrix} & O_{3\times3} \\ O_{3\times3} & O_{3\times3} \\ O_{3\times3} & \dfrac{1}{m}I_{3\times3} \\ O_{3\times3} & O_{3\times3} \end{bmatrix}, \tag{7.17}$$

$$B_i = k_D \begin{bmatrix} \begin{bmatrix} \underline{I}^i_{11} & \underline{I}^i_{12} & \underline{I}^i_{13} \\ \underline{I}^i_{21} & \underline{I}^i_{22} & \underline{I}^i_{23} \\ \underline{I}^i_{31} & \underline{I}^i_{32} & \underline{I}^i_{33} \end{bmatrix} \times \begin{bmatrix} [-r_{\mathrm{I}3}] & [-r_{\mathrm{II}3}] & 0 & r_{\mathrm{I}2} & r_{\mathrm{II}2} & r_{\mathrm{III}2} \\ 0 & 0 & [r_{\mathrm{III}3}] & -r_{\mathrm{I}1} & -r_{\mathrm{II}1} & -r_{\mathrm{III}1} \\ r_{\mathrm{I}1} & r_{\mathrm{II}1} & -r_{\mathrm{III}2} & 0 & 0 & 0 \end{bmatrix} \\ O_{3\times 6} \\ \frac{1}{m} \begin{bmatrix} 0 & 0 & 1 & 0 & 0 & 0 \\ 1 & 1 & 0 & 0 & 0 & 0 \\ 0 & 0 & 0 & 1 & 1 & 1 \end{bmatrix} \\ O_{3\times 6} \end{bmatrix}, \tag{7.18}$$

with $k_D = \frac{1}{2}\mu_o M_o \eta_o N_m G \mathbf{e}^{-\gamma_1 x_{3_o}}$.

The quantities in brackets represent the interaction between the horizontal forces F_i $i = [1, 2]$ and the torques τ_j $j = [2, 1]$ respectively, due to offset between the platen and coils centroids.

From simple inspection, it can be concluded that the open loop system at the equilibrium state is unstable (double integrator because the platen was modeled as a rigid body). Furthermore, it can be shown that all states are controllable from the magnetic torques and forces, and from the direct and quadrature coil currents.

Considering the values of the parameters of the system, shown in Table I, the non-zero eigenvalues and corresponding eigenvectors can be calculated and the results are presented in Table II in the Appendix part. From Table II, it can be seen that three non-zero fundamental modes occur. Two of the modes (modes 1, 2) involve rotations about the η_1 and η_2 axes, the remaining one (mode 3) involves motion along the η_3 axis. Physically, these modes result from the interactions between the platen and the air bearings. Modes 1 and 2, which are oscillatory modes, are related to the terms k_{β_i} $i = [1, 2]$; k_{β_1} (k_{β_2}) initiates a positive rotation in the η_1 axis and a positive (negative) rotation in the η_2 axis after a negative (positive) η_3 displacement.

Mode 3, which is also a oscillatory mode, is related to the term k_{x_3}.

3. Sensing and actuation

Nine physical variables can be indirectly measured, they are the translational velocities, the translational displacements and the rotations of the platen centroid.

For small angles, the rotation and displacements are actually perturbed rotations and displacements around the equilibrium state. The vector of physical variables sensed, denoted as $\vec{y}$, is related to the states as:

$$\vec{y} = C\,\delta\vec{\zeta}, \tag{7.19}$$

where:

$$C = \begin{bmatrix} O_{3\times3} & I_{3\times3} & O_{6\times3} \\ O_{6\times3} & O_{6\times3} & I_{6\times6} \end{bmatrix}. \tag{7.20}$$

In laboratory, the actual measured outputs, denoted by y', are voltages and relative displacements, which are sensed using optical displacement sensors and laser interferometers, respectively. The optical displacement sensors relate voltages to the vertical displacement in η_3 axis and rotations about the η_1 and η_2 axes. The laser interferometers relate the relative displacements to the horizontal displacements/velocities (η_1 and η_2 axes) and rotation/angular velocity about the η_3 axis. Then it follows:

$$\vec{y}' = [p2s]\,\vec{y}, \tag{7.21}$$

where $[p2s]$ is a matrix transformation.

In the case of the laser interferometers, three lasers axes board working with the corresponding receivers give relative position information with 0.6 nm resolution for a plane mirror system. The position data is updated at rate of 10MHz and the axis board provides velocity data up to 1 $\frac{\mathrm{m}}{\mathrm{s}}$. The laser interferometer arrangement is

described in Fig. 38.

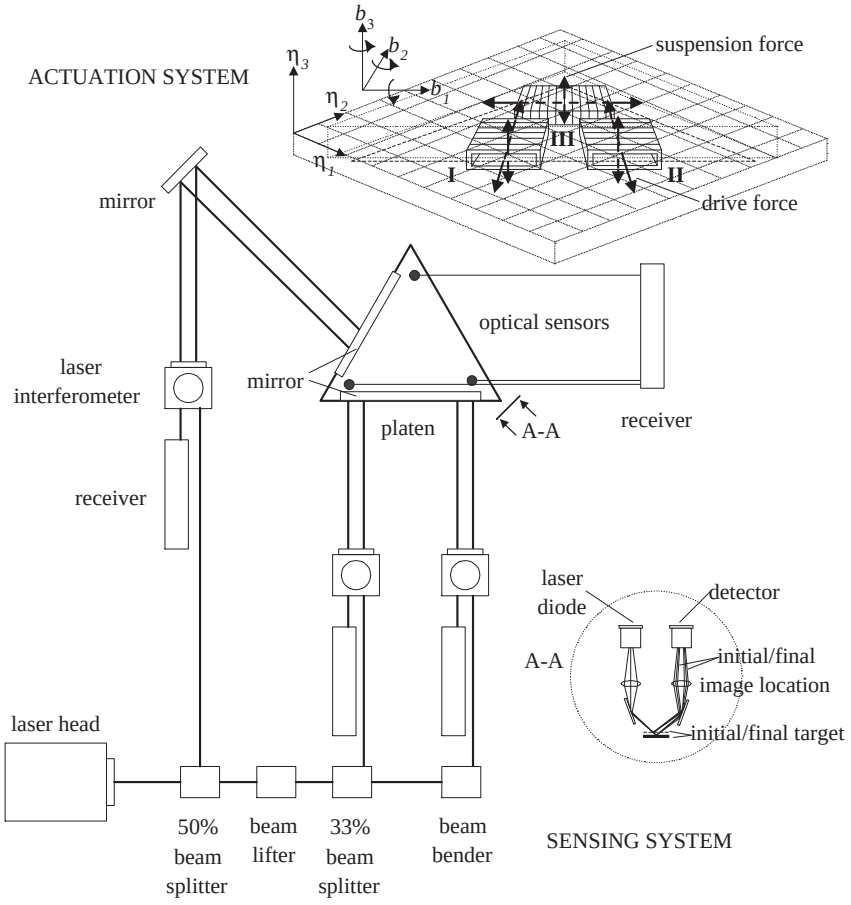

Fig. 38. Sensing and actuation systems.

In the case of the optical sensors, three non-contact ultra precision optical displacement sensors are employed to obtain three measurement channels. The optical sensors have 100μm of measurement range and a resolution of 15 nm. A clock is also used to synchronize the measurements. See Fig. 38.

Figure 39 shows the input and output block diagram of the MPS plant. The input consists of three currents (i_A, i_B and i_C related to i_d and i_q by the matrix transformation T) going into the three coils and the measured outputs involve three voltages and six relative displacements. In short, the current into the coils generates

a magnetic field which interacts with the magnet array and produces a net force and torque on the suspended platen, see Fig. 39. The resulting motion of the platen can be divided into horizontal (unstable) and vertical (stable) motion. The horizontal motion involves displacements in the η_1 and η_2 axes and rotation about the η_3 axis. The vertical motion consists of rotation about the η_1 and η_2 axes and displacement in the η_3 axis. The horizontal motion is sensed by the laser interferometers that give out relative displacement information and the vertical motion is sensed by the optical sensors that produce output voltage signals.

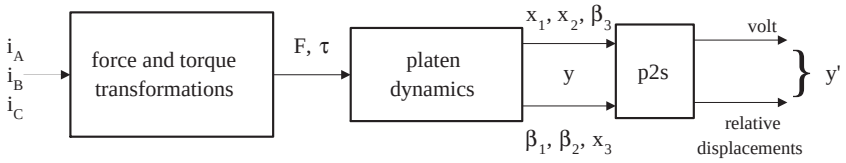

Fig. 39. Open loop block diagram.

B. Model based control of the MPS. A comparison of controller designs with experimental validation

The present study investigates the controlled behavior of the MPS, under the application of model based control techniques (lead-lag, LQR, LQG, LQG-LTR, $\mathcal{H}_\infty$, μ-synthesis and QFT). Particular attention is given to the design, analysis and simulation of the control laws that guarantee tracking performance under modeled uncertainties. Closed-loop identification is used to derive bounds of the variations in magnitude of the experimental data and mathematical models. Results obtained from numerical simulations are presented and judged with respect to the performance and stability achieved and the work needed to perform the designs. Laboratory experiments indicate partial success in the implementation of the designed control systems.

Hence, limited experimental results are presented to validate the performance of the control systems.

The control systems are to be designed such that the MPS tracks simultaneous position and rotation commands for all the six DOF. Similar command following and disturbance rejection specifications in the frequency and time domain are posed for all designs. For design purposes only $\mathcal{H}_\infty$, μ-synthesis and QFT control techniques explicitly incorporate the system uncertainty in the controller design. This uncertainty ideally accounts for the system dynamics not captured in the analytical model.

Using numerical simulations the merits of each controller are analyzed based on the quality of the control system in nominal operation (tracking, disturbance rejection and stability) and under the inclusion of uncertainty (performance and stability robustness) via $\mathcal{H}_\infty$ (μ) constraints on certain frequency weighted transfer matrices. The effort involved in the controller design is also considered (note that no tuning is permitted). From the laboratory experiments shown, a comparison is performed in terms of the agreement, or lack thereof, between simulations and experimental results.

The remainder of this section is organized as follows. The validation of the analytical model is performed first. This validation through comparison with the identified models permits the definition of the uncertainty models. The main differences among the control design approaches are also explained. Following, the numerical results are presented along with limited experimental results. The latter verifies that control objectives are achievable. Finally, the results are discussed and further necessary work is proposed.

1. Model validation and identification of the MPS

System identification is required to verify that the analytical model is valid for controller design. Open loop tests cannot be performed due to the unstable nature of the MPS. Subsequently, identification of the experimental system is carried on the closed loop system with a lead-lag (decentralized) controller under the consideration that the linear model is decoupled. Due to the diagonal dominance of the inertia tensor (see Table I), the linear model corresponding to forces and torques as control inputs can be decoupled and subsequently a decentralized single-input single-output (SISO) control system design is feasible. The joint input-output approach [71] was used for each DOF of the closed-loop. The input test signal, r reference, consisted of a zero mean, white noise random signal with standard deviation of 0.01 and 0.05μm for the horizontal and vertical motion, respectively. The total time of the excitation signal is 2s at a 5kHz sampling rate. Observing the frequency response, Fig. 40, significant mismatch between the analytical and experimental models is apparent, especially at low and high frequencies. The mismatch at low frequencies is likely because the excitation signals did not contain much energy over that frequency range. At high frequencies the mismatch is due to the unmodeled dynamics. Notably, for the horizontal motion, the experimental models present resonances at around 90Hz.

a. Uncertainty model

The uncertainty models are determined by the discrepancy between the derived, simple analytical uncoupled model and the experimental model, with the analytical coupled model serving as the nominal model for controller design. Knowing that for systems such as the MPS the main source of errors are the high frequency dynamics, additive uncertainty models are constructed as shown in Fig. 40. These high

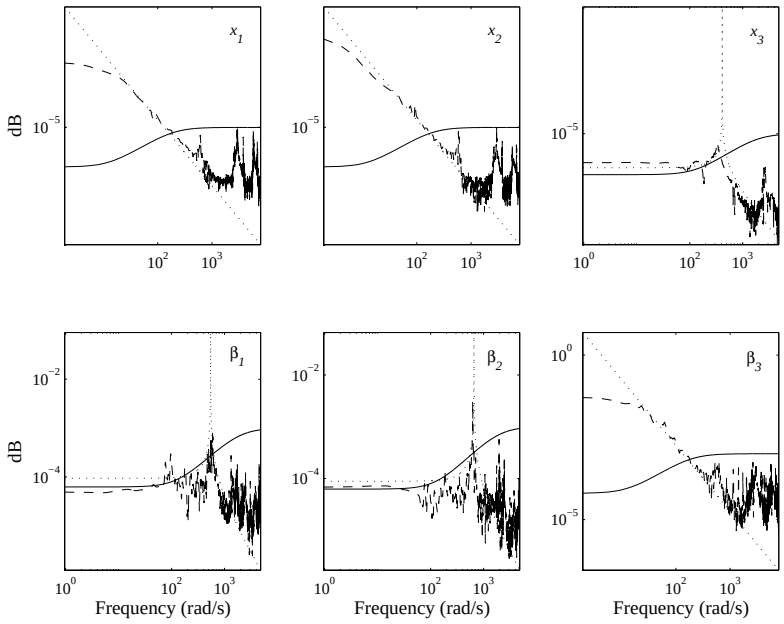

Fig. 40. Comparison of the analytical model (dotted) and the identified model (dashed). Additive uncertainty model (solid line).

frequency dynamics may be caused by nonlinearities, mechanical-electrical couplings and environmental noises. At low frequencies uncertainty is not that important since high gain will be employed at those frequencies. Figure 41 shows the closed-loop system where the uncertainty model maps force and torque inputs to physical outputs.

2. Unconstrained controller design

The main objective of the control systems is to stabilize the platen dynamics and track[1] a command signal about the equilibrium state with 2% steady state error. The challenging aspect of the design is to guarantee a specific tracking performance in spite of imperfect knowledge of the experimental system while accommodating the physical limitations (sampling, etc). The controllers are also designed to attenuate disturbances in the low frequency band from 0 to 30Hz and to have less than 30%

[1]An implicit performance requirement is disturbance rejection of constant inputs.

overshoot with a rise time (to within 80% of the final value) of less than 0.1s for a step change in the reference input, for all axes. For planar movement, the dynamic performance objectives include hundreds of millimeters traveling with a maximum speed capability of 1 $\frac{\mathrm{m}}{\mathrm{s}}$.

In LQG-LTR [72], lead-lag [73], LQR [74] and LQG [74] designs, zero steady state error for step inputs is achieved by inserting an integrating action. In the lead-lag design, the SISO diagonal controller elements are designed independently and have a phase margin of 40^o. The total order of the controller is 12 and the loop bandwidth is 30Hz and 140Hz for the horizontal and vertical motion, respectively. For the LQR and LQG designs, information available from the experimental models is used to choose the weighting matrices. The total order of the LQG-LTR controller for each motion is 12 (horizontal and vertical), the loop bandwidth is 30Hz for the horizontal motion and 100Hz for the vertical one. For the $\mathcal{H}_\infty$ and μ-synthesis designs [8], the uncertainty model is explicitly incorporated in the design. The order of the controllers is reduced to 15, at most, for each motion. The loop bandwidth is 30Hz for the horizontal motion and 110Hz for the vertical one. In the QFT design [75] (two DOF design) the prefilter is designed to enforce closed-loop tracking requirements, increasing the order of the controller. The total order of the QFT controller is 36.

3. Numerical simulation and experimental validation

This section presents the numerical simulations of the controlled MPS response and limited experimental results[2]. The quality of the controllers is analyzed in both the frequency and time domain.

[2]All the results and simulations are computed using the Control, μ-synthesis and QFT Matlab Toolboxes.

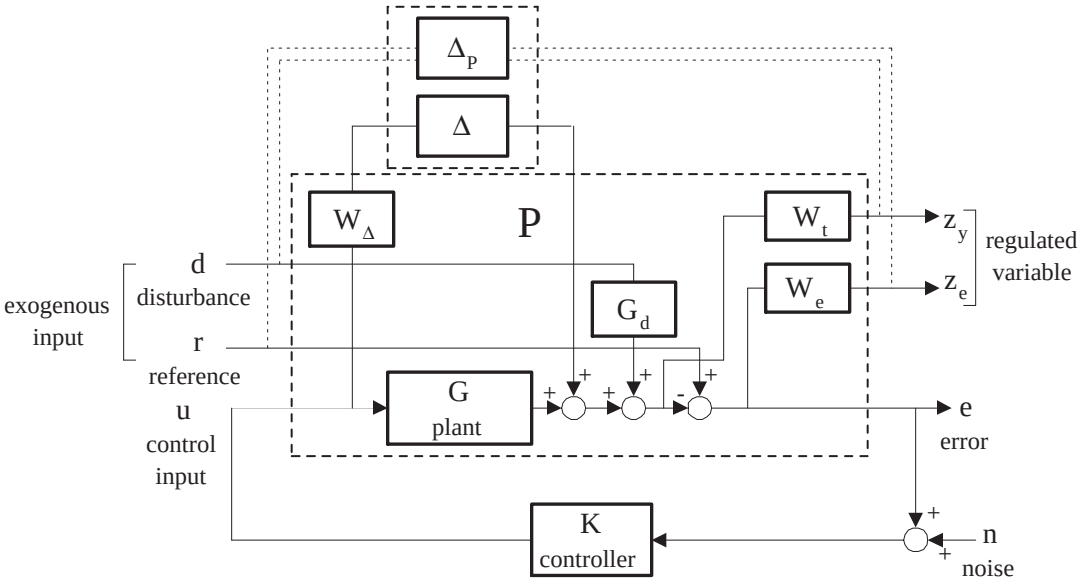

Fig. 41. Closed loop system for comparison.

a. Numerical simulations comparison

In this section we compare the properties of the designed control systems. Notably, there does not exist a general method to compare the designed control systems. However, the use of the $\mathcal{H}_\infty$ norm or μ scalar of the frequency weighted transfer functions, as it is done in the $\mathcal{H}_\infty$ and μ-synthesis designs, proved to be useful for comparing the performance and stability of the designs. In the following, the $\mathcal{H}_\infty$ norm and μ scalar are employed to facilitate comparison and all conclusions are given with respect to the values of the norms (or scalars) associated to the weighted transfer functions, see Fig. 41. The weighting functions employed for the $\mathcal{H}_\infty$ and μ-synthesis designs are also used when comparing the designs.

Frequency domain response

Nominal performance, robust stability and robust performance are investigated.

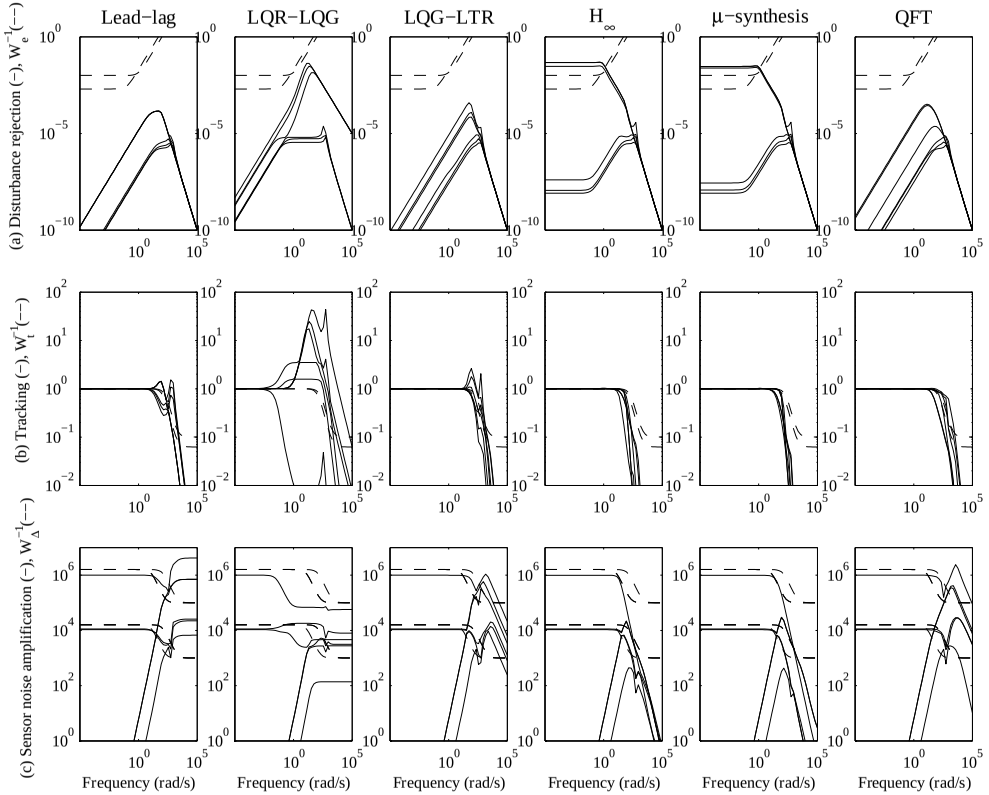

Fig. 42. Singular values (Δ=0): (a) disturbance rejection, (b) tracking and (c) sensor noise amplification.

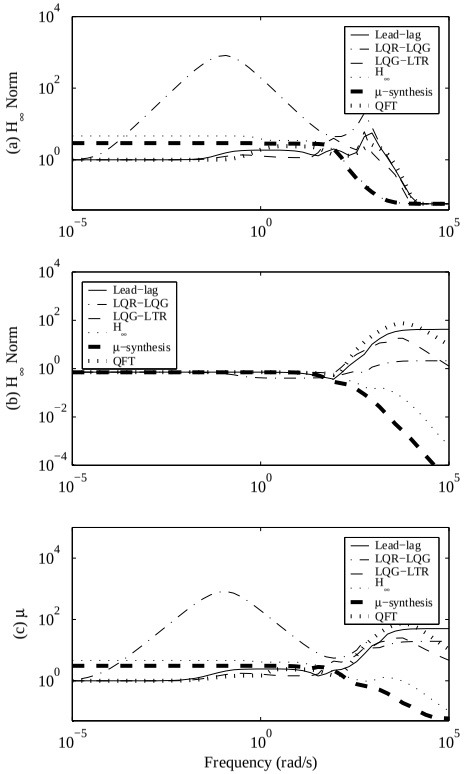

Fig. 43. (a) Nominal performance, (b) robust stability and (c) robust performance.

Nominal performance (NP) The requirements for NP ($\Delta = 0$) are $\|W_e S G_d\|_\infty \leq 1$, for disturbance rejection, and $\|W_t T\|_\infty \leq 1$, for reference tracking. S and T are the sensitivity and complementary sensitivity function, respectively.

From Fig. 42(a) all controllers present good disturbance rejection properties, except for $\mathcal{H}_\infty$ and μ-synthesis controllers which violate the disturbance rejection condition at very low frequencies. While minor in the case of QFT, aside from $\mathcal{H}_\infty$ and μ-synthesis, the other controllers violate the tracking condition (see Fig. 42(b)).

Figure 43(a) shows that no controller presents an $\mathcal{H}_\infty$ norm smaller than one for the NP weighted transfer matrix. This is not surprising as previous plots (Fig. 42(a)-(b)) show that none of the controllers satisfy both performance conditions simultaneously. The worst performance is presented by the LQR-LQG controller that possesses the highest peaks for tracking. The violation of the disturbance rejection by the $\mathcal{H}_\infty$ and μ-synthesis controllers is shown at low frequencies where the $\mathcal{H}_\infty$ norms are 4.5 and 3.0, respectively. For the other controllers, good tracking of signals at low frequencies ($\mathcal{H}_\infty$ norm about 1) and degraded behavior near the crossover frequencies ($\mathcal{H}_\infty$ norm increased by a factor of up to 5) can be seen in the plot. The peaks at intermediate frequencies reflect the peaks the controllers present for tracking. Among the controllers, the QFT controller achieves the best NP.

Robust stability (RS) The consideration of additive uncertainty enforces the condition $\|W_\Delta K S\|_\infty \leq 1$ for RS.

Figure 43(b) shows that only the $\mathcal{H}_\infty$ and μ-synthesis controllers achieve RS. This is to be expected as these controllers were designed considering the weighted uncertainty model. For the $\mathcal{H}_\infty$ and μ-synthesis controllers, the weighted sensor noise amplification matrix, $W_\Delta K S$, present a peak of 0.7. This implies that for diagonal perturbations smaller than $\frac{1}{0.7}$ the closed-loop system remains stable. For the other

controllers it can be said that they are more sensitive to diagonal perturbations. Specifically, the closed-loop system for the QFT controller becomes unstable for the smallest diagonal perturbations. The LQR-LQG controller, which presented the worst NP, has better RS properties than the other controllers, except for the $\mathcal{H}_\infty$ and μ-synthesis controllers. In particular, the RS condition is violated by all the controllers, except $\mathcal{H}_\infty$ and μ-synthesis in the high frequency region. This also can be visualized in Fig. 42(c) where at high frequencies the singular values of KS are not below the inverse of W_Δ.

Robust performance (RP) The closed-loop system achieves RP if it is internally stable for all the plants $G_\Delta = G + W_\Delta\Delta$ ($\|\Delta\|_\infty \leq 1$) and the following performance objectives are satisfied: $\left\| W_e \frac{I}{I + G_\Delta K} G_d \right\|_\infty \leq 1$ and $\left\| W_t \frac{G_\Delta K}{I + G_\Delta K} \right\|_\infty \leq 1$.

Figures 43(a)-(b) show that no controller satisfies NP and RS conditions simultaneously, hence RP is not achievable, as confirmed in Fig. 43(c). Observing the peaks attained for each controller, the μ scalar of the diagonal perturbations that cause deterioration of performance can be calculated. Under this consideration, the $\mathcal{H}_\infty$ and μ-synthesis controllers present better RP properties. This is not unexpected as these controllers considered the performance weighting functions in the design. Figure 43(c) also shows that the NP characteristics of the controlled systems are maintained at low frequencies, while at high frequencies the RS characteristics dominate.

It is worth recalling that the values obtained for the NP, RS and RP are only valid with respect to the performance and stability definitions, and the model of uncertainty considered in the design. If the family of plants considered in the design of the $\mathcal{H}_\infty$ and μ-synthesis controllers, and in the comparison, is erroneous, the resultant RS and RP cannot be reliable.

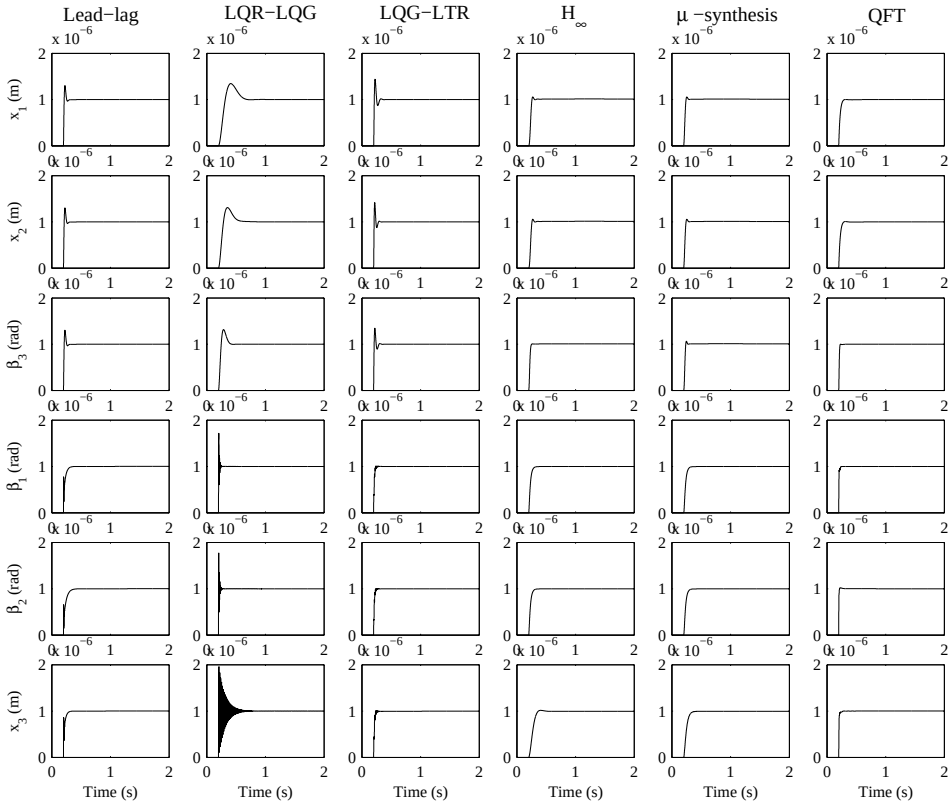

Fig. 44. Numerical simulation results, step response, various controllers.

Time domain response

Figure 44 shows the step responses of the six position variables of the platen, for the nominal model. In general, all controllers present fast tracking of the steps. As stated in the previous analysis, the QFT controller is the one that gives the best performance.

The large peaks in the frequency plots for LQR-LQG tracking are reflected in the large overshoot and slow response presented in the corresponding step response. The $\mathcal{H}_\infty$, μ-synthesis and QFT controllers present well damped responses while the lead-lag and LQG-LTR controllers present overshoot for the horizontal motion responses.

b. Experimental results comparison

The lead-lag, LQR-LQG, LQG-LTR and $\mathcal{H}_\infty$[3] controllers have been implemented and tested with a sampling rate of 5kHz. The performance of each control system is compared with respect to the numerical results. Notably, the MIMO $\mathcal{H}_\infty$, μ-synthesis and QFT controllers have not been successfully implemented and hence are not considered below.

Frequency domain response

Figure 45(a) shows that, except for LQR-LQG, the simulated closed-loop frequency responses of the implemented controllers have good tracking properties for sinusoidal references of frequencies up to $50\frac{\text{rad}}{\text{s}}$ (within a bound of ± 0.01 for T). After the implementation of the discretized controllers on the MPS, it is observed that the tracking characteristics hold at the low frequencies but at intermediate and high frequencies there is an increase in the magnitude. In particular, there is a resonance at about 90Hz in all the frequency responses, the same resonance that appeared during the model validation. The discrepancy at high frequencies is believed to be due to high frequency dynamics not considered in the analytical model (this difference was believed to have been accounted for in the uncertainty models employed in the $\mathcal{H}_\infty$, μ-synthesis and QFT designs). The requirement of a rise time of 0.1s for a step response makes the controlled dynamics important under 100Hz. Hence, even *without* a good match between simulated and experimental responses at high frequencies, it was possible to implement the lead-lag, LQG-LQR, LQG-LTR and SISO $\mathcal{H}_\infty$ controllers. The MIMO $\mathcal{H}_\infty$, μ-synthesis and QFT designs, which considered the modeled uncertainty, were unstable in implementation.

[3]Implemented considering decentralized decoupled SISO $\mathcal{H}_\infty$ designs.

From the control effort plots, Fig. 45(b), the controller $\mathcal{H}_\infty$ requires less energy despite having equal or better tracking performance than the controllers lead-lag and LQG-LTR.

Time domain response

From Fig. 45(c)-(d), there is a fairly close match between the numerical simulation and the experimental results. However, there is a slight difference in transient (damping) of the responses. This difference may be a consequence of high frequency unmodeled dynamics as is evident from the frequency plots. The experimental responses show residual motions not apparent in simulations. The residual motions have envelopes of approximately 0.05μm in all cases, except for the LQR-LQG controller, which shows oscillations with amplitudes of 0.4μm and 0.15μm at about 2 and 1000Hz. The LQG-LTR and lead-lag controllers appear to achieve quicker responses at the expense of higher values of control input.

4. Discussion of results

The present study considered the control of a MPS using a variety of control methods. The MPS employs three novel permanent-magnet linear motors. The employed SISO and MIMO control approaches assumed linearized models that are uncoupled for certain axes, with the actual system's dynamic being nonlinear and coupled. The effectiveness of the control methods was compared analytically, with consideration given to the difference in how the problem is posed and solved for each methodology. The $\mathcal{H}_\infty$ norm and μ scalar of frequency weighted functions facilitated the comparison. Stability robustness was incorporated in the analysis by considering diagonal perturbations. This analysis was performed under the implicit assumption that the uncertainty model considered captures the behavior of the experimental system. The

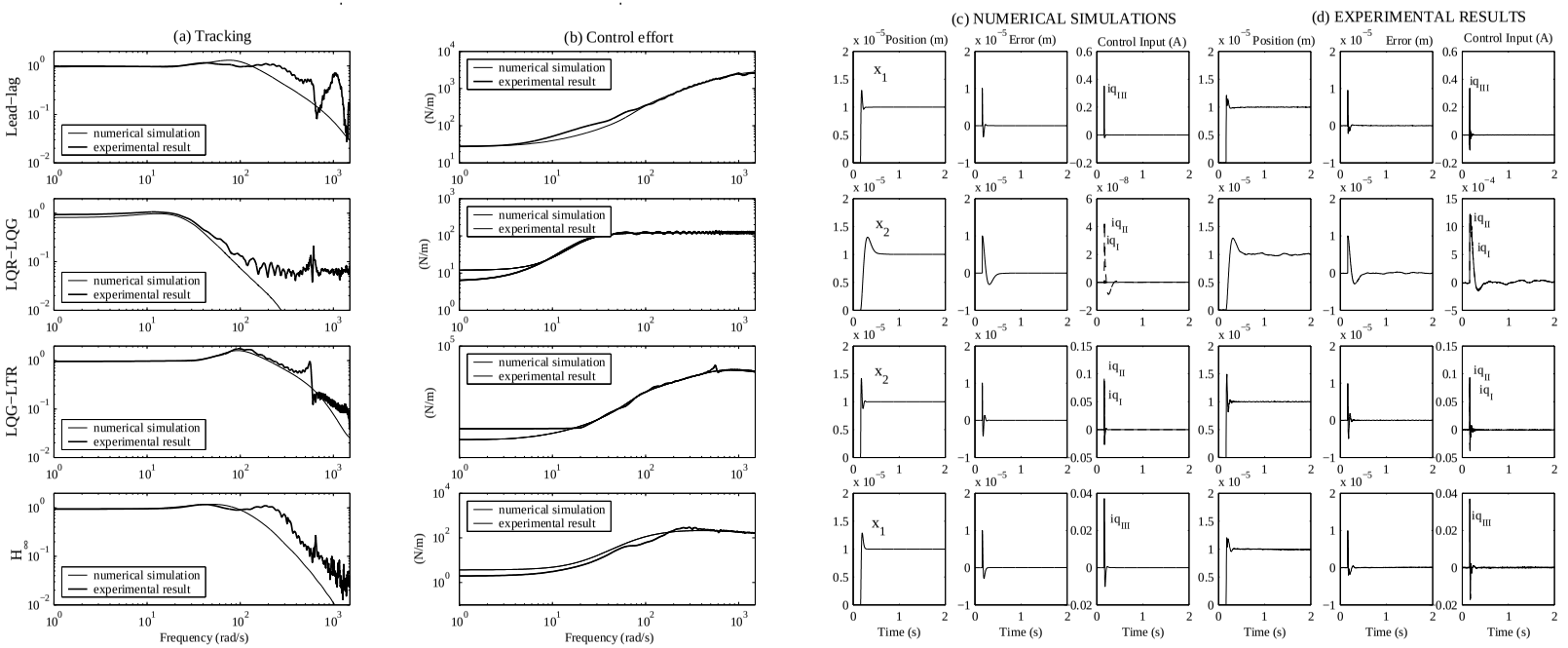

Fig. 45. Numerical simulation and experimental results for step references in x_1 and x_2. Frequency response: (a) tracking and (b) control effort. (c)-(d) Time response: position, position error and control current.

results of the analysis showed that the $\mathcal{H}_\infty$ and μ-synthesis controllers satisfied the RS condition with acceptable performance over the uncertainty range. The remaining controllers violated the RS condition by factors of up to 80, with LQR-LQG having the best RS properties and QFT having the best NP of all the controllers.

Considering the implementation, the lead-lag, LQR-LQG, LQG-LTR and SISO $\mathcal{H}_\infty$ controllers successfully controlled the MPS with positioning capability. Despite the fact that the $\mathcal{H}_\infty$ and μ-synthesis controllers satisfied the RS condition, and were the only ones, they failed in implementation along with the QFT controller. While unexpected, this indicates that the uncertain model failed to capture the dynamics of the real system. Notably, controllers that violated the RS condition were successfully implemented and provided precise response at the operating condition. For these controllers, the frequency and time domain simulations and experimental results confirmed the existence of a mismatch between the analytical model and the real system.

a. Further work

The experimental results indicated that the present nominal model with associated uncertainty is inadequate for reliable controller design. Similar work [76] confirms the importance of both an accurate nominal model and uncertainty description. However, while seemingly feasible [76], simply increasing the level of uncertainty is clearly not sufficient, indicating that the directionality of the uncertainty may have to be taken into account. Subsequently, further work aims to improve the uncertainty description [77] and investigate the presence of unmodeled dominant dynamics that may have contributed to the multivariable design failures. The redesign and implementation of the considered controllers would then be undertaken.

C. System identification and model validation through uncertainty bounds optimization

Success was obtained when implementing the lead-lag, LQR-LQG, LQG-LTR and single-input single-output (SISO) $\mathcal{H}_\infty$ controllers [78], all obtained using the analytical model. Notably, the analytical model presents uncoupling among certain axes even though it was obvious from experimental implementation the existence of coupling among all the axes. Importantly, the multivariable robust control $\mathcal{H}_\infty$, μ-synthesis and QFT designs based on the analytical model and unstructured uncertainty models failed in implementation.

The underlying assumption in previous controller designs was that a sufficient accurate system model and uncertainty models could be obtained from first principles and experimental data. However, the selection of the uncertainty models was not performed following any formal model validation criteria. The uncertainty models were obtained employing the joint input-output identification approach [71] for each input and the related (direct) output of the actual system, and taking the difference in norm of these identified models with respect to their corresponding SISO analytical models.

The aim of this part of the work is to determine improved mathematical representations of the MPS using closed-loop experimental data to facilitate successful control implementation. This data is acquired by operating the system with an existing feedback loop due to the unstable open loop dynamics. A decentralized SISO controller, from a previous successful design, is employed to close the loop. From the collected data, observer/controller based system identification and uncertainty bound optimization methods are employed to determine models of the system and validate these models based on some predefined structure of the uncertainty. The

uncertainty bounds are given in a linear fractional transformation form that enables a direct use in robust control design. Uncertainty bound optimization methods address input directional dependence and differences with respect to each experiment by maximizing uncertainty levels over multiple experimental data sets. Simulations are performed to obtain uncertainty bounds and the effect of parametric uncertainty on the non-modeled dynamics structured uncertainty is observed. There exists a strong possibility that uncertainty bounds obtained using the methods herein shown would overcome the drawback presented in actual implementation by previous designs.

The remainder of this section is organized as follows: the first part comprehends the theory behind the obtention of the identified models of the system and the description of the uncertainty models using model validation ideas. Numerical simulations and results are later shown to prove the potential on improving the modeling of the system and its corresponding uncertainty.

1. System identification from closed-loop data

From the analysis developed in the previous sections, the unstable nature of the actual system constrains the identification of the system to be performed in closed-loop. The system can be operated with any of the previously successfully implemented controllers. However, the decentralized lead-lag controller is employed. The closed-loop is excited by a known excitation signal (gaussian noise) and the time histories of the closed-loop response and feedback signals are measured. Using the time history data, the Markov parameters of the open loop plant are recovered and, subsequently, a state-space model of the open loop plant is realized (observer/controller identification algorithm [79]).

a. Observer/controller identification

Consider the observer/controller Kalman Filter identification algorithm [79]. A schematic diagram of the existing or actual closed-loop system is given in Fig. 46 and shows the measured quantities (output closed-loop response and feedback control signal) and the open loop plant in state space representation. An algorithm is developed to identify the open loop plant, an observer gain and an existing controller gain from closed-loop data. The system input-output relation given in terms of the observer and the controller in discrete time is:

$$\hat{x}(k+1) = \bar{A}\hat{x}(k) + \bar{B}\nu(k), \tag{7.22}$$

$$\begin{bmatrix} \hat{y}(k) \\ u_f(k) \end{bmatrix} = \bar{C}\hat{x}(k) + \bar{D}\nu(k), \tag{7.23}$$

where:

$$\bar{A} = A + GC, \tag{7.24}$$

$$\bar{B} = \begin{bmatrix} B + GD & -G \end{bmatrix}, \tag{7.25}$$

$$\bar{C} = \begin{bmatrix} C \\ -F \end{bmatrix}, \tag{7.26}$$

$$\bar{D} = \begin{bmatrix} D & 0 \\ 0 & 0 \end{bmatrix}, \tag{7.27}$$

$$\nu(k) = \begin{bmatrix} u(k) \\ y(k) \end{bmatrix}, \tag{7.28}$$

and the matrices A, B, C, D, G and F denote suitable state space matrices for the open loop system, and the observer and feedback controller gains respectively.

The observer/controller Markov parameters are identified by solving a least

squares problem directly from the input $u(k)$ and the measured output $y(k)$ time response histories. The error to be minimized is the difference between the estimated outputs and the measured outputs:

$$\bar{e} = \bar{y} - \bar{Y}\bar{V}, \tag{7.29}$$

where:

$$\bar{e} = [\ e(s) \quad e(s+1) \quad \cdot\cdot \quad e(l-1)\ ]^T, \tag{7.30}$$

$$\bar{y} = [\ y(s) \quad y(s+1) \quad \cdot\cdot \quad y(l-1)\ ]^T, \tag{7.31}$$

$$\bar{Y} = [\ D \quad \bar{C}\bar{B} \quad \bar{C}\bar{A}\bar{B} \quad \cdot\cdot \quad \bar{C}\bar{A}^{p-1}\bar{B}\ ], \tag{7.32}$$

$$\bar{V} = \begin{bmatrix} u(p) & u(s+1) & \cdot\cdot & u(l-1) \\ \nu(s-1) & \nu(s) & \cdot\cdot & \nu(l) \\ : & & & : \\ \nu(s-p) & \nu(s-p+1) & \cdot\cdot & \nu(l-1-p) \end{bmatrix}, \tag{7.33}$$

and, the numbers s and l denote the time at which an existing observer has converged to provide the correct state of the plant and the final measured time, respectively. The number p denotes the number of observer/controller Markov parameters $\bar{Y}(k)$ to be solved from the available data. Note that there is an implicit requirement on the Markov parameters after p time steps, they should vanish identically, i.e.

$$\bar{Y}(k) = \bar{C}\bar{A}^{k+1}\bar{B} \equiv 0, \quad k > p. \tag{7.34}$$

By moving the innovation process forward, the following open loop system, ob-

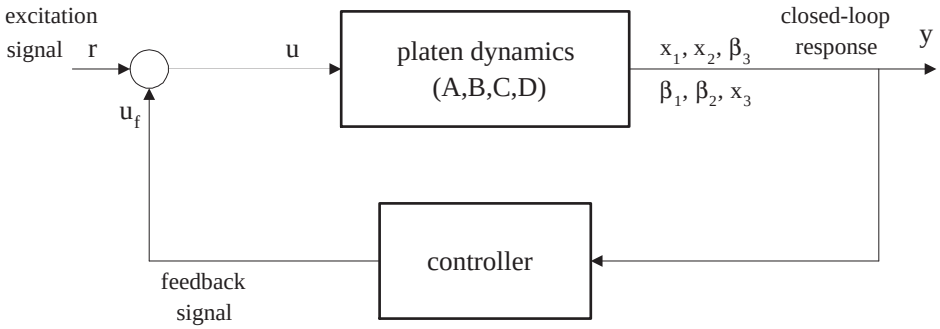

Fig. 46. Existing control system.

server and controller gain Markov parameters:

$$
\begin{aligned}
& Y^{(1,1)}(0) = D \\
Y(k) \;&=\; \begin{bmatrix} C \\ F \end{bmatrix} A^{k-1} \begin{bmatrix} B & G \end{bmatrix} = \begin{bmatrix} CA^{k-1}B & CA^{k-1}G \\ FA^{k-1}B & FA^{k-1}G \end{bmatrix} , \qquad (7.35) \\
&= \begin{bmatrix} Y^{(1,1)}(k) & Y^{(1,2)}(k) \\ Y^{(2,1)}(k) & Y^{(2,2)}(k) \end{bmatrix} , \;\; k = 1, 2, \cdot\cdot
\end{aligned}
$$

are computed from the following identified observer/controller Markov parameters:

$$
\begin{aligned}
\bar{Y}(0) &= \begin{bmatrix} D \\ 0 \end{bmatrix} \equiv \begin{bmatrix} \bar{Y}^{(1,1)}(0) \\ \bar{Y}^{(2,1)}(0) \end{bmatrix} \\
\bar{Y}(k) \;&=\; \begin{bmatrix} C \\ -F \end{bmatrix} (A + GC)^{k-1} \begin{bmatrix} B + DG & -G \end{bmatrix} , \qquad (7.36) \\
&= \begin{bmatrix} \bar{Y}^{(1,1)}(k) & -\bar{Y}^{(1,2)}(k) \\ -\bar{Y}^{(2,1)}(k) & \bar{Y}^{(2,2)}(k) \end{bmatrix} , \;\; k = 1, 2, \cdot\cdot
\end{aligned}
$$

The structure of the observer/controller system identification is shown in Fig. 47.

The realization of the open loop plant, observer and controller gains is performed

using the eigensystem realization algorithm (ERA) and the combined Markov parameters $Y(k)$ determined above. The following Hankel matrix is formed:

$$H(k-1) = \begin{bmatrix} Y(k) & Y(k+1) & \cdot\cdot & Y(k+s) \\ Y(k+1) & Y(k+2) & \cdot\cdot & Y(k+s+1) \\ \vdots & & & \vdots \\ Y(k+r) & Y(k+r+1) & \cdot\cdot & Y(k+r+s)) \end{bmatrix}, \tag{7.37}$$

and the realization below will simultaneously identify the open loop system matrices A, B, C, the observer gain G and the controller gain F:

$$\begin{aligned} A &= D_r^{-1/2} P_r^T H(1) Q_r D_r^{-1/2} \\ \begin{bmatrix} B & G \end{bmatrix} &= D_r^{1/2} Q_r^T E_{(m+q)} \\ \begin{bmatrix} C \\ F \end{bmatrix} &= E_{(m+q)}^T P_r D_r^T \end{aligned}, \tag{7.38}$$

where the order of the realization is determined by the singular value decomposition of the Hankel matrix $H(0)$ as defined by:

$$H(0) = PDQ^T = P_r D_r Q_r^T. \tag{7.39}$$

The subscript r refers to the matrices formed by retained columns in P and Q, and the retained singular values in D, respectively. The matrix E is made up of zeros and identity matrices appropriately.

2. Uncertainty structure

The description of the uncertainty structure must provide physical motivation for its selection. Consider the linearized system with an added weak nonlinearity and

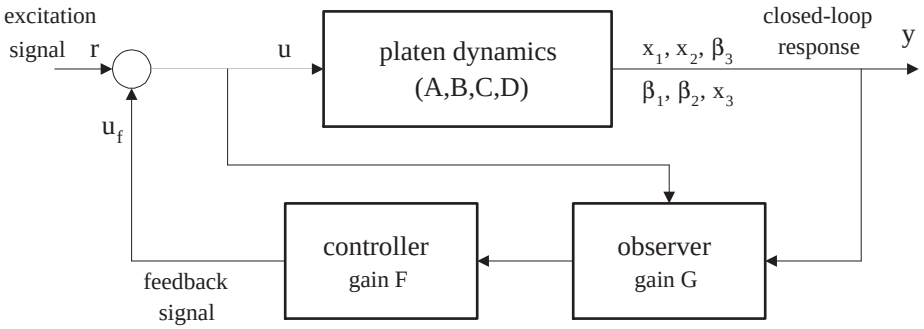

Fig. 47. Identified control system.

defined by the discrete time state equations:

$$x(k+1) = A_P x(k) + B_P a(k) + f(x(k)), \tag{7.40}$$

$$q(k) = C_P x(k) + D_P u(k) + d(k), \quad \text{sensor} \tag{7.41}$$

$$y(k) = g(q(k)) + w(k), \quad \text{output} \tag{7.42}$$

$$a(k) = h(u(k)), \quad \text{actuator} \tag{7.43}$$

where $d(k)$ is the output disturbance (e.g. dynamics of the unmodeled umbilical cables that act on the platen), $w(k)$ is the output noise, $u(k)$ is the control signal, and $y(k)$ is the measured output signal. The term $f(x(k))$ denotes the plant nonlinearities that affect the linearized equation, e.g. nonlinearities such as the damping effect of the air-bearings and the inaccurate knowledge of the spacial distribution of the magnetic field. The $h(u(k))$ and $g(q(k))$ terms are included to incorporate hardware effects such as quantization and saturation, also calibration errors and dynamic range of the sensing system. With this description, the model structure assumed for the platen is given in Fig. 48 with A_P, B_P, C_P and D_P denoting affine parameter dependent

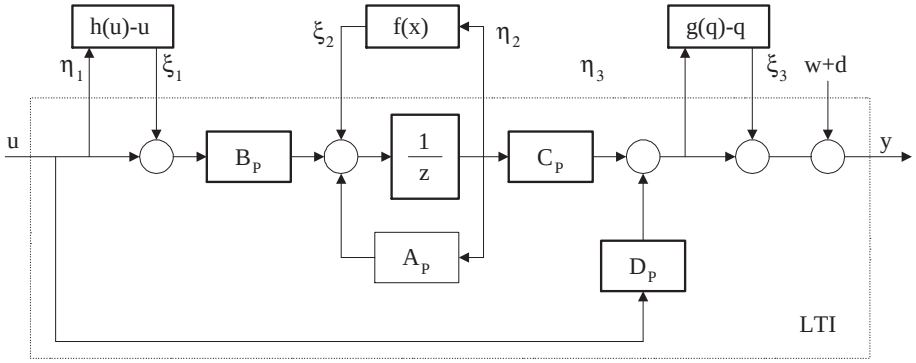

Fig. 48. Model structure of the platen.

linear system matrices as represented below:

$$\begin{bmatrix} A_P & B_P \\ C_P & D_P \end{bmatrix} = \begin{bmatrix} A_o & B_o \\ C_o & D_o \end{bmatrix} + \sum_{i=1}^{n_A} \delta_i \begin{bmatrix} A_{P_i} & 0 \\ 0 & 0 \end{bmatrix} + \sum_{i=n_A+1}^{n_B} \delta_i \begin{bmatrix} 0 & B_{P_i} \\ 0 & 0 \end{bmatrix} + \sum_{i=n_B+1}^{n_C} \delta_i \begin{bmatrix} 0 & 0 \\ C_{P_i} & 0 \end{bmatrix} + \sum_{i=n_C+1}^{n_D} \delta_i \begin{bmatrix} 0 & 0 \\ 0 & D_{P_i} \end{bmatrix}. \quad (7.44)$$

As each of the matrices associated with each Δ_i has rank one they can be factored into row and column vectors using the singular value decomposition [8], then:

$$\begin{bmatrix} A_{P_i} & 0 \\ 0 & 0 \end{bmatrix} = \begin{bmatrix} E_i \\ F_i \end{bmatrix} \begin{bmatrix} G_i & H_i \end{bmatrix}, \quad (7.45)$$

and the following linear system with extra inputs and outputs can be defined:

$$\begin{bmatrix} x(k+1) \\ y(k) \\ \eta_{n_1} \\ \vdots \\ \eta_{n_r} \end{bmatrix} = \begin{bmatrix} A_o & B_o & E_1 & .. & E_n \\ C_o & D_o & F_1 & .. & F_n \\ G_1 & H_1 & 0 & .. & 0 \\ \vdots & \vdots & \vdots & \vdots & \vdots \\ G_n & H_n & 0 & .. & 0 \end{bmatrix} \begin{bmatrix} x(k) \\ u(k) \\ \zeta_{n_1} \\ \vdots \\ \zeta_{n_r} \end{bmatrix}. \quad (7.46)$$

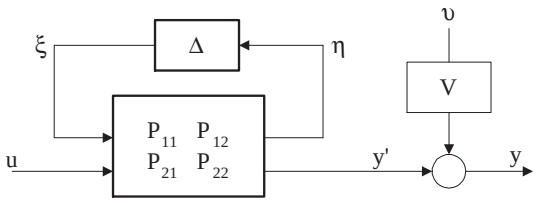

Fig. 49. Plant model structure in the standard LFT form.

In the derivation below of the uncertainty models we assume that Δ belongs to the set of structured uncertainty $\mathcal{D}$, as defined by:

$$\mathcal{D} = \left\{ \begin{array}{ll} \Delta \in \mathcal{C}^{m\times n} : \Delta = & \mathrm{diag}(\delta_1 I_{n_1}, .., \delta_r I_{n_r}, \overbrace{h(u)-u}^{\Delta_{r+1}}, \overbrace{g(q)-q}^{..}, \overbrace{f(x)}^{\Delta_\tau}), \\ & \delta_i \in \mathcal{F}_i, \Delta_i \in \mathcal{C}^{m_i\times n_i} \end{array} \right\}, \quad (7.47)$$

where τ denotes the number of uncertainty blocks and δ_i $i = 1, \cdot\cdot, r$ denotes a set of uncertain repeated scalar parameters. Then, the structure of the plant model can be rewritten in the general form as depicted in Fig. 49.

The transfer function relation for this representation can be written as:

$$y = \mathcal{F}_u(P, \Delta)u + Vv, \quad (7.48)$$

with the upper linear transformation defined by:

$$\mathcal{F}_u(P, \Delta) = P_{22} + P_{21}\Delta(I - P_{11}\Delta)^{-1}P_{12}. \quad (7.49)$$

From this equation note that, when $\Delta = 0$, the nominal (analytical or identified) model can be recovered. Also notice that from system identification only P_{22} and V are to be determined and the other matrices P_{12}, P_{21} and P_{11} can be constructed from the uncertainty structure.

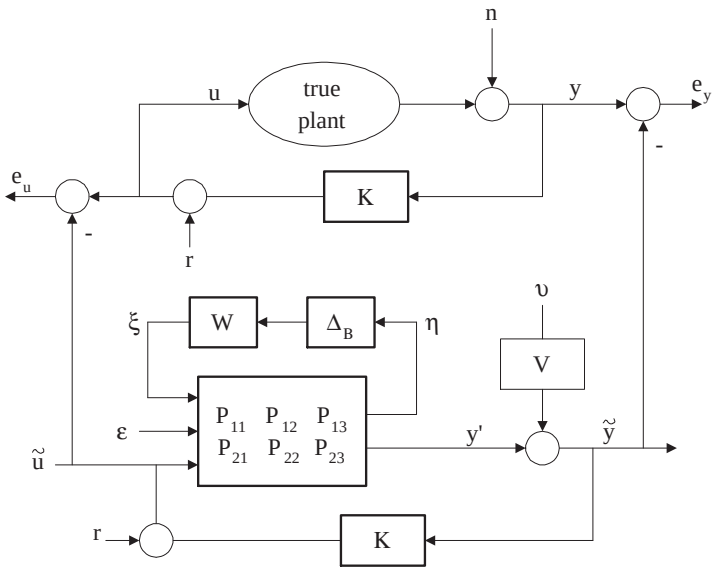

Fig. 50. General block diagram for robust identification.

3. Bounding the uncertainty using model validation

To account for the discrepancies between the available measured outputs and the outputs obtained from the observer/controller based system identification[4], an a priori knowledge of the possible source of uncertainties in the system will be used (see previous subsection). Figure 50 shows the direct connection of the parameterized uncertainties Δ to the residuals between the true system responses and the responses obtained using the identified models. Note that the plant shown in Fig. 50 is in feedback loop with a controller. This goes in accordance with the system identification ideas presented in the last sections due to the unstable nature of the system.

Closing the idealized loop (bottom feedback loop in Fig. 50), the canonical form of the general block diagram can be presented as described in Fig. 51. Then, the

[4]The method to be presented here would also be employed to obtain uncertainty bounds between the measured outputs and the outputs obtained using the analytical model of the plant and the linear controller design.

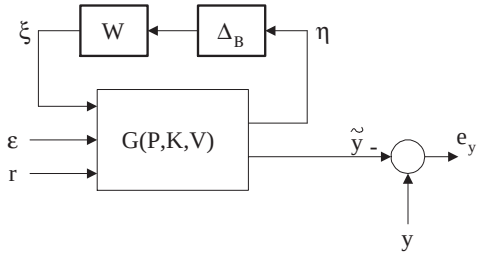

Fig. 51. Canonical form of the general block diagram.

output error is given by:

$$e_y = \underbrace{y - G_{23}r}_{\text{nominal error } e_y^o} \overbrace{-G_{21}\zeta - G_{22}\beta}^{\text{uncertainty freedom}}, \tag{7.50}$$

with the uncertainty weights defined as:

$$W = \text{diag}(w_1 I_1 .. w_\tau I_\tau), \tag{7.51}$$

$$\Delta_B = \text{diag}(\Delta_{B_1} I_1 .. \Delta_{B_\tau} I_\tau), \tag{7.52}$$

where W denotes the radii applied to the blocks of the structured uncertainty unit ball. Since r and K are assumed to be known, the following is satisfied:

$$e_y = 0 \Rightarrow e_u = 0. \tag{7.53}$$

Let $\mathcal{D}_W$ be a bounded structured set. Does there exist $\Delta \in \mathcal{D}_W$, $\beta = \begin{bmatrix} \varepsilon \\ \nu \end{bmatrix}$ and r, where $\|\varepsilon\| \leq 1$, $\|\nu\| \leq 1$ such that:

$$y = \mathcal{F}_u \left(G(P,K,V), \Delta \right) \begin{bmatrix} \varepsilon \\ \nu \\ r \end{bmatrix} \quad ? \tag{7.54}$$

To solve this question, Lim *et al.* [77] addressed the feasibility question, "Does

a model validation $\mathcal{D}_W$ exist?", instead of, "Is $\mathcal{D}_W$ model validating?" The feasibility problem, followed by an appropriate parameterization, is then expressed in the following way:

1. Does (ζ,β) exist, where $\|\beta\| \leq 1$, such that $e_y = 0$?

   Yes, if and only if the following (constant matrix test) passes:

$$e_y^o \in \mathrm{Im}(M) \quad \forall\omega, \tag{7.55}$$

$$\|T_2^H (M^\dagger)_\beta e_y^o\| \leq 1, \quad \forall\omega, \tag{7.56}$$

   where:

$$e_y^o = y - G_{23} r, \tag{7.57}$$

$$M = [\ G_{21} \quad G_{22}\ ], \tag{7.58}$$

$$\mathrm{Im}(N_M) = \mathrm{Ker}(M), \tag{7.59}$$

$$T_2 \in \mathrm{Im}((N_M)\nu)^\perp, \tag{7.60}$$

   else, uncertainty structure and/or noise allowance is limiting and changes in $(P, \mathcal{D}, V)$ are required to increase the possibility of getting a feasible solution.

2. Parameterize all such (ζ,β) and η:

$$\mathcal{S} = \{(\zeta(\phi,\psi), \eta\,[\zeta(\phi,\psi), \beta(\phi,\psi)]), \phi \in \Phi, \psi \in \Psi\}, \tag{7.61}$$

   where (ζ,β,η) is affine in (ϕ,ψ).

3. Does Δ, ζ, η exists, where $\Delta \in \mathcal{D}$, $(\zeta, \beta) \in \mathcal{S}$, such that $\zeta = \Delta\eta$ and $\eta = G_{11}\zeta + G_{12}\beta + G_{13} r$?

   Yes, if and only if (ζ,η) is $\mathcal{D}$-realizable. This condition aims to rule out $\zeta_i \neq 0$ and $\eta_i \neq 0, \forall i$. Fortunately, signal set $\mathcal{S}$ is typically well endowed in application.

If a model validating $\mathcal{D}_W$ exists, it can be shown that all model validating sets can be parameterized by:

$$\mathcal{D}_{W\phi\psi} = \{\Delta \in \mathcal{D} : \Delta = W\Delta_B, \bar{\sigma}(\Delta_B) \leq 1\}, \tag{7.62}$$

where $W = \text{diag}(w_1 I_{n_1}, .., w_\tau I_{n_\tau})$ is any matrix satisfying:

$$|w_i| \geq \frac{\|\zeta_i(\phi, \psi)\|}{\|\eta_i(\phi, \psi)\|}, \quad i = 1, \cdot\cdot, \tau \tag{7.63}$$

with (ζ_i,η_i) parameterized by:

$$\zeta_i = \zeta_{o,i} + \Omega_i \begin{bmatrix} \phi \\ \psi \end{bmatrix}, \tag{7.64}$$

$$\eta_i = \eta_{o,i} + G_{11}\Omega_i \begin{bmatrix} \phi \\ \psi \end{bmatrix}, \tag{7.65}$$

where $\psi \in \mathcal{C}^{n_\psi}$, $\phi \in \mathcal{C}^{n_\phi}$, $\|\phi\| \leq b_o$, and (ζ,η) is $\mathcal{D}$-realizable, $\text{dist}^{(\mathcal{F}_i)}(\zeta_i, \eta_i) = 0$ $i = 1, .., r$. For more explanations see Lim *et al.* [77]. The Appendix shows the smallest model validating set algorithm employed for our calculations.

4. Numerical simulations

Consider the experiment ("truth model") to be simulated with the twelfth order model corrupted at the output with simulated measurement noise. The simulated system consists of the platen having 5% of its weight lifted by some nominal direct current and with the parameters values perturbed by 10%, all of these with respect to the values described in Table I. The obtention of uncertainty bounds employing the smallest set algorithm, and applied at each frequency point, will be elucidated with simulations for the analytical model and an identified model as nominal models. Figures 52

and 53 show two a priori structures of the uncertainty to be considered, additive and multiplicative nonparametric uncertainties together with parametric uncertainty. The scalar parametric uncertainty to be considered for the study will be modeled as perturbations in the real and imaginary eigenvalues of the nominal system matrix A.

a. Data acquisition

The sampling rate assumed is 5000Hz and the data is recorded for 2s with 2^{13} data points used for FFT. The system excitation signal (for identification and calculation of uncertainty bounds) for all channels consists of two added random signals of normal distribution with zero mean and 1 10^{-5}, 5 10^{-5} standard deviations passed trough a fourth order Butterworth filter with passband of 60%, 1% Nyquist frequency respectively. The selection of the excitation signal is consistent with our interest of covering dominant modes at relevant frequency ranges. For the case of system identification (nominal model identification), the excitation inputs are applied individually and data is recorded for all channels. Additionally, measurement noise for all channels is used with standard deviations of 1×10^{-6}. The noise sequence was generated by passing it through a second order Butterworth filter with passband of 90% Nyquist frequency to simulate wideband noise. From sensor measurements, the source of the closed-loop responses is the position (translational and rotational motion) of the platen centroid. The output signals of the feedback control laws and the independent input excitation signals, together with the closed-loop responses, provide the time history necessary for identification and subsequently model validation of the MIMO system. In the Appendix, a detailed description of the tests to be performed for the system identification and uncertainty bounds determination is presented.

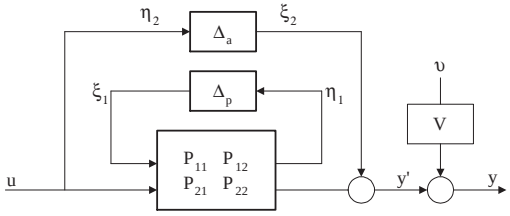

Fig. 52. Structured uncertainty: additive and parametric.

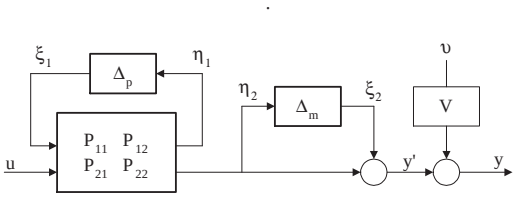

Fig. 53. Structured uncertainty: multiplicative and parametric.

b. Case studies

It is important to point out that the study performed in this part of the work employs a proposed "truth model" for formulating the data. Table III in Appendix presents a number of cases to be considered for the obtention of model uncertainty bounds. These cases (8) arise as a result of choosing either the analytical or identified model as the nominal model, together with a variety of uncertainty structures. In all cases, the uncertainty bounds are determined using the algorithm defined in Section D.3. For the system identification part, the algorithm presented in Section D.1 is employed, with the number of observer/controller Markov parameters set to 30 ($p = 30$) and the assumption that the existing observer converges after 300 steps ($s = 300$).

Nominal model: analytical model

Figure 54 presents the singular value plots for the nominal (analytical) model and the "truth model". Observe some differences between the plots, specially at low and resonance frequencies. To further evaluate the accuracy of the nominal model, the predicted closed-loop responses based on the analytical model are compared to the measured responses, this is shown in Fig. 55. From Fig. 55, we can see a small discrepancy on the responses; however, this discrepancy is a little bigger for the vertical motion variables.

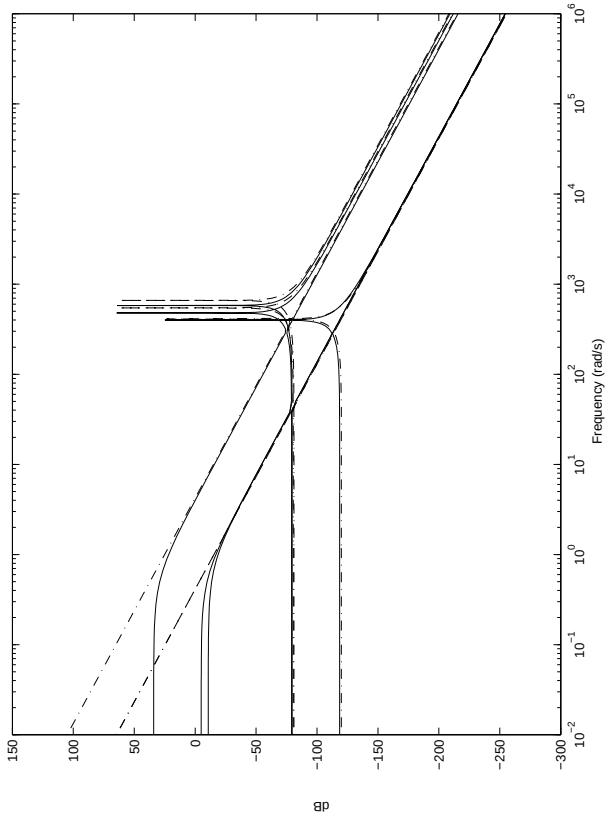

Fig. 54. Case 1,2,3,4. Singular values: "truth model" (-), analytical model (-·).

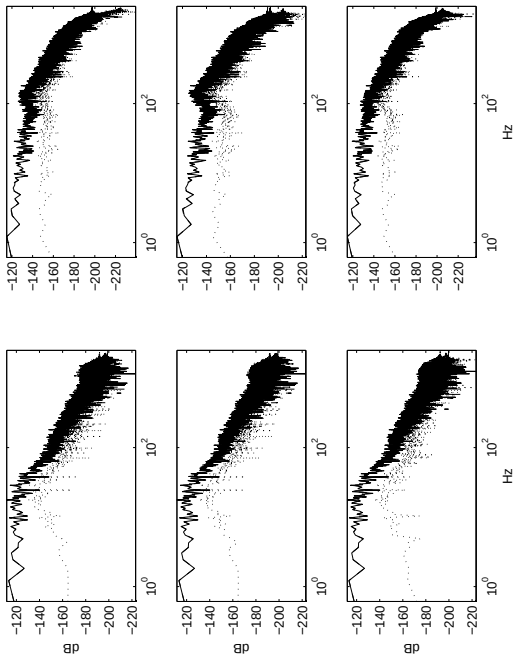

Fig. 55. Case 1,2,3,4. Output responses: y_{meas} (–), $G_{23}u_{\text{id}}$ (-). Error: e_y^o (·).

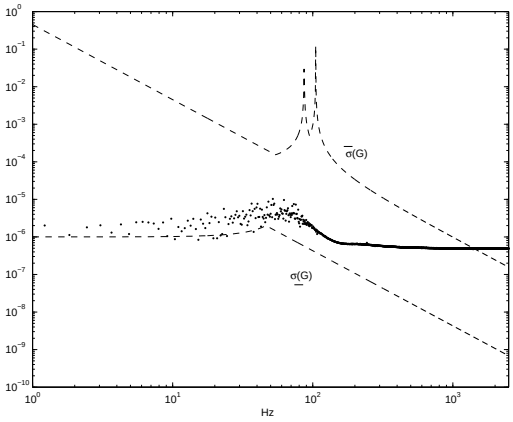

Fig. 56. Case 1. Singular values: nominal model (--), uncertainty bound ($\cdot$).

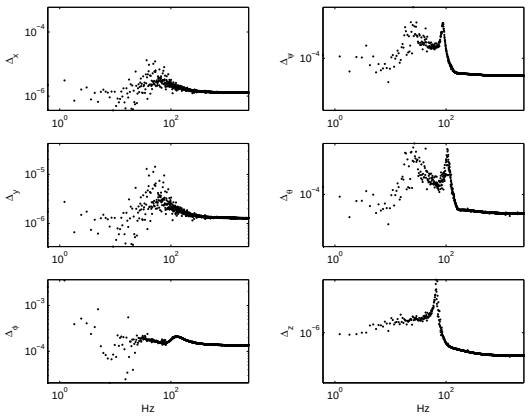

Fig. 57. Case 1. Uncertainty bounds per output channel.

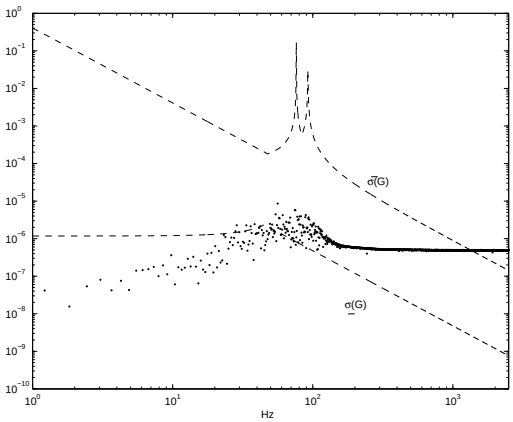

Fig. 58. Case 2 ($\delta = 0.01 I_{12\times 12}$). Singular values: nominal model (--), uncertainty bound ($\cdot$).

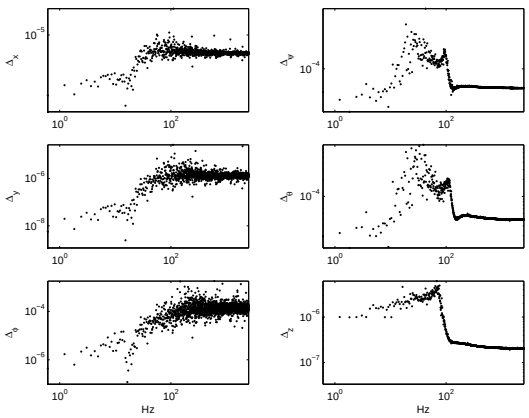

Fig. 59. Case 2 ($\delta = 0.01 I_{12\times 12}$). Uncertainty bounds per output channel.

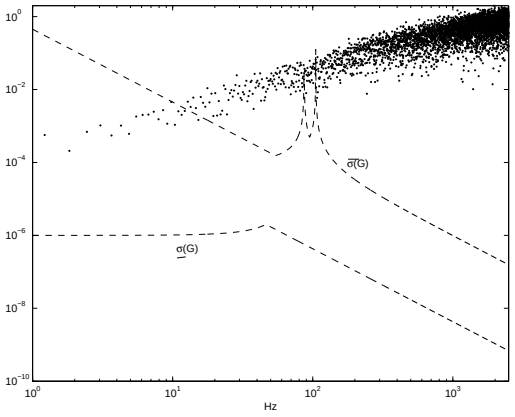

Fig. 60. Case 3. Singular values: nominal model (--), uncertainty bound (·).

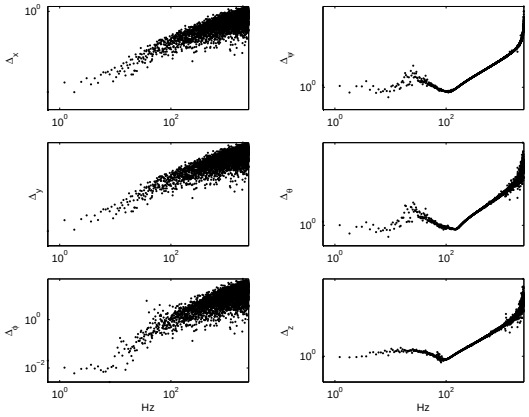

Fig. 61. Case 3. Uncertainty bounds per output channel.

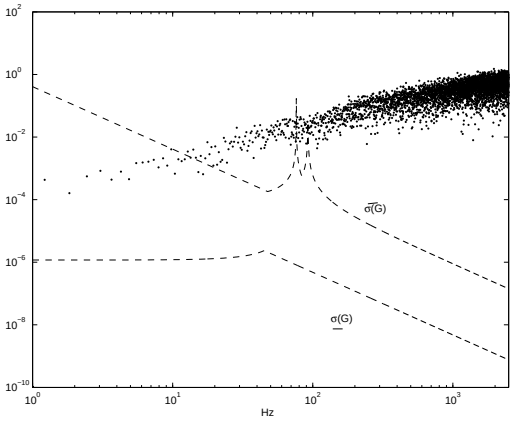

Fig. 62. Case 4 ($\delta = 0.01 I_{12\times 12}$). Singular values: nominal model (--), uncertainty bound (·).

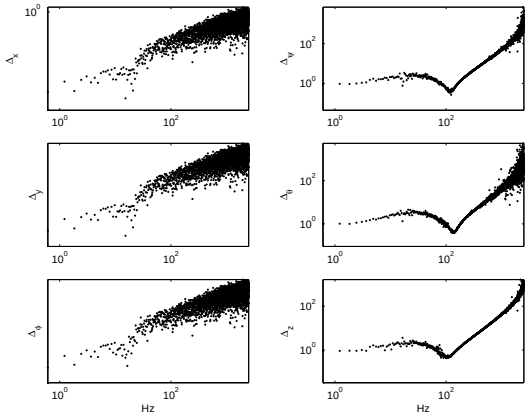

Fig. 63. Case 4 ($\delta = 0.01 I_{12\times 12}$). Uncertainty bounds per output channel.

Figures 56 to 63 correspond to Cases 1 to 4 of Table III. Figure 56 shows the additive uncertainty bound, for the no parametric perturbation case ($\delta = 0$), in contrast to the singular values of the nominal plant. It can be seen that the uncertainty bound is slightly bigger than the minimum singular values but much smaller than the maximum singular values, this at low and intermediate (resonance) frequencies. This tendency changes at high frequencies where the uncertainty bound becomes much greater than the maximum singular values of the nominal model. Note that, noise has been employed to obtain the uncertainty bounds, hence at high frequencies this noise could be the one appearing in this plot. Importantly, Fig. 57 complements the information provided by Fig. 56 and permits to distinguish the uncertainty bounds for each output channel. These plots show that the uncertainty bounds for the vertical motion are the ones that contribute more to the order of magnitude of the uncertainty bound depicted in Fig. 56. Again, at high frequencies, the effect of the simulated noise is present in all channels. Note that the validity of the predicted additive uncertainty is assured only over all the excitation signal frequency band.

Figures 58 and 59 show Case 2 of Table III with parametric scalar uncertainty set to $\delta = 0.01 I_{12\times 12}$. It is important to highlight that the inclusion of significant neighboring eigenvalue allowance in the nominal system matrix resulted in decreased additive uncertainty bounds at low frequencies. However, at high and intermediate (resonance) frequencies, the additive uncertainty bounds maintained similar behavior to the previous case of no parametric uncertainty.

From the multiplicative uncertainty bounds in Figs. 60 and 61 (Case 3 of Table III), it is evident the influence of the vertical dynamics on the determination of the uncertainty bounds. With the consideration of parametric uncertainty, Case 4 of Table III with $\delta = 0.01 I_{12\times 12}$, Figs. 62 and 63 show that the multiplicative uncertainty

bounds can be decreased at low frequencies.

Nominal model: identified model

Figures 64, 65, 66 and 67 show two identified models and their corresponding observer and plant Markov parameters. These two identified models differ in the generation of simulated data, one set of data has been collected considering that the "truth model" (system) has noisy outputs whereas the other set has been gathered in a noise free setting. The computed plant Markov parameters, obtained from the observer Markov parameters, are then used to determine a state space model of the open loop plant, termed the identified model. The plots of the plant Markov parameters present responses increasing in amplitude with the time, these plots reveal the open loop unstable nature of the "truth model", see Figs. 65 and 67. A comparison of Figs. 64 and 66 shows the effect that the consideration of noise has in the identification procedure, specifically at low and high frequencies. The difference in the plots emphasizes the attention that should be given to the signal-to-noise ratio in the identification of the actual dynamics of the platen.

Figure 68 presents a small discrepancy between the predicted responses based on the identified model (with noise) and the measurements. However, when comparing the order of magnitude of these discrepancies, the horizontal motion variables present the bigger differences. This is in accordance to Fig. 66 where, at low frequencies, significant mismatch exists between the "truth model" and the identified model. Recall that the dynamics of the platen at low frequencies is mainly described by the horizontal motion.

From previous experimental closed-loop responses, it is clear the existence of significant level of exogenous input and disturbance (at approximately 90Hz) on the platen [78]. Following the ideas described in the uncertainty structure section, an

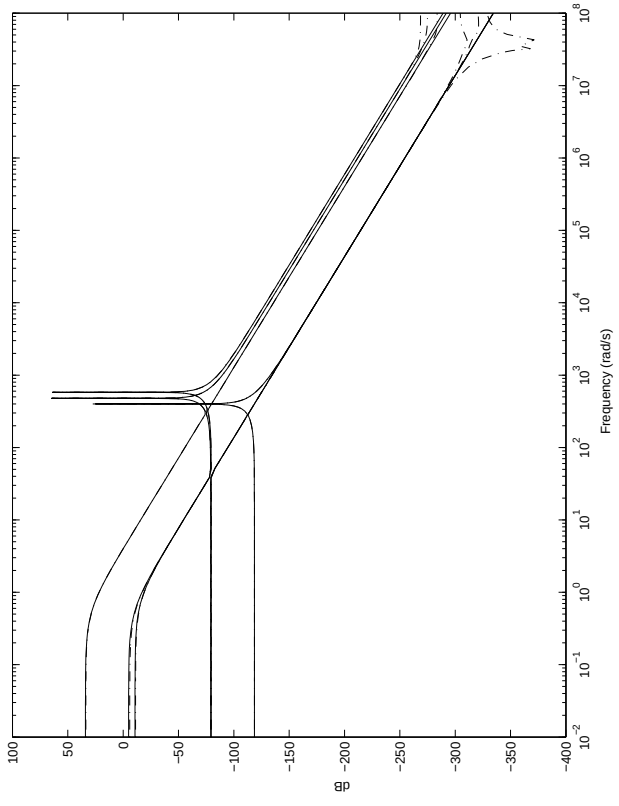

Fig. 64. Singular values: "truth model" identified (-), model (-·). No noise at the output.

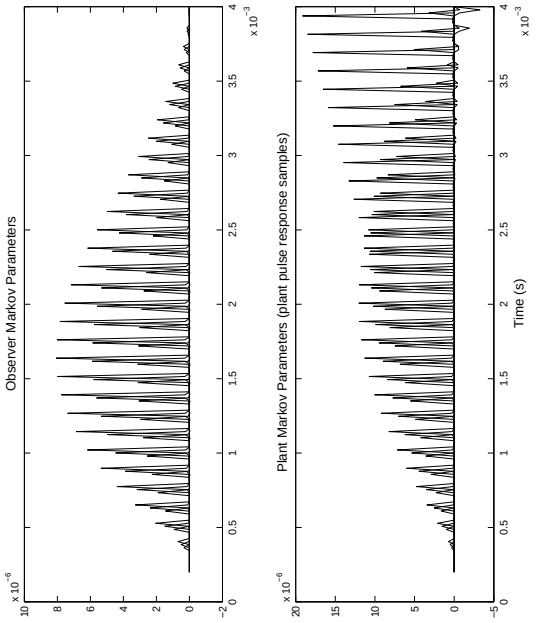

Fig. 65. Markov parameters. No noise at the output.

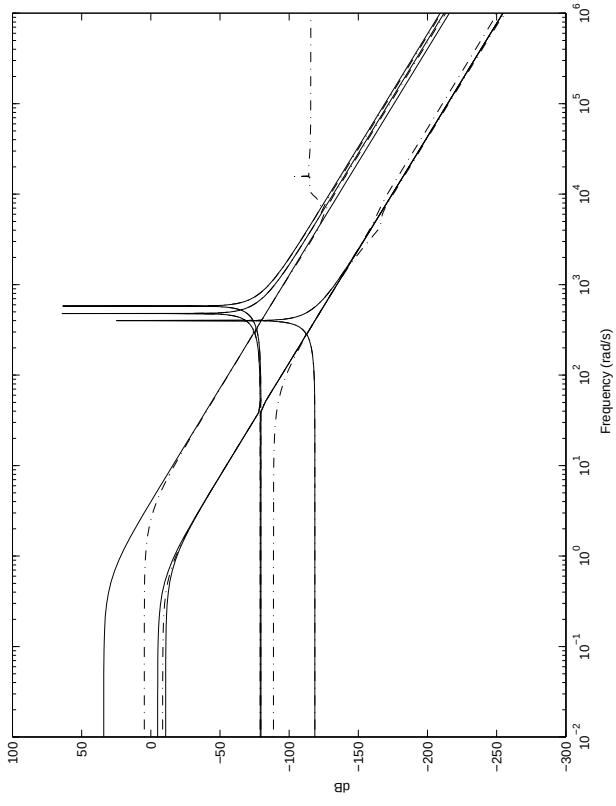

Fig. 66. Case 5,6,7,8. Singular values: "truth model" (-), identified model (-·). Noise at the output.

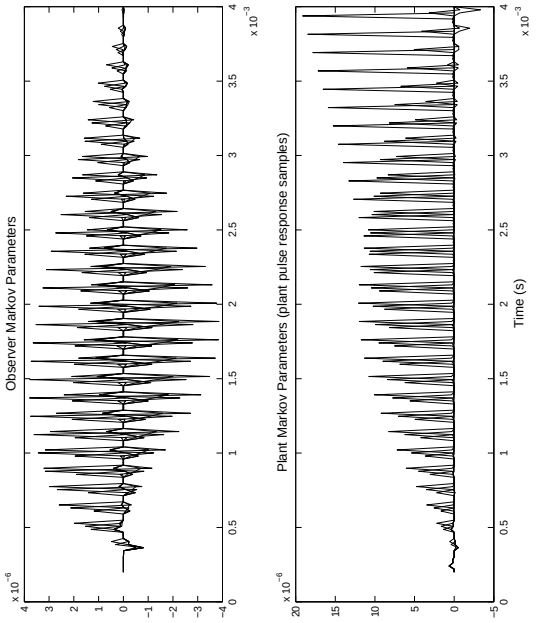

Fig. 67. Case 5,6,7,8. Markov parameters. Noise at the output.

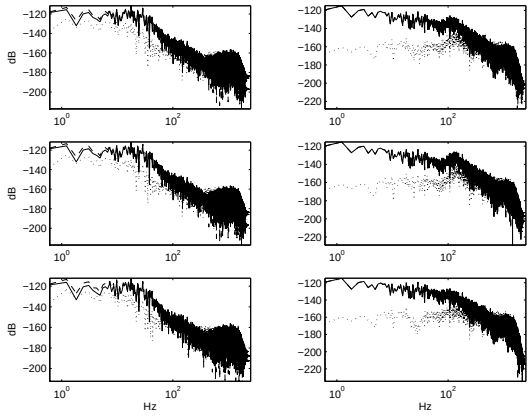

Fig. 68. Case 5,6,7,8.
Output responses: y_{meas} (–), $G_{23}u_{\text{id}}$ (-). Error: e_y^o (··).

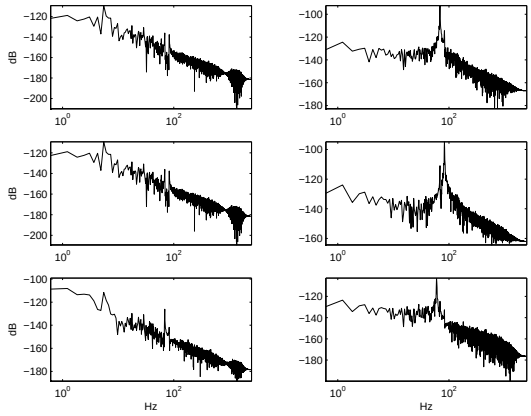

Fig. 69. Case 5,6,7,8.
Identified noise per output channel.

equivalent noise can be identified in closed-loop. This equivalent noise may account for the 90Hz disturbance and also for the acoustic noise generated by the air bearings. Figure 69 shows the identified noise for each output channel, the knowledge of this equivalent noise provides an extra freedom in the determination of uncertainty bounds.

With respect to Case 5 in Table III, at very low frequencies, Figs. 70 and 71 present smaller additive uncertainty bounds in comparison to the bounds presented in Case 1. This tendency changes at high frequencies where the uncertainty bounds for Case 5 appear to be higher. The behavior for the uncertainty models at very low frequencies is expected as the identified model was obtained from the data collected for the "truth model" (system) whereas the analytical model (Case 1) incorporated a double integrator as part of its dynamics. The high bounds at low frequencies can also be expected from Fig. 69 because at this frequency range the identified model fails to match the "truth model". Notably, the incorporation of parametric uncertainty in the uncertainty structure does not reflect an important improvement (decrement) in

the uncertainty bounds, as observed in Case 6 of Table Table III (Figs. 72 and 73). Hence, from Figs. 72 and 73, one can conclude that if a good system identification is performed the necessity of having a high allowance for parametric uncertainty is decreased.

Cases 7 and 8 of Table III are visualized in Figs. 74, 75, 76 and 77, they simply corroborate what was previously stated for the additive uncertainty structure with and without parametric uncertainty consideration. There is a significant mismatch between the "truth model" and the identified model at low and high frequencies, and no major improvement on the size of the bounds is achieved when parametric uncertainty is considered.

5. Discussion of results

In the present study it was demonstrate a viable approach to determine identified models and uncertainty bounds. The approaches mentioned here for closed-loop identification and determination of model uncertainty bounds have been successfully tested in experimental air and spacecraft tests, [80], [81]. This encourages us to think that we can obtain illustrative results in the MPS.

An improved and optimal description of the uncertainty models, obtained through model validation, could incorporate the actual difference between the experimental system and the analytical model, and lead to a successful multivariable controller implementation. The latter could also be achieved using a better model of the real system (i.e. identified models). From simulations it was observed that the identified models reduced the parametric uncertainty consideration relative to the analytical models. Moreover, determining accurate models of the MPS will give us more insight about some dynamics not considered in the analytical model and which, from practical implementation test, seems to be playing an important role when robust based

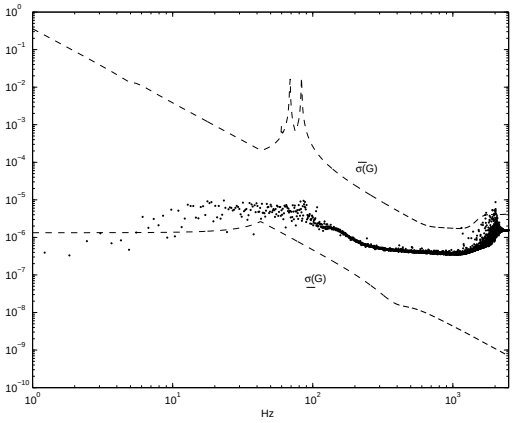

Fig. 70. Case 5. Singular values: nominal model (--), uncertainty bound ($\cdot$).

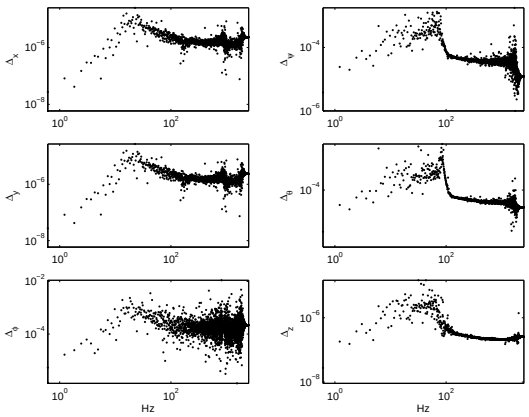

Fig. 71. Case 5. Uncertainty bounds per output channel.

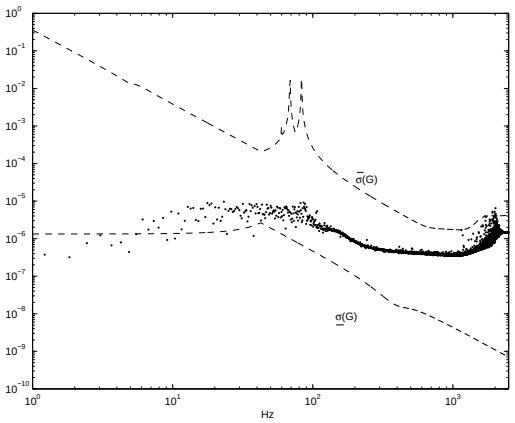

Fig. 72. Case 6 ($\delta = 0.01 I_{16\times 16}$). Singular values: nominal model (--), uncertainty bound ($\cdot$).

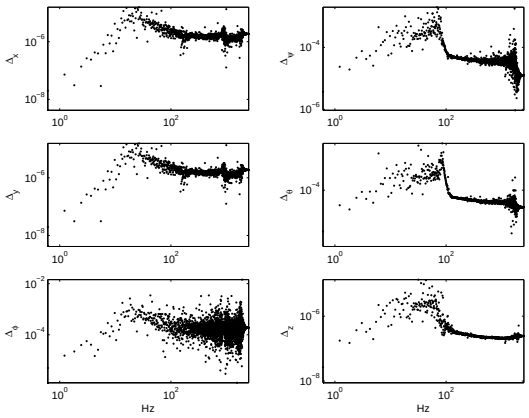

Fig. 73. Case 6 ($\delta = 0.01 I_{16\times 16}$). Uncertainty bounds per output channel.

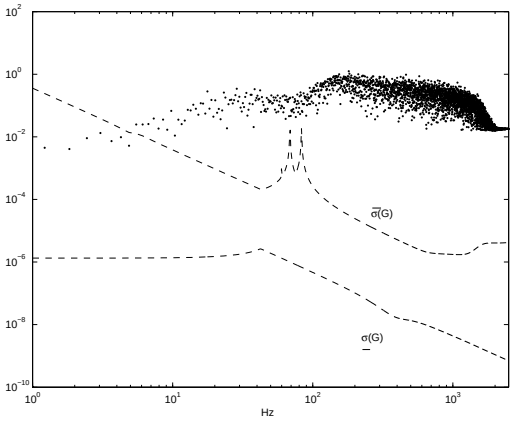

Fig. 74. Case 7. Singular values: nominal model (--), uncertainty bound $(\cdot)$.

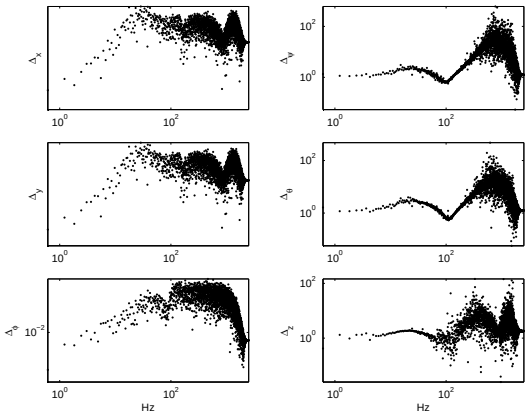

Fig. 75. Case 7. Uncertainty bounds per output channel.

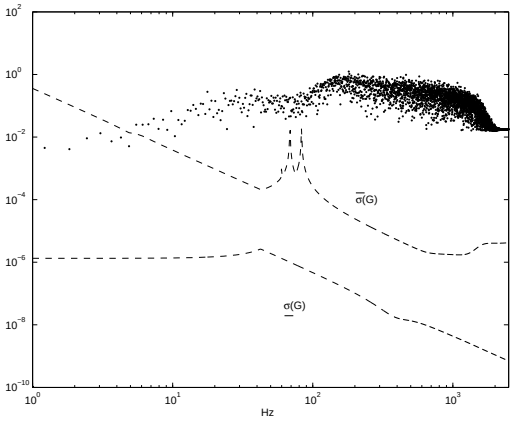

Fig. 76. Case 8 ($\delta = 0.01 I_{16\times 16}$). Singular values: nominal model (--), uncertainty bound $(\cdot)$.

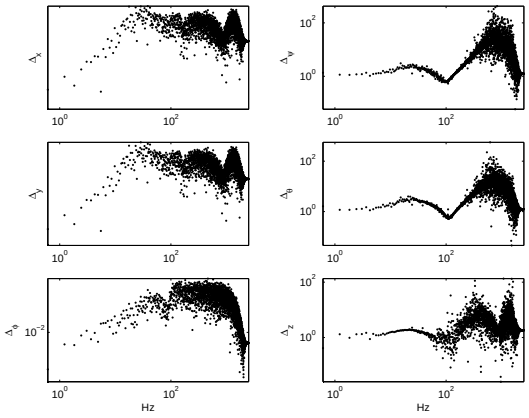

Fig. 77. Case 8 ($\delta = 0.01 I_{16\times 16}$). Uncertainty bounds per output channel.

control designs are implemented. Also the level of uncertainty will provide or justify the need of robust controller design along with the acknowledgment of robustness issues.

D. Remedial compensation

This part requires more theoretical work as the MPS is not an asymptotically stable system.

CHAPTER VIII

SUMMARY AND FUTURE WORK

The idea of this dissertation was to bring simplicity in constrained control. Control theory has arrived to a stage in which the aim is to find unifying control theories. In that sense, I hope our work has contributed to clarify some of the basic design principles underlying the control of systems subject to constraints. However, a number of issues still remain open.

A. Anti-windup compensation design

One can think that having identified three parameters, i.e. (H_1, H_2, Q), which contribute to quantify the potential success of anti-windup compensation, presents an advantage in terms of the synthesis problem. To see this, let's take the case of static anti-windup compensation with (H_1, H_2, I_{n_u}). H_1 and H_2 correspond to a certain coprime factorization of the unconstrained controller, and then, by an appropriate redefinition of the anti-windup closed-loop system[1], the synthesis problem can be reduced to that of finding H_1 and H_2. With the unconstrained controller being fixed, working directly in its coprime factorization representation seems interesting. Even more when consideration of uncertainty is an emphasis. In this context, the idea of a one-step anti-windup design can also be linked, maybe with some iterative process. The more general case can also be considered by adding the effects of dynamics through Q. However, is Q independent? one can say that H_1 and H_2 depend on

[1]In fact, this idea is related to the schemes that incorporate a model of the plant in the design. They, further employ the Bezout identity and get the synthesis problem redefined in terms of the coprime factors of the plant, or equivalently, some H_1 and H_2. Note, however, that the issue of uncertainty must be considered, and hence employing the Bezout identity does not look appealing.

the configuration chosen but is this also true for Q?. Probably, Q needs to satisfy extra requirements. These questions need to be resolved if one aims to design for (H_1, H_2, Q) for anti-windup compensation. Additionally, an issue of convexity when designing for Q needs also to be studied. If Q is general enough wouldn't it contain the structures that inherently render.

The advantages or disadvantages of employing the $\mathcal{L}_2$ gain can also be further exploited. With the synthesis algorithms in Chapter V given in terms of LMIs, results on the level of feasibility conditions for optimal global performance can be pursued. We can contribute by showing that, when employing the $\mathcal{L}_2$ gain, under what conditions, the variety of anti-windup compensation schemes are likely to provide the same performance level.

Robust anti-windup compensation presented in this dissertation still does not account for structured dynamic (non-parametric) uncertainty. Aiming for an anti-windup compensator that guarantees a given level of uncertainty with those characteristics is ideal when attempting to move towards the complete solution of the robust ant-windup control problem.

The parametrization of the anti-windup control problem is also of importance, some results show that embedding the dynamics of the prefilter in the unconstrained controller can improve the overall level of performance. Can this effect be quantified? Would it be of help to also incorporate some disturbance dynamics? These remain as open questions.

Note that, when attempting to control the multidimensional positioning system, we have to deal with unstable systems. Hence, an interesting problem to work on is that of developing remedial compensation synthesis techniques to guarantee local stability in the presence of uncertainty and constraints.

B. Override compensation design

A first step has been given towards the systematization of solutions for override compensation. However, still many details need to be worked out. In particular, one regarding the implications of not having the parameters (H_1, H_2, Q) being all independent. How does it constrain our design problem? Furthermore, working with the conditioning of the plant does not seem a good idea in order to design compensators, not at least if the issue of uncertainty is of importance. This idea also holds for the plant model based anti-windup schemes. However, working with the conditioning of the plant cannot be disregarded unless more concluding results are obtained regarding the complications of incorporating uncertainty in the conditioning of the plant. Other issues of importance are related to providing synthesis algorithms for other override compensation schemes. At this point the general architecture for remedial compensator can be of help.

C. Simultaneous problem of input and output constraints

This problem looks very challenging, being limited in both the plant output and plant input further constrains or reduces the solution set. Importantly, to work on this problem, a lot of the bases provided in this dissertation can be employed.

REFERENCES

[1] G. Stein, "Respect the unstable," *IEEE Control Systems Magazine*, vol. 23, no. 4, pp. 12–25, August 2003.

[2] G.G. Hanson and R.F. Stengel, "Effects of displacement and rate saturation on the control of statically unstable aircraft," *Journal of Guidance, Control and Dynamics*, vol. 7, no. 2, pp. 197–205, 1984.

[3] D. McRuer and M. Graham, "Retrospective essay on nonlinearities in aircraft fight control," *Journal of Guidance, Control and Dynamics*, vol. 14, no. 6, pp. 1089–1098, 1991.

[4] M. A. Dornheim, "Report pinpoints factors leading to YF-22 crash," *Aviation Week and Space Technology Magazine*, pp. 52–54, Nov. 9 1992.

[5] Anon, "Why the gripen crashed," *Aerospace America*, vol. 32, no. 2, pp. 11, 1994.

[6] I. Eckerman, "The Bhopal gas leak: Analyses of causes and consequences by three different models," *Journal of Loss Prevention in the Process Industries*, vol. 18, no. 4-6, pp. 213–217, July-November 2005.

[7] D. Bernstein and A. Michel, "A chronological bibliography on saturating actuators," *International Journal of Robust and Nonlinear Control*, vol. 5, no. 5, pp. 375–380, 1995.

[8] K. Zhou, J. Doyle, and K. Glover, *Robust and Optimal Control*, Prentice Hall, Upper Saddle River, NJ, 1996.

[9] E.G. Gilbert and K.T. Tan, "Linear systems with state and control constraints: The theory and application of maximal output admissible sets," *IEEE Transactions on Automatic Control*, vol. 36, no. 9, pp. 1008–1020, September 1991.

[10] Z. Lin and A. Saberi, "Semi-global exponential stabilization of linear systems subject to 'input saturation' via linear feedbacks," *System & Control Letters*, vol. 21, no. 3, pp. 225–239, 1993.

[11] A. Saberi, L. Zongli, and A.R. Teel, "Control of linear systems with saturating actuators," *IEEE Transactions on Automatic Control*, vol. 41, no. 3, pp. 368–378, 1996.

[12] F.Z. Chaoui, F. Giri, and M.M'Saad, "Asymptotic stabilization of linear plants in presence of input and output constraints," *Automatica*, vol. 27, no. 1, pp. 37–42, 2001.

[13] M. Morari and J.H. Lee, "Model predictive control: Past, present and future," *Computers & Chemical Engineering*, vol. 23, no. 4, pp. 667–682, 1999.

[14] G. Dullerud and F. Paganini, *Course in Robust Control Theory - A Convex Approach*, Springer, New York, 2000.

[15] J. C. Doyle, R. S. Smith, and D. F. Enns, "Control of plants with input saturation nonlinearities," in *American Control Conference*, Green Valley, AZ, 1987, pp. 1034–1039.

[16] H. A. Fertik and C. W. Ross, "Direct digital control algorithms with anti-windup feature," *Instrument Society of America Transactions*, vol. 6, no. 4, pp. 317–328, 1967.

[17] M.V. Kothare, P.J. Campo, M. Morari, and C.N. Netts, "A unified framework for the study of anti-windup designs," *Automatica*, vol. 30, no. 12, pp. 1869–1883, 1994.

[18] M. Kothare and M. Morari, "Multiplier theory for stability analysis of anti-windup control systems," *Automatica*, vol. 35, no. 5, pp. 917–928, May 1999.

[19] A.R. Teel and N. Kapoor, "The $\mathcal{L}_2$ anti-windup problem: Its definition and solution," in *European Control Conference*, Brussels, Belgium, July 1997.

[20] E. Mulder, M.V. Kothare, and M. Morari, "Multivariable anti-windup controller synthesis using linear matrix inequalities," *Automatica*, vol. 37, no. 9, pp. 1407–1416, 2001.

[21] G. Grimm, J. Hatfield, I. Postlethwaite, A. Teel, M. Turner, and L. Zaccarian, "Antiwindup for stable linear system with input saturation: An LMI-based synthesis," *IEEE Transactions on Automatic Control*, vol. 48, no. 9, pp. 1509–1525, 2003.

[22] I. Horowitz, "A synthesis theory for a class of saturating systems," *International Journal of Control*, vol. 38, no. 1, pp. 169–187, 1983.

[23] S. Miyamoto and G. Vinnicombe, "Robust control of plants with saturation nonlinearity based on coprime factor representations," in *Control and Decision Conference*, Kobe, Japan, December 1996, pp. 2838–2840.

[24] C. Edwards and I. Postlethwaite, "Anti-windup and bumples-transfer schemes," *Automatica*, vol. 34, no. 2, pp. 199–202, 1998.

[25] B.J. Lurie and P.J. Enright, *Classical Feedback Control with MATLAB*, Marcel Dekker, New York, 2000.

[26] P.F. Weston and I. Postlethwaite, "Linear conditioning for systems containing saturating actuators," *Automatica*, vol. 36, no. 9, pp. 1347–1354, 2000.

[27] G. Grimm, A. Teel, and L. Zaccarian, "Linear LMI-based external anti-windup augmentation for stable linear systems," *Automatica*, vol. 40, no. 11, pp. 1987–1996, 2004.

[28] M.C. Turner and I. Postlethwaite, "A new perspective on static and low order anti-windup synthesis," *International Journal of Control*, vol. 77, no. 1, pp. 27–44, 2004.

[29] M.C. Turner, G. Herrmann, and I. Postlethwaite, "Accounting for uncertainty in anti-windup synthesis," in *American Control Conference*, Boston, MA, 2004, pp. 5292–5297.

[30] G. Grimm, A. Teel, and L. Zaccarian, "Robust linear anti-windup synthesis for recovery of unconstrained performance," *International Journal of Robust and Nonlinear Control*, vol. 14, pp. 1133–1168, May 2004.

[31] W. Wu and S. Jayasuriya, "A new QFT design methodology for feedback systems under input saturation," *Journal of Dynamic Systems, Measurement and Control*, vol. 123, no. 2, pp. 225–232, June 2001.

[32] T. Hu, A.R. Teel, and L. Zaccarian, "Nonlinear gain and regional analysis for linear systems with anti-windup compensation," in *American Control Conference*, Portland, OR, 2005, pp. 3391–3396.

[33] A. H. Glattfelder and W. Schaufelberger, "Stability analysis of single-loop control systems with saturation and antireset-windup circuits," *IEEE Transactions on Automatic Control*, vol. 28, no. 12, pp. 1074–1081, 1983.

[34] P. Kapasouris and M. Athans, "Multivariable control systems with saturating actuators antireset windup strategies," in *American Control Conference*, Boston, MA, June 1985, pp. 579–1584.

[35] P.J. Campo, M. Morari, and C.N. Nett, "Multivariable anti-windup and bumpless transfer: A general theory," in *American Control Conference*, Pittsburgh, PA, 1989, pp. 1706–1711, June.

[36] K.J. Astrom and L. Rundqwist, "Integrator windup and how to avoid," in *American Control Conference*, Pittsburgh, PA, 1989, pp. 1693–1698.

[37] B. Romanchuk and B.C. Smith, "Incremental gain analysis of linear systems with bounded controls and its application to the anti-windup problem," in *Control and Decision Conference*, Kobe, Japan, December 1996, pp. 2942–2947.

[38] N. Kapoor, A. Teel, and P. Daoutidis, "An anti-windup design for linear systems with input saturation," *Automatica*, vol. 34, no. 5, pp. 559–574, 1998.

[39] V. Kulkarni, "Multipliers for memoryless incrementally positive MIMO nonlinearities," Ph.D. dissertation, USC, Los Angeles, CA, May 2001.

[40] S.T. Impram and N. Munro, "Absolute stability of nonlinear systems with disc and norm-bounded perturbations," *International Journal of Robust and Nonlinear Control*, vol. 14, no. 1, pp. 61–78, December 2004.

[41] R.A. Hess and S.A. Snell, "Flight control system design with rate saturating actuators," *Journal of Guidance, Control and Dynamics*, vol. 20, no. 1, pp. 90–96, 1997.

[42] W. Wu and S. Jayasuriya, "A QFT design methodology for feedback systems

with input rate or amplitude and rate saturation," in *American Control Conference*, Arlington, VA, June 2001, pp. 376–383.

[43] T. Pare, H. Hindi, J. How, and D. Banjerdpongchai, "Local control design for systems with saturating actuators using the Popov criteria," in *American Control Conference*, San Diego, California, June 1999, pp. 3211–3215.

[44] A. Teel, "Anti-windup for exponentially unstable linear systems," *International Journal of Robust and Nonlinear Control*, vol. 9, no. 10, pp. 701–716, 1999.

[45] R. Hanus, M. Kinnaert, and J.L. Henrotte, "Conditioning technique, a general anti-windup and bumpless transfer method," *Automatica*, vol. 23, no. 6, pp. 729–739, 1987.

[46] I. Horowitz, "Feedback systems with rate and amplitude limiting," *International Journal of Control*, vol. 40, no. 6, pp. 1215–1229, 1984.

[47] T. Hu, Z. Lin, and B.M. Chen, "An analysis and design method for linear systems subject to actuator saturation and disturbance," *Automatica*, vol. 38, no. 2, pp. 351–359, 2002.

[48] K.C. Goh, "Robust control synthesis via bilinear matrix inequalities," Ph.D. dissertation, USC, Los Angeles, CA, May 1995.

[49] J.H.Q. Ly, "A multiplier approach to robust analysis and synthesis," Ph.D. dissertation, USC, Los Angeles, CA, May 1995.

[50] H.-H. Meng, "Stability analysis and robust control synthesis with generalized multipliers," Ph.D. dissertation, USC, Los Angeles, CA, June 2002.

[51] A.H. Glattfelder and W. Schaufelberger, "Stability of discrete override and cascade-limiter single-loop control systems," *IEEE Transactions on Automatic Control*, vol. 33, no. 6, pp. 532–540, June 1988.

[52] M.C. Turner and I. Postlethwaite, "Output violation compensation for systems with output constraints," *IEEE Transactions on Automatic Control*, vol. 47, no. 9, pp. 1540–1546, September 2002.

[53] M.C. Turner and I. Postlethwaite, "Multivariable override control for systems with output and state constraints," *International Journal of Robust and Nonlinear Control*, vol. 14, pp. 1105–1131, June 2004.

[54] A.H. Glattfelder and W. Schaufelberger, "A path from antiwindup to override control," in *IFAC Symposium on Nonlinear Control Systems*, Stuttgart, Germany, September 2004, pp. 1379–1384.

[55] W. Wu and S. Jayasuriya, "Criteria for recovery of the output response of unstable plants under input saturation," in *ASME International Mechanical Engineering Congress & Exhibition*, Orlando, FL, November 2000, vol. 1, pp. 503–508.

[56] G. Grimm, "Constructive sotutions to the anti-windup problem," Ph.D. dissertation, UCSB, Santa Barbara, CA, June 2003.

[57] E. Villota, M. Kerr, and S. Jayasuriya, "A study of configurations for anti-windup control of uncertain systems," in *Control and Decision Conference*, San Diego, CA, December 2006, pp. 6193–6198.

[58] F. Tyan and D.S. Bernstein, "Dynamic output feedback compensation for linear systems with independent amplitude and rate saturations," *International*

Journal of Control, vol. 67, no. 1, pp. 89–116, 1997.

[59] J.-K. Park and C.-H. Choi, "Dynamic compensation method for multivariable control systems with saturating actuators," *IEEE Transactions on Automatic Control*, vol. 40, no. 9, pp. 1635–1640, 1995.

[60] G. Herrmann, M. Turner, and I. Postlethwaite, "Some new results on anti-windup-conditioning using the Weston-Postlethwaite approach," in *Control and Decision Conference*, Bahamas, 2004, pp. 5047–5052.

[61] L. Zaccarian and A.R. Teel, "Nonlinear scheduled anti-windup design for linear systems," *IEEE Transactions on Automatic Control*, vol. 49, no. 11, pp. 2055–2061, 2004.

[62] R.A. Horn and C.R. Johnson, *Matrix Analysis*, Cambridge University Press, New York, 1990.

[63] S. Galeani, M. Massimetti, A. Teel, and L. Zaccarian, "Reduced order linear anti-windup augmentation for stable linear systems," *International Journal of Systems Science*, vol. 37, no. 2, pp. 115–127, 2006.

[64] M. Vidyasagar, *Control System Synthesis: A Factorization Approach*, The MIT Press, Cambridge, MA, 1988.

[65] E. Villota, W. Wu, M. Kerr, and S. Jayasuriya, "An analysis of model-based conditioning schemes for uncertain plants with input saturation," in *Symposium on QFT and Robust Frequency Methods*, Lawrence, KA, 2005.

[66] S. Galeani and A. Teel, "On performance and robustness issues in the anti-windup problem," in *American Control Conference*, Bahamas, December 2004, vol. 5, pp. 5022–5027.

[67] S. Boyd, L.El. Ghaoui, E. Feron, and V. Balakrishnan, *Linear Matrix Inequalities in System and Control Theory*, SIAM, Philadelphia, PA, 1994.

[68] P. Gahinet and P. Apkarian, "A linear matrix inequality approach to $\mathcal{H}_\infty$ control," *International Journal of Robust and Nonlinear Control*, vol. 4, no. 4, pp. 421–448, 1994.

[69] N. Bhat, "ATP project report," Internal report, Mechanical Engineering Department, Texas A&M University, 2003.

[70] W.J. Kim, "High precision planar magnetic levitation," Ph.D. dissertation, MIT, Cambridge, MA, June 1997.

[71] U. Forssell and L. Ljung, "Closed-loop identification revisited," *Automatica*, vol. 35, no. 9, pp. 1215–1241, July 1999.

[72] M. Athans, "A tutorial on the LQG/LTR method," Research report, Laboratory for Information and Decision Systems, MIT, 1986.

[73] G. Franklin, A. Emami-Naeini, and J. Powell, *Feedback Control of Dynamic Systems*, Addison-Wesley Longman Publishing Co., Boston, MA, 1994.

[74] B.D.O. Anderson and J.B. Moore, *Linear Optimal Control*, Prentice Hall, Upper Saddle River, NJ, 1971.

[75] O. Yaniv, *Quantitative Feedback Design of Linear and Nonlinear Control Systems*, Kluwer Academic Pub., The Netherlands, 1999.

[76] K.B. Lim and D.E. Cox, "Experimental robust control studies on an unstable magnetic suspension system," in *American Control Conference*, Baltimore, MD, June 1994, vol. 3, pp. 3198–3203.

[77] K.B. Lim and D.P. Giesy, "Parameterization of model validating sets for uncertainty bound optimizations," in *AIAA Guidance, Navigation and Control Conference and Exhibit*, Boston, MA, August 1998, vol. 1, pp. 336–346.

[78] E. Villota, S. Jayasuriya, and M. Kerr, "Model based control of a multidimensional positioning system - A comparison of controllers with experimental validation," in *American Control Conference*, Portland, OR, June 2005, vol. 2, pp. 1365–1370.

[79] J. Juang, *Applied System Identification*, Prentice Hall, Upper Saddle River, NJ, 1994.

[80] K.B. Lim, "A methodology for model validation and uncertainty modeling for linear multivariable robust control," in *AIAA Guidance, Navigation and Control Conference and Exhibit*, Portland, OR, August 1999, vol. 2, pp. 1145–1155.

[81] K.B. Lim, G.L. Balas, and T.C. Anthony, "A minimum-norm model validation identification for robust control," in *AIAA Guidance, Navigation and Control Conference*, San Diego, CA, July 1996, vol. 1, pp. 1–11.

APPENDIX A

A. Mechanical and electromagnetic parameters of the MPS

Table I. Mechanical and electromagnetic parameters of the MPS.

parameter	value	units
	mechanical parameters	
mass (m)	5.91	kg
inertia tensor ($\underline{I}$)	$\begin{bmatrix} 0.0357 & -0.0012 & -0.0008 \\ -0.0012 & 0.0261 & 0.0003 \\ -0.0008 & 0.0003 & 0.0561 \end{bmatrix}$	kgm^2
linear spring constant (k_{x_3})	10^6	$\frac{\mathrm{N}}{\mathrm{m}}$
rotational spring constant (k_{β_1})	$1.065\,10^4$	$\frac{\mathrm{N\ m}}{\mathrm{rad}}$
rotational spring constant (k_{β_2})	$1.131\,10^4$	$\frac{\mathrm{N\ m}}{\mathrm{rad}}$
	electromagnetic parameters	
turn density (η_o)	$3.5246\,10^6$	$\frac{\mathrm{turns}}{\mathrm{m}^2}$
number of magnet pitches (N_m)	2	-
magnet remanence ($\mu_o M_o$)	0.71	T
motor geometry constant (G)	$1.0722\,10^{-5}$	m^3
fundamental wave number (γ_1)	123.25	m^{-3}

B. Non-zero eigenvalues and eigenvectors for the open loop system

Table II. Non-zero eigenvalues and eigenvectors for the open loop system.

	mode 1 eigenvalue	mode 2 eigenvalue	mode 3 eigenvalue
	$\pm 659.85i$	$\pm 545.44i$	$\pm 411.35i$
states	eigenvector	eigenvector	eigenvector
ω_1	-0.1060	-0.9949	0
ω_2	-0.9944	+0.0999	0
ω_3	0	0	0
β_1	$\pm 0.0002i$	$\pm 0.0018i$	0
β_2	$\pm 0.0015i$	$\mp 0.0002i$	0
β_3	0	0	0
v_1	0	0	0
v_2	0	0	0
v_3	+0.0031	-0.01479	+1
x_1	0	0	0
x_2	0	0	0
x_3	$\mp 0.000005i$	$\pm 0.00003i$	$\mp 0.0024i$

C. A smallest model validating set algorithm

The following steps need to be followed for the obtention of the smallest model validating set.

1. Select (P, Δ, V).
2. Test feasibility of (P, Δ, V) against (r,y) (if infeasible, return to Step 1).
3. Select W.
4. Find the smallest w such that $\mathcal{D}_W$ is model validating. Tradeoff, repeat Steps 3 and 4.

The introduction of nonparametric uncertainty is recommended to satisfy the feasibility condition in Step 2. Parametric uncertainties can be included to reduce the nonparametric uncertainty levels in Step 4.

a. Optimal Problem:

$$\begin{aligned} \min \quad & w^2 \\ \phi, \psi, \delta_1, .., \delta_r, w^2 \quad & \text{subject to} \\ & \|\zeta_i(\phi,\psi) - \delta_i \eta_i(\phi,\psi)\|^2 = 0, \quad \delta_i \in \mathcal{F}_i, \ \forall i = 1, \cdot\cdot, r, \\ & |\delta_i|^2 - |w_i|^2 \leq 0, \ \forall i = 1, \cdot\cdot, r, \\ & \|\zeta_i(\phi,\psi)\|^2 - |w_i|^2 \|\eta_i(\phi,\psi)\|^2 \leq 0, \forall i = r+1, \cdot\cdot, \tau, \\ & \|\phi\|^2 \leq b_o^2. \end{aligned} \tag{A.1}$$

D. Approach to determine identified models and uncertainty bounds experimentally

The proposed approach to determine identified models and uncertainty bounds has two well-defined phases: i) identification of state space realization of the plant by obtaining the open loop Markov parameters from the closed-loop Markov parameters and employing the observer/controller identification algorithm, and ii) calculation of the uncertainty bounds by employing the smallest model validation set algorithm[2]. For these two phases, time histories from the actual experiment need to be collected, this can be done following the procedures described below.

a. Test for system identification (steps)

1. Use two added noise signals for one channel input and zero signal for the other channel inputs.

   Signal 1: zero mean noise with 1×10^{-5} standard deviation filtered by a Butterworth filter of order 4 ($n = 4$), with break frequency of 60% Nyquist frequency.

   Signal 2: zero mean noise with 5×10^{-5} standard deviation filtered by a Butterworth filter of order 4 ($n = 4$), with break frequency of 1% Nyquist frecuency.

2. Total time excitation 2s at a sampling rate of 5000Hz.

   Save input and output time histories.

3. Repeat Steps 1 and 2 ten times ($N = 10$).

4. Repeat Steps 1 to 3 interchanging the input signals (the total number of input signals is 6).

[2]To solve the minimization problem, a nonlinear optimization approach based on sequential quadratic programming techniques is used.

b. Test for uncertainty bounds (steps)

1. Use two added noise signals for all the channels simultaneously. These added noise signals could be the same of previous test.

2. Total time excitation 2s at a sampling rate of 5000Hz.

   Save input and output time histories.

3. Repeat Steps 1 and 2 ten times ($N = 10$).

E. Case studies for uncertainty bounds generation

Table III. Description of case studies for uncertainty bounds generation.

case number	nominal model	uncertainty	noise for ID
1	analytical, 12th order	add	-
2	analytical, 12th order	add+par	-
3	analytical, 12th order	mult	-
4	analytical, 12th order	mult+par	-
5	identified, 16th order	add	yes
6	identified, 16th order	add+par	yes
7	identified, 16th order	mult	yes
8	identified, 16th order	mult+par	yes

VITA

Elizabeth Roxana Villota Cerna received her Bachelor of Science degree from the Universidad Nacional de Ingenieria, Peru, in March 1999 and her Master of Science degree from the Pontificia Universidade Catolica do Rio de Janeiro, Brazil, in August 2001. Her research interests lie at the intersection of modeling, analysis and control of complex systems with emphasis on the applications to interdisciplinary fields ranging from electromechanical systems to biological systems. Broadly, her goal is to find shared principles of design that may simplify the picture when analyzing and synthesizing complex systems.

Ms. Villota can be reached at elvillota@gmail.com. Mailing address: 100 ENPH, Texas A&M University, College Station, TX 77843-3123.